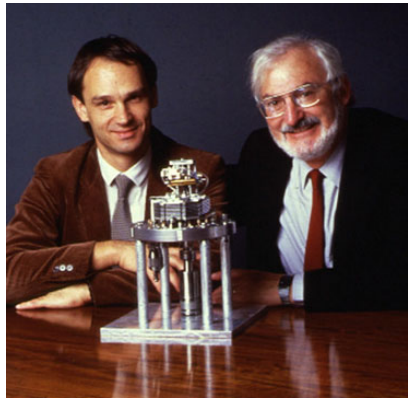


Polymers in Nanotechnology

History of Nanotechnology

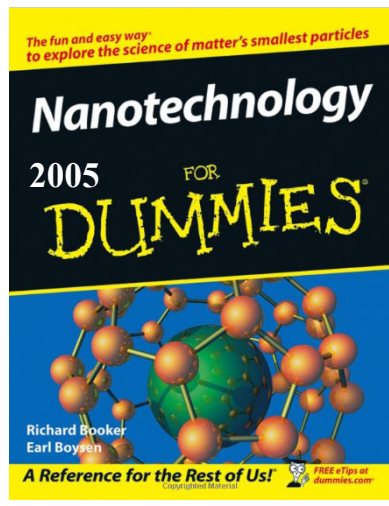
The Big Picture on Nanotechnology

The Beginning

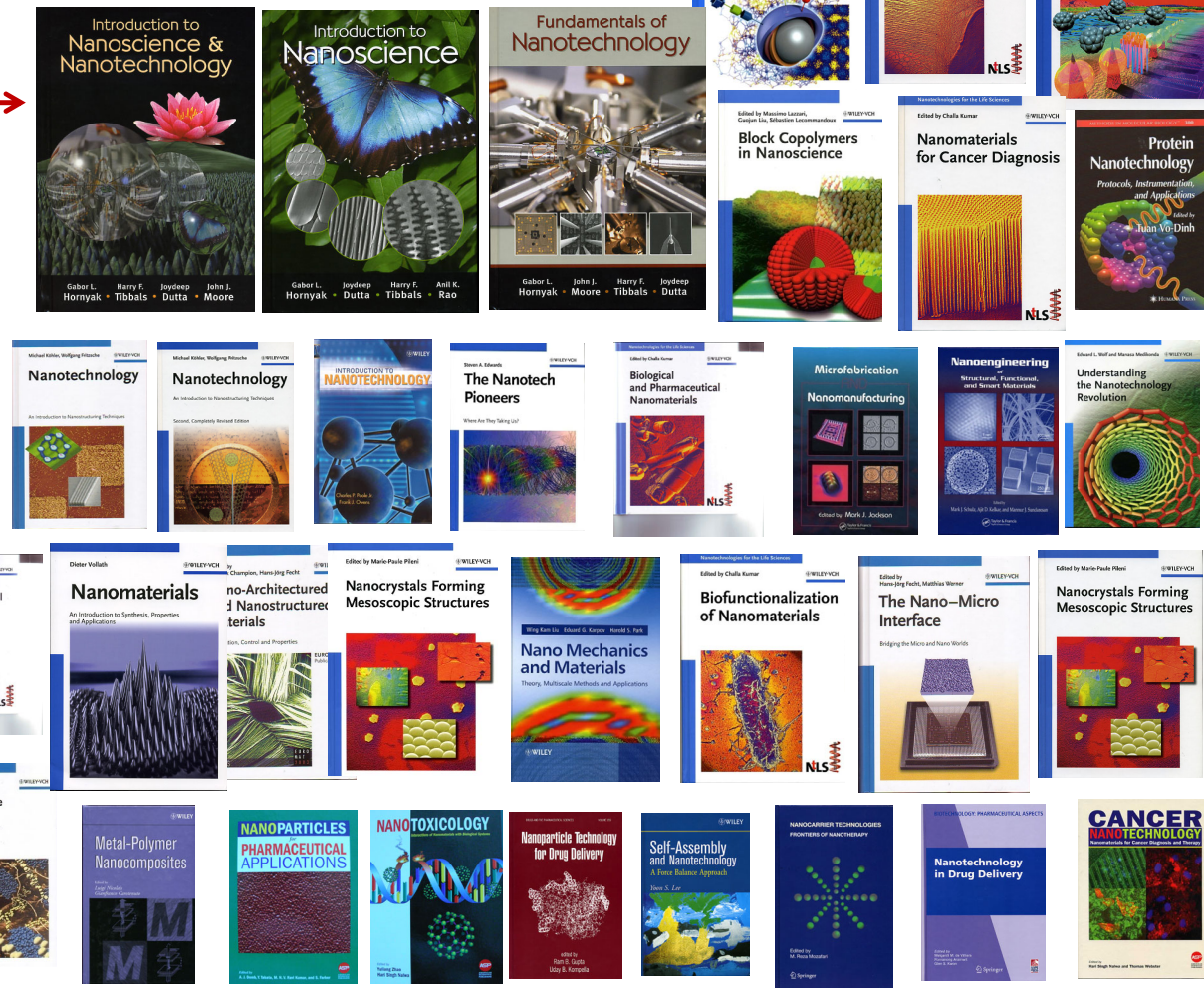


Gerd Binnig & Heinrich Rohrer
Inventors of the Scanning tunneling microscope (STM)

The Trending



The Boom



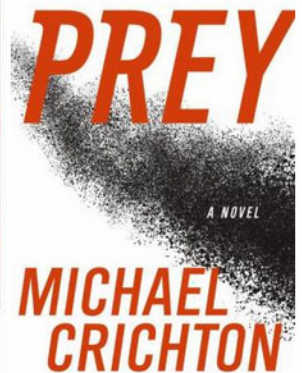
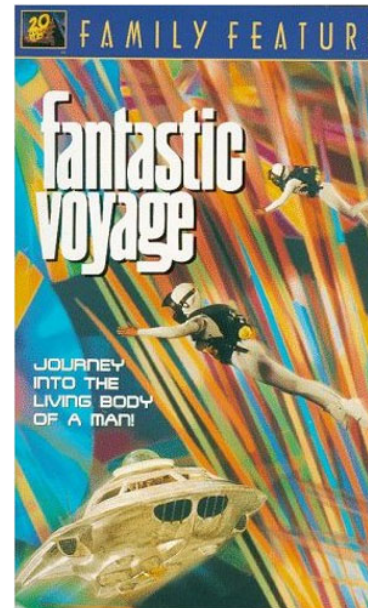
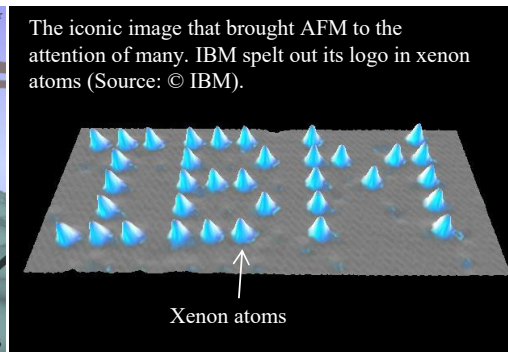
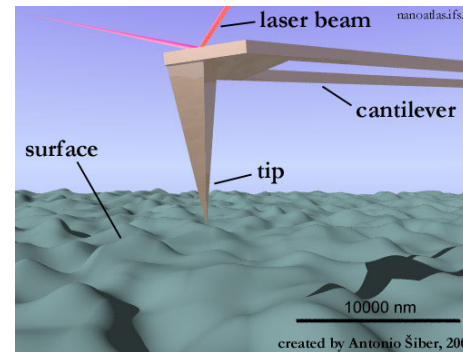
Nanotechnology: Introduction

It is debatable when nanotechnology, as we now know it, began. Perhaps, we can trace the beginnings to the invention of the scanning tunneling microscope in 1980, as it and the subsequently developed atomic force microscope enabled manipulation of individual atoms and molecules.

The nanotechnology fever began when the United States launched the National Nanotechnology Initiative (<https://www.nano.gov/>), the world's first program of its kind, in 2000. Since then, we have been bombarded by the dazzling images and cartoons of nanotechnology, such as nanorobots killing cancer cells resembling the plot of *Fantastic Voyage*. Tens of thousands of articles have been published on nanotechnology, and the press feed the public a steady diet of potential advances due to nanotechnology.

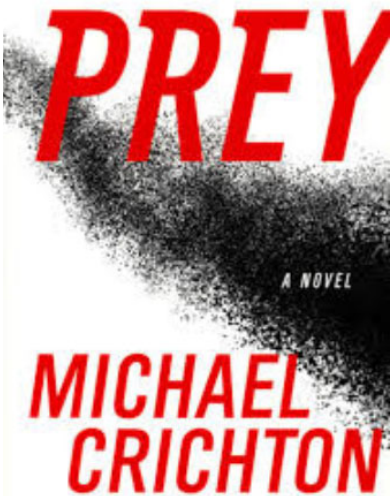
Park 2013, Facing the truth about nanotechnology in drug delivery

Scanning tunneling microscope → atomic force microscope



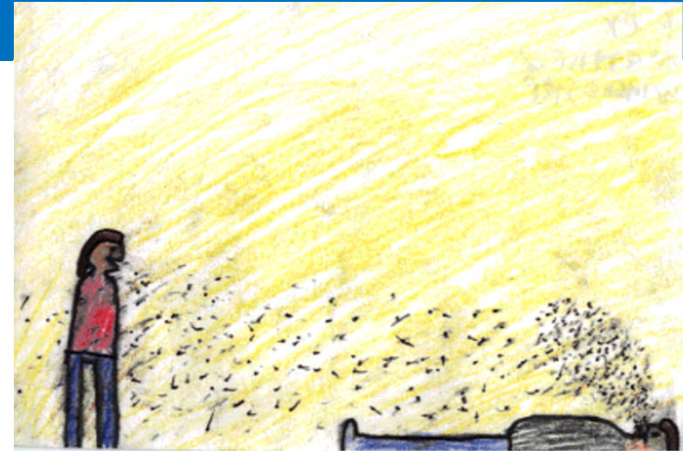
1966
1989
2002
Hollywood versions of nanotechnology

Nanotechnology Future: Fiction and Fact



MAKING PREHISTORY Michael Crichton at the Natural History Museum of Los Angeles County, in 2004. BY BLAKE LITTLE/CONTOUR/GETTY IMAGES.

2002



Prey- Written by Michael Crichton
Illustrated by Will Staehle, Reviewed by Matthew W. (age 10, 4th Grader))

Have you ever heard of a nano particle? Well Prey is about a company called Xmos that develops nano technology and creates nano particles. Nano particles are micro super computer robots capable of intelligent life. Jack (a father of three kids who had been working at Xmos but was fired several weeks ago) has been asked to come back to Xmos by his best friend, Ricky. Ricky says that they have a runaway swarm of nano particles. After several days at Xmos, Jack gets suspicious of his wife, Julia, who is working to solve the mystery as well. She is acting very strangely toward him and Jack wants to know what's wrong. What Jack doesn't know is that the answer could get him killed!

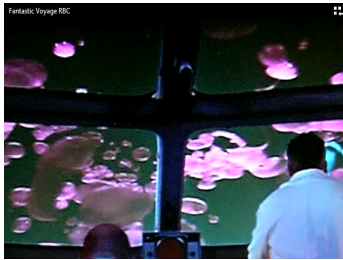
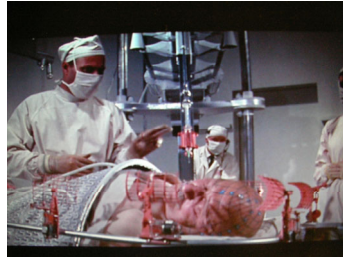
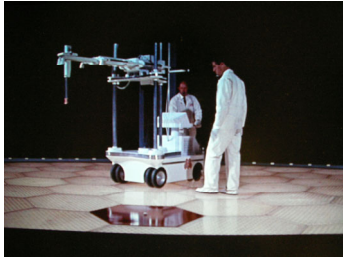
I highly recommend this book. The plot was fantastic and exiting. I was never bored because the book moved fast and there was always an adventure going on. Jack was very interesting. His brightness and curiosity helped solve the mystery. He knows a lot about computers and he saves many lives. The book was scary and strange. I do not recommend this book for all ages. Unless you are a good reader and your parents will let you read it you should not read this book. If you read it, I hope you like it.

I recommend this book to boys who like scary and weird books. You can find this book at your local library. I hope you like it!

<https://www.spaghettibookclub.org/review.php?reviewId=4396>
<https://www.goodreads.com/review/show/203477000>

Nanoparticles in the Blood

Fantastic Voyage (1966)



US Airways Flight 1549 in the Hudson River, New York, USA (January 15, 2009)

~
~

↕
C



<https://simpleflying.com/the-miracle-on-the-hudson/>
<https://www.sciencephoto.com/media/852378/view/us-airways-flight-1549-incident-illustration>

Nanotechnology: Chip to Machine

K. Eric Drexler

1992

Nanosystems

Molecular Machinery, Manufacturing, and Computation

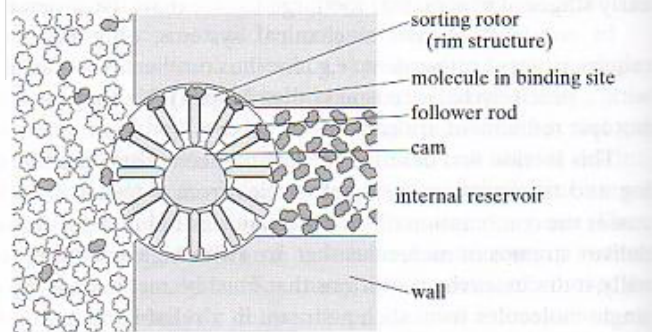


Figure 13.1. A sorting rotor based on modulated receptors. In this approach (illustrated schematically), a cam surface modulates the position of a set of radial rods. In the binding position (mapping the illustration onto a 12-hour clock dial, 10:00), the rods form the bottom of a site adapted to bind molecules of the desired type. Between 10:00 and 2:00, the receptors undergo transport to the interior, driven by shaft power (coupling not shown). Between 2:00 and 4:00, the molecules are forcibly ejected by the rods, which are thrust outward by the cam surface. Between 4:00 and 8:00, the sites, now blocked and incapable of transporting molecules, undergo transport to the exterior. Between 8:00 and 10:00, the rods retract, regenerating an active receptor. Section 13.2.1c discusses receptor properties; Section 13.2.1e discusses energy dissipation.

Machine-Phase Nanotechnology

A molecular nanotechnology pioneer predicts that the tiniest robots will revolutionize manufacturing and transform society

By K. Eric Drexler

IN 1959 PHYSICIST Richard Feynman gave an after-dinner talk exploring the limits of miniaturization. He set out from known technology (at a time when an adding machine could barely fit in your pocket), surveyed the limits set by physical law and ended by arguing the possibility—even inevitability—of “atom by atom” construction.

What at the time seemed absurdly ambitious, even bizarre, has recently become a widely shared goal. Decades of technological progress have shrunk microelectronics to the threshold of the molecular scale, while scientific progress at the molecular level—especially on the

to put every atom in a selected place (where it would serve as part of some active or structural component) with no extra molecules on the loose to jam the works. Such a system would not be a liquid or gas, as no molecules would move randomly, nor would it be a solid, in which molecules are fixed in place. Instead this new machine-phase matter would exhibit the molecular movement seen today only in liquids and gases as well as the mechanical strength typically associated with solids. Its volume would be filled with active machinery.

The ability to construct objects with molecular precision will revolutionize

molecular repair of the human body. Medical nanorobots are envisioned that could destroy viruses and cancer cells, repair damaged structures, remove accumulated wastes from the brain and bring the body back to a state of youthful health.

Another surprising medical application would be the eventual ability to repair and revive those few pioneers now in suspended animation (currently regarded as legally deceased), even those who have been preserved using the crude cryogenic storage technology available since the 1960s. Today’s vortification techniques—which prevent the forma-

In principle, Drexler says, a molecular construction system called an assembler could build almost anything, including copies of itself.

molecular machinery of living systems—has now made clear to many what was envisioned by a sole genius so long ago.

Inspired by molecular biology, studies of advanced nanotechnologies have focused on bottom-up construction, in which molecular machines assemble molecular building blocks to form products, including new molecular machines. Biology shows us that molecular machine systems and their products can be made cheaply and in vast quantities.

Stepping beyond the biological analogy, it would be a natural goal to be able

manufacturing, permitting materials properties and device performance to be greatly improved. In addition, when a production process maintains control of each atom, there is no reason to dump toxic leftovers into the air or water. Improved manufacturing would also drive down the cost of solar cells and energy storage systems, cutting demand for coal and petroleum, further reducing pollution. Such advances raise hope that those in the developing world will be able to reach First World living standards without causing environmental disaster.

Low-cost, lightweight, extremely strong materials would make transportation far more energy efficient and—finally—make space transportation economical. The old dreams of expanding the biosphere beyond our one vulnerable planet suddenly look feasible once more.

Perhaps the most exciting goal is the

tion of damaging ice crystals—should make repair easier, but even the original process appears to preserve brain structure well enough to enable restoration.

Those researchers most familiar with the field of molecular nanotechnology see the technology base underpinning such capabilities as perhaps one to three decades off. At the moment, work focuses on the earliest stages finding out how to build larger structures with atomic precision, learning to design molecular machines and identifying intermediate goals with high payoff.

To understand the potential of molecular manufacturing technology, it helps to look at the macroscale machine systems used now in industry. Picture a robotic arm that reaches over to a conveyor belt, picks up a loaded tool, applies the tool to a workpiece under construction, replaces the empty tool on the belt,



picks up the next loaded tool, and so on—as in today’s automated factories.

Now mentally shrink this entire mechanism, including the conveyor belt, to the molecular level to form an image of a nanoscale construction system. Given a sufficient variety of tools, this system would be a general-purpose building device, nicknamed an assembler. In principle, it could build almost anything, including copies of itself.

Molecular nanotechnology as a field does not depend on the feasibility of this particular proposal—a collection of less general building devices could carry out the functions mentioned above. But because the assembler concept is still controversial, it’s worth mentioning the objections being raised.

One prominent chemist speaking at a recent event sponsored by the American Association for the Advancement of Science asked how one could power and direct an assembler and whether it could really break and re-form strong molecular bonds. These are reasonable questions that can be answered only by de-

scribing designs and calculations too bulky to fit in this essay. Fortunately, technical literature providing seemingly adequate answers has been available since at least 1992, when my book *Nanosystems* was published.

Another well-known chemist objects that an assembler would need 10 robotic “fingers” to carry out its operations and that there isn’t room for them all. The need for such a large number of manipulators, however, has never been established or even seriously argued. In contrast, the designs that have received (and survived) the most peer review use one tool at a time and grip their tools without using any fingers at all.

These examples point to the difficulty of finding appropriate critiques of nanotechnology designs. Many researchers whose work seems relevant are actually the wrong experts—they are excellent in their discipline but have little expertise in

systems engineering. The shortage of molecular systems engineers will probably be a limiting factor in the speed with which nanotechnology can be developed.

It is important that critiques of nanotechnology are well executed, because vital societal decisions depend on them. If molecular nanotechnology as described here is correct, policy issues can look quite different from what is generally expected. Today most people believe that global warming will be hard to correct—with nanotechnology, excess greenhouse gases could be inexpensively removed from the atmosphere. Current Social Security projections assume increasing numbers of aged citizens in poor health. With advanced medical nanotechnology, nanorobots’ services could be more active and healthy than they are now, bringing new meaning to the “golden years.”

Likewise, we need to focus now on avoiding accidents and preventing abuse of this powerful technology. Solid work has been done on the problem of heading off major nanotechnology accidents. The Foresight Guidelines, available on the World Wide Web, sketch out proposed safety rules [see below].

But the challenge of preventing abuse—the exploitation of this technology by aggressive governments, terrorist groups or even individuals for their own purposes—still looms large. The closest analogy to this problem these days is the difficulty of controlling the proliferation of chemical and biological weapons. The advance toward molecular nanotechnology highlights the urgency in finding effective ways to manage emerging technologies that are powerful, valuable and open to misuse.

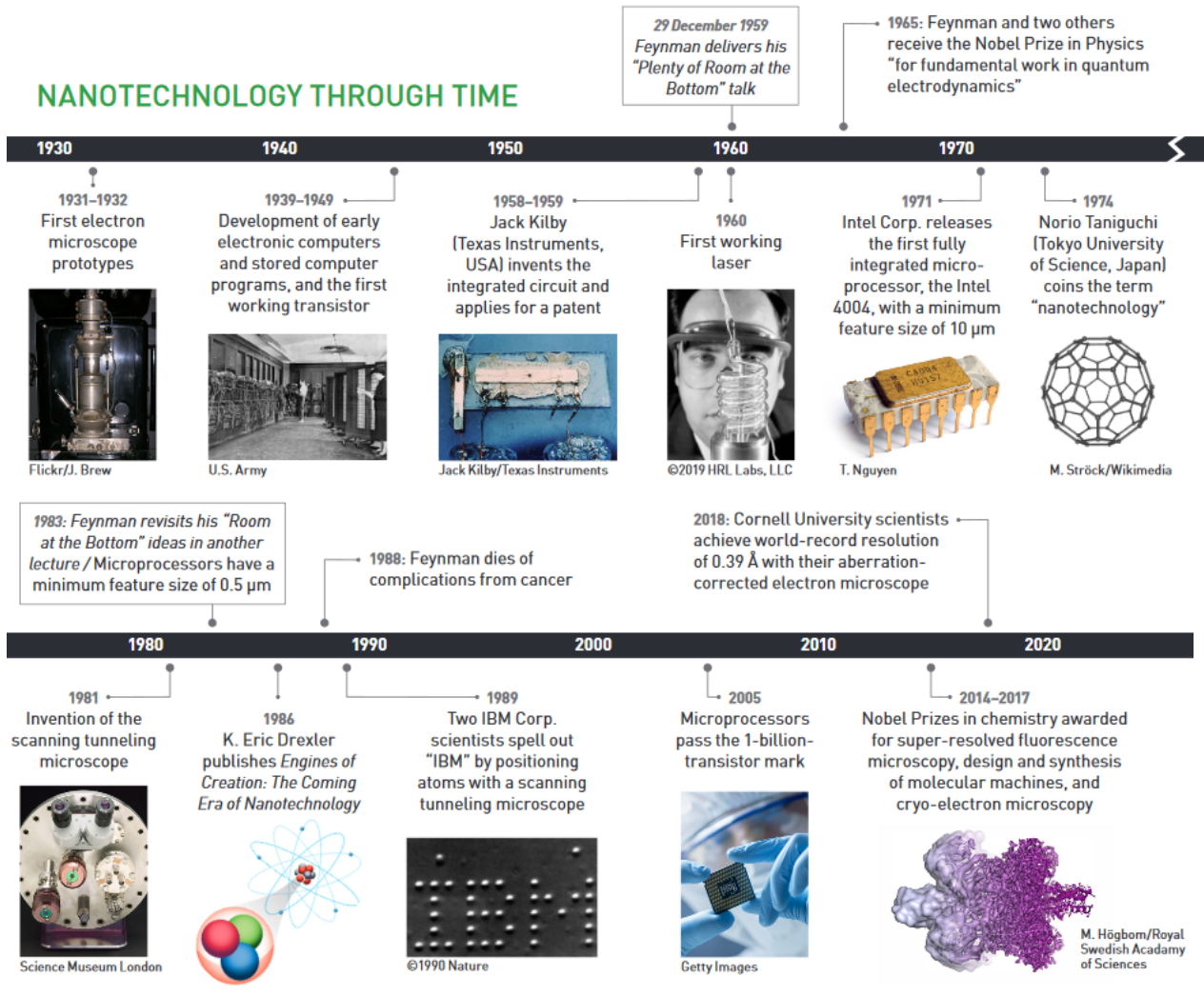
MORE TO READ
Engines of Creation: The Coming Era of Nanotechnology, K. E. Drexler, Fourth Estate, 1986.
Nanosystems: Molecular Machinery, Manufacturing, and Computation, K. E. Drexler, John Wiley & Sons, 1992.
 The Foresight Institute and the Foresight Guidelines: www.foresight.org
 Richard Feynman’s lecture “There’s Plenty of Room at the Bottom” can be found at www.zyxx.com/nanosuch/feynman.html

Nanomachines, such as the one described above in Figure 13.1, looks great on paper. But the nanomotor in the figure has immediate and obvious difficulties for practical use. What are the problems?



Nanotechnology through Time


https://www.osa-opn.org/opn/media/Images/PDF/2019/07_0819/24-31_OPN_07_08_19.pdf?ext=.pdf

NANOTECHNOLOGY THROUGH TIME

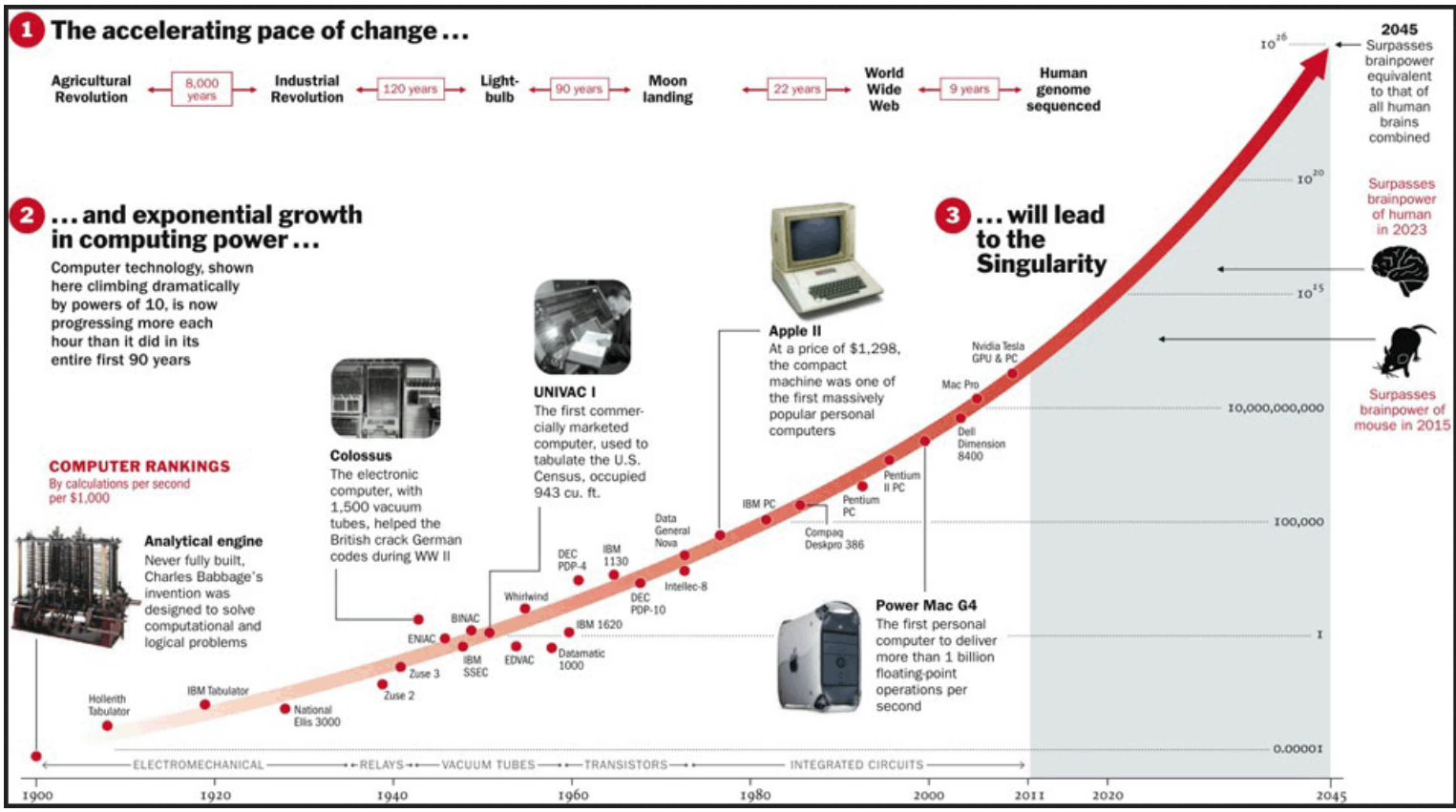


Patricia Daukantas: Still plenty of room at the bottom, *Optics & Photonics News*, July/August, 25-31, 2019.

How do Electron Microscopes Work?  
Taking Pictures of Atoms - part 1

 **TikTok**
@mimicsporton1111996jh

The Accelerating Pace of Change & Growth



Whatever has been done can be
outdone.

Gordon Moore

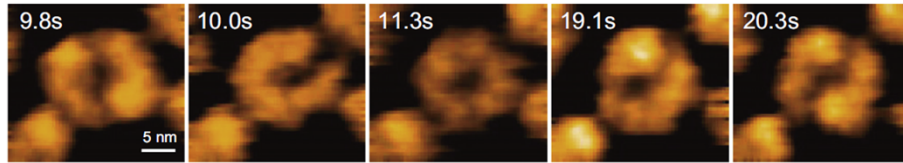
In 1965, Gordon Moore made a prediction that would set the pace for our modern digital revolution. From careful observation of an emerging trend, Moore extrapolated that computing would dramatically increase in power, and decrease in relative cost, at an exponential pace. The insight, known as **Moore's Law** (the number of transistors in a dense integrated circuit (IC) doubles about every two years), became the golden rule for the electronics industry, and a springboard for innovation. As a co-founder, Gordon paved the path for Intel to make the ever faster, smaller, more affordable transistors that drive our modern tools and toys. Even over 50 years later, the lasting impact and benefits are felt in many ways.

<https://www.intel.com/content/www/us/en/silicon-innovations/moores-law-technology.html>

<https://ourworldindata.org/technological-progress>

https://external-preview.redd.it/IHdaR-B3P5UvLf0n520AVuKE_qQhbBuIjB44JA7GZRM.png?auto=webp&s=9ce56fd8924ba75aee566c1dc53d417938831c0b

High-Speed Atomic Force Microscopy (AFM)



HS-AFM images showing massive conformational changes of DN-ClpB during the ATPase reaction. Different structures appeared, including a twisted-half-spiral ring (9.8 s, 20.3 s), a round ring (11.3 s), a spiral ring (10.0 s), and an intermediate between spiral and twisted-half spiral rings (19.1 s). Imaging rate, 10 fps.

HS-AFM for biomolecular imaging was established in 2008. The feedback bandwidth (FB) of our system, which determines the system's speed performance, is about 110 kHz when it is used together with a short cantilever with resonant frequency of 1.2 MHz in water. HS-AFM has been used for not only imaging proteins but also live cell imaging [8,9], chemically oriented studies on DNA/RNA, mechanical measurements of cells and biopolymers, and others. However, in this mini review I focus on HS-AFM imaging of proteins (other than transmembrane proteins).

The advent of high-speed atomic force microscopy (HS-AFM) has changed the field of biology considerably. Unlike conventional AFM, which has a slow scanning rate, **HS-AFM can scan a biological molecule (100 nm size) in 100 ms or less.** The feedback bandwidth and short cantilever in HS-AFM allow **high spatiotemporal resolution scanning** without affecting the integrity of biomolecules. The greatest advantage of HS-AFM is **the real-time imaging of biomolecules.** In addition, sample preparation, for example, crystallization or fixation, is unnecessary for HS-AFM scanning to observe native or transformed conformations of target biomolecules. Therefore, this advantage overcomes the technical limitations that exist in the aforementioned techniques. By using HS-AFM, we have achieved several remarkable breakthroughs in biomolecular imaging, including structural characterization, visualization of conformational dynamics, and revealing the dynamic interactions of biomolecules and organelles. Recently, we have successfully conducted a pilot study regarding realtime visualization of the native structure and conformational dynamics of the hemagglutinin precursor (HA0) of H5N1 in the physiological buffer.

Ando 2019, High-speed atomic force microscopy

Lim 2020, High-speed AFM reveals molecular dynamics of human influenza a hemagglutinin and its interaction with exosomes

Lim 2023, Nanoscopic assessment of anti-SARS-CoV-2 spike neutralizing antibody using high-speed AFM

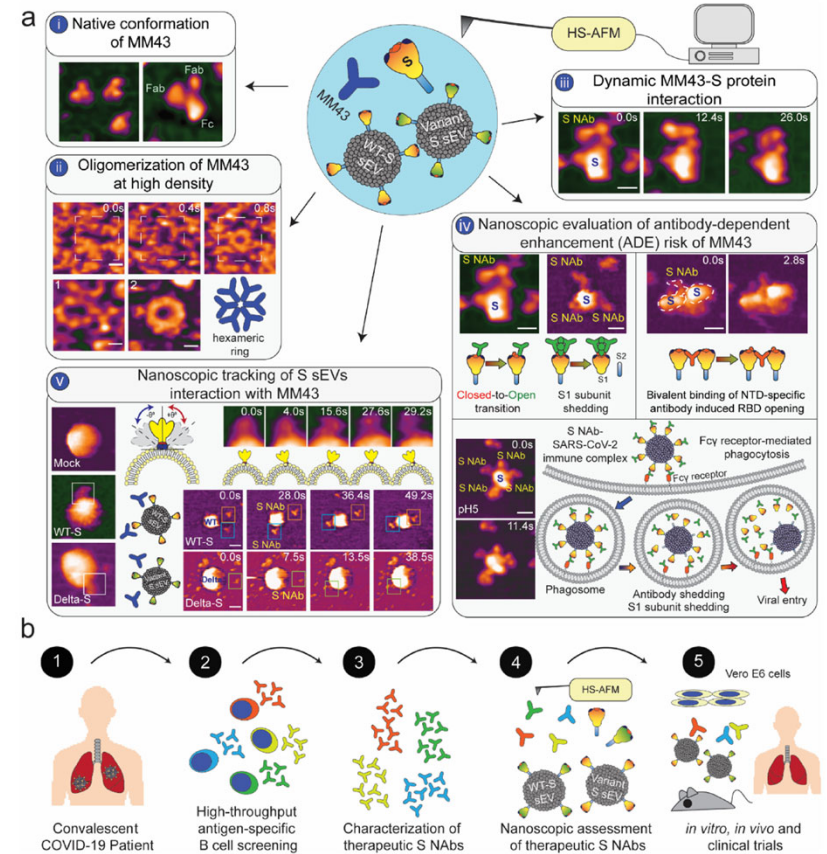


Figure 5. A nanoscopic perspective of S NAb and S protein interaction is essential for the assessment of S NAb therapeutic potential. (a) Nanoscopic observation of MM43 using HS-AFM reveals its native conformation (i) and intrinsic properties (ii), oligomerization for example. High spatiotemporal resolution enables HS-AFM to capture the dynamic MM43-S protein interaction and its binding pattern (iii). Direct visualization of S protein conformation in an immune complex at either neutral or acidic pH could provide important information related to antibody-dependent enhancement (ADE) such as RBD "Closed"-to-"Open" transition,^{31,10} S1 subunit shedding,⁶ and antibody shedding¹¹ (iv). S sEVs are safe alternative materials for nanoscopic tracking of the MM43 and SARS-CoV-2 interaction (v). Topology of S sEV and dynamic movement of S protein on sEV surface resemble SARS-CoV-2 virus. (b) Our results as summarized in (a) demonstrate that HS-AFM is feasible for nanoscopic assessment of potential therapeutic S NAbs. Patients recovered from COVID-19 have acquired immunity against SARS-CoV-2 (1). High-throughput screening of antigenic-specific B cells (2) is performed to isolate S NAbs for further evaluation of their therapeutic values (3). Nanoscopic assessment of these candidates using HS-AFM could provide essential information for better selection of S NAbs (4). Finally, the selected S NAbs will be used for downstream *in vitro* and *in vivo* experiments as well as clinical trials to validate their therapeutic efficacies (5).

Single-Molecule Optical Biosensing

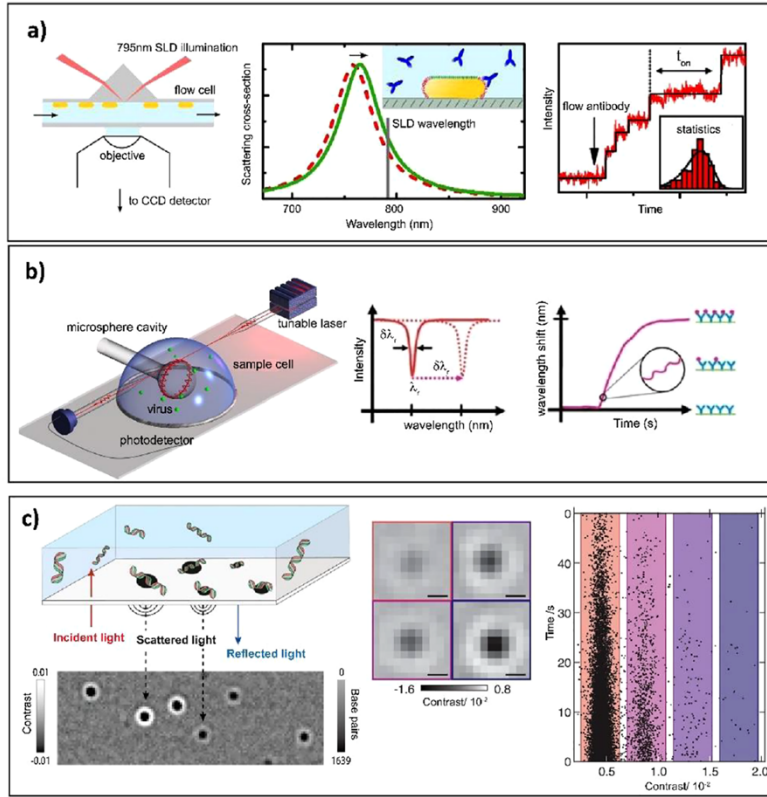


Figure 2. Examples of single-molecule direct assays. (a) Left: Schematic of the optical setup for monitoring stochastic protein interactions using plasmon sensing. Middle: Illustration of detection principle; gold nanorods are functionalized with receptors (depicted in red), whereas the sides are blocked by tetra ethylene glycol (depicted in green). The binding of individual antibodies results in a red shift of the plasmon resonance. Right: Time trace of the normalized scattered intensity of a single gold nanorod. Stepwise changes in the signal indicate stochastic binding of single antibodies. The distribution of waiting times between events is used to determine the antibody concentration. Reproduced with permission from 23. Copyright 2015 American Chemical Society. (b) Left: Experimental design of a Whispering Gallery Mode (WGM) based sensing platform showing detection of single virus particles. Middle: The resonance is identified at a specific wavelength from a dip in the transmission spectrum acquired with a tunable laser. A resonance shift associated with molecular binding; $\Delta\lambda_r$, is indicated by the dashed arrow. Bottom panel: Binding of analyte is identified from a shift $\Delta\lambda_r$ of resonance wavelength. Reproduced with permission from 28. Copyright 2008 Proceedings of the National Academy of Sciences. (c) Left: Concept of interferometric scattering mass spectrometry (iSCAMS) and working principle of label-free DNA detection employing iSCAMS. Middle: Binding events cause changes to the reflectivity of the interface, visualized by a contrast-enhanced interferometric scattering microscope through the interference between scattered and reflected light. Right: Statistics of the image contrast provide a single-molecule readout of molecular mass. Adapted with permission from ref 33. Copyright 2020 Oxford University Press. Adapted with permission from 36. Copyright 2018 American Association for the Advancement of Science.

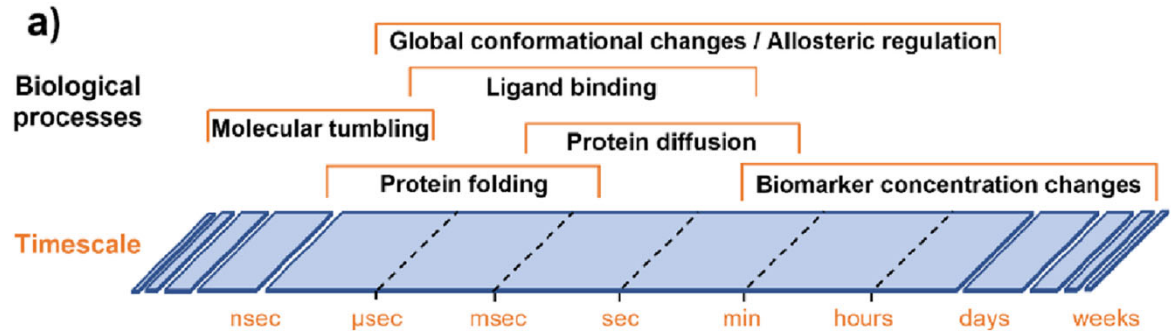


Figure 5. (a) Characteristic time scales for various biomolecular processes.

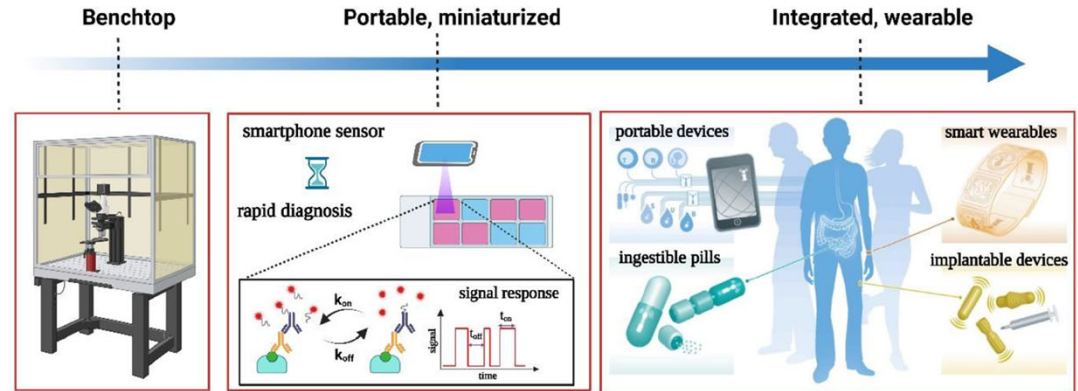


Figure 8. Timeline depicting the evolution of optical biosensors (left, benchtop detection ; middle, rapid, diagnostic field testing kits and portable smartphone based sensors; right, integrated smart biosensors for personalized health monitoring. Reprinted with permission from ref 102. Copyright 2016 Nature Publishing Group.

Optical Sensing of Single Cell Secretion

ABSTRACT: Measuring cell secretion events is crucial to understand the fundamental cell biology that underlies cell–cell communication, migration, proliferation, and differentiation. Although strategies targeting cell populations have provided significant information about live cell secretion, they yield ensemble profiles that obscure intrinsic cell-to-cell variations. Innovation in single-cell analysis has made breakthroughs allowing accurate sensing of a wide variety of secretions and their release dynamics with high spatiotemporal resolution. This perspective focuses on the power of single-cell protocols to revolutionize cell-secretion analysis by allowing real-time and real-space measurements on single live cell resolution. We begin by discussing recent progress on single-cell bioanalytical techniques, specifically optical sensing strategies such as fluorescence, surface plasmon resonance, and surface-enhanced Raman scattering-based strategies, capable of in situ real-time monitoring of single-cell released ions, metabolites, proteins, and vesicles. Single-cell sensing platforms which allow for high-throughput high-resolution analysis with enough accuracy are highlighted. Furthermore, we discuss remaining challenges that should be addressed to get a more comprehensive understanding of secretion biology. Finally, future opportunities and potential breakthroughs in secretome analysis that will arise as a result of further development of single-cell sensing approaches are discussed.

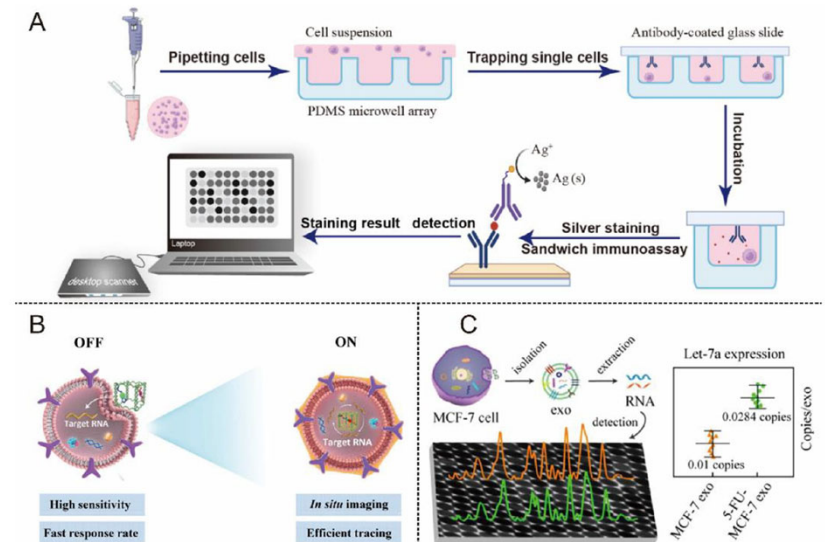
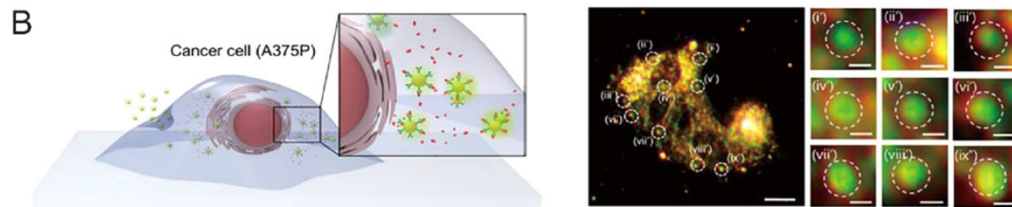
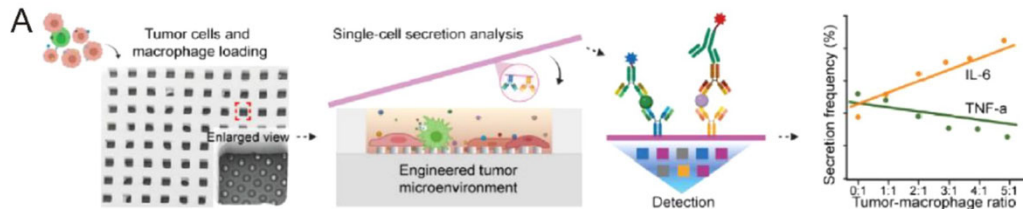
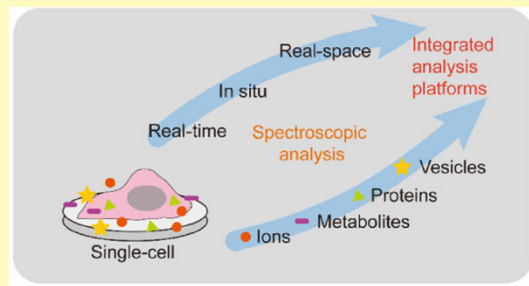


Figure 4. (A) Workflow illustration of trapping of single cells and using gold nanoparticle-enhanced silver staining to enable detection with the desktop scanner for the single-cell EV secretion assay. Reprinted with permission from ref 102. Copyright 2021 American Chemical Society. (B) In situ monitoring of exosomal miRNAs with double-accelerated DNA cascade amplifier nanocubes. Reprinted with permission from ref 106. Copyright 2022 American Chemical Society. (C) Schematic illustration of the SERS sensing exosomal microRNAs. Reprinted with permission from ref 111. Copyright 2021 American Chemical Society.

Figure 3. (A) Engineering and characterization of single-cell secretion analysis platform. **A fluorescent immunoassay-based single cell analysis platform** has been developed for investigating the differential modulation effect in cytokine secretions by the tumor microenvironment (B) Immunoplasmonic approach for transforming growth factor- β . The method used antibody-conjugated single gold nanoparticles as optical detection probes.

Patterning Wettability

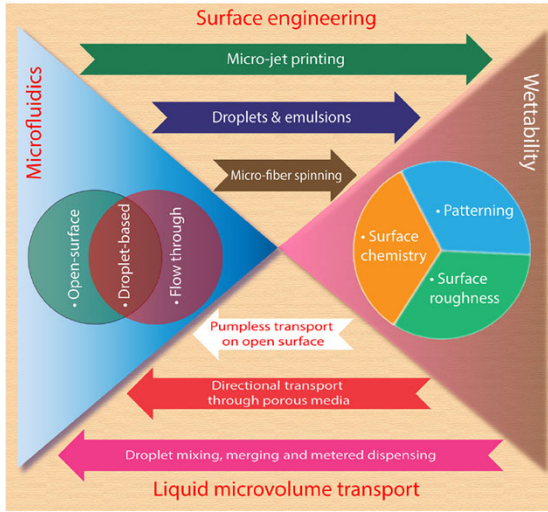
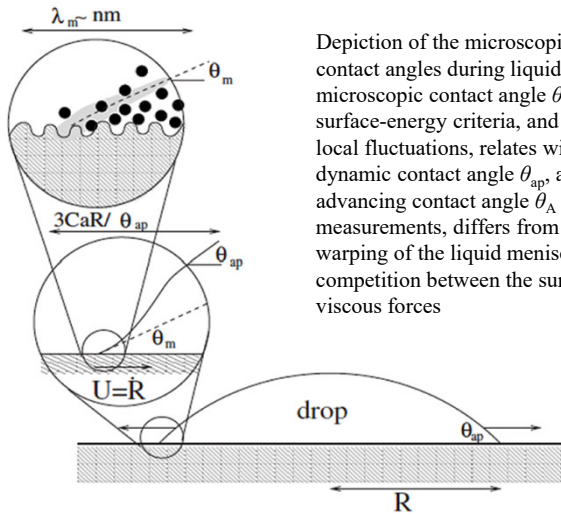
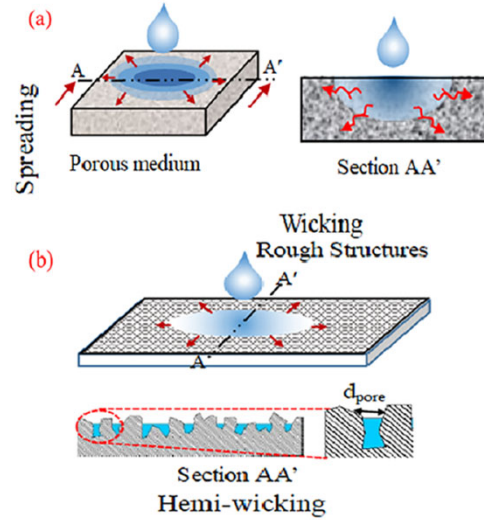
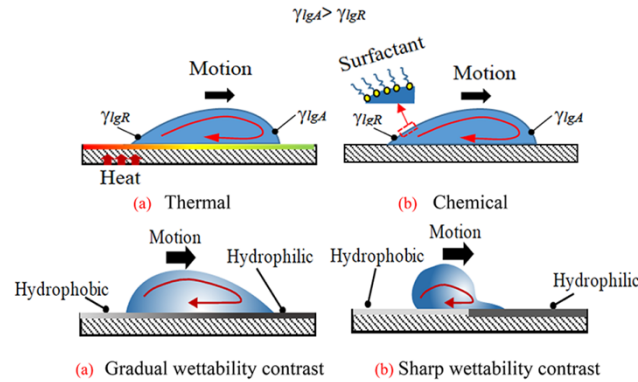


Figure 1. Mutual relationship between microfluidics and wettability. For attributes of microfluidic flows offering a number of enabling technologies for surface engineering. The lower quadrant elucidates different modes of liquid microvolume transport realized by leveraging wettability engineering.



Depiction of the microscopic and macroscopic contact angles during liquid spreading; the microscopic contact angle θ_m ensues from surface-energy criteria, and accounting for local fluctuations, relates with θ_{eq} ; the apparent dynamic contact angle θ_{ap} , also known as the advancing contact angle θ_A from macroscopic measurements, differs from θ_m because of the warping of the liquid meniscus from the competition between the surface tension and viscous forces

(i) Surface tension gradient in liquid
(ii) Surface tension gradient on substrate



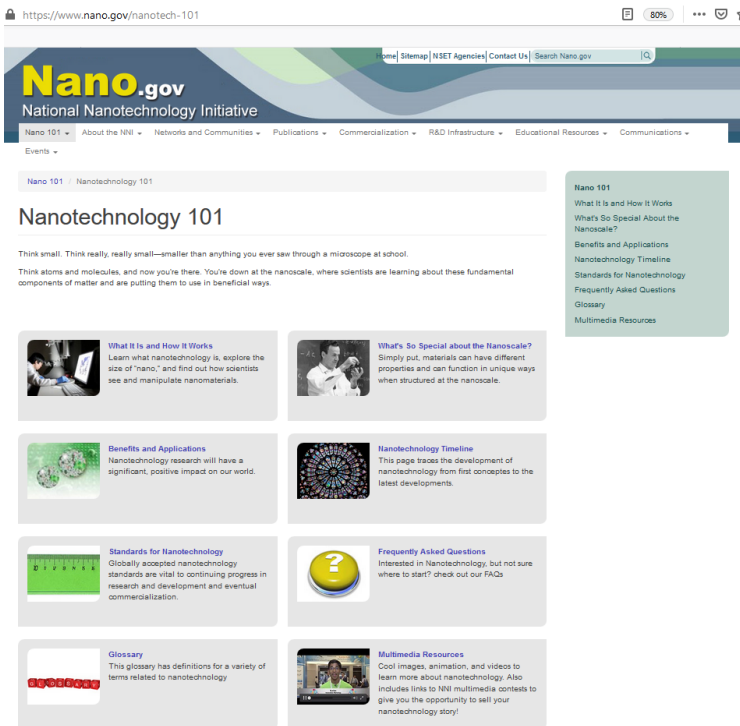
Liquid spreading and Laplace pressure basics: (i) Schematic showing spreading of a liquid droplet on a porous substrate (a, classical wicking) and a solid impermeable substrate with shallow micronano roughness structures (b, hemiwicking). For both cases, spreading distance varies with time as $x \sim t^{0.5}$.

Figure 5. Passive liquid-transport mechanisms driven by surface-energy differentials: (i) Thermal (a) and chemical (b) surface tension gradients in the liquid promote fluid actuation. In (a), a temperature gradient on the substrate changes the local surface tension at the advancing (right) and receding (left) edge of the liquid volume. (b) Surfactants can alter local surface tension chemically, hence mobilizing the droplet by the differential capillary force between the advancing (right) and receding (left) front. γ_{lgR} and γ_{lgA} denote the liquid surface tension at the receding and advancing front, respectively. (ii) Droplet actuation by patterning the wettability of the substrate. (a) Substrate with spatially gradual wettability changes. The droplet moves from the hydrophobic (left) to the hydrophilic region (right). (b) Droplet actuation by a sharp wettability contrast line on the underlying solid. The property of the substrate suddenly shifts from hydrophobic to hydrophilic at the wettability contrast line. Note the distorted shape of the droplet at the onset of transport.

Definitions of Nanotechnology

National Nanotechnology Initiative

A very good place to learn the basic of nanotechnology is the National Nanotechnology Initiative (NNI) (<https://www.nano.gov/>).



The screenshot shows the website <https://www.nano.gov/nanotech-101>. The main heading is "Nano.gov National Nanotechnology Initiative". Below the navigation bar, the "Nanotechnology 101" section is highlighted. The page content includes a sub-heading "Nanotechnology 101" and a brief introduction: "Think small. Think really, really small—smaller than anything you ever saw through a microscope at school. Think atoms and molecules, and now you're there. You're down at the nanoscale, where scientists are learning about these fundamental components of matter and are putting them to use in beneficial ways." The page features several interactive tiles with images and text:

- What It Is and How It Works:** Learn what nanotechnology is, explore the size of "nano," and find out how scientists see and manipulate nanomaterials.
- What's So Special about the Nanoscale?:** Simply put, materials can have different properties and can function in unique ways when structured at the nanoscale.
- Benefits and Applications:** Nanotechnology research will have a significant, positive impact on our world.
- Nanotechnology Timeline:** This page traces the development of nanotechnology from first concepts to the latest developments.
- Standards for Nanotechnology:** Globally accepted nanotechnology standards are vital to continuing progress in research and development and eventual commercialization.
- Frequently Asked Questions:** Interested in Nanotechnology, but not sure where to start? Check out our FAQs.
- Glossary:** This glossary has definitions for a variety of terms related to nanotechnology.
- Multimedia Resources:** Cool images, animation, and videos to learn more about nanotechnology. Also includes links to NNI multimedia contents to give you the opportunity to tell your nanotechnology story!

Learning from Nature and mimicking natural materials!

Nanomedicine: What are the Fundamental Concepts?

Nanotechnology has been considered as an **enabling technology**. If nanotechnology is such an enabling technology, however, why have nanoformulations been used only for targeted delivery to tumors? Why has none of the nanotechnology been used to treat other important diseases? Even for tumor targeting, no nanoformulations have been effective. The main problem is that nanoparticles have been simply assumed to have a targeting property. It was just an assumption based on in vitro cell culture studies.

NIH Nanomedicine website (<https://commonfund.nih.gov/nanomedicine/overview>) does not provide any scientific reasons or evidence **why nanomedicine will be better in treating various diseases**. The National Nanotechnology Initiative does not provide any scientific evidence either.

Under the section of "Fundamental concepts in nanoscience and nanotechnology", the National Nanotechnology Initiative says, "Although modern nanoscience and nanotechnology are quite new, nanoscale materials were used for centuries. **Alternate-sized gold and silver particles created colors in the stained glass windows of medieval churches hundreds of years ago.** The artists back then just didn't know that the process they used to create these beautiful works of art actually led to changes in the composition of the materials they were working with".

It is well known that Michael Faraday was fascinated by the ruby color of colloidal gold (<https://link.springer.com/content/pdf/10.1007/BF03215598.pdf>). The size of colloidal gold particles ranges from a few nanometers to micrometers. Does this mean that the current nanotechnology is simply a rehash of the hundreds-year old technology? Then, what does nanotechnology really mean? The National Nanotechnology Initiative further describes, "**Nanotechnology is not simply working at ever smaller dimensions; rather, working at the nanoscale enables scientists to utilize the unique physical, chemical, mechanical, and optical properties of materials that naturally occur at that scale**" (<https://www.nano.gov/nanotech-101/special>). It continues, "Nanoscale materials have far larger surface areas than similar masses of larger-scale materials. As surface area per mass of a material increases, a greater amount of the material can come into contact with surrounding materials, thus affecting reactivity". The larger surface area of nanoscale materials has a few advantages in drug delivery, but it still does not explain how nanotechnology, or nanomedicine, brings new properties that traditional drug delivery systems do not have, and thus improved treatment.

Definitions of Nanotechnology and Nanomedicine

The term “**nanotechnology**” was defined as “science, engineering, and technology conducted at the nanoscale, which is **about 1 to 100 nanometers**” (<https://www.nano.gov/nanotech-101/what/definition>).

The term “**nanomedicine**” refers to “highly specific medical intervention at the molecular scale for curing disease or repairing damaged tissues, such as bone, muscle, or nerve”. It is further explained that “**It is at this size scale - about 100 nanometers or less - that biological molecules and structures operate in living cells**” (<https://commonfund.nih.gov/nanomedicine/overview>).

These definitions sound magnificent and futuristic, but closer examination of the definitions to acquire better understanding makes it confusing. First, if the matter we are dealing with is larger than 100 nm, is it not qualified to be called nanotechnology? **What are the scientific criteria that set the boundary at 100 nm?** Would it make a sense, if the size is limited to 200 nm, 300 nm, or larger?

Second, the description of nanomedicine is so generic that the term “nanomedicine” can be easily named by others, e.g., “molecular medicine”. After all, **if medical interventions are made at the molecular scale, isn't it better to call it “molecular medicine”?** If engineering occurs at the molecular level, isn't it what we call chemistry, biochemistry, and molecular biology? The prefix “nano” has dominated the science throughout the world with no particular rationale; just like the prefix “i” dominated the market since the successful introduction of iPod. It is these arbitrary, generic definitions of nanotechnology and nanomedicine that set the stage of a decades-long stray from the otherwise more productive, useful, and practical path. Even nowadays, many scientists, engineers, and clinicians who are not familiar with the drug delivery field think that nanotechnology or nanomedicine, will solve their research problems regardless of the nature of the problems.

In drug delivery systems, there are not many systems that are truly less than 100 nm in size. The drug delivery systems exist to deliver a drug, and the system less than 100 nm does not have enough reservoir space for effective drug delivery. Most polymer micelles, which are one of the main representatives of nanomedicine, are much larger than 100 nm, especially after a drug is loaded. **The drug delivery systems are usually larger than 100 nm by necessity, but they are not really nanosystems according to the definition provided by the National Nanotechnology Initiative [14]. What nonsense! More correctly, what nano-nonsense!**

Park 2017, The drug delivery field at the inflection point- Time to fight its way out of the egg

For the drug delivery field **the definition of nanomedicine described by the FDA** may be more relevant. According to the FDA Guidance for Industry regarding nanotechnology products, nanomaterials are defined as **materials that have at least one dimension in the size range of approximately 1 nm to 100 nm** (<https://www.fda.gov/regulatory-information/search-fda-guidance-documents/considering-whether-fda-regulated-product-involves-application-nanotechnology>). This follows the definition by the National Nanotechnology Initiative. The FDA, however, chose to include a much broader meaning of nanomaterials by asking “**Whether a material or end product is engineered to exhibit properties or phenomena, including physical or chemical properties or biological effects, that are attributable to its dimension(s), even if these dimensions fall outside the nanoscale range, up to one micrometer (1,000 nm)**”. This definition is very forgiving in the size limitation, and indeed many products can fall into the definition of the nanotechnology product. This is why when drug products containing nanomaterials in the U.S. were analyzed, more than 350 products were shown to contain nanomaterials (<https://www.nature.com/articles/nnano.2017.67>). This number, however, is misleading, because the number is based on mostly traditional formulations, such as liposome, emulsion, and drug crystals which were introduced several decades ago.

Look at the Data, Nothing Else

To understand why and how we ended up where we are now, we need an “independent” examination. The term “independent” here means an impartial approach between “**confirmation bias**” and “**negativity bias**”. A mind with a confirmation bias seeks out data that support the preconceived idea, while a mind with a negativity bias does the same with the opposite goal.

Talking about the truth and criticizing something that most believe is difficult. Quite often, those who criticize the mainstream idea are labeled as pessimistic or politically motivated, as if science has to rely on the majority opinion or blind optimism. Accurate data interpretation has nothing to do with one's feeling. If the data point to a different direction from the expected, a new direction should be explored. This is of course assuming that the data are not fake. In his book “Only the Paranoid Survive”, Andy Grove pointed out that an industry going through a strategic inflection point follows a sequence of denial, anger, bargaining, depression, and ultimately, acceptance (Only the Paranoid Survive). Going through an unknown future requires an accurate grasp of the reality, identification of the source of the problems, and preparation for the future. Only those with an independent mindset can go through such due diligent work, because they are not biased and not influenced by internal and external factors.

Think, Think, and Think

Then, You Will Become Better than the Most.

Do Not Fall into the Nanotechnology Trap

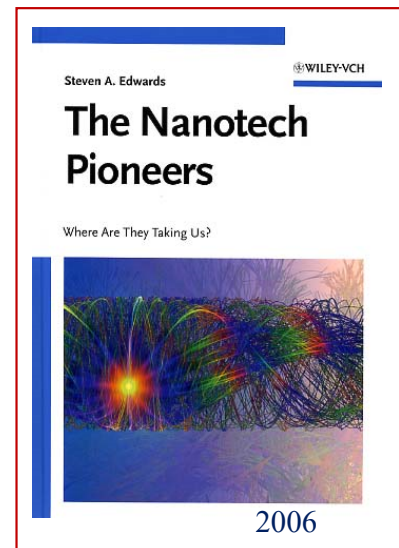
Table 2 The proliferation of "Nano" as a Prefix.

nanoage	nanocrystals	nanomagnetic	nanoscale
nanoarray	nanocube	nanomanipulator	nanoscience
nanoassembly	nanodevice	nanomaterial	nanoscope
nanobacteria	nanodivide	nanomedicine	nanosecond
nanobiologist	nanodomain	nanometer	nanoshell
nanobiomedicine	nanoelectromechanical	nanomicelle	nanostructured
nanobiotechnology	nanoelectronics	nanoparticle	nanostructures
nanobot	nanoencapsulation	nanoparticulate	nanoswarm
nanocapsule	nanofabrication	nanophase	nanosystems
nanocassette	nanofibers	nanoplatelates	nanotechnology
nanocatalyst	nanofilter	nanoporous	nanotool
nanocomponent	nanofluidics	nanopowder	nanotube
nanocomposite	nanolayer	nanoproduct	nanotweezers
nanconnections	nanoliter	nanoreactor	nanowire
nanocosm	nanolithography	nanoreplicator	nanoworks
nanocrystalline	nanomachine	nanorobotics	nanoworld

Table 2 is hardly an exhaustive list, particularly if you start including the names of companies – NanoInk, NanoSphere, Nano-Opto, Nanoproprietary, Nanoset, Nanosys, etc. – or the names of products – Nano-fur, NanoReader, NanoSolve, Nanobac.

Scientists are supposed to have a clear, open mind just following the data, and should not fall into the populism and the fashion. At the height of the nanofashion, many started adding the prefix 'nano' to almost all words in the dictionary.

Does anybody know what 'nanoage' means? Or 'nanoworld'? Isn't nanocomponent called atom or molecule?



When iPod was first introduced and became hugely popular, almost all product names in Walmart began with 'i', such as iFlower, iChair, etc.

Simply changing the name to more fancy names, like including 'i' or 'nano', does make things better.

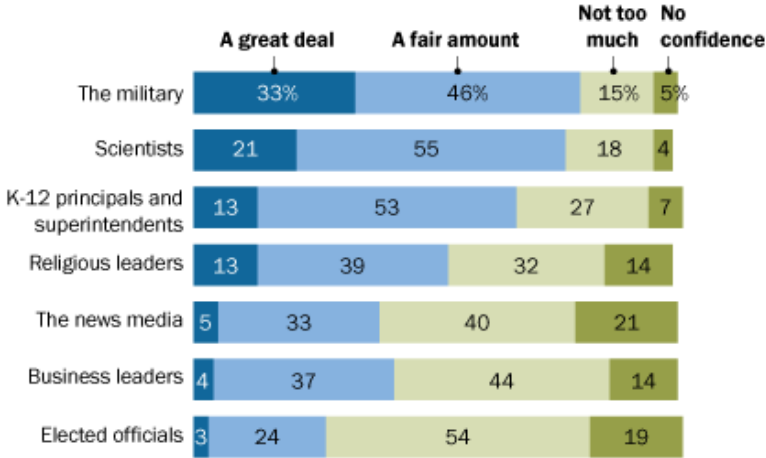
How about “*i*NanoPurdue”?

Trust Scientists? Earn the Trust

America and many countries around the world have systematically downplayed the importance of science for the special interest groups who increase their political power through dismissing science and promoting their agendas. Even then, the trust in scientists is as high as that in the military. It is not surprising that the trusts in business leaders and politicians are very low. Scientists need to work hard to tell the truth and improve the public's trust to close to 100%. Telling the truth based on accurate data is the best weapon scientists have.

Americans' trust in military, scientists relatively high; trust in media, business leaders, elected officials low

% of U.S. adults who say they have ___ of confidence in each of the following groups to act in the best interests of the public

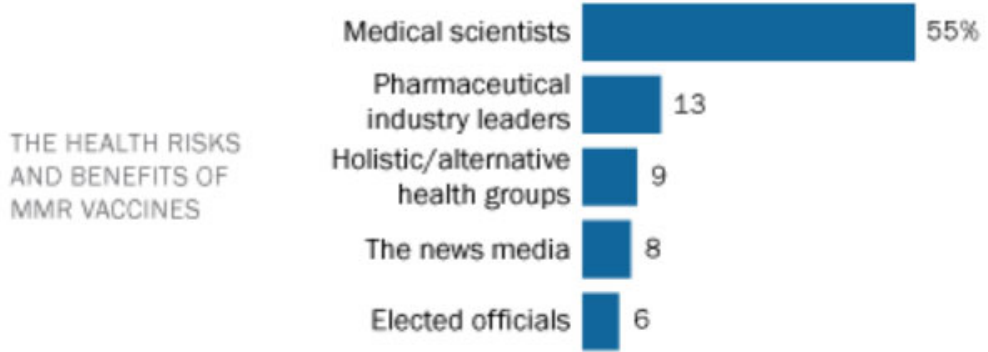


Note: Those who gave other responses or who did not give an answer are not shown. Source: Survey of U.S. adults conducted May 10–June 6, 2016.

PEW RESEARCH CENTER

Public trust of information from scientists is higher than for industry leaders, news media, elected officials

% of U.S. adults who say that they trust each of these groups a lot to give full and accurate information on these topics



<https://www.pewresearch.org/science/2017/12/08/mixed-messages-about-public-trust-in-science/>

Why We Must Rebuild Trust in Science

A scientific endeavor that is not trusted by the public cannot adequately contribute to society (February 9, 2021, BySudip Parikh)

Despite failures in our public health response to the pandemic, the biomedical research enterprise has **never worked more quickly than during its quest to understand and address COVID-19**. While basic researchers work around-the-clock to answer fundamental questions about the coronavirus' structure, transmission, and impacts, clinicians and physician scientists are testing therapeutics and vaccines.

One element is absolutely critical to the success of our mission to improve the human condition: trust. It's a foundational element of any relationship, but for the mutual benefit of the scientific enterprise and the people who support it, trust is essential. Simply put, a scientific endeavor that is not trusted by the public cannot adequately contribute to society and will be diminished as a result. The COVID-19 pandemic presents us with just such an example. Late last year two of the vaccine candidates in clinical trials demonstrated **safety and effectiveness in preventing infection of the virus that causes COVID-19**. Although this was a remarkable accomplishment on its own, **manufacturing and delivering these vaccines to the world's population** will be an enormous challenge. To further complicate this situation, a public that is generally trusting of scientists and health professionals is **receiving vastly different information, guidance, and recommendations based on its news consumption, political leaders, and geography**. A September 2020 Pew Research Center survey found that Americans were evenly divided as to whether they would get a vaccine to prevent COVID-19 if one were available now.

Importantly, it is not enough to say the public should trust scientists because we know better or because we know more. **Trust must be earned**. Unfortunately, science and scientists have not consistently earned and nurtured this trust. In some respects, this is the result of the advancement of the scientific enterprise. **Science in the 21st century is much more removed from daily life** because of the necessity of speaking with precision by using technical terms and jargon.



The COVID-19 pandemic will not be the last time that science will be essential to society's triumph over existential threats.

The practice of science is messy. Hypotheses are put forward and tested. Understanding evolves and comes in fits and starts. The trial and error in research methodology and the repetitive testing in laboratories are often hidden behind the end products of scientific research - a new treatment, a new piece of technology, a new or revised piece of public health guidance - without the public seeing the puts and takes that are required along the way. When that process is then seen in real time, as we're all experiencing during the COVID-19 pandemic, **the public has little context for updates in public health guidance, such as the change to recommending wearing face masks to limit and prevent infection.**

More disturbingly, science has sometimes lost the trust of the public through researchers' own painful missteps and blatant violations of that trust. **Science, engineering, and medicine are not immune to the discrimination, subjugation, and silencing of marginalized people and voices.** We have too often been unwitting perpetrators of the status quo, and the reasons are deeply ingrained in the systems that govern our society.

At the same time, **increased political polarization and an outspoken faction of Americans who distrust experts**, including scientists who develop evidence-based findings that may challenge closely held opinions, have also widened the gap between Americans' trust in science and scientists. **Science is not just for the few. It is for everyone and can be used by anyone.**

Why are Americans so slow to get booster shots?

The New York Times (February 7, 2022, By David Leonhardt)

The enemy of the good

The United States has a vaccination problem. And it is not just about the relatively large share of Americans who have refused to get a shot. The U.S. also trails many other countries in the share of vaccinated people who have received a booster shot. In Canada, Australia and much of Europe, the recent administering of Covid-19 booster shots has been rapid. In the U.S., it has been much slower. The booster shortfall is one reason the U.S. has suffered more deaths over the past two months than many other countries

Two explanations

What explains the American booster shortfall? I think there are two main answers, both related to problems with the American health system.

First, **medical care in the U.S. is notoriously fragmented**. There is neither a centralized record system, as in Taiwan, nor a universal insurance system, as in Canada and Scandinavia, to remind people to get another shot. Many Americans also do not have a regular contact point for their health care.

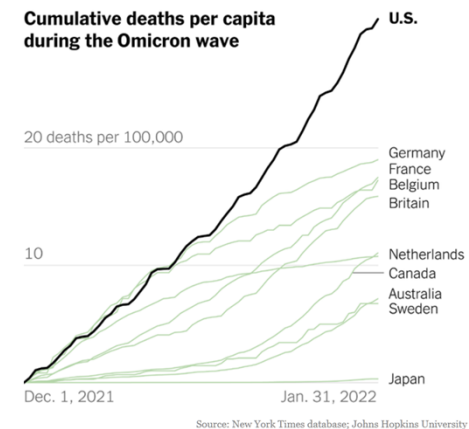
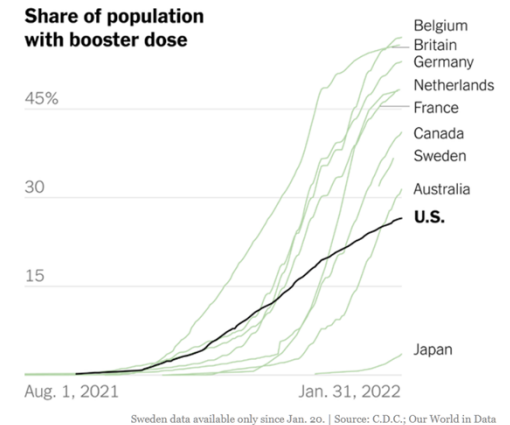
The second problem is one that has also bedeviled other aspects of U.S. Covid response: **Government health officials, as well as some experts, struggle to communicate effectively with the hundreds of millions of us who are not experts. They speak in the language of academia, without recognizing how it confuses people. Rather than clearly explaining the big picture, they emphasize small amounts of uncertainty that are important to scientific research but can be counterproductive during a global emergency.** They are cautious to the point of hampering public health. **As an analogy, imagine if a group of engineers surrounded firefighters outside a burning building and started questioning whether they were using the most powerful hoses on the market.** The questions might be reasonable in another setting — and pointless if not damaging during a blaze. A version of this happened early in the pandemic, when experts, including the C.D.C. and the World Health Organization, discouraged widespread mask wearing. They based that stance partly on the absence of research specifically showing that masks reduced the spread of Covid. But obviously there had not been much research on a brand-new virus. Multiple sources of scientific information did suggest that masks would probably reduce Covid's spread, much as they reduced the spread of other viruses. Health officials cast aside this evidence.

Tests, vaccines, boosters

Similar problems have occurred since then, especially in the U.S.: (1) slow to give formal approval to the Covid vaccines, (2) slow to approve rapid tests, and (3) slow to tell people who had received the Johnson & Johnson vaccine to get a follow-up shot. In the U.S., some officials and experts continue to raise questions about whether the evidence is strong enough to encourage boosters for younger adults. Two top F.D.A. officials quit partly over the Biden administration's recommendation of universal boosters. The skeptics say they want to wait for more evidence.

I don't fully understand why statistical precision seems to be a particularly American obsession.

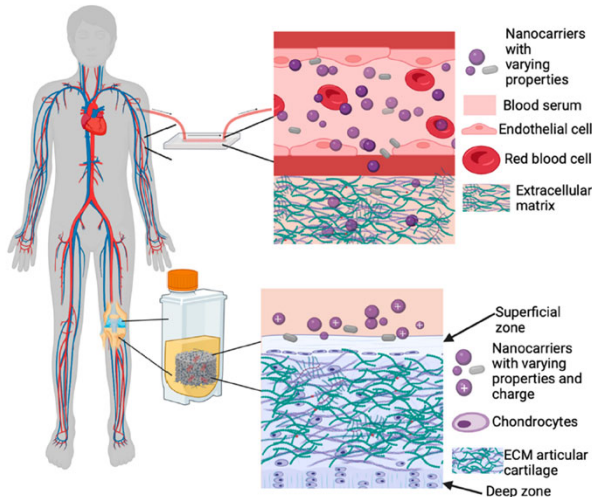
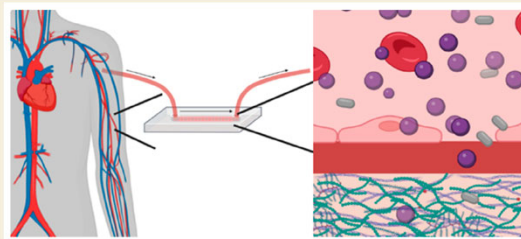
The New York Times



Precision Healthcare through Nanomedicine

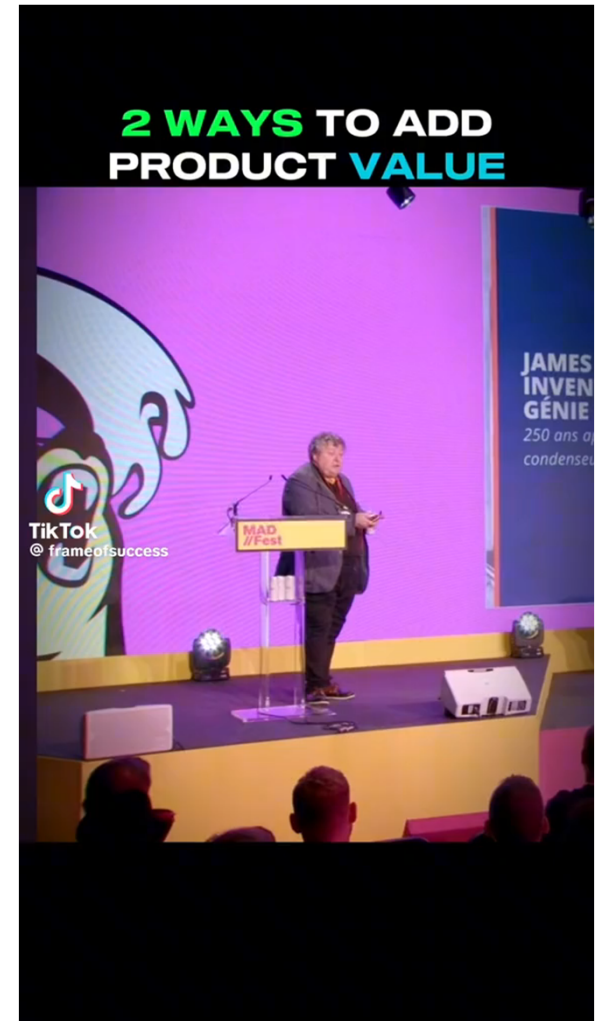
ABSTRACT: The ability to customize medical choices according to an individual's genetic makeup and biomarker patterns marks a significant advancement toward overall improved healthcare for both individuals and society at large. By transitioning from the conventional one-size-fits-all approach to tailored treatments that can account for predispositions of different patient populations, nanomedicines can be customized to target the specific molecular underpinnings of a patient's disease, thus mitigating the risk of collateral damage. However, for these systems to reach their full potential, our understanding of how nano-based therapeutics behave within the intricate human body is necessary. Effective drug administration to the targeted organ or pathological niche is dictated by properties such as nanocarrier (NC) size, shape, and targeting abilities, where understanding how NCs change their properties when they encounter biomolecules and phenomena such as shear stress in flow remains a major challenge. This Review specifically focuses on vessel-on-a-chip technology that can provide increased understanding of NC behavior in blood and summarizes the specialized environment of the joint to showcase advanced tissue models as approaches to address translational challenges. Compared to conventional cell studies or animal models, these advanced models can integrate patient material for full customization. Combining such models with nanomedicine can contribute to making personalized medicine achievable.

KEYWORDS: Personalized Medicine, Precision Medicine, Nanomedicine, Drug Delivery, Model Systems, Vessel-on-a-Chip, Bioreactors, Joint Drug Delivery, Cartilage Transport



Details?
How?
Simple explanation?

Figure 1. Models of NC delivery to target organs and cells.



Self-Assembly

Life began with self-assembly.

Natural (Bottom-up) and Synthetic Systems (Top-down)

Natural Systems

Efficacy and Simplicity
at the Molecular Level
(Bottom-up)



Survival



Biological Needs

In nature, bottom-up approaches are achieved through self-assembly of molecules. No matter how small or large a structure is, it must have a building block. If building blocks are assembled by themselves, it can be called self-assembly. But if the building blocks have to be assembled by external forces, it cannot be called self-assembly.

Synthetic Systems

Efficiency and Selectivity
at the Macro Level
(Top-down)



Miniaturization



Clinical Efficacy



Bottoms-up Approach: Building brick by brick the Great Wall (>20,000 km long) or the Great Pyramid (230 m x 230 m x 147 m).

Natural (Bottom-up) and Synthetic Systems (Top-down)

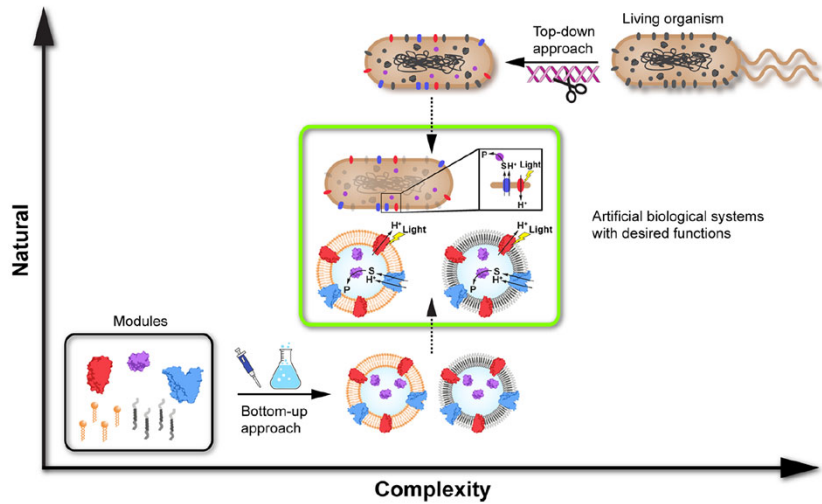


Figure 1. Schematic depiction of the core concepts in synthetic biology. Artificial biological systems with desired functions (green box) can be created by using two main methodologies. The **top-down approach** focuses on the modification of living organisms, usually through introduction of artificial elements by **genetic engineering**, whereas the **bottom-up approach** involves the combination of isolated biological and synthetic modules. The latter can include, but are not limited to, soluble (purple) or membrane proteins (red and blue) as functional modules and lipids or block copolymers (brown and gray) as scaffolds for vesicular systems. The example used to illustrate this concept is a simple reaction system including a light-driven proton pump (red), a proton-driven symporter (blue) that imports a specific substrate (S) using the established proton gradient, and an enzyme capable of converting the imported substrate into a desired product (P). These modules are either genetically introduced into a simplified host organism (top-down) or assembled from isolated components into functionalized liposome or polymersome systems (bottom-up).

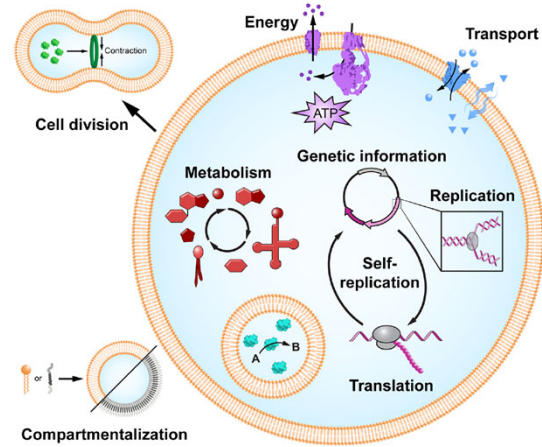


Figure 2. Bottom-up engineering of an ideal artificial cell. Isolated biological and chemical components are assembled in a modular fashion to create an artificial cell with desired traits and functions. The artificial cell is based on at least one main compartment and optional subcompartments that can harbor individual processes, each enclosed by lipid (brown) or polymer (gray) membranes. A compartmentalized process is exemplified by a reaction catalyzed by encapsulated enzymes (cyan). Energizing modules provide energy for energy-dependent modules; transport modules supply nutrients and building blocks and dispose of waste products, and a minimal metabolism (red) ensures replenishment of essential components. Replication, transcription, and translation (enzymes in gray) of genetic information enables continuous and autonomous function, while the ability to divide (component of a minimal divisome illustrated in green) ensures sustainable growth and proliferation.

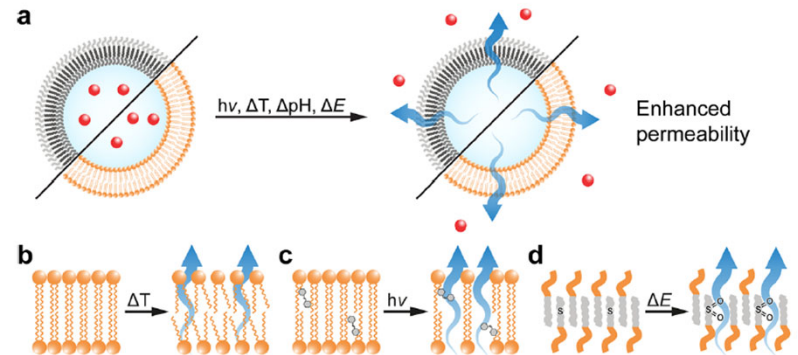


Figure 5. Controlled release of cargo from **stimuli-responsive vesicles**. (a) The release of molecules (red) stored within stimuli-responsive polymersomes (gray) or liposomes (brown) can be triggered by irradiation ($h\nu$), heat (ΔT), or by change in pH or redox potential (ΔE). (b) Heat-sensitive lipid bilayers exhibit a gel-to-liquid phase transition at a particular temperature, rendering the membrane permeable to hydrophilic molecules. (c) Photosensitive molecules such as azobenzene derivatives of lipids undergo photoisomerization upon UV irradiation, which enforces significant changes in conformation and polarity, leading to permeabilization of the membrane. (d) Redox-sensitive polymer membranes can change from hydrophobic to hydrophilic under oxidative conditions, resulting in increased permeability.

Building Blocks

TABLE 1. **Synthetic and Biological Building Blocks** Used in Supramolecular Self-Assembly for Obtaining Diverse Complex Structures and Their Potential Biomedical Applications.

Building-Blocks		Supramolecular Assemblies	Applications
Synthetic	Polymers	Linear (e.g. block-co-polymers) AB ABA ABC Branched (e.g. dendrimers) Dendrons	Micelles Vesicles Tubes Nanoreactors; artificial organelles; nanocarriers drug delivery ^{21, 22}
	Surfactants	Anionic Cationic Neutral Micelles Vesicles	Nanoparticles Nanofibers Nanocarriers for drug and gene delivery ²³⁻²⁵
	Others	Porphyrin Rotaxane Graphene Nanotubes Toroids Carbon nanotubes	Nanomedicine; drug delivery; hydrogels ^{8, 28, 29}
	Viruses	CPMV λ phage hHPeV Aligned phage film Fibrils Particles	Biomaterials; cell culture substrates ³⁰⁻³³
Biological	Nucleic acids	RNA DNA DNA origami	Therapeutics (vehicles for drug delivery); diagnostics (biosensing) ^{11, 34, 35}
	Lipids	Fatty acid Phospholipid Cholesterol Lipid bilayer Vesicles Films	Nanoreactors; artificial organelles; controlled drug delivery ^{19, 36-37}
	Saccharides	Amylose (helical) Cyclodextrin (cyclic)	Drug delivery; biosensors ^{38, 39}
	Peptides	VSYK EACO Random coil β-sheet α-helix Helix protein	Hydrogel biomaterials; drug delivery; tissue engineering; 3D cell culture ⁴⁰⁻⁴⁸

Mendes 2013, Self-assembly in nature,

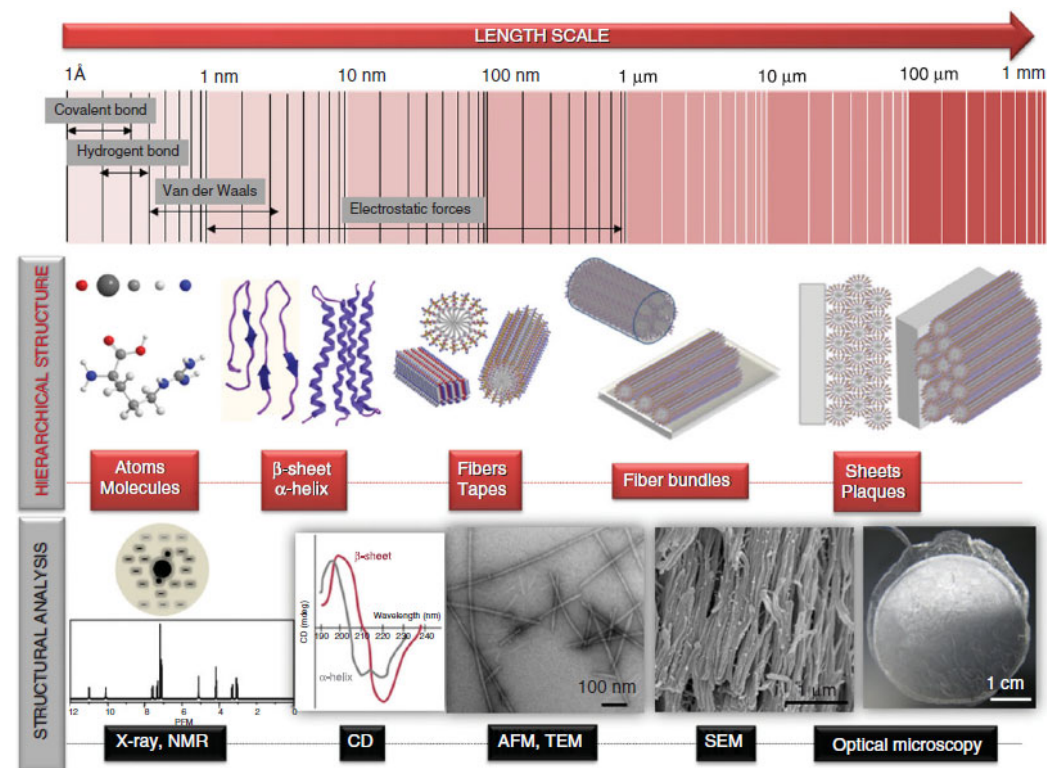
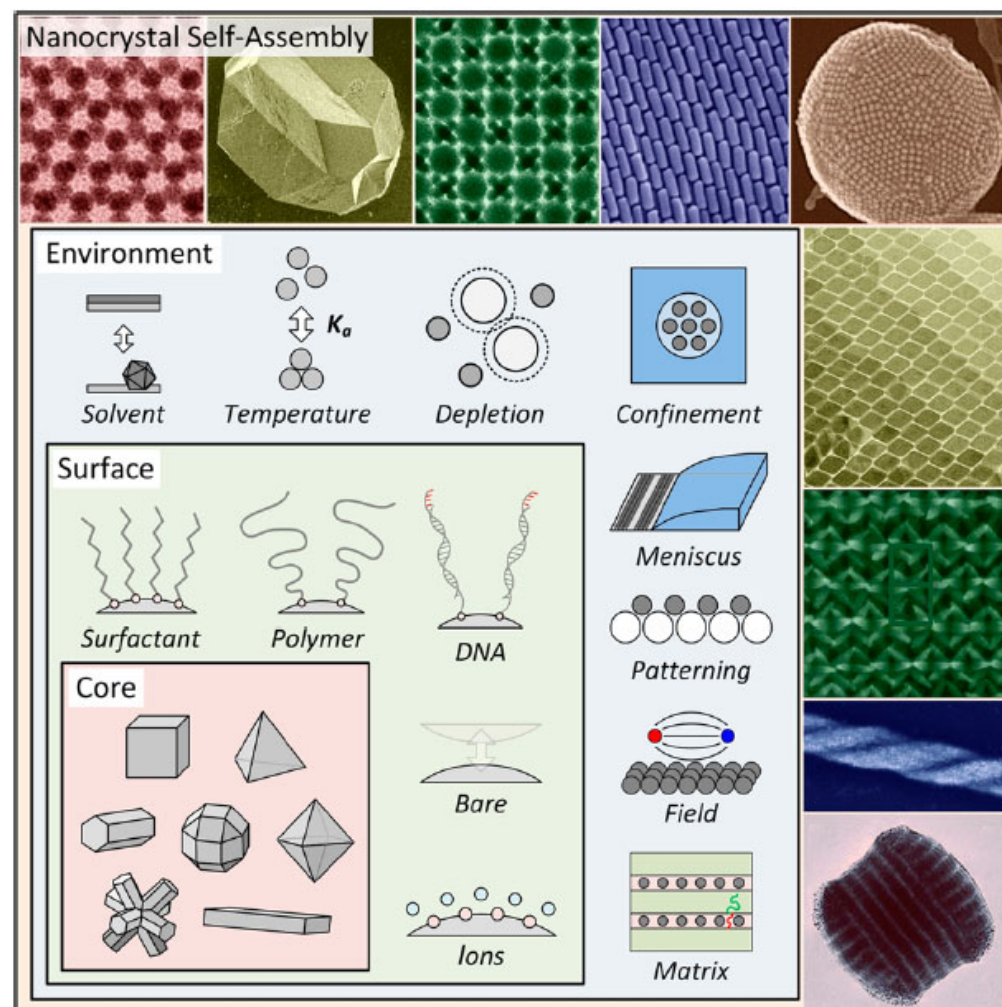


FIGURE 4. Length scales of the forces involved in self-assembly (first panel) and the hierarchical complex structures generated by peptide self-assembly (second panel). Spectroscopy and microscopy techniques used for structural characterization of peptide molecules and assemblies from the nanometer to centimeter length scales (third panel). NMR, nuclear magnetic resonance; X-ray, X-ray diffraction; CD, circular dichroism; AFM, atomic force microscopy; TEM, transmission electron microscopy; SEM, scanning electron microscopy.

Self-Assembly

Self-assembly is the process by which individual components arrange themselves into an ordered structure. While sufficiently broad to include crystallization of atomic solids, the term is generally reserved for building blocks not linked together via covalent bonds but ordered through weak forces (e.g., van der Waals, hydrogen bonding) or hard-particle (e.g., excluded volume) interactions. Following this classification, examples of self-assembled structures include DNA, proteins, lipid vesicles, block copolymer melts, opals, and nanocrystal superlattices. Self-assembly can also make use of external forces such as electric/magnetic fields or fluid flows, but the term does not extend to serial manipulation of building blocks (e.g., dragging individual particles into position).

Figure 2. Nanocrystal self-assembly is a process that involves control over several length scales. The nanocrystal core (typically 1–100 nm across) is surrounded by a layer of surface ligands (with length typically between 1 nm and up to tens of nanometers). The assembly environment can be used to control interparticle interactions and impart geometric constraints with characteristic length scale exceeding nanocrystal size. **The resulting superstructures are typically produced with domain size falling between 1 μm and several millimeters.** Details about the nanocrystal composition, assembly conditions, and references for the systems shown in this figure are given in Table 1.



Self-Assembly

10.3 PRINCIPLES OF SELF-ASSEMBLY

Self-assembly is **the reversible and cooperative assembly of predefined parts into an ordered structure**, which assembles with no external influences after the initial trigger. Currently, self-assembly has been broken down into two categories: static and dynamic. **Static self-assembly** refers to systems at equilibrium which do not dissipate energy. The formation of the nanostructure may require energy, but the structure is stable once it has been formed. **Dynamic self-assembly** refers to the formation or patterning of structures when the system does, in fact, dissipate energy.

Self-assembly in materials relies on the fact that **the fluctuations in the orientation and position** of the molecules or particles due to random movements have energies in the order of **thermal energy**. Thermal energy has a significant impact on materials on the nanoscale as non-covalent bonds are often broken and reformed in a new manner. **Due to these non-covalent interactions between molecules**, structure changes can be obtained by changes in the conditions provided for the molecules. For instance, temperature and pH changes help to initiate the transition of a structure to another.

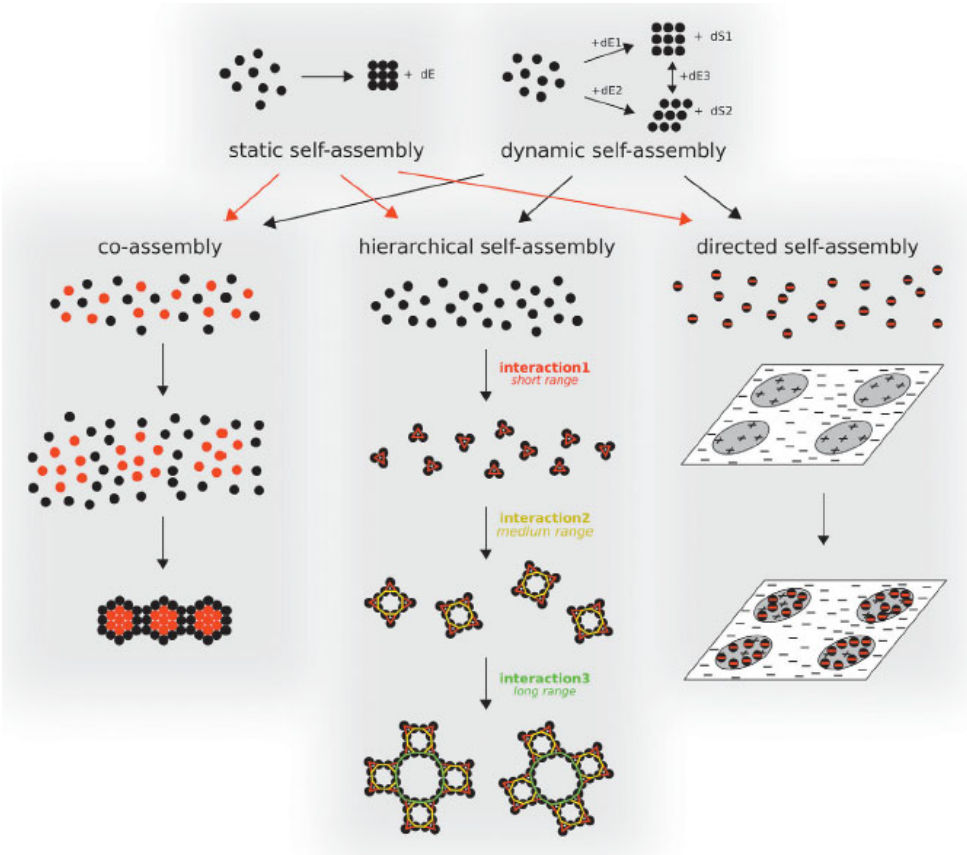


Fig. 1. Graphical rendition of static and dynamic self-assembly and how they relate to co-assembly, hierarchical assembly and directed assembly.

Self-Assembly

10.3.1 NON-COVALENT INTERACTIONS

In order for self-assembly to occur, the non-covalent forces between the molecules need to be **broken and reformed**. In doing so, the molecules are not changed chemically, but are **structured in a different orientation**. The weak intermolecular interactions that govern molecular ordering in materials include hydrogen bonds, ionic interactions, dipolar interactions, van der Waals forces, and hydrophobic interactions.

Hydrogen bonding is especially important in biological systems. Protein structures in water are held together by hydrogen bonds (Kelsall et al., 2005). **Hydrogen bonds** are weaker than covalent bonds (about 20 kJ/mol compared to about 500 kJ/mol for hydrogen bonds and covalent bonds, respectively) (Kelsall et al., 2005). As a result, structures can self-assemble without chemical reactions needing to occur, and the bonds are strong enough to hold the structures together once they have been formed.

Dipolar interactions follow the same principles as hydrogen bonding, except they are not limited to just hydrogen atoms. Dipolar interactions refer to the direct interactions between two magnetic dipoles. The dipoles are a result of the difference in electronegativity within molecules creating partial positive and negative charges within the molecule.

The van der Waals forces are the sum of the attractive or repulsive forces between molecules—other than those due to covalent bonds. The forces include those between a permanent dipole and a corresponding dipole, as well as the London dispersion forces.

The hydrophobic effect arises when a nonpolar solute is inserted into water. The hydrophobic effect is attributed to the ordering of water molecules around a hydrophobic molecule. The ordering leads to a reduction in entropy (Kelsall et al., 2005). **The entropy loss can be offset when association of hydrophobic molecules into micelles occurs, as this results in an increase in entropy.**

Self-Assembly

10.3.2 INTERMOLECULAR PACKING

At higher concentrations, the packing of block copolymer or amphiphilic molecules in solution leads to the formation of **lyotropic liquid crystal phases** (Kelsall et al., 2005). These crystal phases include cubic-packed spherical micelles, hexagonal-packed cylindrical micelles, lamellae, and bicontinuous cubic phases. The phase that forms is dependent on the curvature of the surfactant–water interface. To understand the lyotropic phase behavior, there exist two approaches. The first approach computes the free energy associated with curved interfaces; the curvature is analyzed using differential geometry, while not incorporating details of the organization of the molecules. The second approach uses a molecular packing parameter to describe the interfacial curvature.

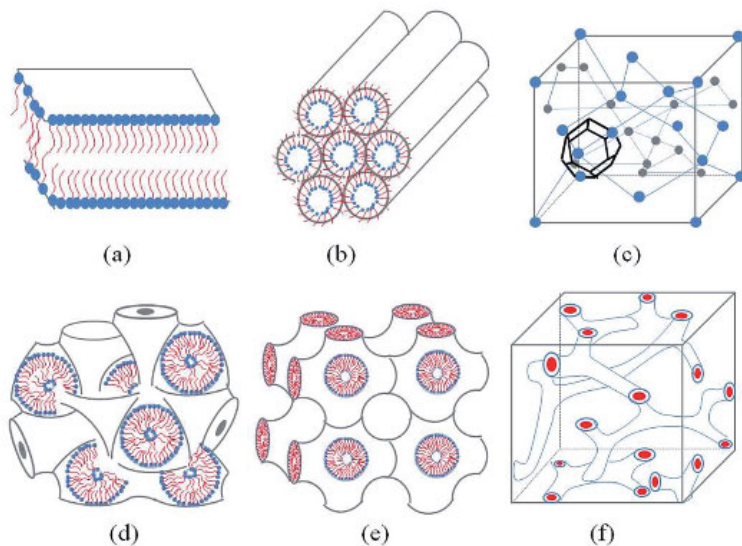


Fig. 1. Schematic representation of the lyotropic liquid crystalline phases commonly found in neutral lipid/water systems. (a) Lamellar phase (b) reverse hexagonal phase (c) reversed micellar cubic of Fd3m (d) reversed bicontinuous cubic (Im3m) (e) reversed bicontinuous cubic (Pn3m) (f) reversed bicontinuous cubic (Ia3).

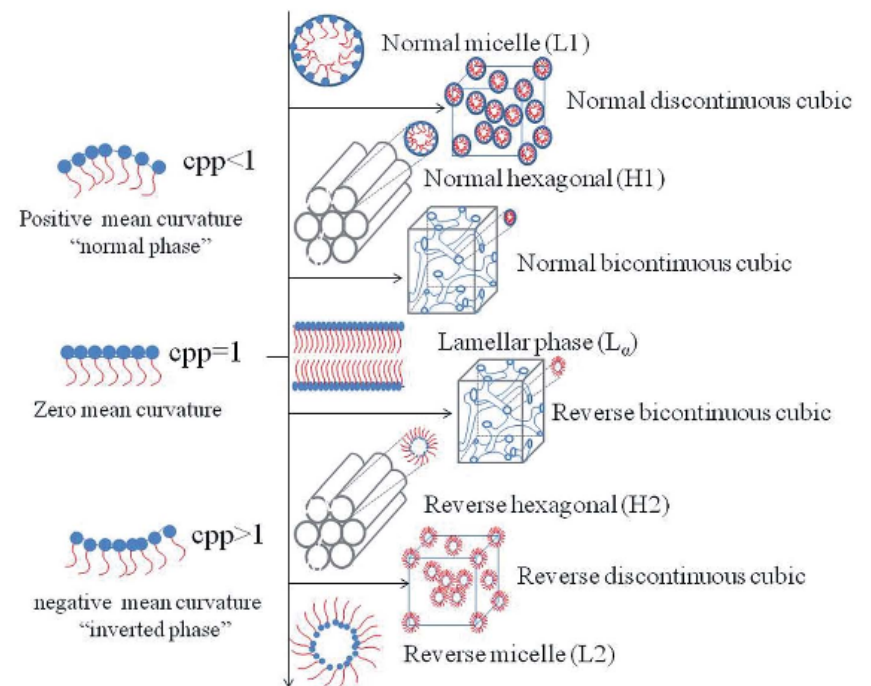


Fig. 2. Schematic representations of common structures and their corresponding CPP. bicontinuous cubic (Ia3).

Dahman 2017, Self-assembling nanostructures, Nanotechnology and Functional Materials for Engineers, pp. 207-228.

Huang 2018, Factors affecting the structure of lyotropic liquid crystals and the correlation between structure and drug diffusion, RSC Adv., 2018, 8, 6978-6987.

Self-Assembly to Generate Complex Structure

Only some selected classes of chemical compounds are capable to lead to useful self-assembled structures. Amphiphiles, simultaneously possessing polar and apolar moieties within their molecular architecture, can give a wide scenario of possible intermolecular interactions: polar–polar, polar–apolar, apolar–apolar interactions, eventual directional H-bonds, steric hindrance and so on. This peculiarity efficiently triggers the possibility of originating complex behavior, i.e., the formation of interacting structures at hierarchical length-scales characterized by emerging and specific properties and functions. However, if one places in a becher the molecules constituting a living cell, he does not observe the formation of a living cell even after vigorous and prolonged stirring and/or heating. This consideration suggests that the building up of complex structures is not only an affair of molecular structure, system composition and self-assembling processes but additional subtle features can contribute to the overall process.

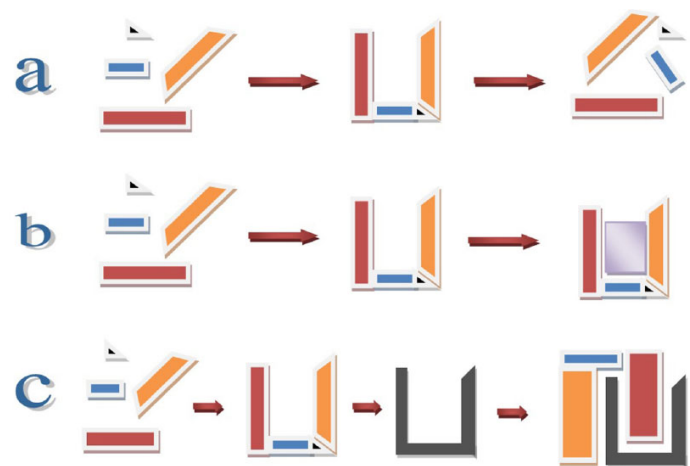


Fig. 3. Different mechanisms for complexity generation. (a) the building blocks are assembled through soft interactions. The structure formation is reversible and usually temperature-dependent. The assemblies show emerging properties with respect to those possessed by their constituents. (b) the building blocks are assembled in such way to template or to drive the formation of successive structures. See for example nanoparticle synthesis through the use of microemulsions. (c) the building blocks are assembled through strong interactions. Such structures are less sensitive to temperature changes and may be needed for the preparation of building blocks for the formation of complex structures of successive level of complexity.

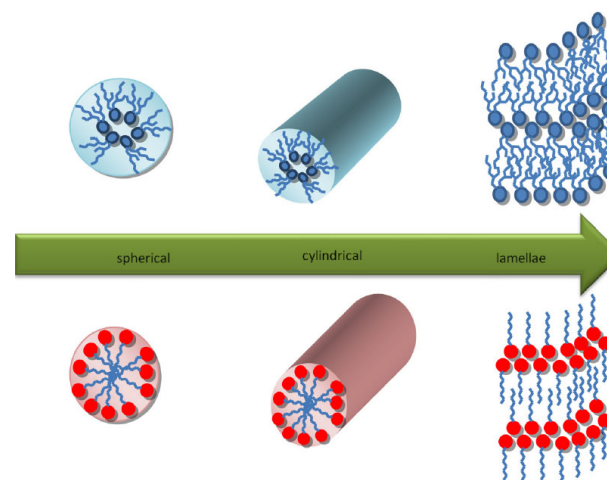
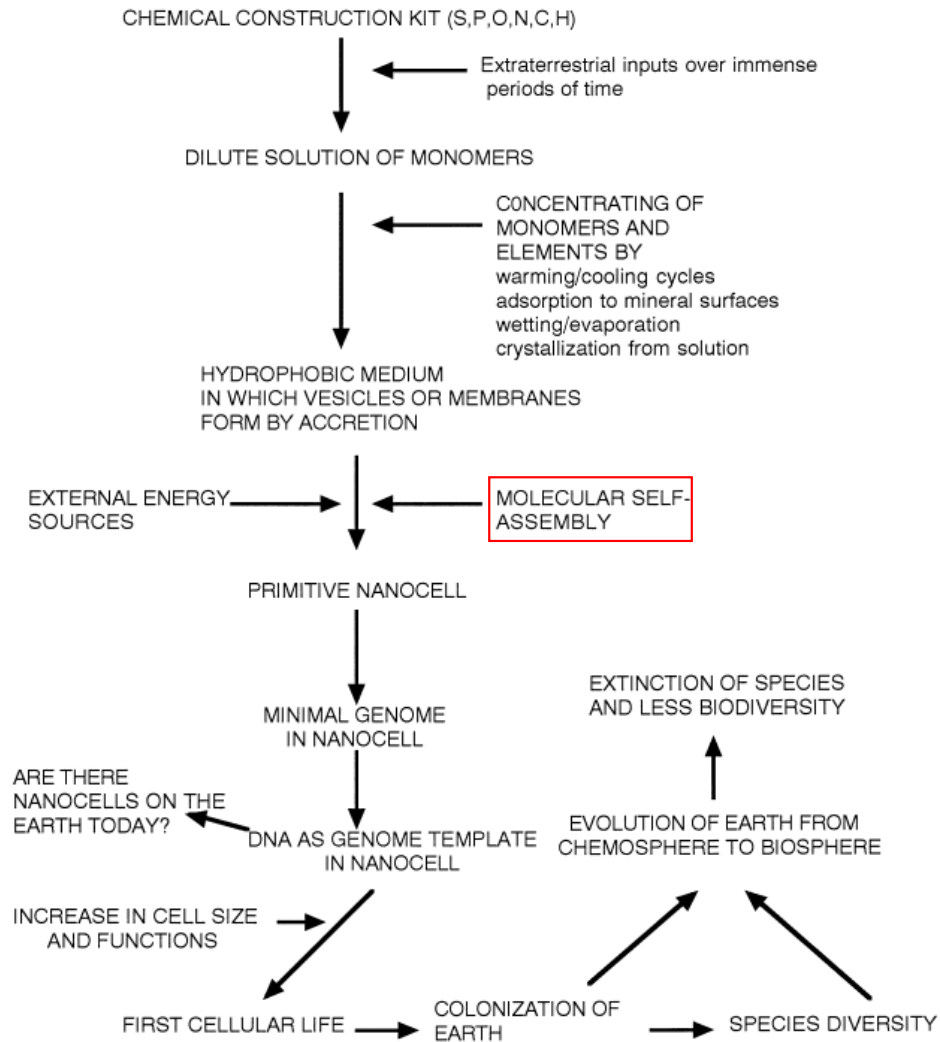


Fig. 4. The aggregation of amphiphiles can give supra-structures with various dimensionalities: 0D (micelles) 1D (cylinders or cylindrical micelles), 2D (lamellae). The structures can be reversed (upper panel) or direct (lower panel) depending on the polarity of the solvent. In apolar solvent reversed structures are formed, in polar solvent direct structures are the stable ones.

Calandra 2015, How self-assembly of amphiphilic molecules can generate complexity in the nanoscale.

Colloids and Surfaces A: Physicochemical and Engineering Aspects, Volume 484, 5 November 2015, Pages 164-183.

Self-assembly of Life

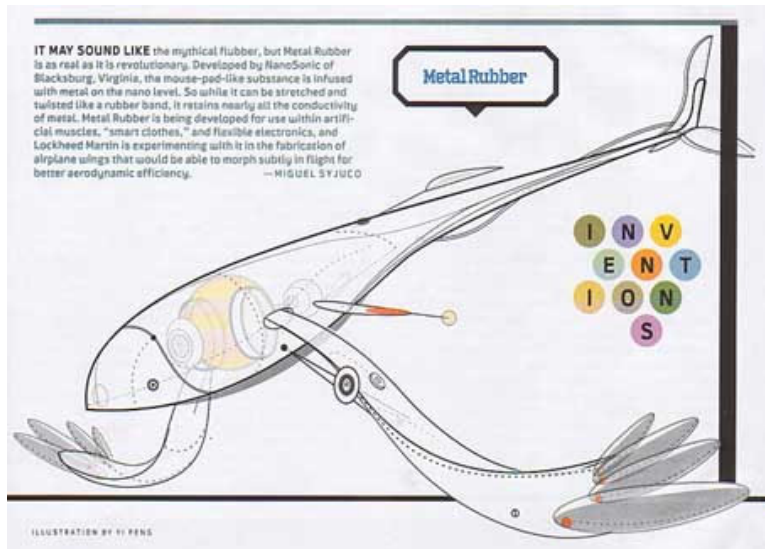


Trevors 2001, From self-assembly of life to present-day bacteria, FEMS Microbiology Reviews 25 (2001) 573-582.

The self-assembly events that led to the first minimal cell and genome capable of growth and division are highly debated. Fig. 1 is a proposed sequence of major events that may have occurred initially at a molecular level and then progressed to a nanocell level and finally to the bacterial cell dimensions (μm) that we know today. In this review we will examine **the major self-assembly events for cells** as outlined in Fig. 1. We will also discuss the possibility that nanobacteria, which are small spherical and ovoid structures discovered in rocks and minerals, may be the fossil evidence of the earliest life forms on Earth and outer space. Fig. 1 also indicates a role for extraterrestrial inputs which may have included living spores.

Fig. 1. Proposed sequence of major events in the origin of a cell capable of growth, division and diversification.

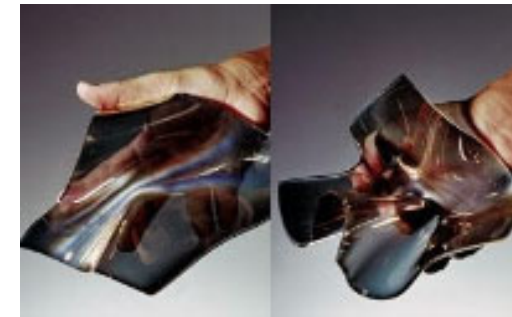
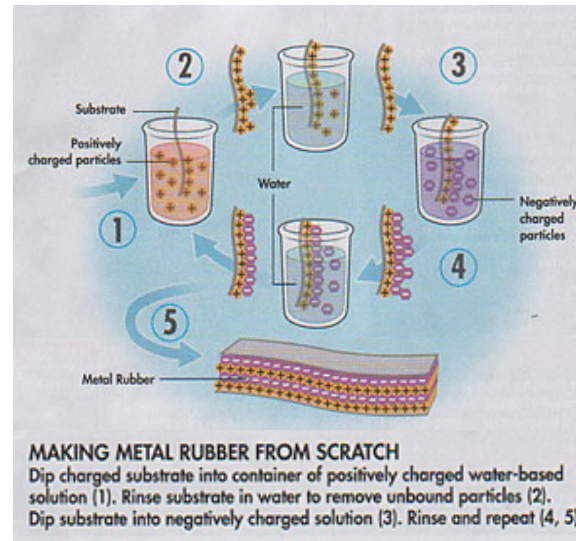
Metal Rubber



NanoSonic's Metal Rubber™ is a highly electrically conductive and highly flexible elastomer. It can be mechanically strained to greater than 1000 percent of its original dimensions while remaining electrically conductive. As Metal Rubber can carry data and electrical power and is environmentally rugged, it opens up a new world of applications requiring robust, flexible and stretchable electrical conductors in the aerospace/defense, electronics and bioengineering markets.

<http://www.nanosonic.com/80/4/metalrubber.html>

<http://videos.howstuffworks.com/sciencentral/2938-metal-rubber-video.htm>



Popular Science. August 2004. p. 36.

“Today in class you mentioned "metal rubber" briefly and the graphic showed the process of dipping a polymer sheet into solutions of positive and negative ions to build up layers on the polymer. This got me thinking, can you build epitaxial layers on top of malleable polymers? and more so, can you do this by **atomic layer deposition**? I assume nastier deposition methods (like plasma assisted vapor deposition) would most likely destroy or heavily alter the polymer base, but the idea of vapor deposition of say hexagonal boron nitride would be neat though I'm not sure how useful. Just something my mind latched on to during lecture.”

Layer-by-layer (LBL) process takes a long time for molecule by molecule. Atom by atom will take even longer, but automation can be easily done.

Two-dimensional (2D) Materials

The atomiewise chemical approaches and reactions suitable for 2D structures.

These approaches work as a “lancet” which can add, remove, and replace the desired atoms in 2D materials at will, with the rest of the atoms well preserved (Figure 1). In this way, the physical and chemical properties can be finely tuned, and various new properties can emerge. The rise in precision chemistry for 2D materials will enable a boom in relevant fields in materials science, physics, and engineering.

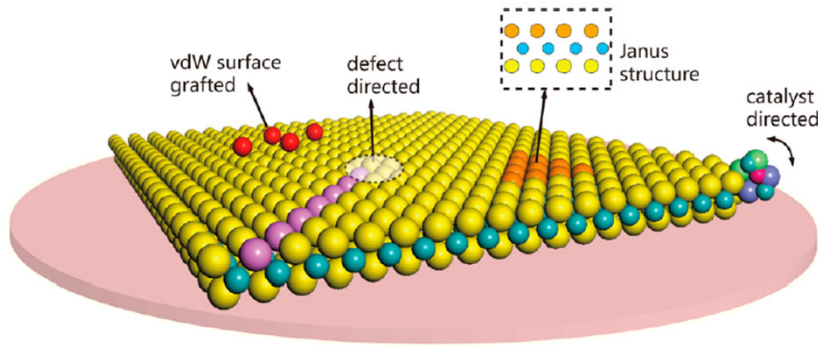


Figure 1. Scheme of some 2D structures enabled by precision chemistry.

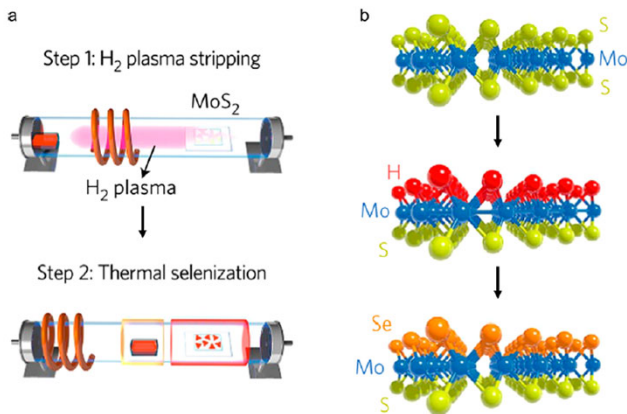


Figure 2. (a) Two-step plasma-assisted chemical vapor deposition method. (b) 3D atomic structure illustration of the MoS₂ monolayer, Janus H-Mo-S monolayer, and Janus Se-Mo-S monolayer.

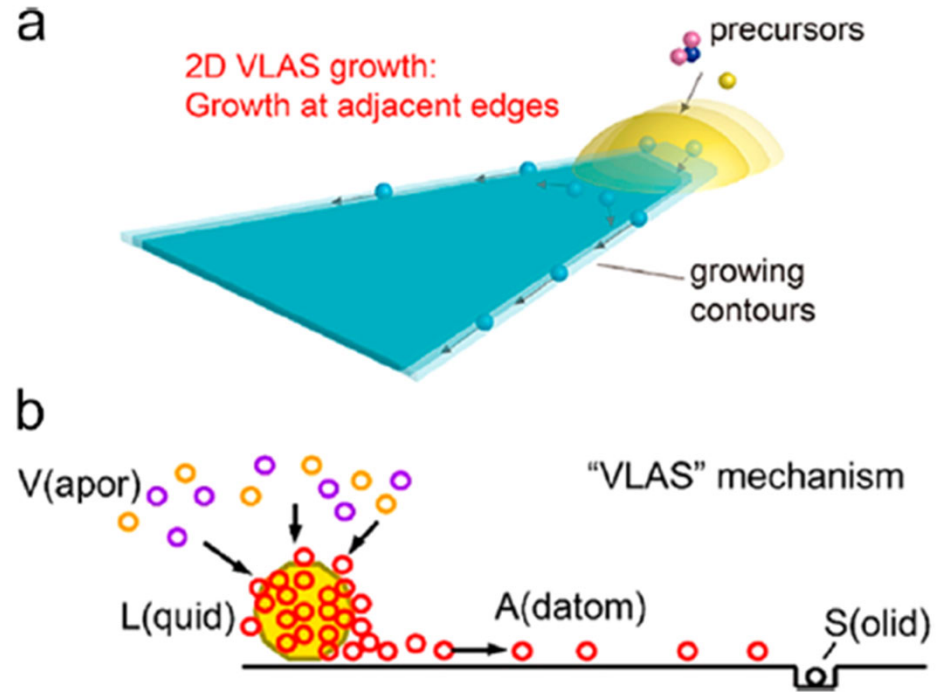


Figure 4. (a) Schematic illustration of the KCl-catalyzed growth of the 2D MoS₂ nanosheet. (b) Schematic illustration of the vapor-liquid-atom-solid (VLAS) mechanism. An adatom is an atom that lies on a crystal surface.

Self-Assembly of Virus

Viruses infect cells in all kingdoms of life and, from a physicochemical perspective, can be regarded as **molecular machines** that have successfully evolved to spread between related organisms. They hijack their host cell's machineries in a highly efficient and minimalistic manner, in order to ensure their propagation. The molecular mechanisms behind the viral life cycle are not only complex, these processes also **require a remarkably low number of essential viral components to be successful**.

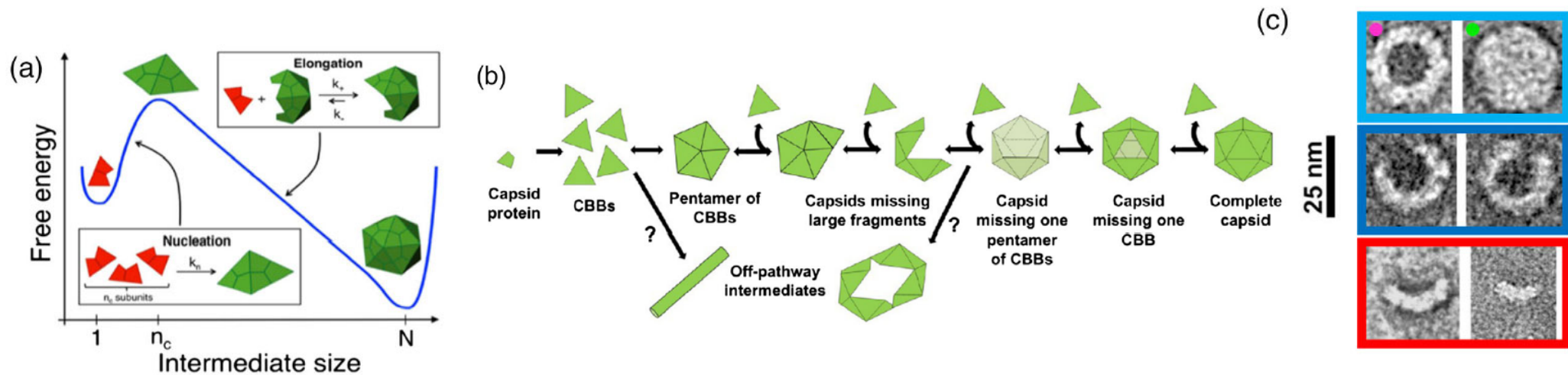


FIGURE 1 Assembly of empty particles through the nucleation, growth, and completion pathway. (a) Schematic representation of the free energy profile of the nucleation-and-growth/elongation pathway: first, nuclei are formed; then, the reaction proceeds downhill until the complete closure of the capsid. (Reprinted with permission from Michaels, Bellaiche, Hagan, and Knowles (2017)). (b) Self-assembly model proposed for MVM empty capsids based on the sequential addition of trimeric subunits, or CBBs (capsid building blocks). (Reprinted with permission from Medrano et al. (2016)). (c) MVM particles imaged by TEM (left): light blue, Types I + II particles (complete capsids); green, Type I (complete capsids in basal state); magenta, Type II (complete rearranged capsids); blue, Type IIIA (large incomplete capsids); red, Type IIIB (smaller incomplete capsids). Progression of the total number of particles during disassembly (left graph) and assembly (right graph) over time. (Reprinted with permission from Medrano et al. (2016)).

Self-Assembly of Virus

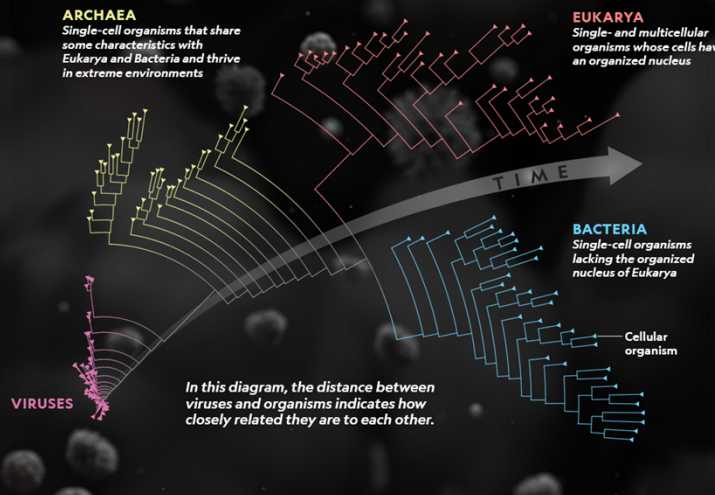


BY JASON TREAT, MESA SCHUMACHER, AND EVE CONANT
ILLUSTRATIONS BY MARKOS KAY
PUBLISHED JANUARY 14, 2021

Cells are considered the foundation of life, but viruses—with all their genetic diversity—may share in that role. Our planet's earliest viruses and cells likely evolved in an intertwined and often symbiotic relationship of predator and prey. Evidence even suggests that viruses may have started out as cells but lost their autonomy as they evolved to thrive as parasites on other cells. This dependent relationship began a long history of coevolution. Viruses living in cells cause their hosts to adapt, and those changes then cause viruses to adapt in a never ending cycle of one-upmanship.

A MORE INCLUSIVE TREE OF LIFE?

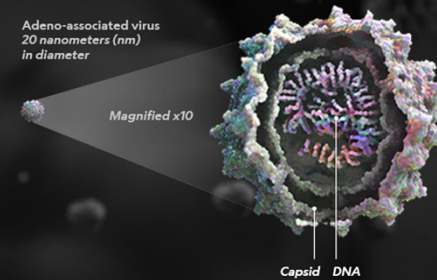
Billions of years ago life on Earth diverged into three branches: Archaea, Bacteria, and Eukarya. But recent research suggests viruses should be considered a fourth branch. This diagram, based on comparing the shapes of proteins in viruses and cellular organisms, shows that viruses share many primitive characteristics with early cellular ancestors—and likely evolved alongside them.



FROM SMALL AND SIMPLE TO LARGE AND COMPLEX

Viruses are shown here at 10,000 to 20,000 times actual size, depending on screen size.

Adeno-associated virus
20 nanometers (nm)
in diameter

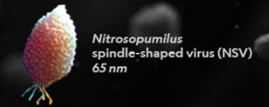


A USEFUL TOOL

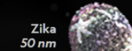
Scientists are now able to insert DNA into the genome of many rudimentary viruses, then use them to deliver this material to specific cells. This promising research may lead to safer methods of gene therapy.

Marine viruses

These tiny viruses infect ammonia-oxidizing Archaea, oceanic microorganisms that play a major role in carbon and nitrogen cycling. Regular infection of Archaea by these viruses may help regulate these cycles, impacting entire ecosystems.



Zika
50 nm



About 55 million Zika viruses could fit on the period at the end of this sentence.

West Nile
50 nm



Mosquito-borne viruses

Medium-size viruses like West Nile and dengue are transmitted to humans via saliva in a mosquito's bite and travel throughout the body in the bloodstream.

Dengue
50 nm

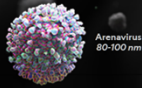


Jason Treat, Mesa Schumacher, & Eve Conant
Illustrations By Markos Kay
Published January 14, 2021,
National Geographic

Self-Assembly of Virus

DRIVERS OF EVOLUTION

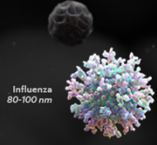
Rodent-borne arenaviruses typically pass through a cell's membrane by using receptors that import iron into cells. In response to the viruses, these receptors have been continually modified, an example of how viruses shape the evolution of life.



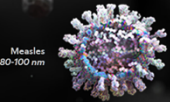
Arenavirus
80-100 nm

VIRAL INSTRUCTORS

Vaccination is like a training exercise for the immune system. Exposure to a weakened virus, dead virus, or a component of a virus teaches the body to recognize and attack that specific invader. If the virus is encountered, the immune system will be able to respond faster. Measles and influenza are viruses successfully controlled with vaccines.



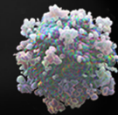
Influenza
80-100 nm



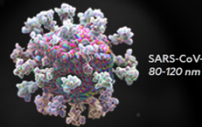
Measles
80-100 nm

VIRAL EDITORS

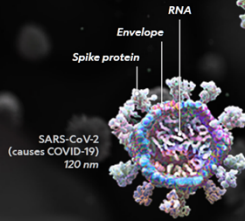
Viruses enter a cell and hijack its machinery to replicate, but retroviruses such as HIV do it by inserting their genes into the cell's DNA. If they do it in germ cells, the DNA can end up as part of the host's genome. There are thousands of fragments of ancient retroviruses in the human genome. Scientists found that a crucial membrane in the mammalian placenta—which makes internal pregnancy possible—evolved with the help of ancient retroviral genes.



Human
Immunodeficiency
virus (HIV)
80-100 nm



SARS-CoV-1
80-120 nm

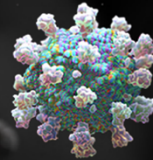


SARS-CoV-2
(causes COVID-19)
120 nm

Envelope
Spike protein
RNA

Coronaviruses

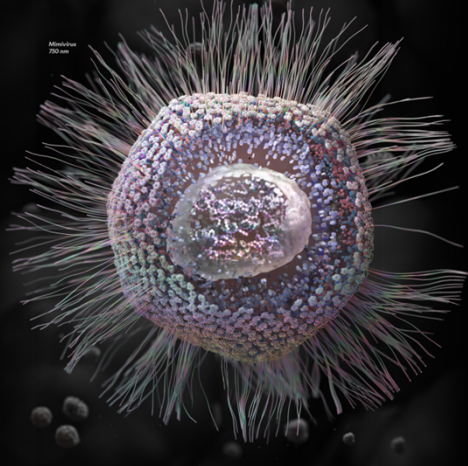
There are seven coronaviruses known to infect humans; one has led to the current pandemic. Named for their spiky proteins—"corona" is Latin for crown—that help them attack cells, they spread through respiratory droplets and aerosols.



MERS-CoV
120-135 nm

BIG CLUES TO EARLY ORIGINS

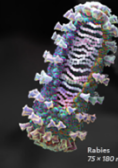
The reduction hypothesis supposes that viruses downsized in favor of using their host's machinery to reproduce. New support for the idea arrived in the form of the giant viruses of the Mimiviridae family. They set up "virus factories" in host cells that may resemble some of the earliest virus-cell interactions.



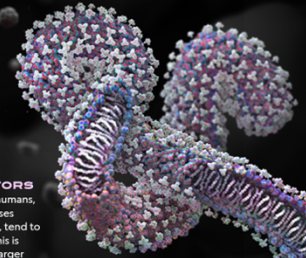
Mimivirus
200 nm

BIG CLUES TO EARLY ORIGINS

The reduction hypothesis supposes that viruses downsized in favor of using their host's machinery to reproduce. New support for the idea arrived in the form of the giant viruses of the Mimiviridae family. They set up "virus factories" in host cells that may resemble some of the earliest virus-cell interactions.



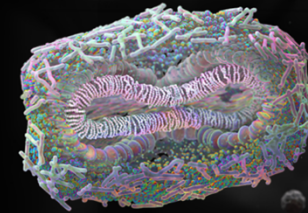
Rabies
75 x 180 nm



Ebola virus
970 x 80 nm

DEADLY ADAPTORS

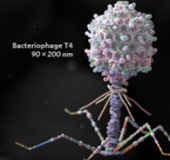
Large viruses that infect humans, such as variola (which causes smallpox) and Ebola virus, tend to have a high death rate. This is probably because many larger viruses carry viral proteins, in addition to their genes, that overwhelm and shut down the host's defenses.



Variola
(causes smallpox)
325 x 260 nm

Bacteriophages

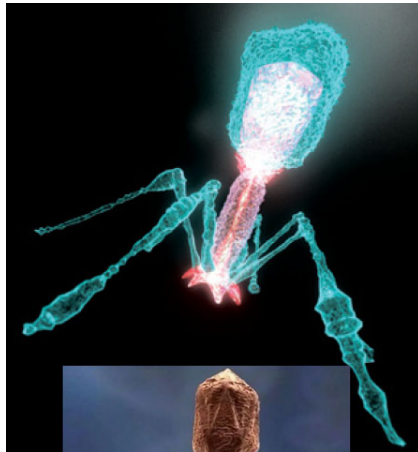
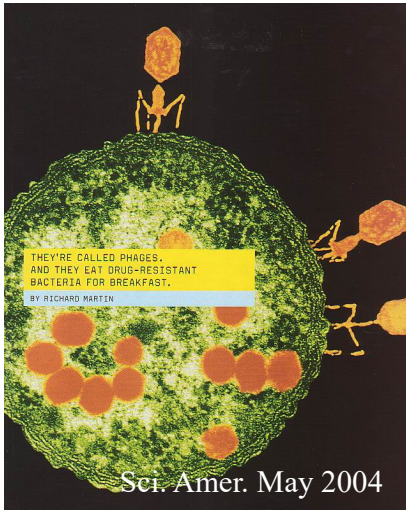
As viruses get larger, they also get more sophisticated. Bacteriophages are viruses that target bacteria; this one (at right) infects E. coli. Bacteriophages have complex heads that carry DNA and intricate tail structures that identify and bind to host cells, then inject viral genetic material through specialized tubes.



Bacteriophage T4
90 x 200 nm

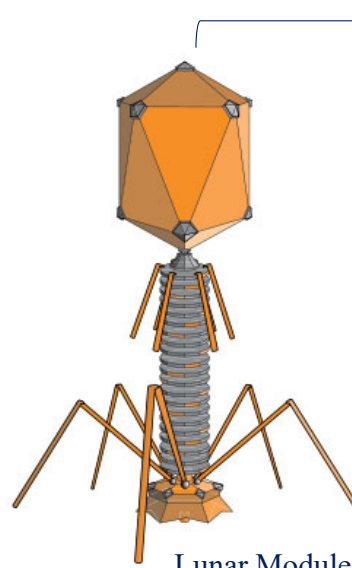
The Ultimate Nanofabrication: Synthetic Bacteriophage

The ultimate nanofabrication will be the technology that can fabricate synthetic bacteriophage-type machines that can deliver a high drug load into only the targeted cells and, if necessary, reproduce itself in the cell to continuously supply the drug, e.g., insulin. The nanofabrication that scientists are talking about now is basically Lego assembly by babies. Probably 100 years from now, scientists can engineer such an artificial machine, and you will be at the forefront of these efforts. Dream Big!

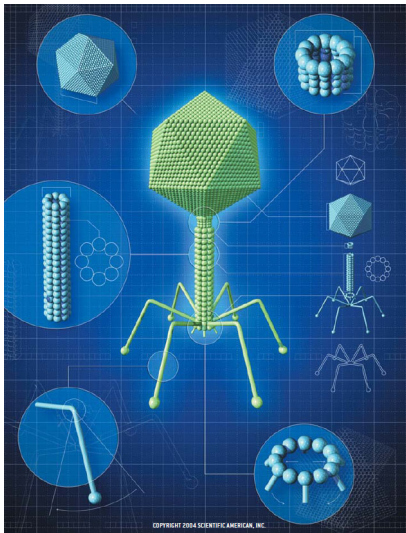


<https://tigerscroll.com/rare-pictures-that-will-show-you-the-unseen-side-of-things-long/22/>

See the similarity in the structures? Engineers can copy what the nature provides, as the nature has learned the good-enough form through millions of years of evolution.



Lunar Module Eagle



Artificial Viral Vectors

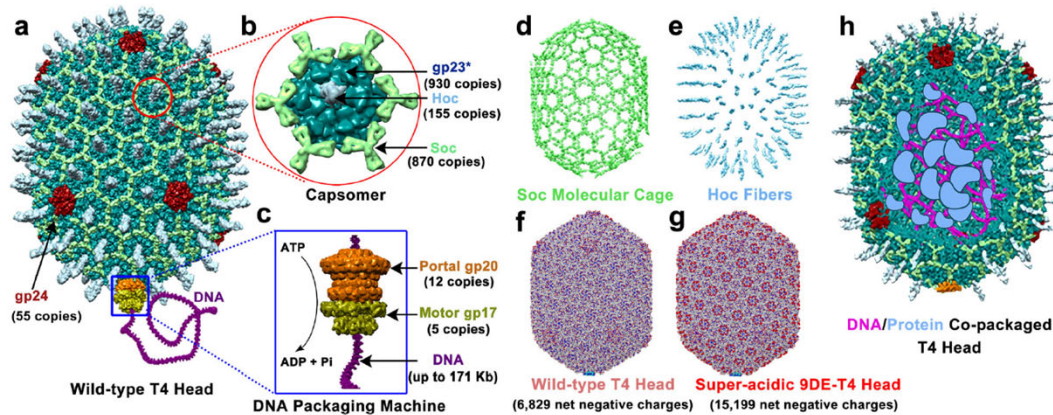


Fig. 1 | Structural components for assembly of bacteriophage T4-AVVs.

a Structural model of phage T4 head (capsid)⁴⁴. Pentameric gp24 vertices are shown in red. **b** Enlarged capsomer shows the hexameric arrangement of major capsid protein gp23 (dark green), Soc trimers (light green), and Hoc fiber (cyan)⁴⁴. **c** Enlarged DNA packaging machine structural model comprised of gp20 portal dodecamer (PDB 3JA7) (brown) and pentameric gp17 DNA packaging motor (PDB 3CPE) (yellow)^{24,44}. **d** Eight hundred and seventy Soc molecules assembled at the quasi-three-fold axes form a molecular cage around T4 capsid²¹ (PDB 5VF3). **e** One

hundred and fifty-five Hoc fibers emanate from the centers of capsomers³⁴ (PDB 3SHS). **f, g** Molecular surfaces of wild-type (WT) T4 capsid²² (3.4 Å, PDB 7V55) (**f**) and super-acidic 9DE-T4 capsid (3.9 Å) (**g**) are colored according to electrostatic potential. The color ranges from red, corresponding to a potential of -5 kT/e^- , to blue, corresponding to a potential of $+5 \text{ kT/e}^-$. The WT-T4 capsid has 6,829 net negative charges and the 9DE-T4 capsid has 15,199 net negative charges. **h** Schematic of head packaged with foreign proteins and DNAs in its interior space.

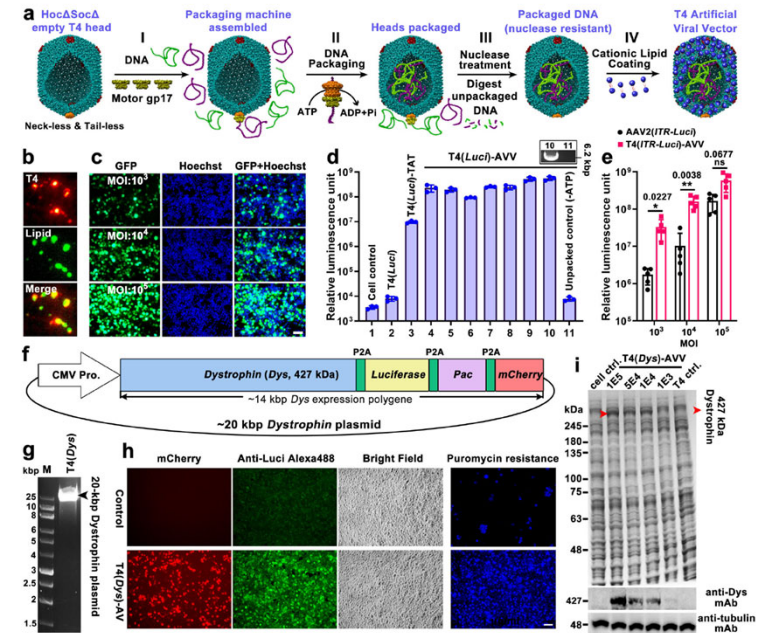


Fig. 2 | T4-AVVs efficiently deliver genetic payloads into human cells.

a Schematic of sequential assembly of DNA-packaged T4-AVVs. **b** Alexa Fluor 594 (red) labeled T4 capsid colocalized with nitrobenzoxadiazole (NBD, green) labeled cationic lipid molecules. **c** T4(*GFP*)-AVVs efficiently delivered packaged *GFP* DNA into 293 T cells, as determined by GFP expression at different MOIs (multiplicity of infection, ratio of AVV particles to cells). Cell nuclei were stained with Hoechst. Bar = 50 μm . **d** Transduction efficiencies of T4(*Luciferase*)-AVVs coated with different cationic lipids, as determined by luciferase expression. 1, cell control (no treatment); 2, T4(*Luciferase*) control (no lipid coating and no TAT); 3, T4(*Luciferase*)-TAT control (TAT-displayed, no lipid); 4-10, T4(*Luciferase*)-AVVs coated with various lipids; 4, LPF3K-AVVs; 5, LPFLTX-AVVs; 6, LPFStem-AVVs; 7, EXPI-AVVs; 8, FECT-AVVs; 9, LPFRNAiMAX-AVVs; 10, LPF2K-AVVs; 11, unpackaged control (same as #10 but no ATP). The top right box shows the packaged *Luciferase* DNA in groups 10 and 11. Values represent mean with standard deviation (SD) ($n = 3$). **e** Transduction efficiencies of T4(*UTR-Luciferase*)-AVV and single-stranded AAV2(*UTR-Luciferase*) at a MOI of 10^3 , 10^4 , or 10^5 . The T4-packaged *UTR-Luciferase* plasmid has the same sequence as the one packaged into AAV2 particles. Values represent mean with SD ($n = 5$). * $P < 0.05$, ** $P < 0.01$, and ns, not significant. Paired *t* test (two-tailed) was used for comparison in each MOI. **f** Schematic of $\sim 20 \text{ kbp}$ *dystrophin* (*Dys*) plasmid. **g** Agarose gel electrophoresis showing T4-packaged *Dys* plasmid (~ 2.5 molecules per head). **h** *mCherry* expression, *luciferase* expression, and puromycin resistance (*Pac* expression) in 293 T cells transduced by T4(*Dys*)-AVVs. *Luciferase* expression was detected by cellular immunofluorescence using Alexa488-labeled anti-*Luciferase* antibody. Puromycin-resistant 293 T cells following transduction with T4(*Dys*)-AVVs were stained by Hoechst, while the sensitive cells floated and were washed off. Bar = 50 μm . **i** *Dystrophin* expression in 293 T cells transduced by T4(*Dys*)-AVVs. Top, SDS-PAGE of whole cell extracts showing the appearance of $\sim 427 \text{ kDa}$ dystrophin protein band (red arrowhead). Middle, Western blotting using anti-dystrophin mAb. Bottom, Western blotting using control anti-tubulin mAb.

Luciferase plasmid (AAV2(*UTR-Luciferase*)-CMV enhancer and promoter-fireflyLuciferase-hGH polyA) has the same sequence as the one packaged into AAV2 particles. Values represent mean with SD ($n = 5$). * $P < 0.05$, ** $P < 0.01$, and ns, not significant. Paired *t* test (two-tailed) was used for comparison in each MOI. **f** Schematic of $\sim 20 \text{ kbp}$ *dystrophin* (*Dys*) plasmid. **g** Agarose gel electrophoresis showing T4-packaged *Dys* plasmid (~ 2.5 molecules per head). **h** *mCherry* expression, *luciferase* expression, and puromycin resistance (*Pac* expression) in 293 T cells transduced by T4(*Dys*)-AVVs. *Luciferase* expression was detected by cellular immunofluorescence using Alexa488-labeled anti-*Luciferase* antibody. Puromycin-resistant 293 T cells following transduction with T4(*Dys*)-AVVs were stained by Hoechst, while the sensitive cells floated and were washed off. Bar = 50 μm . **i** *Dystrophin* expression in 293 T cells transduced by T4(*Dys*)-AVVs. Top, SDS-PAGE of whole cell extracts showing the appearance of $\sim 427 \text{ kDa}$ dystrophin protein band (red arrowhead). Middle, Western blotting using anti-dystrophin mAb. Bottom, Western blotting using control anti-tubulin mAb.

Engineering Next-Generation Adenoviral Gene Therapies

Synthetic biology centers on the design and modular assembly of biological parts so as to construct artificial biological systems.

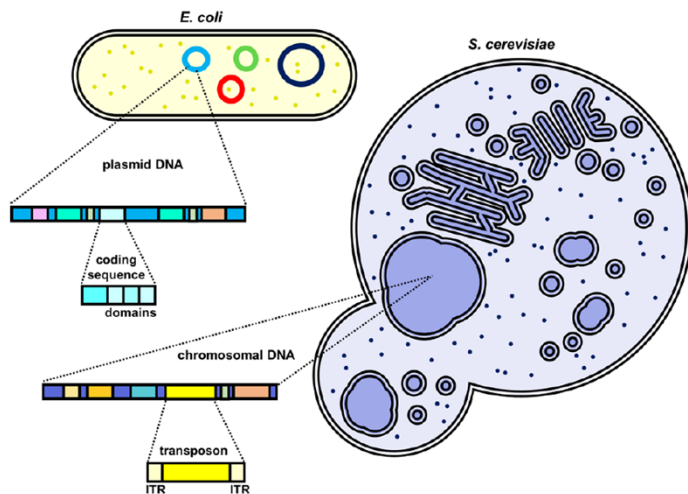


Figure 1. Philosophy of synthetic biology. From the perspective of a synthetic biologist, **all biology is decomposable into modular biological parts which can be synthesized, characterized, and rearranged like LEGO bricks to create functional systems.** A few examples of biological parts are plasmids, chromosomes, coding sequences, transposons, protein domains, and inverted terminal repeats. Synthetic biologists also employ chassis, which are existing biological systems that incorporate edits and parts. Two canonical examples of chassis are *E. coli* and *S. cerevisiae*. The Ad represents another important chassis system.

Collins 2021, Synthetic biology approaches for engineering next-generation adenoviral gene therapies

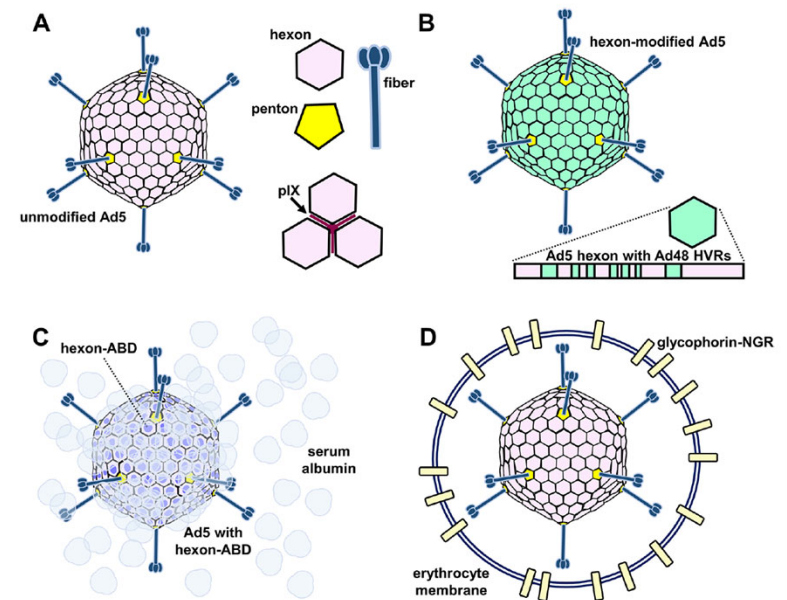


Figure 2. Synthetic biology strategies to help mitigate the immunogenicity of Ads. (A) Structure of the Ad capsid and its external components. Three more structural proteins (not shown) can be found on the inner surface of the Ad capsid: pIIIa, pVI, and pVIII. (B) The Ad hexon includes seven highly immunogenic HVR sequences. Replacing these sequences with versions from rare Ad serotypes such as Ad4812 can mitigate immunogenicity since the human body has fewer antibodies against rare Ad serotypes. (C) Insertion of an albumin binding domain (purple) into the hexon protein has sterically shielded the Ad from neutralizing antibodies by sequestering serum albumin upon injection.³⁸ (D) Encapsulation of the entire Ad inside of erythrocyte-derived membrane has protected the Ad from immunological assaults.³⁹ To facilitate tissue targeting, glycoprotein proteins with an NGR tripeptide have been included in the encapsulating membrane.

Nanomaterials: From Natural To Synthetic

Microfabrication: Sticky Fingers

Sticky fingers: Novel robotic grippers expand role in fulfillment

These cool gecko-inspired grippers show how the best innovations don't add complexity, but eliminate it. Greg Nichols, 2020.

Robots with gecko-inspired hands are becoming more important during the rise of on-demand-everything. That's prompting a leader in robotic end-of-arm tooling to expand its lineup of the biologically-inspired gripper pads for robots that work in various industries, including fulfillment and logistics.

The company's gripper uses millions of "micro-scaled fibrillar stalks" to stick to smooth surfaces using van der Waals forces, which is the mechanism geckos use to climb. The technology was first developed with space in mind and grew out of a Stanford research project that inspired work at the NASA Jet Propulsion Lab. NASA was exploring van der Waals forces as an effective way to capture orbiting satellites for salvage or repair. Suction cups and vacuum grippers aren't effective in space, and traditional robotic end effectors can push objects away in zero gravity.

OnRobot's Gecko no-mark adhesive gripper seemed like a grippy solution to a sticky situation, and the company's success with its grippers has reinforced the market need for this sort of product. Last year OnRobot won silver at the Edison Awards Gala, which came on the heels of the Gecko Gripper winning the Robotics Award at the Hannover Messe in Germany.

<https://www.zdnet.com/article/sticky-fingers-novel-robotic-grippers-expand-role-in-fulfillment/#ftag=CAD-03-10abf5f>



Gecko Gripper – SPECIAL ADHESIVE TECHNOLOGY, NO-MARK GRIPPING

No compressed air requirement saves maintenance costs and provides faster payback in as little as 5 months.

Precise, no-mark gripper technology increases productivity in pick-and-place tasks.

Innovative gecko technology enables gripping of flat, porous objects such as PCBs to extend automation capabilities. <https://onrobot.com/en/products/gecko-gripper>

Microfabrication: Gecko's Attachment Pads

This review paper discusses design parameters that were found to be instrumental to the adhesive properties of **synthetically fabricated adhesive structures, currently available fabrication methods** for producing these adhesive structures, as well as the various testing methods that have been used experimentally to characterize adhesion performance.

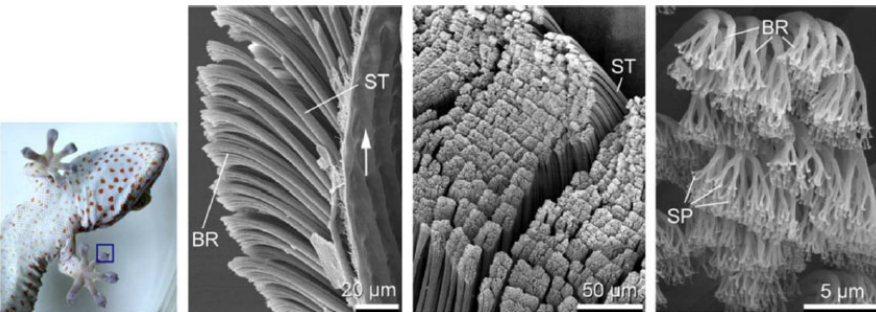


Fig. 2. Adhesion map for spherical tip contacts.

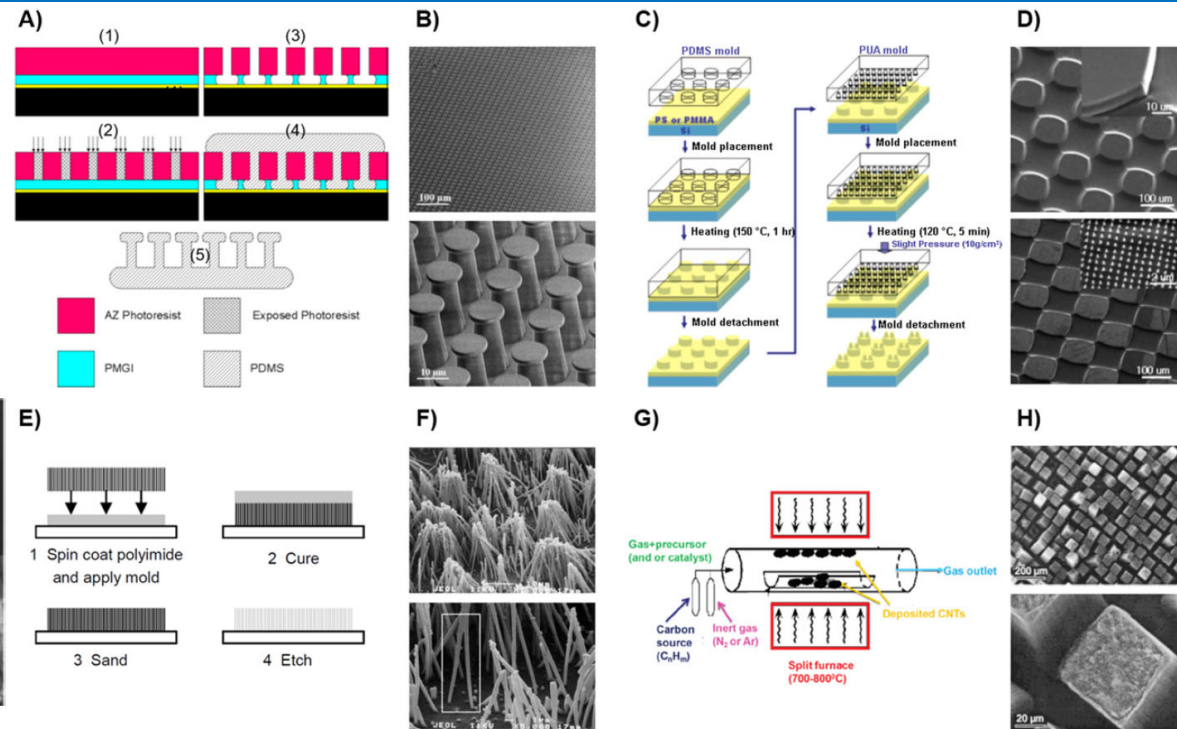
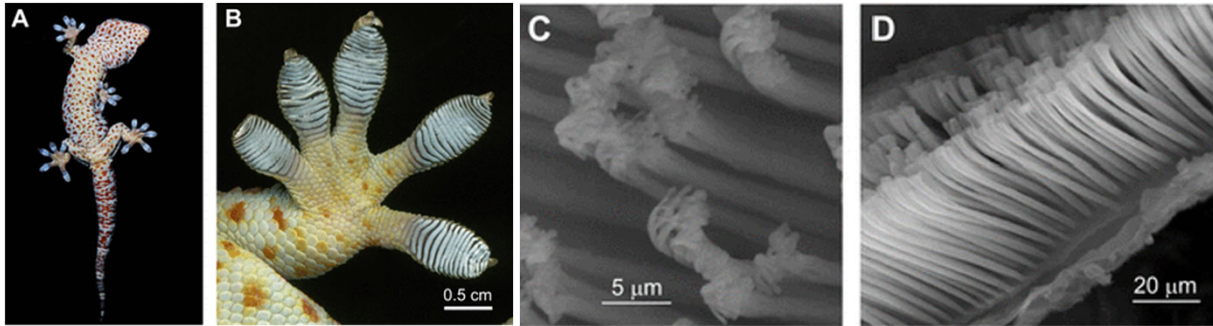


Fig. 3 (A) (1) A silicon wafer is coated with Cr/Au followed by spin-coating and baking PMGI and AZ 9260 photoresists. (2) The AZ 9260 is UV-exposed under the post array mask. (3) Following exposure, the photoresist is developed and dried, leaving undercut areas. (4) Sylgard[®] 184 is poured onto the mold and cured. (5) The cured silicone is removed by hand, producing the final dry adhesive. (B) SEM images of 10 μm diameter posts with a cap thickness of 1.5 μm and post height of ~ 20 μm. (C) Schematic of the two-step capillary force lithography process. Polymer microstructures were fabricated using a micropatterned PDMS mold followed by nanofabrication on top of the preformed microstructure using a nanopatterned PUA mold. (D) SEM images of PS microstructures and micro/nanoscale hierarchical structures. A microstructure with 120 μm posts and 25 μm spacing was used. The nanostructure is 100 nm in diameter and 400 nm in spacing with a height of 450 nm. (E) Synthetic fiber fabrication by nanocasting. (F) Clumping in an array of 0.6 μm diameter polyimide fibers. (G) Schematic diagram of chemical vapor deposition (CVD) setup. (H) SEM images of MWCNTs deposited on a masked pattern after 10 min of CVD. Reproduced with permission from

Nanostructures in Nature



An overview of the hierarchical nature of the gecko adhesive system. (A) A ventral view of a tokay gecko on glass, showing the toe pads. (B) Lamellae on the gecko toe pads. (C) The setae that make up the lamellae. (D) The flattened tips of branched setae (spatulae). <https://jeb.biologists.org/content/219/7/912.figures-only>

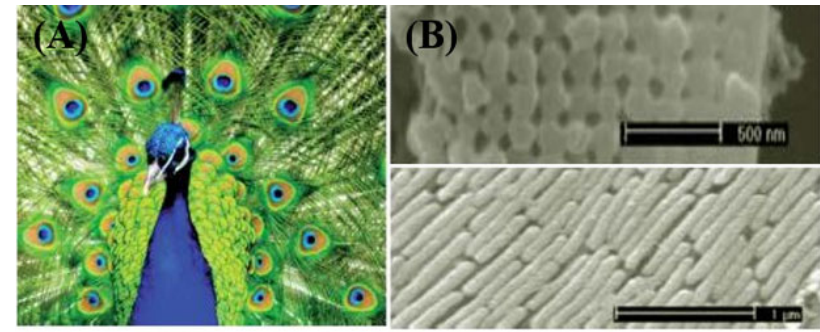


Figure 7: (A) Photograph of peacock feathers showing various colors and patterns. (B) Cross-sectional SEM images of the transverse (top) and longitudinal (bottom) sectionals of green barbule cortex.

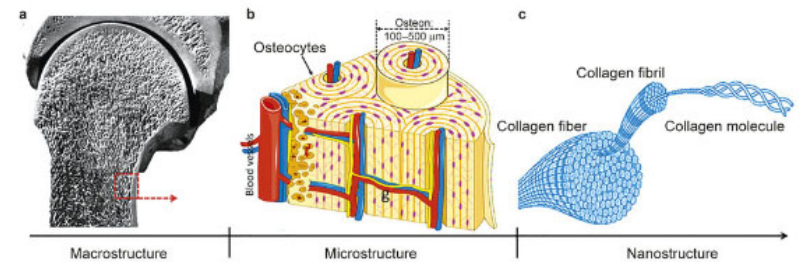


Figure 8: The macro- and microstructure of bone and its components with nanostructured materials employed in the regeneration of bone. (a) Macroscopic bone details with a dense cortical shell and cancellous bone with pores at both ends. (b) Repeating osteon units within cortical bone. (c) Collagen fibers (100–2000 nm) comprised of collagen fibrils.

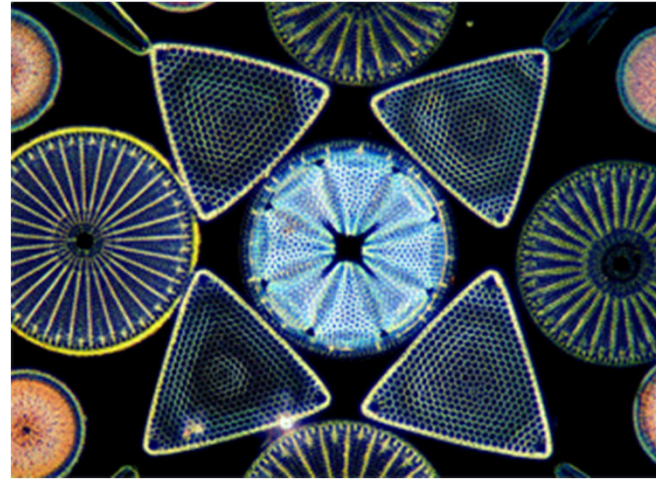
Jeevanandam 2018, Review on nanoparticles and nanostructured materials

Nanostructures in Nature: Planktonic Diatoms

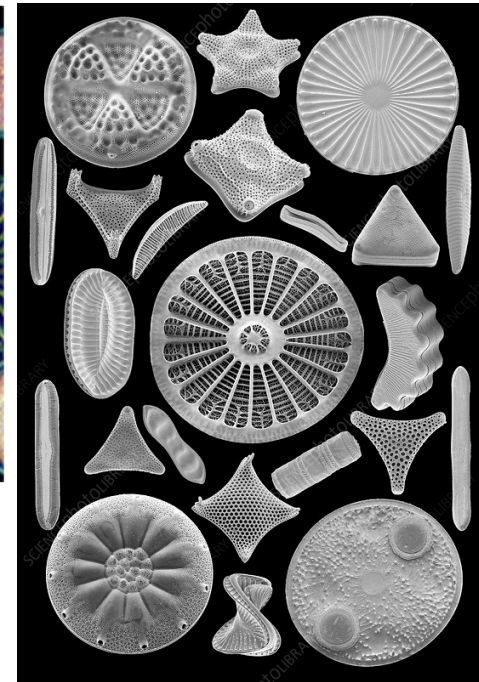
Diatoms are single-celled algae that live in houses made of glass. They are the only organism on the planet with cell walls composed of transparent, opaline silica. Diatom cell walls are ornamented by intricate and striking patterns of silica.

Diatoms turn energy from the sun into sugar.
 Diatoms produce 50% of the air we breathe.
 Diatoms remove carbon dioxide (CO₂) from the atmosphere.
 Diatoms are food for the entire food web.

<https://diatoms.org/what-are-diatoms>



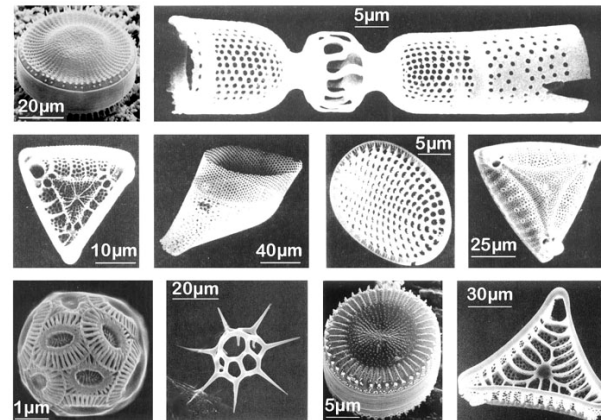
<http://www.go-star.com/antiquing/diatoms-victorian-microscope-slides.htm>



<https://www.sciencephoto.com/media/943455/view/diatoms-sem>

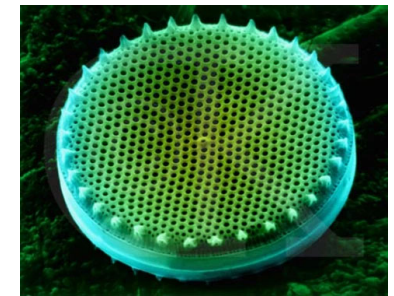


<https://bukuipa.co.id/kingdom-protista/>



Selection of planktonic diatoms
 (not representative for the mediterranean)

<https://www.pinterest.com/pin/16881468600330498/>



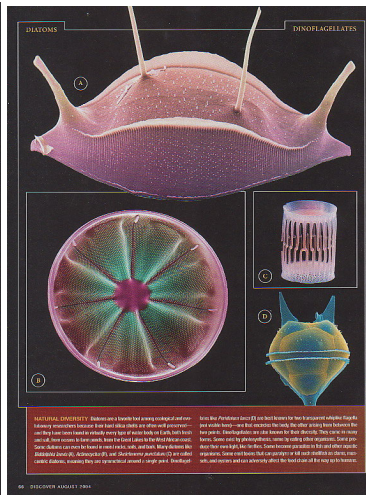
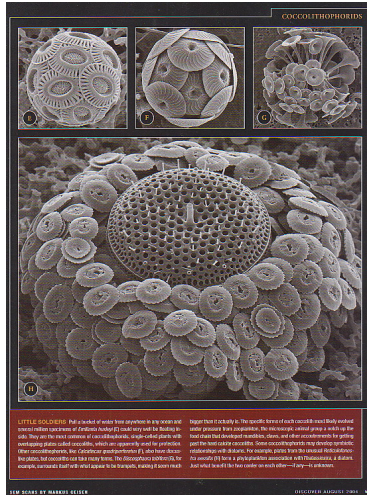
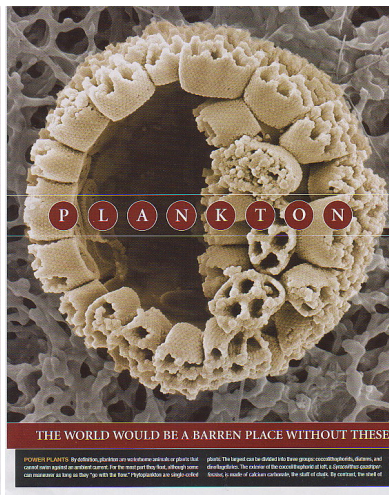
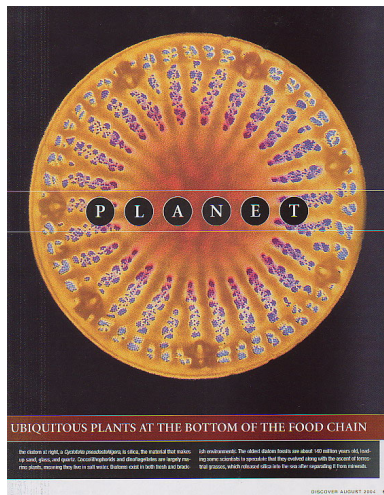
<https://wyrdsience.wordpress.com/2011/01/10/205/>

Nanostructures in Nature: Planktonic Diatoms

By definition, plankton are waterborne animals or plants that cannot swim against an ambient current. For the most part they float, although some can maneuver as long as they “go with the flow.” Phytoplankton are single-celled plants. The largest can be divided into three groups: coccolithophorids, diatoms, and dinoflagellates. The exterior of the coccolithophorid, a *Syracolithus quadriperforatus*, is made of **calcium carbonate**, the stuff of chalk. By contrast, the shell of the diatom *Cyclotella pseudostelligera* is **silica**, the material that makes up sand, glass, and quartz. Coccolithophorids and dinoflagellates are largely marine plants, meaning they live in salt water. Diatoms exist in both fresh and brackish environments. The oldest diatom fossils are about 140 million years old, leading some scientists to speculate that they evolved along with the ascent of terrestrial grasses, which released silica into the sea after separating it from minerals. | SEM scan courtesy of Markus Geisen.

Plankton are literally at the bottom of the food chain, a source of nourishment for virtually every animal in the sea. They are ancestors to terrestrial plants, which seem to have evolved from certain ocean phytoplankton hundreds of millions of years ago.

Scanning electron microscope (SEM) images show that they can be arrestingly beautiful. Coccoliths are not always round, flat plates, like hubcaps; many look like trumpets, cabbage leaves, or stars.



From Nature to Fabrication

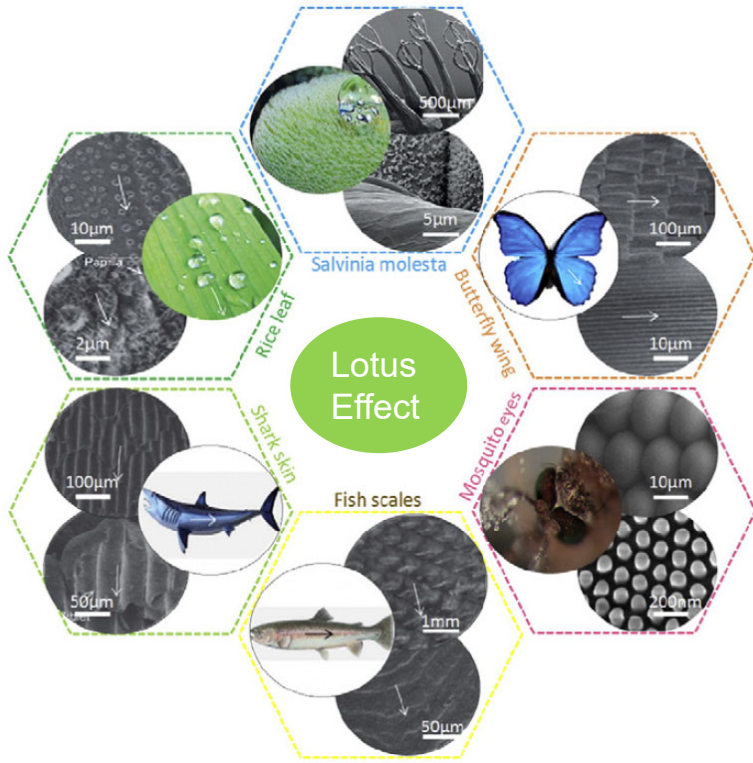


Fig. 1. The typical self-cleaning surfaces in nature and their SEM images. The droplets of water on the surfaces can roll off following a preferential direction dictated by the structural features.

Zhang 2016, Lotus effect in wetting and self-cleaning

From natural

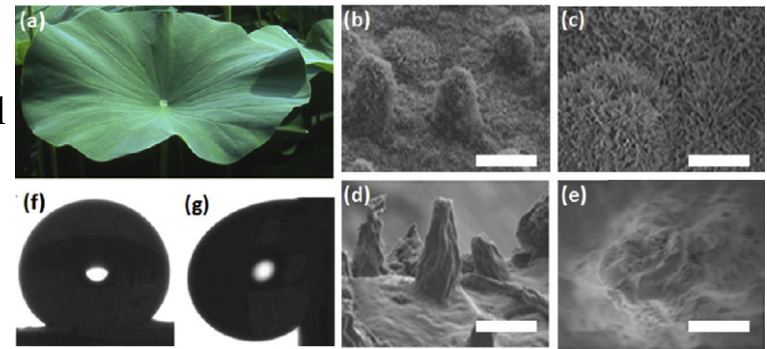


Fig. 2. Image and SEM images of lotus leaf surface. (a) A fresh lotus leaf in nature, (b) the micro-structure of lotus leaf, (c) the nano-structure of lotus leaf, (d) the micro-structure of annealed lotus leaf, (e) the nano-structure of annealed lotus leaf, (f) a droplet placed on an untreated lotus leaf, and (g) a droplet placed on an annealed lotus leaf, then tilted to an angle of 90°. (Scale bar: (b and d) 10 μm , (c and e) 3 μm).

to synthetic
surface structures

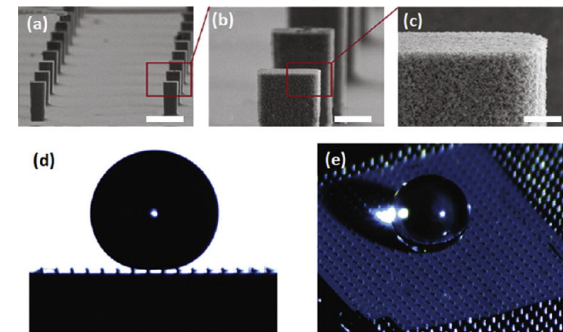


Fig. 6. Droplet on the fabricated micro/nano roughened hierarchical surface. (a-c) Nano-scaled roughness etched by XeF₂ gas that conformally covers the micro-scale array of pillars fabricated through deep reactive etching. (d-e) Droplet sitting on the double roughness with the value of the pillar spacing to width ratio at 7.5, supported by only several pillars. The contact angle at this state is 173°. (Scale bar: (a) 50 μm , (b) 10 μm , and (c) 2 μm).

Superhydrophobic Paper

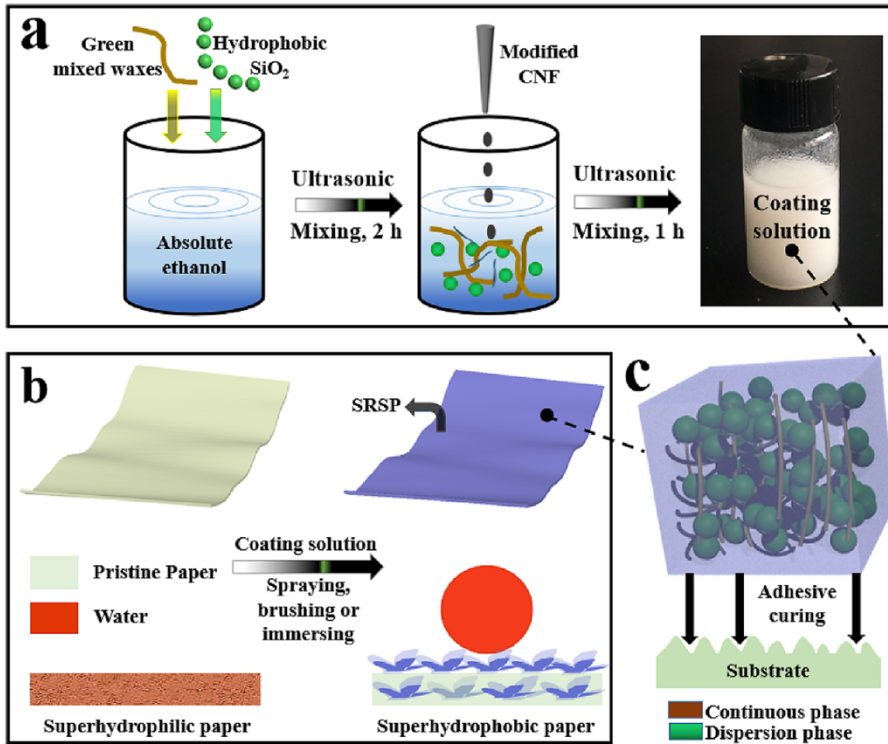


Fig. 1. Design of SRSP. (a) Fabrication process schematic illustration of targeted coating solution, and the building block of SRSP. (b) Schematic illustration of the procedure for coating treatment procedure to obtain the SRSP. (c) Illustration of the superhydrophobic composite coating layer (consisting of the continuous phase: brown part and dispersion phase: green part) was formed on the surface of the pristine paper-based substrate through synergistic reinforcement of cross-linking reaction.

Long 2022, Synergistic reinforced superhydrophobic paper with green, durability, and antifouling function

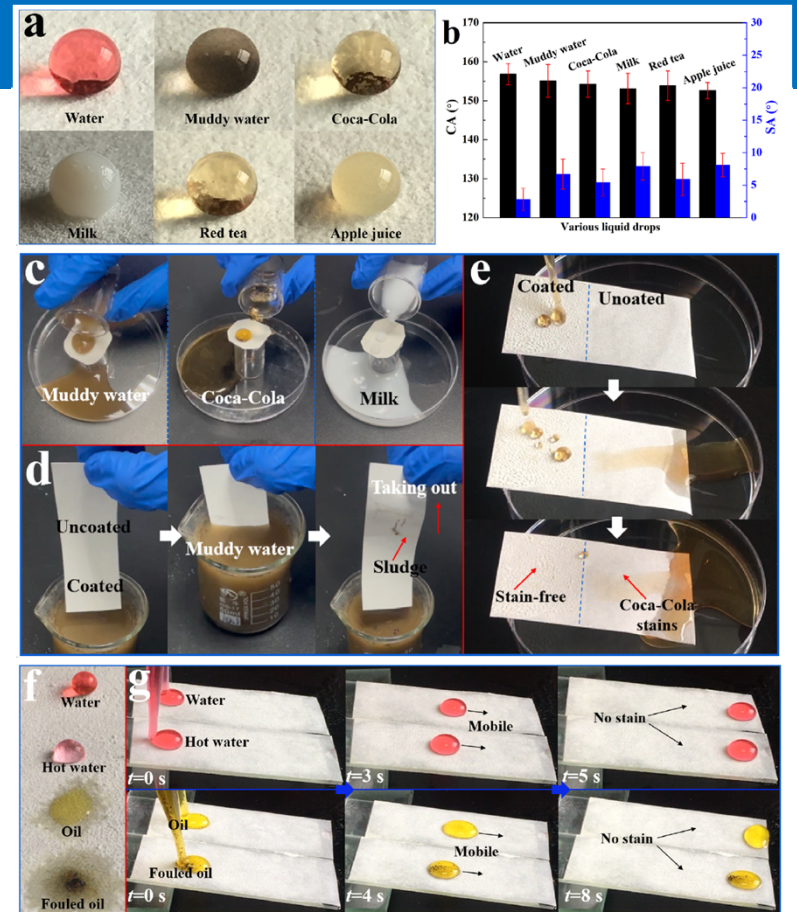
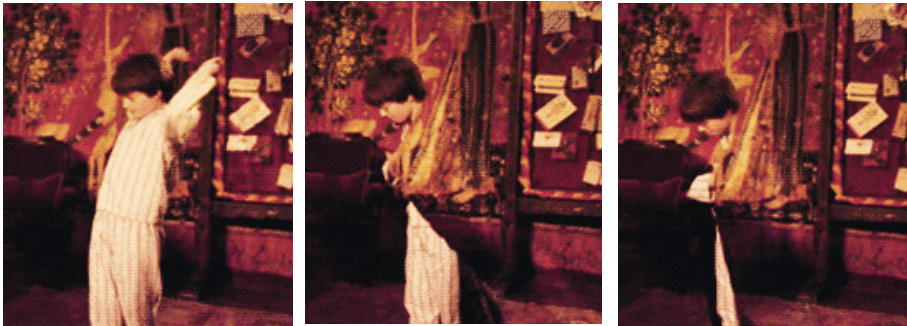


Fig. 6. Direct antifouling ability of SRSP. (a) Different types of liquid droplets with spherical shape on SRSP surface: red-colored water, muddy water, Coca-Cola, milk, red tea, and apple juice. (b) CAs and SAs of different liquids on the SRSP surface. (c) Three water-based liquids including muddy water, Coca-Cola, and milk were poured onto the SRSP surface. (d) Uncoated pristine paper surface (upper image) and SRSP surface (lower image) was dipped into muddy water and brought out. (e) Movement of Coca-Cola on the substrate composed of uncoated pristine paper surface (right) and SRSP surface (left). (f) Wetting behavior of water, hot-water (~100 °C), oil, and foul-oil droplets on SRSP surface. (g) Time-sequence images of the free mobility of water, hot-water, oil, and foul-oil droplets down along the tilted SLIPS-SRSP surfaces with a tile angle of ~10°.

Nano (Maybe Pico) Camouflage Technology

Invisibility in Movies



Harry Potter's Cloak of Invisibility



Invisibility — like time travel, teleportation, flying, and super-speed — has been a fixture in science fiction ever since science fiction has existed. The most well-known examples range from the one used by the Romulans in Star Trek, Harry Potter's deathly hallows cloaking device, and the elven cloak Frodo and Sam used to evade Sauron's army at the gates of Mordor.

<http://www.iaat.tech/article/215b5c38ac473f65bf2d8d39.html>

<https://futurism.com/scientists-have-found-a-way-to-interfere-with-light-to-make-objects-invisible>

Human Camouflage



@rody_eug1, TikTok

<https://www.proapto-camouflage.com/neuropsychology-of-camouflage>

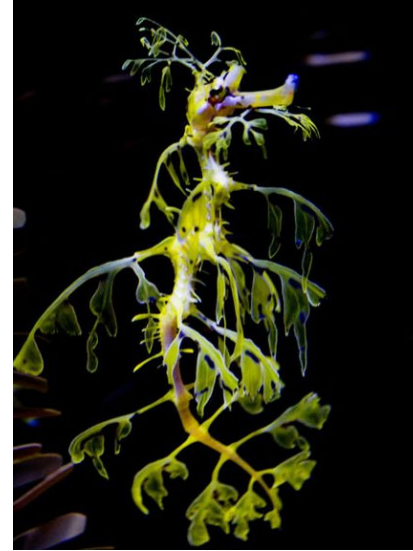
Invisibility in Real World through Camouflage



Tasseled Anglerfish



Cuttlefish



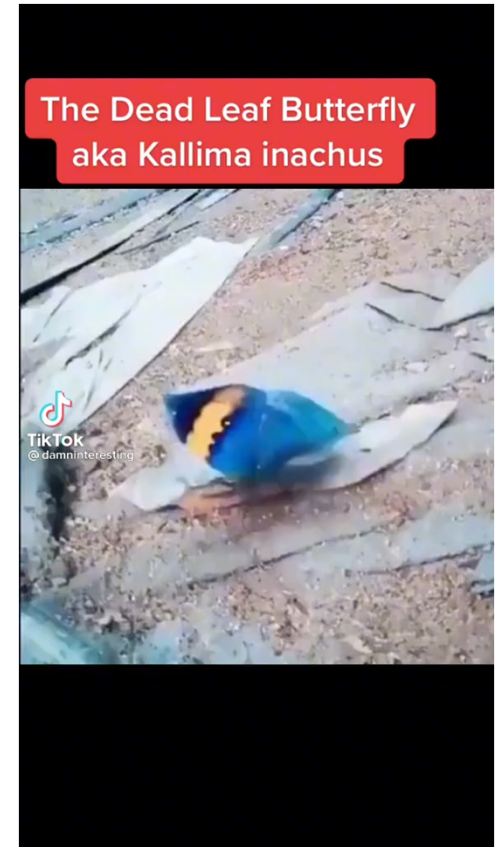
Leafy Sea Dragon



Trumpetfish



Reef Stonefish



http://ocean.nationalgeographic.com/ocean/photos/undersea-camouflage/#/camouflage05-trumpetfish_13511_600x450.jpg

Invisibility in Real World



Octopus Camouflage

An amazing transformation of colors that match with the background in a matter of seconds.



<http://www.youtube.com/watch?v=eS-USrwuUfA>

Invisibility in Real World

Octopus Camouflage

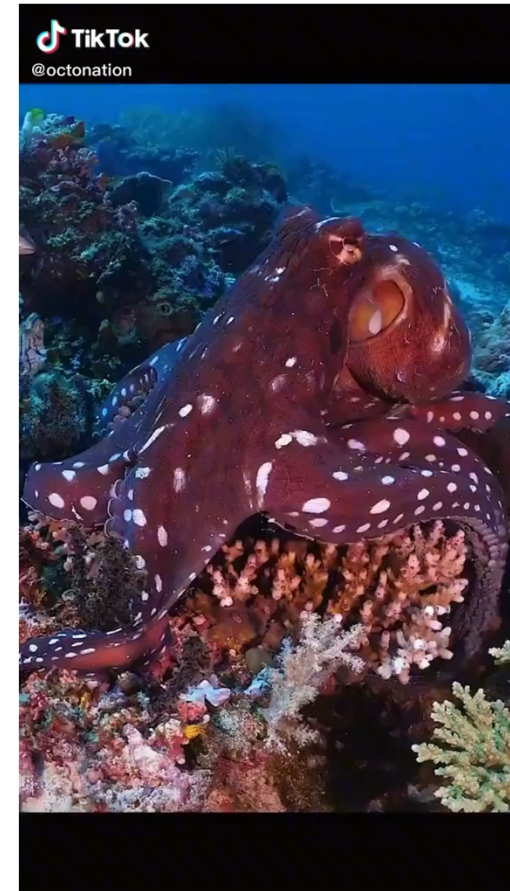
It is even more amazing that octopus is color blind.



<http://www.youtube.com/watch?v=eS-USrwuUfA>



Octopus Camouflage



TikTok. @oceanwild247

My Octopus Teacher (Netflix 2020)

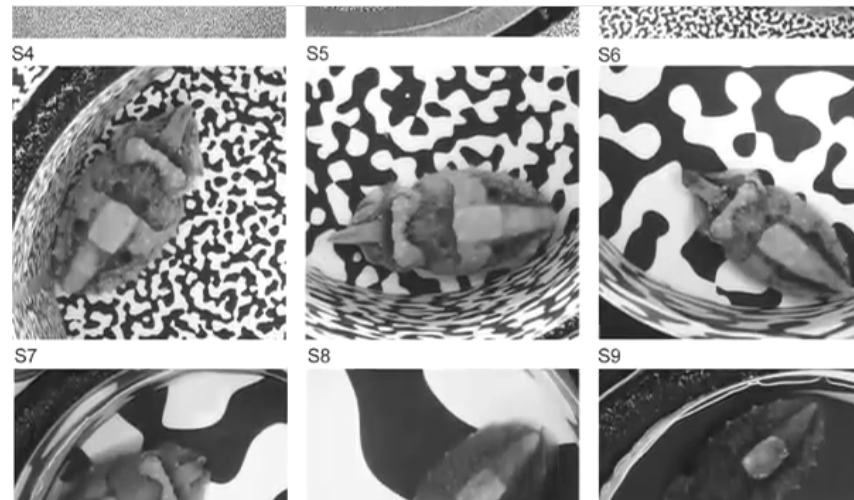
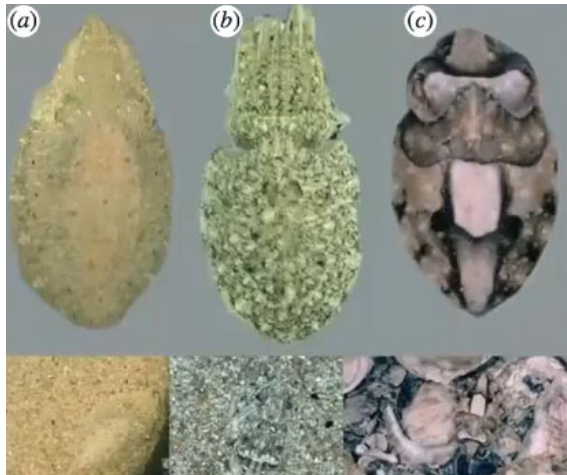
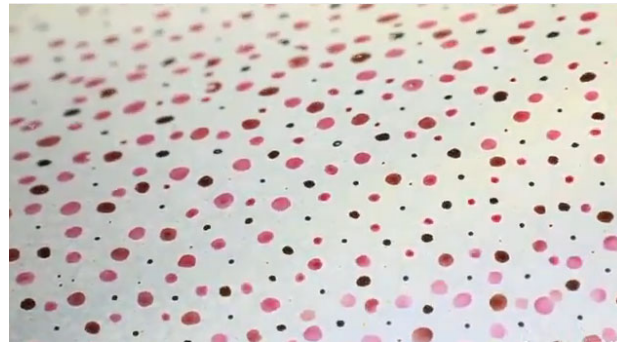


A filmmaker forges an unusual friendship with an octopus living in a South African kelp forest, learning as the animal shares the mystery of her world (1:05:34)

Almost Instant Changes in Color, Pattern, and Shape of the Skin

Cephalopods (Squid, Octopus, Cuttlefish) have several tricks for blending in with their undersea surroundings: they can change color, pattern and even the shape of their skin.

<http://www.youtube.com/watch?v=eS-USrwuUfA>



<http://www.sciencefriday.com/segment/08/05/2011/squid-octopus-cuttlefish-masters-of-camouflage.html>

Smart Camouflage for Sneakier Soldiers: (DO NOT OVERPROMISE)

Cuttlefish-inspired smart camouflage could make for sneakier soldiers. The US Army has pondered the development of camouflage that mimics how cephalopods rapidly change their colour and patterning. They call it 'signature management'. By Stilgherrian | February 12, 2020

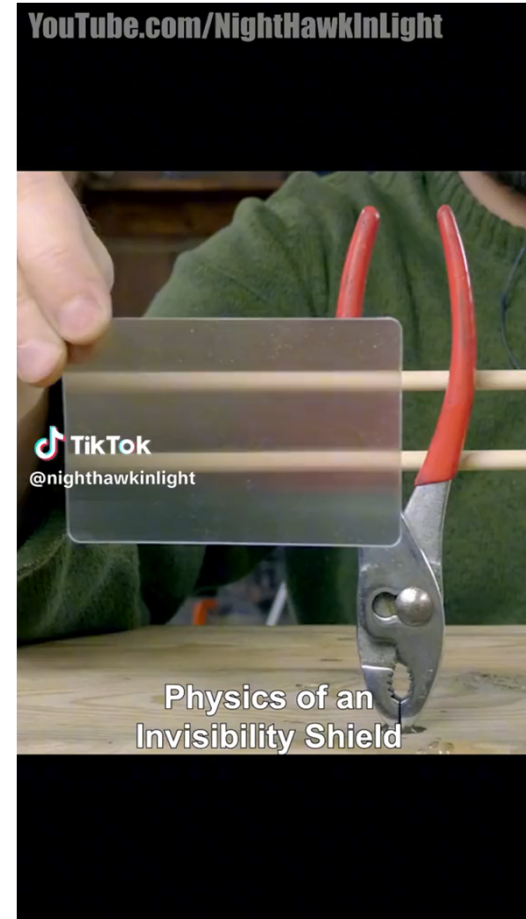
For some time, engineers have been experimenting with robotic tentacles modelled on the octopus. Now they're being inspired by their camouflage. **Cephalopods -- cuttlefish, octopus, and squid -- are renowned for their ability to rapidly change their skin colour and patterns to match their surroundings or warn off attackers. Their skin is studded with sacs full of pigment called chromatophores, each one surrounded by 18 to 30 muscle fibres that can rapidly change how much pigment is exposed.** It also seems that the skin itself is somehow "smart" and can, in some circumstances, work independently from the animal's brain.

According to Alon Gorodetsky Associate Professor of Chemical and Biomolecular Engineering at the University of California, Irvine, understanding these biological capabilities could inspire the engineering of **dynamic materials for military camouflage applications**. That could include reconfigurable infrared (IR) camouflage coatings and IR invisibility covering -- something that's of increasing importance as more IR sensors are deployed on the battlefield. Gorodetsky and his colleagues have already demonstrated the potential of such a "dynamic thermoregulatory material" which was inspired by squid skin. "We draw inspiration from the static infrared-reflecting space blanket and active colour-changing squid skin to design and develop a tuneable thermoregulatory material," they wrote. By varying the mechanical strain on the fabric, thereby changing its characteristics, they could regulate the body temperature of its wearer. The potential military applications of such technology were discussed at a workshop, called Bio-Inspired Signature Management for the US Army, convened by the National Academies of Sciences, Engineering, and Medicine.

While the workshop was held in September 2019, the in-brief proceedings were published last week. It's a fascinating read. Participants discussed the possibility of **"smart skin" fabrics** that would include light sensors that could enable **"adaptive optoelectronic camouflage systems inspired by cephalopod skins"**. The fabric wouldn't have to be smart enough to exactly match its surroundings. Disruptive dazzle patterns could be more effective than background-matching, particularly against edge-detection algorithms, participants said. Dazzle markings make estimates of speed and trajectory difficult.

One example cited was a school of stripe-patterned fish, which utilize their speed and shifting direction to confuse predators. Predators also use disruptive camouflage. A cuttlefish might do five primary camouflage changes in the course of 20 minutes to approach prey. The challenge, participants said, is how you would actually manufacture a smart skin. **Smart skins would have to include micro-structure components yet be made in metre-scale fabric.** They would also have to be **flexible**. The possibility of commercial manufacturing techniques are "nearing short-term now", said Dr Michelle Povinelli from the University of Southern California. But not all participants agreed. "To date, the participants had not seen engineered systems actively change shape after receiving cues with an active skin," said the proceedings. "Knowledge is lacking as to the level of effort needed to understand **these observed capabilities from biology and bring them to practical systems**. Its associated timeline -- be it a 1-year, 10-year, 20-year, or beyond challenge -- is unknown as well."

<https://www.zdnet.com/article/cuttlefish-inspired-smart-camouflage-could-make-for-sneakier-soldiers/#ftag=CAD-03-10abf5f>



Nanofabrication & Microfabrication

Nanofabrication deals with smaller structural sizes than microfabrication, but the borderline size is not well-defined and unnecessary.

Except for the manufacturing of evermore powerful computer chips, nanofabrication and microfabrication in most applications, especially in biomedical applications, are intimately tied together.

Thus, the two terms are frequently used together and/or used interchangeably.

Miniaturization



https://defense-update.com/20101231_miniature_weapons.html

<https://news.mit.edu/2017/miniaturizing-brain-smart-drones-0712>

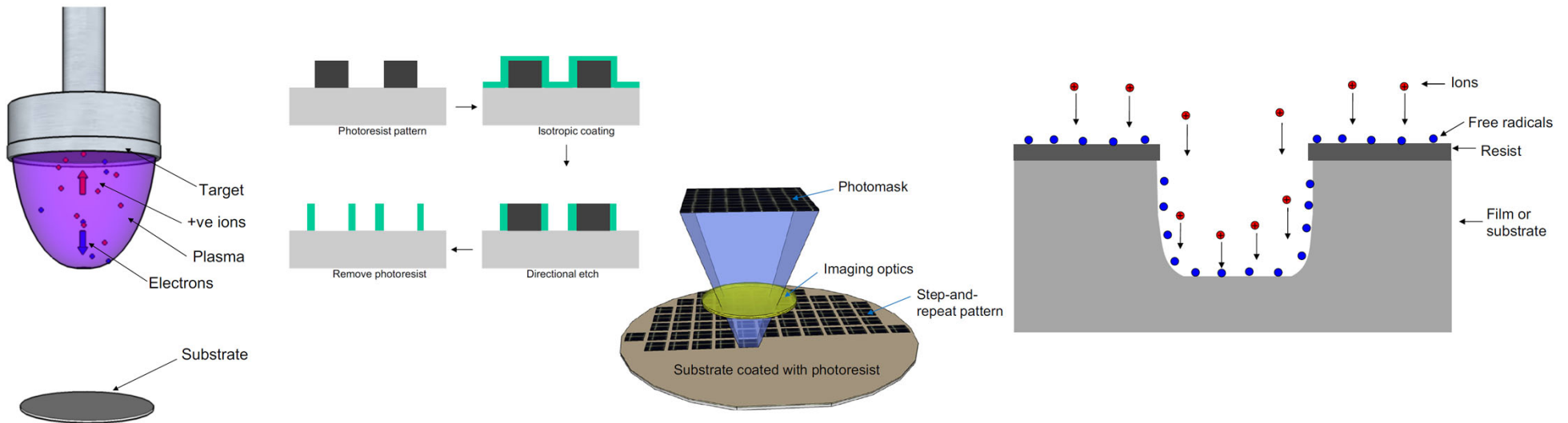
<https://www.islamtimes.org/en/news/183106/us-military-developing-insect-surveillance-drones>

<https://www.defenceiq.com/defence-technology/articles/nano-drone-tech-is-advancing>

Nanofabrication: Introduction

There is no single accepted definition of nanofabrication, nor a definition of what separates nanofabrication from microfabrication. To meet the continuing challenge of shrinking component size in microelectronics, new tools and techniques are continuously being developed. Component sizes that were in tens of micrometers became single-digit micrometers, and then hundreds of nanometers, and then went down to a few tens of nanometers where they stand today. As a result, what used to be called microfabrication was rebranded as nanofabrication, although the governing principles have remained essentially the same. The main driver of this technology has been the manufacture of integrated circuits, but there have been tremendous fallout benefits to other areas, including photonics.

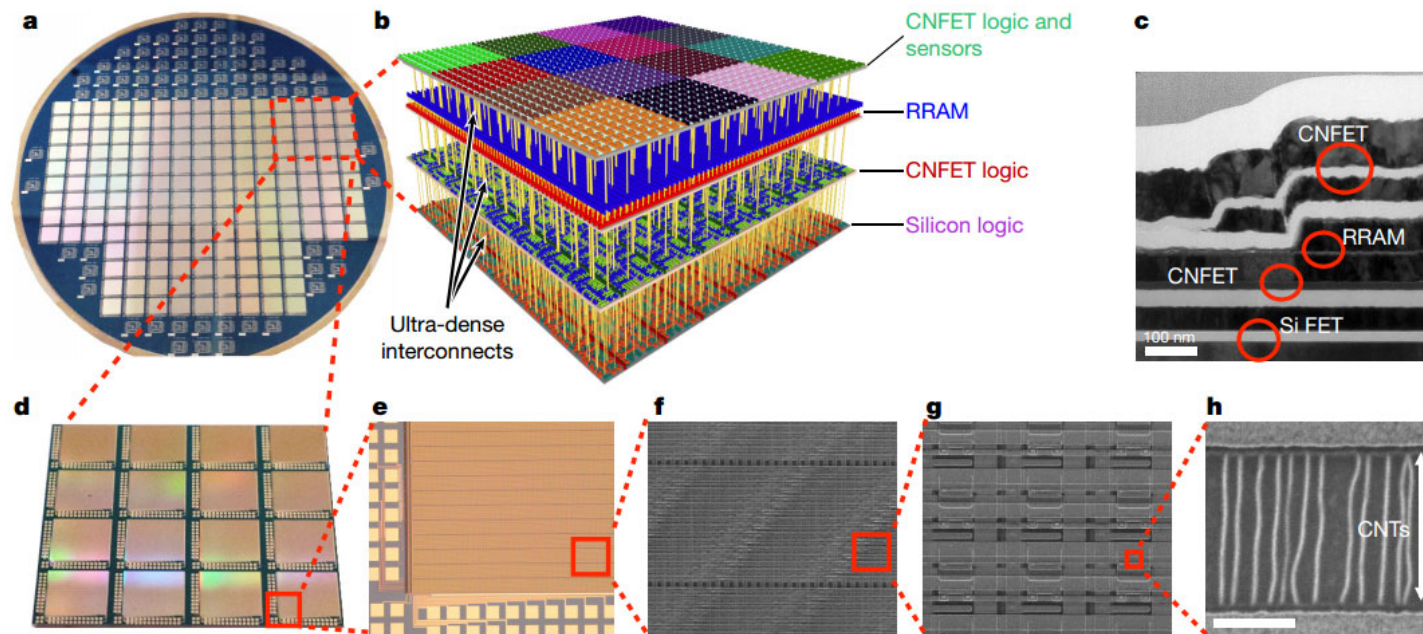
Nanofabrication can be loosely divided into three major areas: thin films, lithography, and etching.



Nanofabrication: Three-Dimensional Chip

Nanofabrication

Computers today comprise different chips cobbled together. There is a chip for computing and a separate chip for data storage, and the connections between the two are limited. As applications analyze increasingly massive volumes of data, the limited rate at which data can be moved between different chips is creating a critical communication "bottleneck." And with limited real estate on the chip, there is not enough room to place them side-by-side, even as they have been miniaturized (a phenomenon known as Moore's Law).



The new prototype chip is a radical change from today's chips. It uses multiple nanotechnologies, together with a new computer architecture, to reverse both of these trends. Instead of relying on silicon-based devices, the chip uses carbon nanotubes, which are sheets of 2-D graphene formed into nanocylinders, and resistive random-access memory (RRAM) cells, a type of nonvolatile memory that operates by changing the resistance of a solid dielectric material. The researchers integrated over 1 million RRAM cells and 2 million carbon nanotube field-effect transistors, making the most complex nanoelectronic system ever made with emerging nanotechnologies. The RRAM and carbon nanotubes are built vertically over one another, making a new, dense 3-D computer architecture with interleaving layers of logic and memory. By inserting ultradense wires between these layers, this 3-D architecture promises to address the communication bottleneck.

<https://phys.org/news/2017-07-three-dimensional-chip-combines-storage.html>

Nanofabrication & Microfabrication: Cardiac Tissue Engineering

The following example describes interchangeable use of nanofabrication (nanoengineering in this article) and microfabrication, and the difficulty of separating the two.

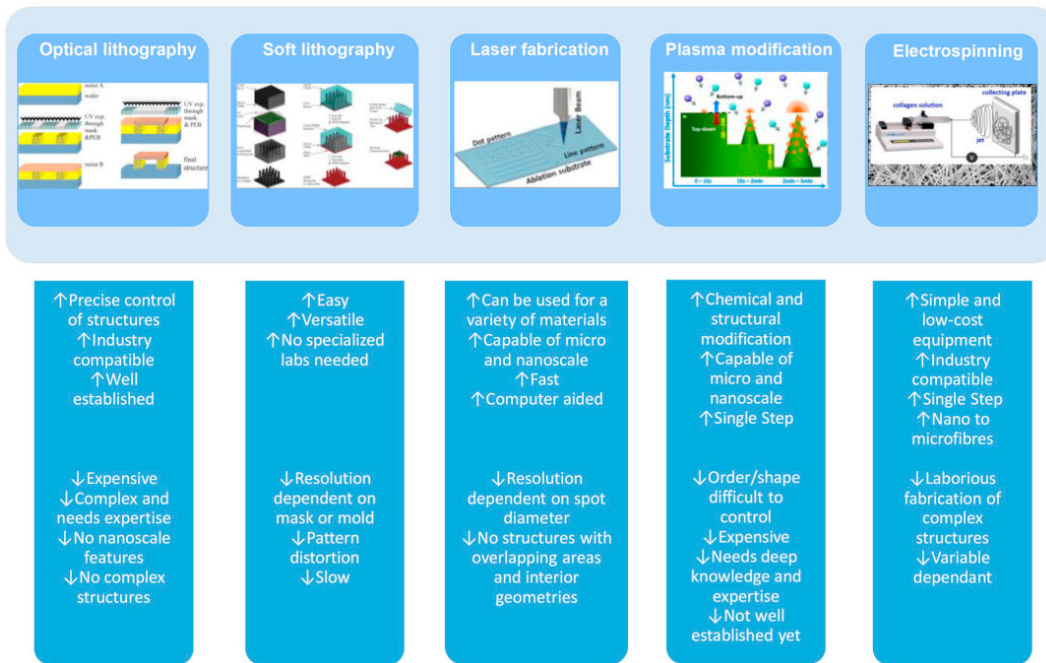


Fig. 3. Basic micro and nanoengineering methods used in cardiac tissue engineering. Schematic representations of the method, followed by advantages and disadvantages for their use in cardiac tissue engineering.

Kitsara 2019, Heart on a chip - Micro-nanofabrication and microfluidics. *Microelectronic Engineering* 203–204 (2019) 44–62.

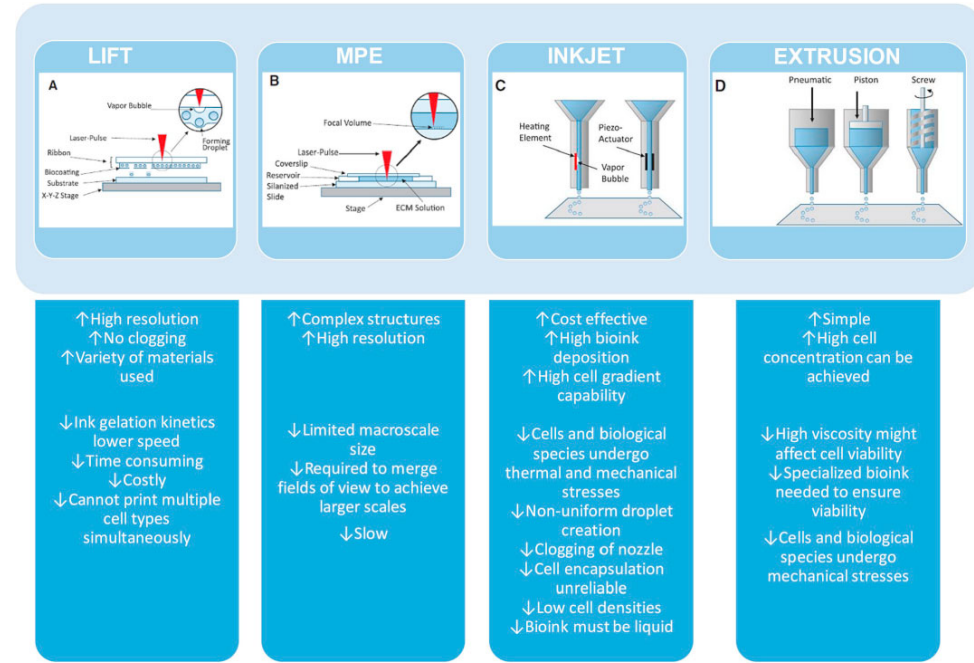


Fig. 5. Schematic representations of the four most widely used techniques of 3D printing for cardiac tissue engineering (reprinted with permission). (A) Laser-assisted bioprinting (LAB) which is based on laser-induced forward transfer (LIFT). (B) Multiphoton excitation (MPE) which is also called stereolithography. (C) Inkjet printing. (D) Microextrusion ink deposition.

Nanofabrication for Functional 3D Architectures

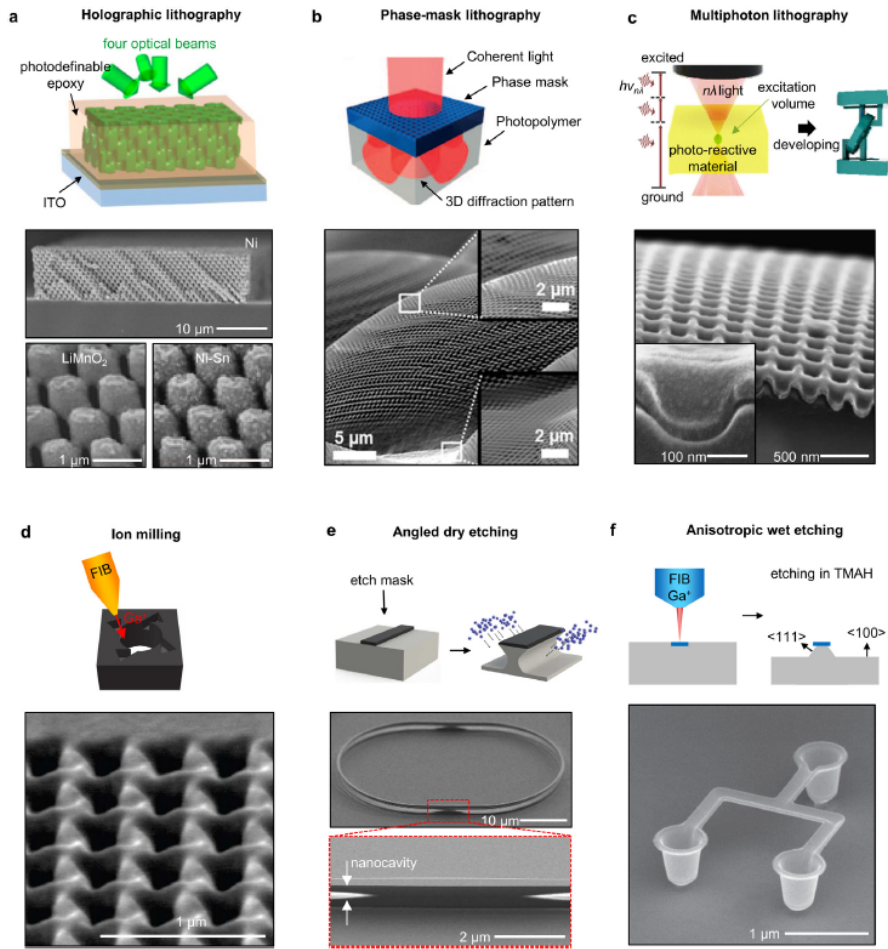


Fig. 1. Top-down approaches for the fabrication of functional 3D nanostructures.

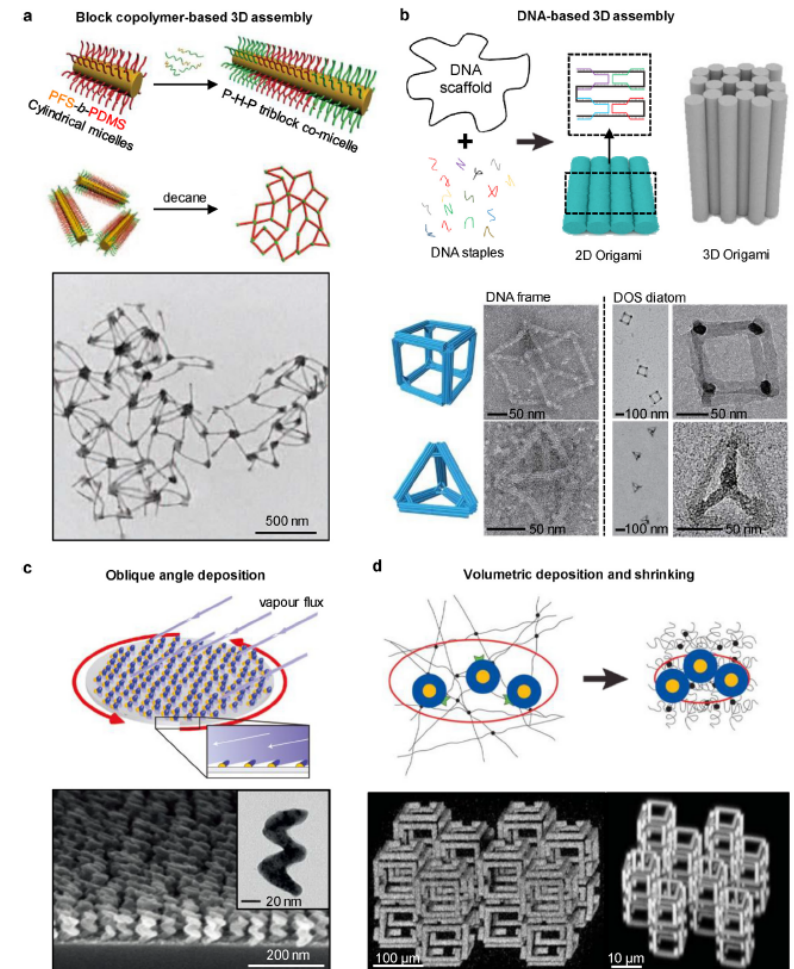


Fig. 2. Bottom-up approaches for the fabrication of functional 3D nanostructures.

Zhao, Lee, Han, Sharma. Chen, Ahn, and Rogers: Nanofabrication approaches for functional three-dimensional architectures.

Micro & Nanofiber Production by Large-Scale Centrifugal Multispinning

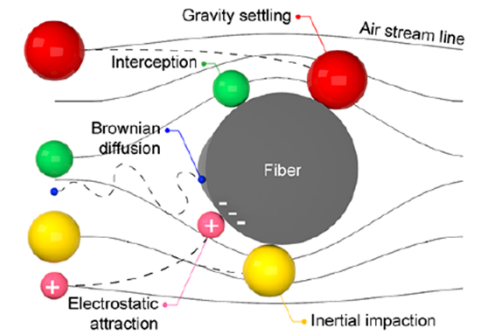
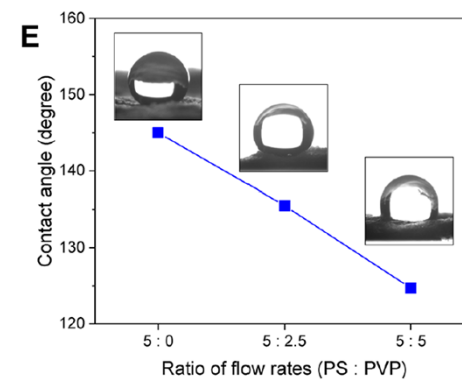
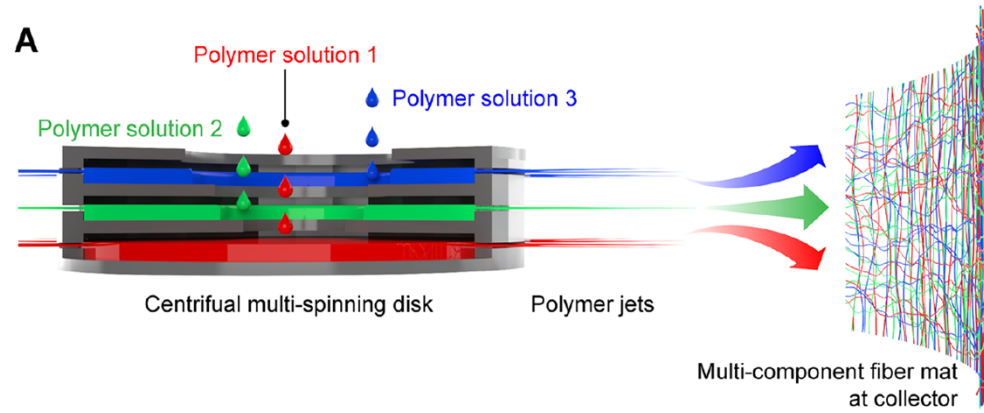


Figure 3. (E) Contact angle of spun nanofiber webs with different ratios of flow rates of PS and PVP solutions. Deionized water was used to measure the contact angle.

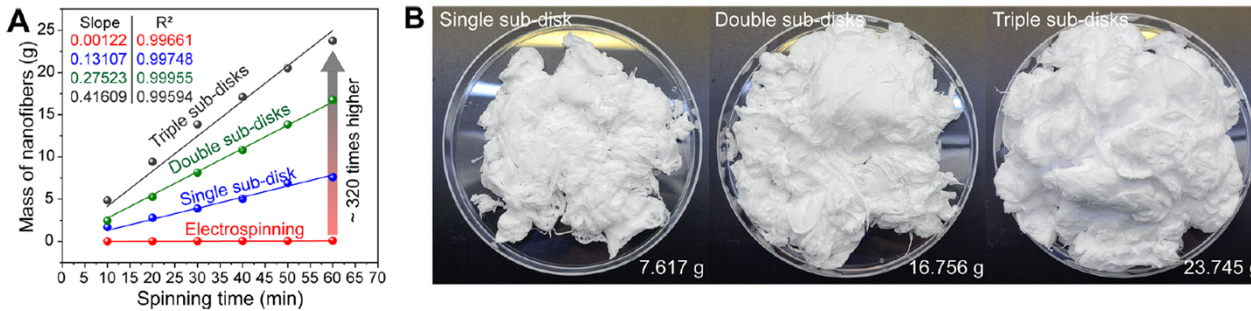


Figure 2. Production rate calculation of PS nanofibers. (A) Weight of nanofibers that were spun by centrifugal spinning and electrospinning according to spinning time. (B) Photographs of the prepared PS nanofibers spun by centrifugal multispinning with a different number of sub-disks

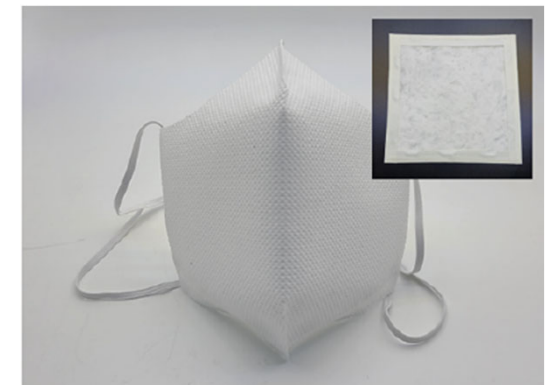


Figure 4. Mask filter application of PS nanofibers. The fabricated PS nanofiber-based mask for fine dust capture and filter for measurements of capture efficiency and resistance (inset).

Microfabrication of Microfluidics

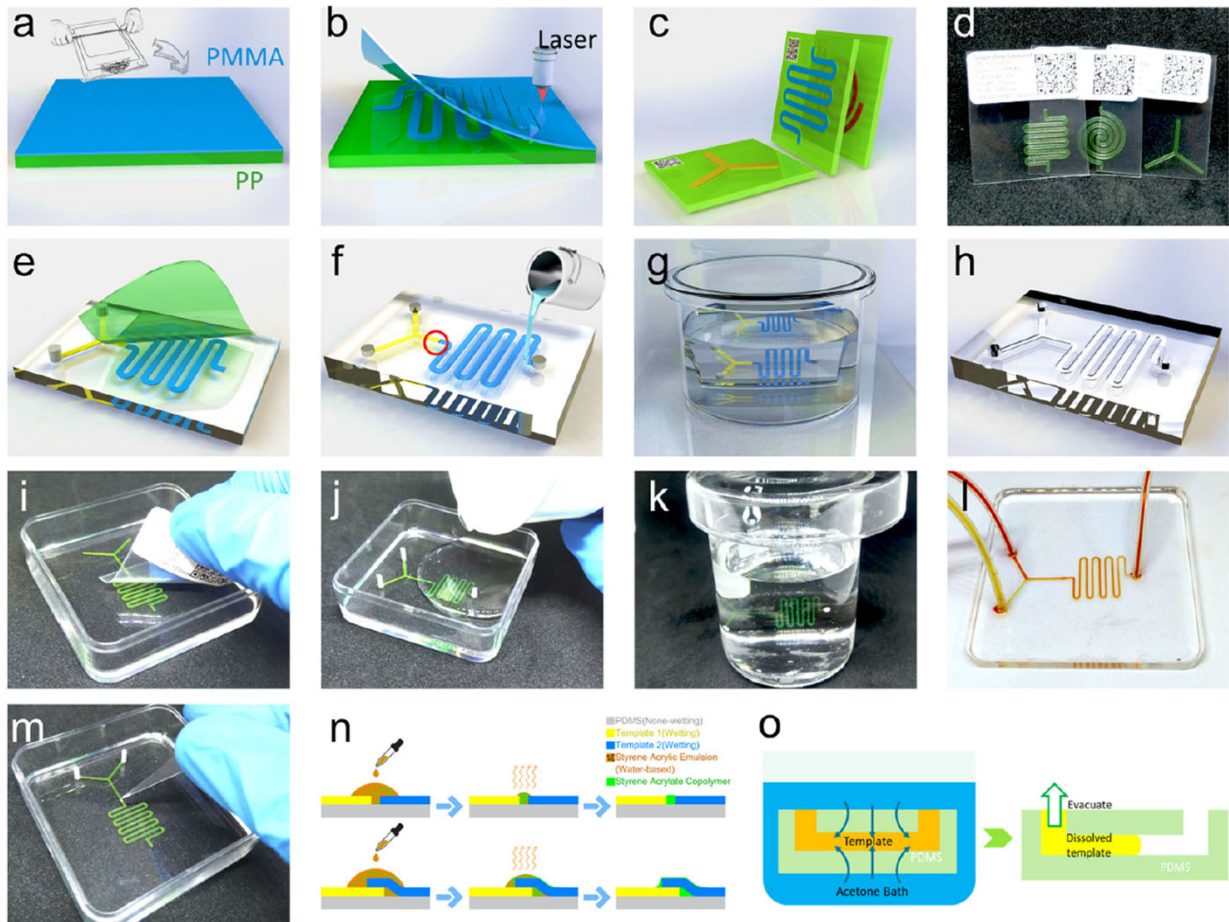


Figure 2. Fabrication process of creating microfluidic devices. (a–c) Schematic illustrations of preparing PMMA stickers on PP backing using laser cutting.

- (a) Coating the PMMA film on the PP sheet.
- (b) Laser cutting of PMMA patterns and removal of the unnecessary PMMA film.
- (c) Stickers of different microfluidic structures.
- (d) Laser-cut microfluidic stickers.
- (e–h) Schematic illustrations of creating microfluidics using the stickers.
- (e) Arranging and sticking the stickers on PDMS substrate.
- (f) Casting liquid PDMS and curing.
- (g) Acetone bathing.
- (h) Completed microfluidic chip.
- (i–l) Photograph of the process shown in (e)–(g).
- (m) Photograph of linking separate stickers with styrene acrylate copolymer emulsion.
- (n) Schematic illustration of wettability-guided emulsion linking of the stickers shown in (f) when two stickers are not in contact (top) and stickers overlap (bottom).
- (o) Schematic illustration of dissolving the template and evacuating the chip. Left: dissolving the template sticker in an acetone bath. Right: evacuation of the chip.

Microinjection Moulding

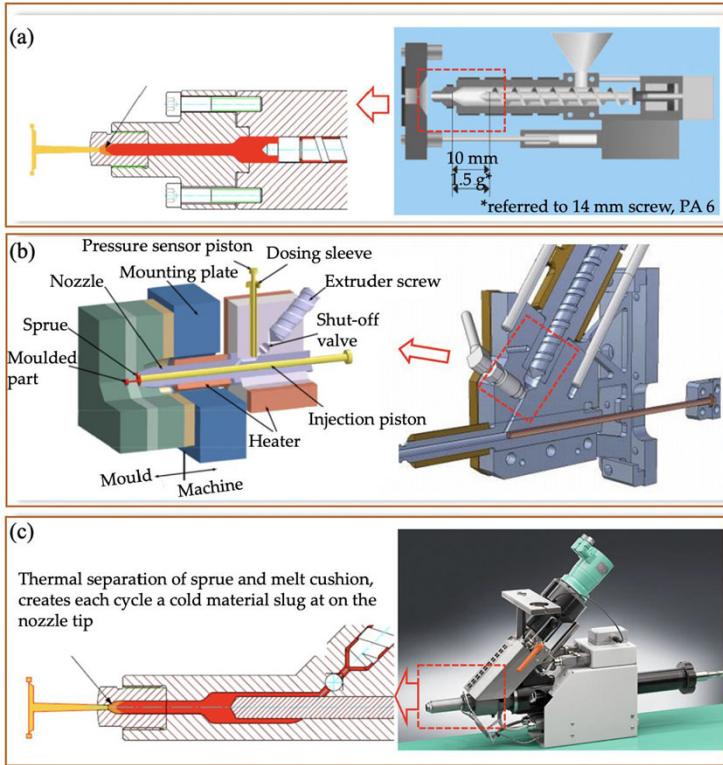


Figure 5. Microinjection moulding system: (a) one-step system, (b) two-step system (Arburg new microinjection module), and (c) three-step system (Microsystem50).

Zhang 2022, A review of microinjection moulding of polymeric micro devices

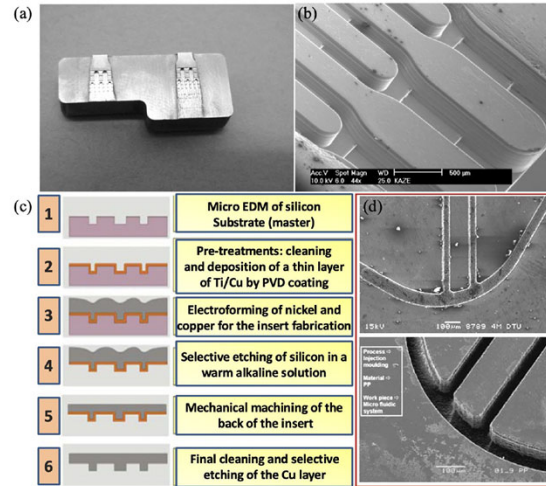


Figure 20. (a) Details of microchannel network of electroplated nickel mould insert and (b) microinjection moulded part for agglutination assays [93], (c) process chain, and (d) nickel mould insert and microchannels on microinjection moulded part [95].

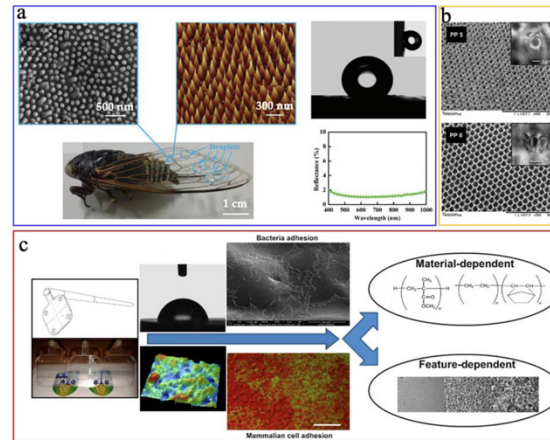


Figure 29. Applications of microinjection moulded functional micro/nano structured surfaces: (a) antireflective surfaces [127], (b) hydrophobic surfaces [128], (c) cell-adhesion surface [131].

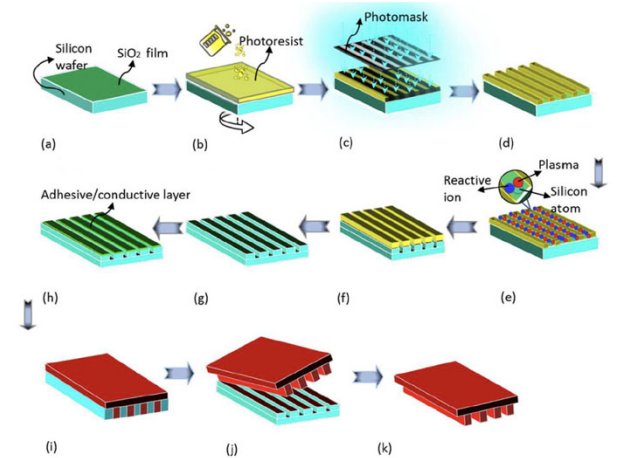


Figure 21. Processing steps required for preparing nickel mould insert: (a) silicon wafer preparation, (b) spin coating of photoresist, (c) exposure, (d) development, (e) silicon etching, (f) etched silicon with the photoresist, (g) patterned silicon, (h) metallization, (i) electroforming, (j) demoulding, and (k) electroformed nickel mould [96].

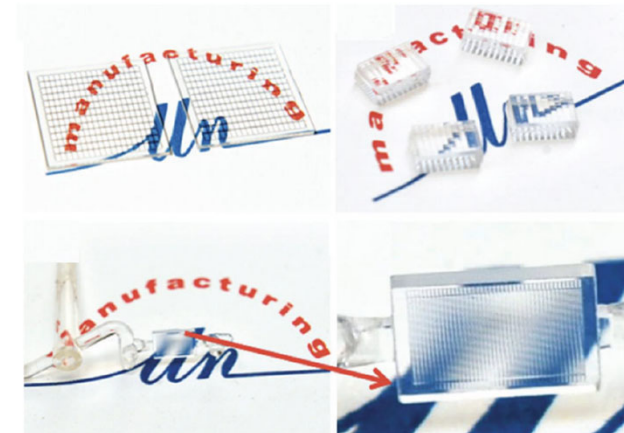


Figure 30. Microinjection moulded micro lenses array [133].

PLGA Coating on Water Droplets

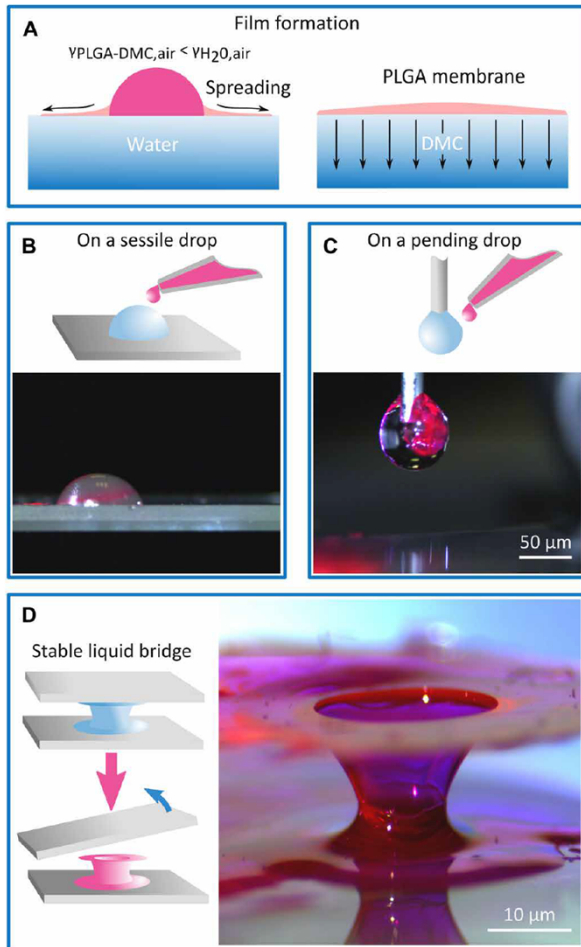


Fig. 1. Polymer packaging on water surface. (A) The mechanism for the formation of the PLGA membrane is composed of a phase of polymer solution spreading by surface tension over the free water surface while the DMC solvent diffuses, leading to the solidification of the PLGA membrane. Water packaging methods are shown in stable/static and dynamic/unstable conditions: (B) on a sessile drop on hydrophobic substrate and (C) wrapping, in real time, a drop flowing out of a needle. (D) Explanation of the 3D packaging approach over the wall of a stable liquid bridge between two plates.

Coppola 2019, Quick liquid packaging-Encasing water silhouettes by three-dimensional polymer membranes

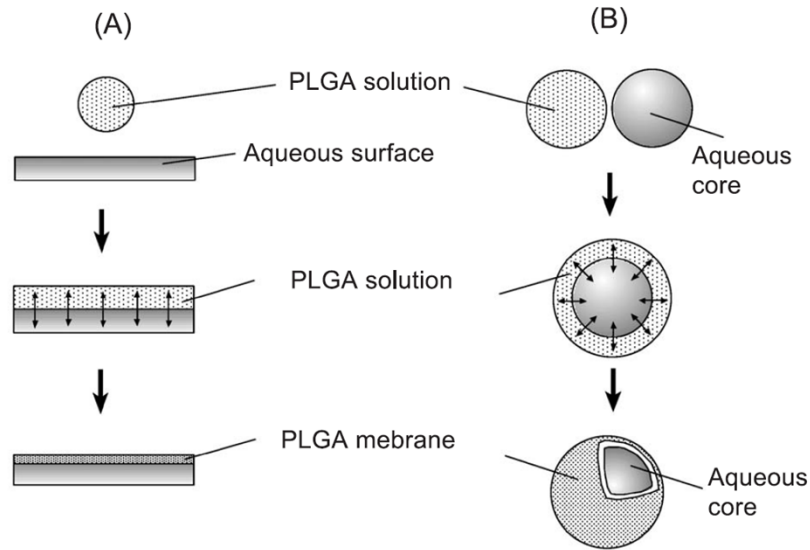


Fig. 1. Schematic description of the formation of a polymer membrane on an aqueous (A) film and (B) droplet through solvent exchange at the interface between the aqueous and the polymer solutions.

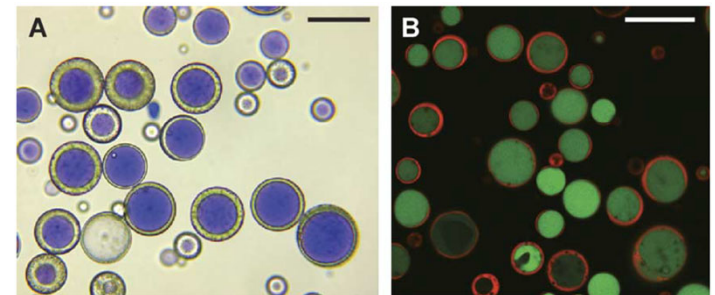
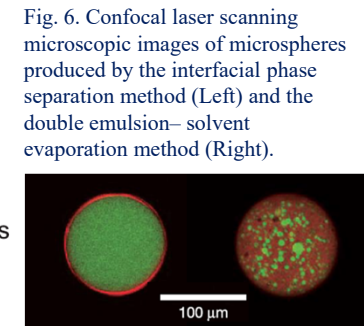
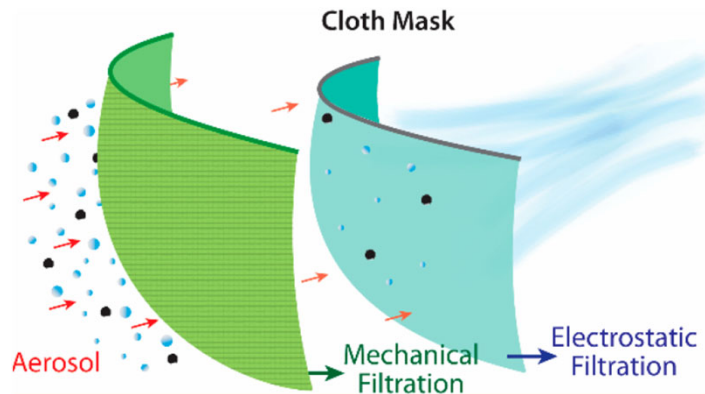


Fig. 2. (A) Bright-field microscopic image of the microcapsules produced by the coaxial ultrasonic atomizer. The aqueous cores look blue due to the presence of Coomassie brilliant blue R-250. (B) CLSM cross-sectional image of the microcapsules. The cores were labelled with FITC-dextran (green), and the polymer layer with Nile Red (red). Scale bars=100 μ m.

Yeo 2003, A new process for making reservoir-type microcapsules using ink-jet technology and interfacial phase separation
 Yeo 2004, A new microencapsulation method using an ultrasonic atomizer based on interfacial solvent exchange
 Yeo 2004, Solvent exchange method A novel microencapsulation technique using dual microdispensers

Aerosol Filtration Efficiency of Common Fabrics



Although the filtration efficiencies for various fabrics (cotton, silk, chiffon, flannel, various synthetics, and their combinations) when a single layer was used ranged from 5 to 80% and 5 to 95% for particle sizes of <300 nm and >300 nm, respectively, the efficiencies improved when multiple layers were used and when using a specific combination of different fabrics. Filtration efficiencies of the hybrids (such as cotton–silk, cotton–chiffon, cotton–flannel) was $>80\%$ (for particles <300 nm) and $>90\%$ (for particles >300 nm). The enhanced performance of the hybrids is likely due to the combined effect of **mechanical and electrostatic-based filtration**. **Cotton**, the most widely used material for cloth masks performs better at **higher weave densities** (i.e., thread count) and can make a significant difference in filtration efficiencies. **Gaps (as caused by an improper fit of the mask) can result in over a 60% decrease in the filtration efficiency**, implying the need for future cloth mask design studies to take into account issues of “fit” and leakage, while allowing the exhaled air to vent efficiently. Combinations of various commonly available fabrics used in cloth masks can potentially provide significant protection against the transmission of aerosol particles.

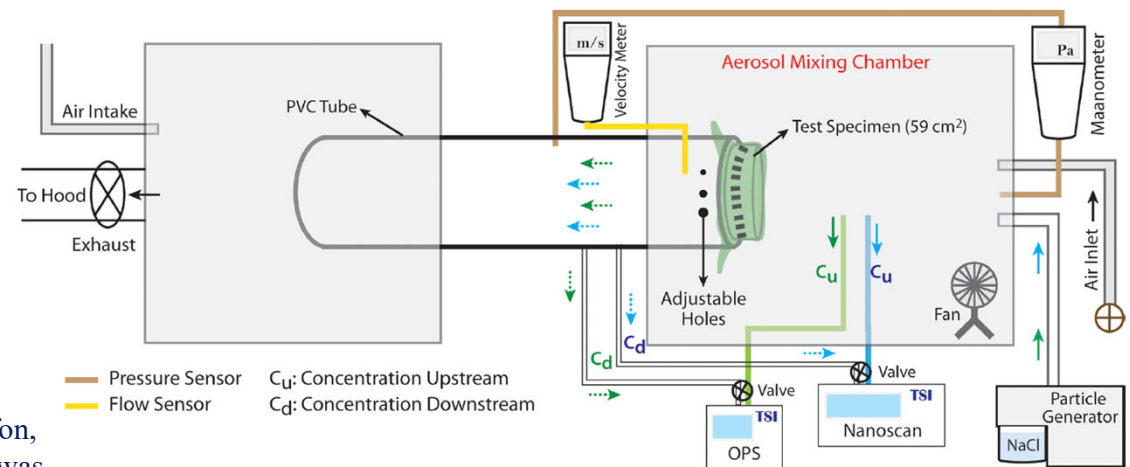


Figure 1. Schematic of the experimental setup. A polydisperse NaCl aerosol is introduced into the mixing chamber, where it is mixed and passed through the material being tested (“test specimen”). The test specimen is held in place using a clamp for a better seal. The aerosol is sampled before (upstream, C_u) and after (downstream, C_d) it passes through the specimen. The pressure difference is measured using a manometer, and the aerosol flow velocity is measured using a velocity meter. We use two circular holes with a diameter of 0.635 cm to simulate the effect of gaps on the filtration efficiency. The sampled aerosols are analyzed using particle analyzers (OPS and Nanoscan), and the resultant particle concentrations are used to determine filter efficiencies.

Nanopores & Molecular Imprinting

Dynamics of Driven Polymer Transport through a Nanopore

Molecular transport in confined nanoscale geometries is the basis for many emerging biotechnologies and biological processes. Polymer translocation across a nanoscale pore has been one of the most intensively studied topics in this field. Motivated in part by the goal of **DNA sequencing**, a rich phenomenology of behaviour has been observed, requiring ideas from polymer physics, surface science and fluid mechanics. **Nanopore sensors** work by measuring the modulations in ionic current as single molecules are electrophoretically driven through the pore. Ever since the first demonstration of nucleic acid detection, intensive efforts have focused on understanding the physics governing key experimental observables such as the translocation time (τ).

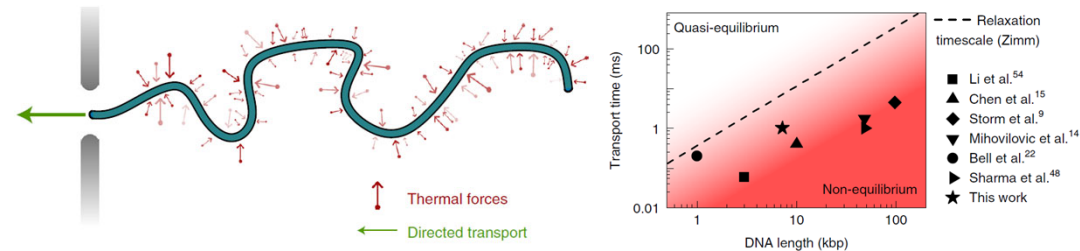


Fig. 1 | Translocation of dsDNA through synthetic nanopores is a non-equilibrium process. Schematic illustrating directed polymer translocation through a nanoscale aperture. The entropic forces due to thermal noise are indicated together with the driving force, for example, an electrophoretic force due to an applied potential difference.

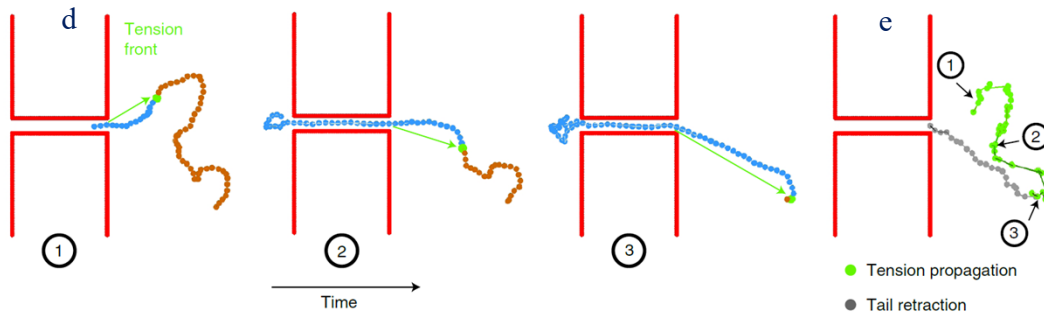
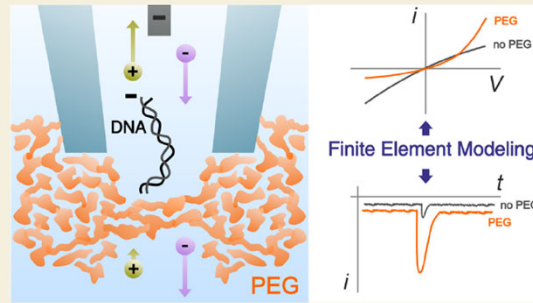


Fig. 5 | Simulations show that correlated motion arises from initial distribution of DNA conformations. d, Three snapshots (time increasing from left to right) of a simulation with the position of the tension front indicated by the bead in green. The chain is coloured blue for the section that has already been pulled taut and orange for the remainder of the chain. Loops in the DNA structure are successively straightened during the translocation as the tension front follows a random path set by the initial conformation of the DNA. e, Overall path of tension front for the translocation illustrated in d, with the green line showing the path traced out during the tension propagation phase and the grey line showing the path of the last bead once the tension reaches the end of the molecule. The numbers highlight the position of the tension front at the three snapshots shown in d.

Synthetic nanopores and nanostructured DNA molecules were used to directly measure the velocity profile of driven polymer translocation through synthetic nanopores. The results reveal a two-stage behaviour in which **the translocation initially slows with time before accelerating close to the end of the process**. Distinct local velocity correlations as the DNA polymer chain passes through the nanopore. Brownian dynamics simulations show that the two-stage behaviour is associated with tension propagation, with correlations arising from the random-walk conformation in which the DNA begins.

Enhanced Single-molecule Detection in a Nanopore

ABSTRACT: Solid-state nanopores have been widely employed in the detection of biomolecules, but low signal-to-noise ratios still represent a major obstacle in the discrimination of nucleic acid and protein sequences substantially smaller than the nanopore diameter. The addition of 50% poly(ethylene) glycol (PEG) to the external solution is a simple way to enhance the detection of such biomolecules. Here, we demonstrate with finite-element modeling and experiments that the addition of PEG to the external solution introduces a strong imbalance in the transport properties of cations and anions, drastically affecting the current response of the nanopore. We further show that the strong asymmetric current response is due to a polarity-dependent ion distribution and transport at the nanopipette tip region, leading to either ion depletion or enrichment for few tens of nanometers across its aperture. We provide evidence that a combination of the decreased/increased diffusion coefficients of cations/anions in the bath outside the nanopore and the interaction between a translocating molecule and the nanopore–bath interface is responsible for the increase in the translocation signals. We expect this new mechanism to contribute to further developments in nanopore sensing by suggesting that tuning the diffusion coefficients of ions could enhance the sensitivity of the system.



KEYWORDS: nanopipette, nanopore, finite-element modeling, nanofluidic diode, DNA, poly(ethylene) glycol, PEG

Marcuccio 2023, Mechanistic study of the conductance and enhanced single-molecule detection in a polymer–electrolyte nanopore

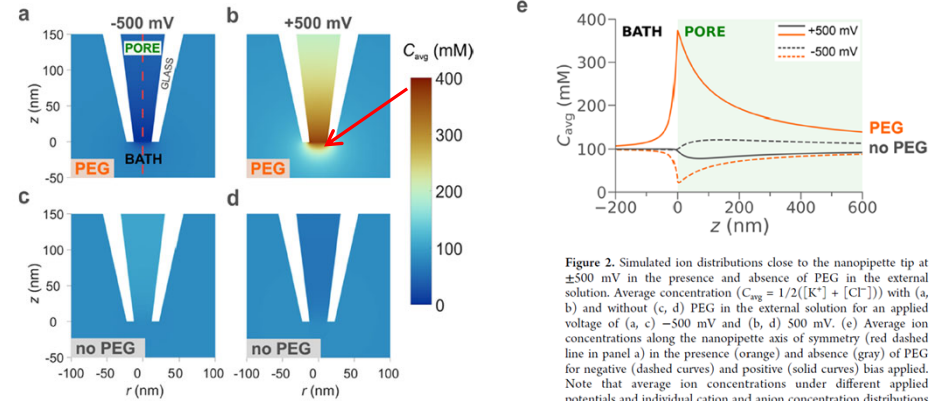
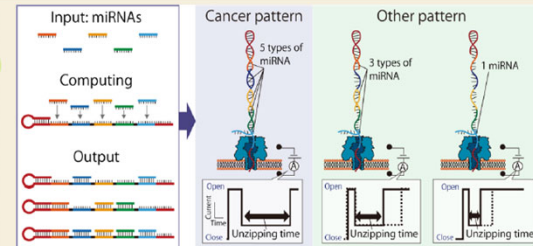


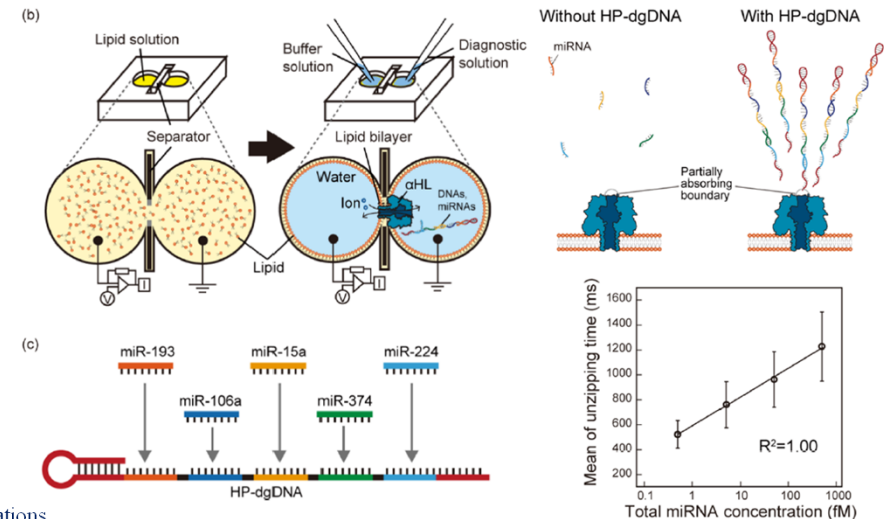
Figure 2. Simulated ion distributions close to the nanopipette tip at ± 500 mV in the presence and absence of PEG in the external solution. Average concentration ($C_{\text{avg}} = 1/2([K^+] + [Cl^-])$) with (a, b) and without (c, d) PEG in the external solution for an applied voltage of (a, c) -500 mV and (b, d) 500 mV. (e) Average ion concentrations along the nanopipette axis of symmetry (red dashed line in panel a) in the presence (orange) and absence (gray) of PEG for negative (dashed curves) and positive (solid curves) bias applied. Note that average ion concentrations under different applied potentials and individual cation and anion concentration distributions are included in the Supporting Information (Section S5).

ABSTRACT: This paper describes a method for detecting microRNA (miRNA) expression patterns using the nanopore-based DNA computing technology. miRNAs have shown promise as markers for cancer diagnosis due to their cancer type specificity, and therefore simple strategies for miRNA pattern recognition are required. We propose a system for pattern recognition of five types of miRNAs overexpressed in bile duct cancer (BDC). The information of miRNAs from BDC is encoded in diagnostic DNAs (dgDNAs) and decoded electrically by nanopore analysis. With this system, we succeeded in the label-free detection of miRNA expression patterns from the plasma of BDC patients. Moreover, our dgDNA–miRNA complexes can be detected at subfemtomolar concentrations, which is a significant improvement compared to previously reported limits of detection ($\sim 10^{-12}$ M) for similar analytical platforms. Nanopore decoding of dgDNA-encoded information represents a promising tool for simple and early cancer diagnosis.



KEYWORDS: DNA computing technology, nanopore, microRNA, cancer, membrane

Takeuchi 2022, Pattern Recognition of microRNA expression in body fluids using nanopore decoding at subfemtomolar concentrations



A Nanopore Protein Reader

Since the 1990s, nanopores have been used for sequencing strands of DNA. A voltage is applied across the nanopore, which is embedded in a thin lipid membrane, causing a stretch of DNA to thread through the pore. A helicase enzyme then methodically pulls the molecule back through. As this happens, the nitrogenous bases that make up the DNA affect the ion current flowing through the pore, and by measuring these current changes, researchers can decode the DNA sequence. Now, biophysicist Cees Dekker of Delft University of Technology in the Netherlands and colleagues have repurposed this technology for deciphering amino acid differences among peptides (*Science*, 374:1509–13, 2021).

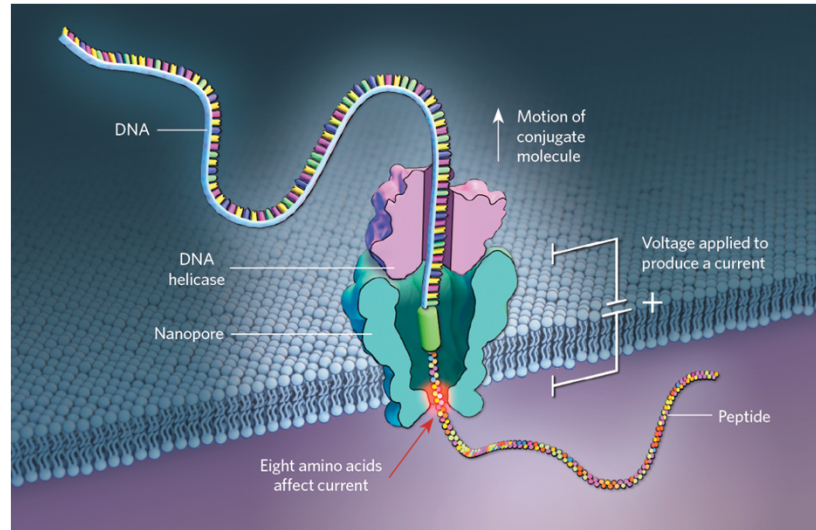
Dekker's team starts by linking a synthetic peptide with the 5' end of a single strand of DNA. After a zap of voltage sends the conjugated molecule through the nanopore, the Hel308 helicase walks on the DNA section, pulling both the DNA and the attached peptide back through the nanopore. As with DNA sequencing, ratcheting the peptide through the nanopore changes the ion current, and the researchers can link the changes to a specific sequence of amino acids in their designed peptide. The target peptide is read in this way multiple times, threading back through the pore as the helicase falls off and being pulled back through again by another, improving the technique's fidelity. In a proof-of-principle study, the researchers were able to distinguish three different 26-amino-acid-long peptides that only varied by a single amino acid.

The method cannot be used to decode protein sequences without a known reference for comparison, however. That's because not only does the amino acid at the pore's entrance affect the ion current, but the eight surrounding amino acids do as well. "Right now, it is not yet a full de novo sequencing tool," Dekker writes in an email to *The Scientist*. "Yet it is very powerful since we showed that by changing even a single amino acid within the chain, we observed dramatic differences in the current step signals." The new method therefore could be useful for detecting amino acid mutations or identifying the presence of a specific peptide of interest within a mixture of proteins, he says.

In theory, this method is "perfect" for analyzing proteins, says Giovanni Maglia, a chemical biologist at the University of Groningen who recently published a proteasome-nanopore that can unfold proteins for sequencing. The helicase is already known to work for DNA sequencing, he notes, and it pulls the DNA through the pore in a controlled way. Maglia points out that the approach is limited to peptides that are 26 amino acids or shorter, however. This is because the helicase sits on top of the pore and can only pull the molecule by its DNA tail.

Dekker acknowledges this limitation but notes that this read length is enough to discriminate all proteins in the human proteome if they are broken into pieces. Also, the nanopore-based approach requires smaller samples than does mass spectrometry—a commonly used protein analysis approach—and would be able to detect rare variants, something mass spec can't, Dekker says. ■

Researchers link a stretch of DNA to a peptide of interest and measure changes in electrical current as the molecule is pulled by a helicase through a nanopore (Sophie Fessl).



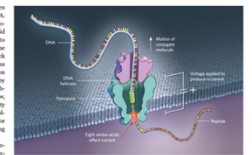
Protein Reader

PULL AND READ: In a proof-of-concept study, researchers show that nanopore sequencing techniques can be used to interrogate the sequence of a peptide. First they link the peptide to a stretch of DNA and apply a voltage to feed the conjugated molecule through a nanopore embedded in a thin membrane. A helicase molecule then walks along the DNA strand, effectively pulling the DNA and attached peptide back through the pore. As the peptide passes through, changes in the current across the membrane can be measured, providing clues to the amino acid composition of that stretch of the peptide.

Researchers link a stretch of DNA to a peptide of interest and measure changes in electrical current as the molecule is pulled by a helicase through a nanopore.

BY SOPHIE FESSL

Since the 1990s, nanopores have been used for sequencing strands of DNA. A voltage is applied across the nanopore, which is embedded in a thin lipid membrane, causing a stretch of DNA to thread through the pore. A helicase enzyme then methodically pulls the molecule back through. As this happens, the nitrogenous bases that make up the DNA affect the ion current flowing through the pore, and by measuring these current changes, researchers can decode the DNA sequence. Now, biophysicist Cees Dekker of Delft University of Technology in the Netherlands and colleagues have repurposed this technology for deciphering amino acid differences among peptides (*Science*, 374:1509–13, 2021).



Dekker's team starts by linking a synthetic peptide with the 5' end of a single strand of DNA. After a zap of voltage sends the conjugated molecule through the nanopore, the Hel308 helicase walks on the DNA section, pulling both the DNA and the attached peptide back through the nanopore. As with DNA sequencing, ratcheting the peptide through the nanopore changes the ion current, and the researchers can link the changes to a specific sequence of amino acids in their designed peptide. The target peptide is read in this way multiple times, threading back through the pore as the helicase falls off and being pulled back through again by another, improving the technique's fidelity. In a proof-of-principle study, the researchers were able to distinguish three different 26-amino-acid-long peptides that only varied by a single amino acid.

The method cannot be used to decode protein sequences without a known reference for comparison, however. That's because not only does the amino acid at the pore's entrance affect the ion current, but the eight surrounding amino acids do as well. "Right now, it is not yet a full de novo sequencing tool," Dekker writes in an email to *The Scientist*. "Yet it is very powerful since we showed that by changing even a single amino acid within the chain, we observed dramatic differences in the current step signals." The new method therefore could be useful for detecting amino acid mutations or identifying the presence of a specific peptide of interest within a mixture of proteins, he says.

In theory, this method is "perfect" for analyzing proteins, says Giovanni Maglia, a chemical biologist at the University of Groningen who recently published a proteasome-nanopore that can unfold proteins for sequencing. The helicase is already known to work for DNA sequencing, he notes, and it pulls the DNA through the pore in a controlled way. Maglia points out that the approach is limited to peptides that are 26 amino acids or shorter, however. This is because the helicase sits on top of the pore and can only pull the molecule by its DNA tail.

Dekker acknowledges this limitation but notes that this read length is enough to discriminate all proteins in the human proteome if they are broken into pieces. Also, the nanopore-based approach requires smaller samples than does mass spectrometry—a commonly used protein analysis approach—and would be able to detect rare variants, something mass spec can't, Dekker says. ■

A Nanopore Protein Reader

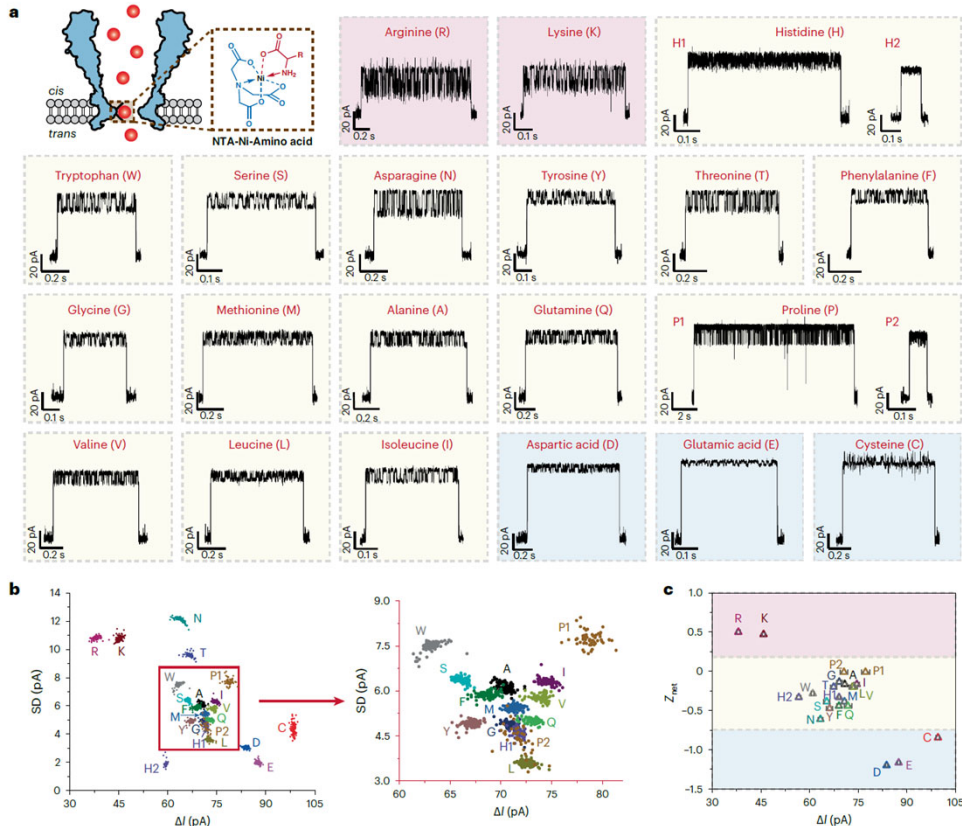


Fig. 2 | Discrimination of 20 amino acids using MspA-NTA-Ni. **a**, The schematics of amino acid sensing (top left) and representative events generated by different amino acids when measured with MspA-NTA-Ni. The measurements were carried out as described in Methods. A total of 20 proteinogenic amino acids were separately added to *cis* with a final concentration of 2 mM (A, C, F, G, H, K, M, N, Q, R, S, T, V, W, Y), 4 mM (D, E, I, L) or 40 mM (P) (Supplementary Figs. 8–11 and Supplementary Table 4). The final concentration of proline was set higher to compensate for its low rate of event appearance. Histidine and proline both produce two types of nanopore events, defined respectively as H1/2 and P1/2. According to their net charge (Z_{net}), all 20 amino acids were classified into three groups, in which amino acids with positive charge, weak negative charge and strong negative charge were marked with a red, yellow or blue background,

respectively. **b**, The scatter plot of ΔI versus SD of events acquired with different amino acids. One hundred events acquired with each amino acid were used to generate the plot, according to which, most amino acid events are fully distinguishable. To clarify the detail, the events inside the red box are further zoomed in and shown on the right. Although the events corresponding to P2 and H1 appear to overlap in the plot, their event characteristics are visually different and can be discriminated when other event features such as dwell time, skewness and kurtosis are simultaneously considered. **c**, The correlation between ΔI and Z_{net} of amino acids. Generally, the blockage amplitude (ΔI) is larger when the net charge of the amino acid is more negative. The color background in the plot is consistent with that in **a**.

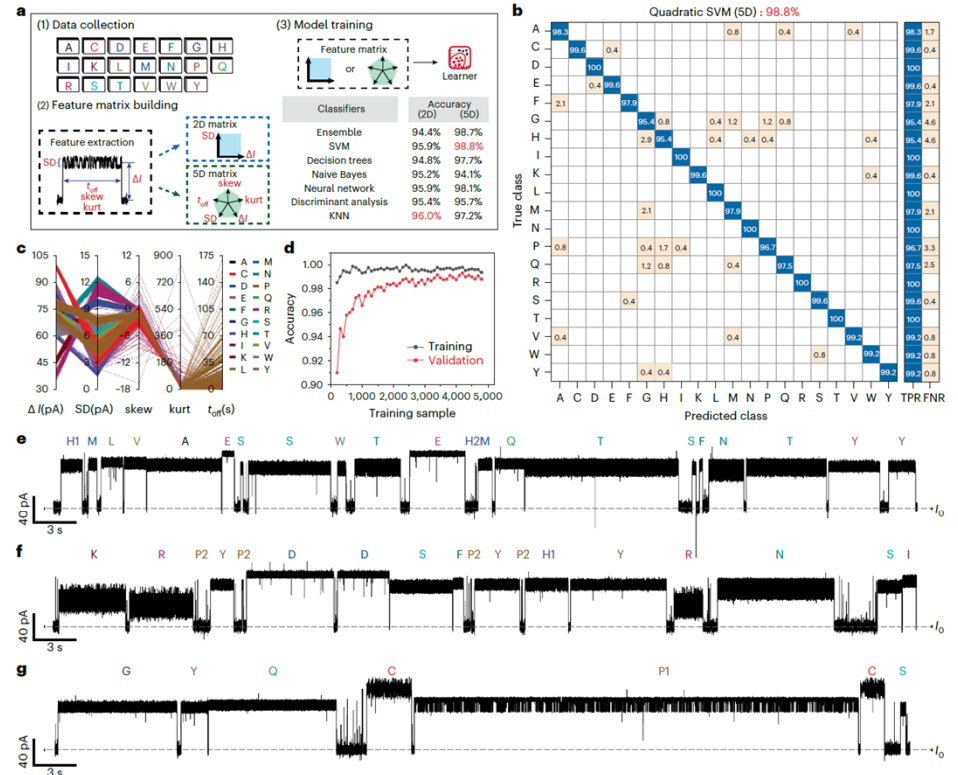


Fig. 3 | Identification of 20 amino acids by machine learning. **a**, The workflow of machine learning. In brief, sensing events separately acquired with 20 amino acids were collected to form a dataset. Five event features (ΔI , SD, skewness (skew), kurtosis (kurt) and t_{off}) were extracted from each event to form a feature matrix. A 2D feature matrix and a 5D feature matrix were built for machine learning. The 2D matrix contains only two features (ΔI and SD), similar to that in a 2D scatter plot (Fig. 2b). The 5D matrix, which contains all five features, includes more information from sensing. Machine learning was performed with the Classification Learner toolbox of MATLAB. Seven classifiers were evaluated with 10-fold cross-validation to screen the best-performing model. For the 2D matrix, the highest validation accuracy is 96.0% (Supplementary Table 6). For the 5D matrix, the highest validation accuracy reaches 98.8%, achieved by the quadratic SVM model (Supplementary Table 7). **b**, The confusion matrix of

amino acid classification generated by the quadratic SVM model using the 5D feature matrix. TPR (true-positive rate) and FNR (false-positive rate) represent the correct or false classification of each true class, respectively. **c**, The parallel coordinate plots generated from the 5D feature matrix. **d**, The learning curve of the quadratic SVM model for varying sample size. **e–g**, Representative traces acquired during simultaneous sensing of all 20 amino acids. The measurements were performed as described in Methods. All amino acids were simultaneously added to *cis*. The final concentration of H and C was 0.1 mM. The concentration of F, M, N, I, S was 0.5 mM. The concentration of P was 20 mM. The concentration of all remaining amino acids was 1 mM. Zoomed-in views of these traces are shown in Supplementary Figs. 21–23. The events were predicted with the trained quadratic SVM model.

Wang 2024, Unambiguous discrimination of all 20 proteinogenic amino acids and their modifications by nanopore

Molecular Imprinting

Molecular imprinting refers to **the creation of specific recognition sites in polymer networks by cross-linking in the presence of a template molecule**, which represents the target to be recognized. This process is performed by mixing a solution of one (or several) monomer(s) with the template, thereby forming temporary interactions between the two. Subsequent cross-linking and polymerization, followed by removal of the template, lead to the formation of a polymer structure with embedded complementary cavities for the superstructure of the imprinted molecule. These nanocavities preserve not only the shape and size but also the molecular interactions necessary for the recognition of the target. The resulting **molecularly imprinted polymers (MIPs)** are thus able to selectively recognize and bind the target via a “lock and key” mechanism similar to those found in biological systems (e.g., antibodies and enzymes). These biomimetic polymeric networks can be prepared by designing interactions between the building blocks of a biocompatible network and the desired specific ligand and stabilizing these interactions by a three-dimensional (3D) structure. These structures are at the same time flexible enough to allow for diffusion of solvent and ligand into and out of the network.



Tour groups at the Chinese Theatre on Feb. 22, 1983 (George Rose/ LA Times)

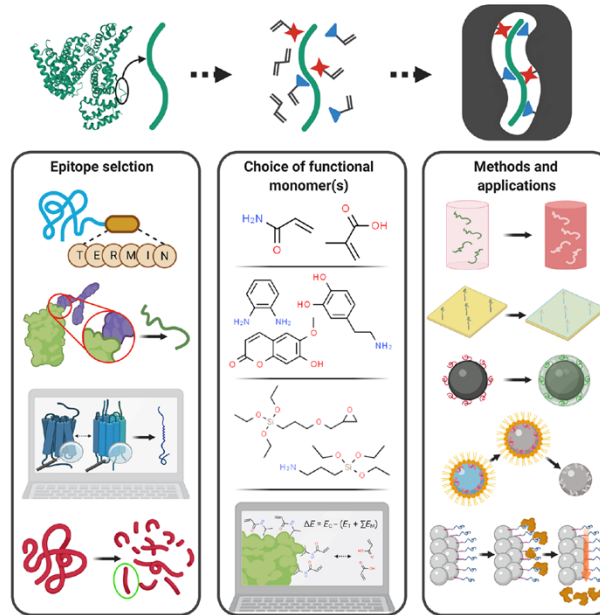


Fig. 2. Major steps in the process of epitope imprinting. Each one presents an array of options that must be carefully considered to optimize MIP efficacy considering the target application.

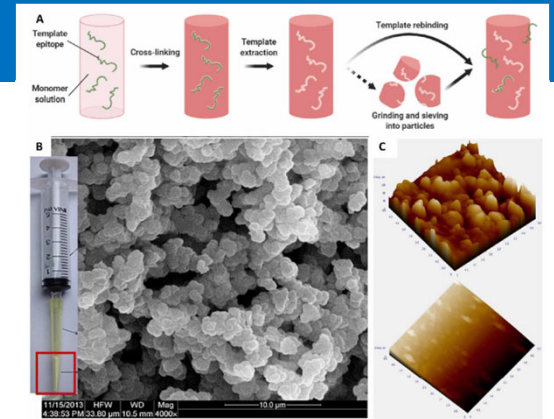


Fig. 6. Bulk molecular imprinting method and representative applications. (A) Bulk imprinting procedure; bulk MIPs can further be processed into microparticles/nanoparticles by grinding and sieving (dashed arrow). (B) Scanning electron microscopy micrographs of imprinted (MIP C) and nonimprinted (NIP C) poly(2-hydroxyethyl methacrylate-co-N-methacryloyl-L-aspartic acid) cryogels for IgG purification.

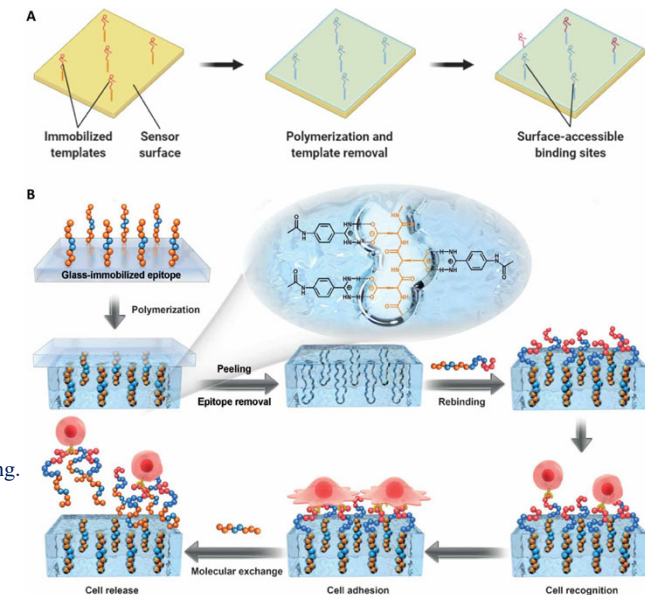


Fig. 7. Surface imprinting on thin flat films. (A) Surface MI procedure, allowing the creation of surface-accessible binding sites for the target molecule. (B) Generation of an epitope-imprinted biointerface for dynamic cell adhesion and harvesting.

Telxelra 2021, Epitope-imprinted polymers-Design principles of synthetic binding partners for natural biomacromolecules

Molecularly Imprinted Polymers

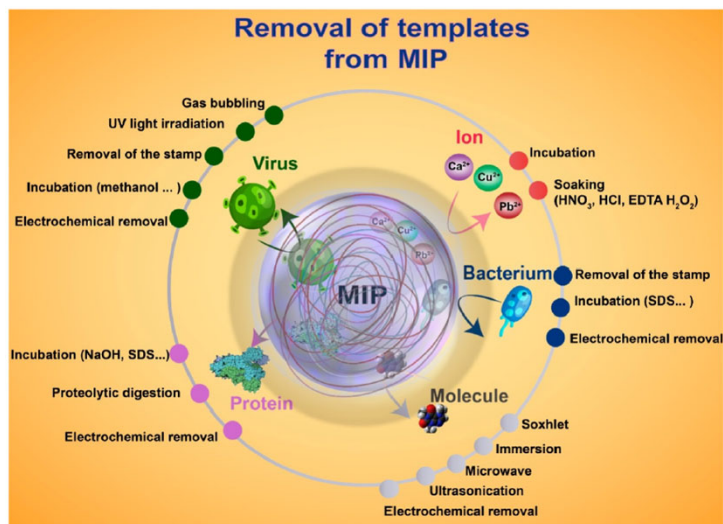


Fig. 2. Summary of selected removal approaches of templates from MIPs. EDTA: ethylenediaminetetraacetic acid; SDS: Sodium dodecyl sulfate.

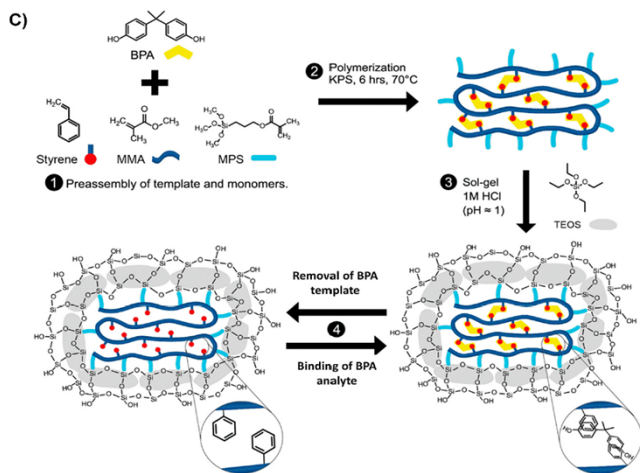


Fig. 9. C): Preparation of MIP and its coating with SiO₂.

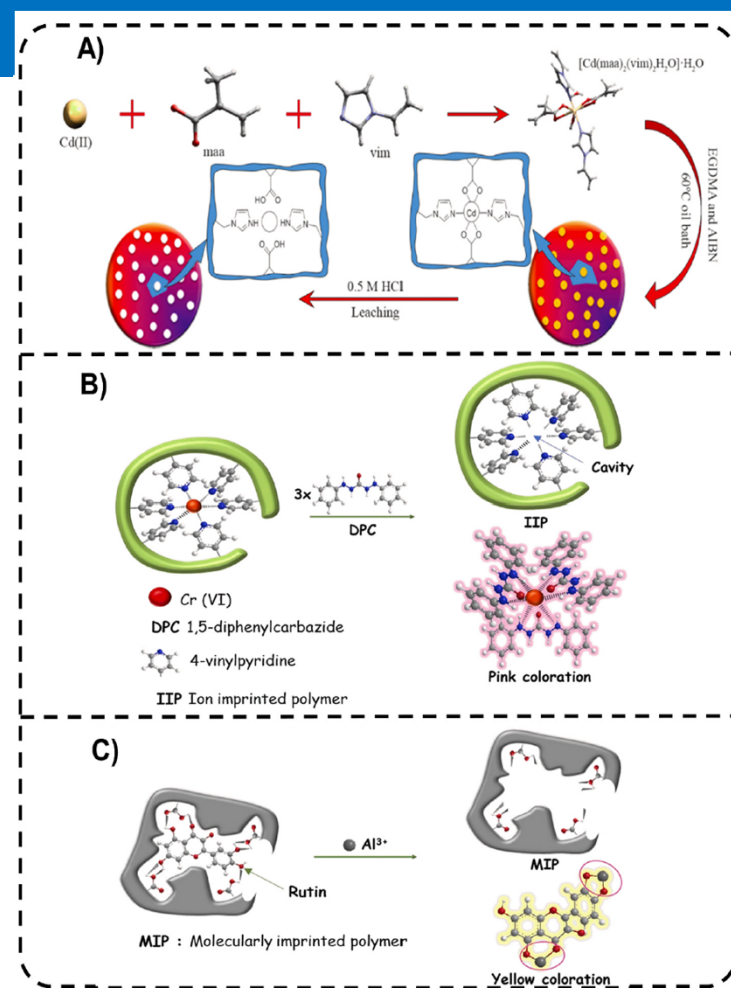
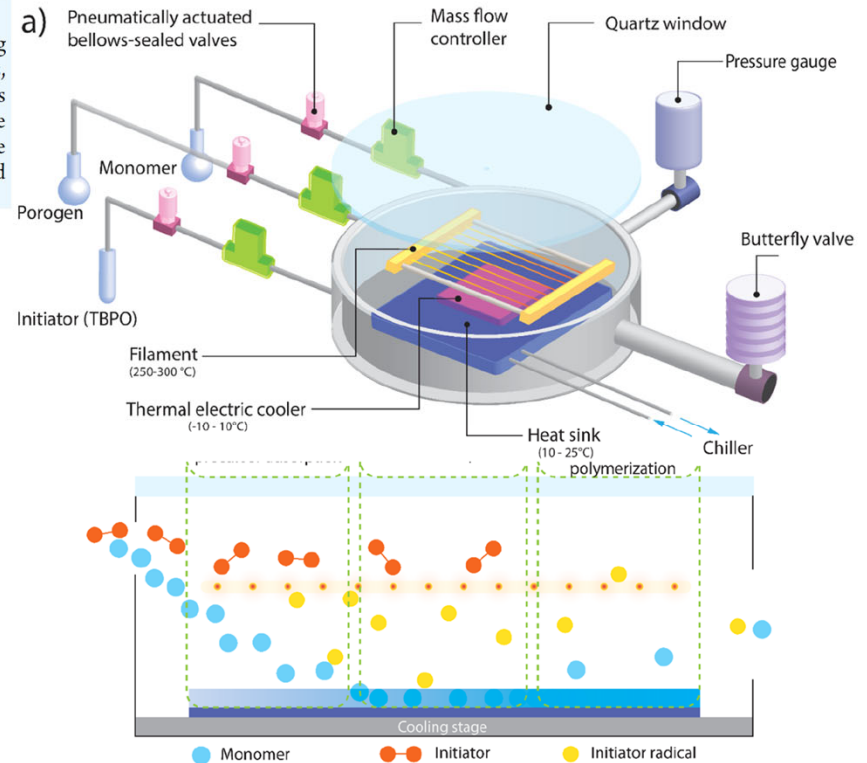
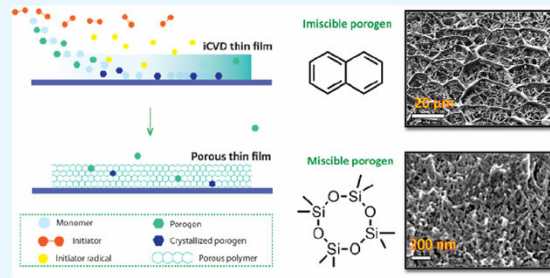


Fig. 3. A) Synthesis of Cd⁺² imprinted polymer and removal of Cd⁺² using HCl as a template removal agent. Removal mechanism of B) Cr⁶⁺ from ion-imprinted polymers (IIPs) and C) Rutin from MIP. MAA: Methacrylic acid; VIM: 1-vinylimidazole; EGDMA: Ethylene glycol dimethacrylate; AIBN: Azobisisobutyronitrile.

Porous Polymer Films with Tunable Pore Size and Morphology

ABSTRACT: The fabrication of porous polymer thin films with precise thickness and morphological control through conventional solvent-based techniques is challenging. Herein, we present a fabrication method for porous polymer thin films based on chemical vapor deposition that provides control over pore size, pore morphology, and film thickness. The porous films are prepared by co-depositing crystallizable porogen molecules with cross-linked poly(glycidyl methacrylate) (pGMA) thin films, which are synthesized by initiated chemical vapor deposition (iCVD). As the porogen is deposited, it crystallizes and phase-separates from the polymer film; simultaneous polymerization of pGMA limits porogen crystal growth, controlling the size of crystals. Using naphthalene as porogen resulted in thin films with pore sizes from 5.9 to 24.2 μm and porosities ranging from 59.4 to 78.4%. Using octamethylcyclotetrasiloxane as porogen, which is miscible with the GMA monomer, drastically reduced the pore dimensions, ranging from 14.4 to 65.3 nm with porosities from 8.0 to 33.2%. The film morphology was highly dependent on the relative kinetics of porogen crystallization, phase separation, and heterogeneous polymerization. The kinetics of these competing processes are discussed qualitatively based on nucleation theory and Cahn–Hilliard theory. Fourier-transform infrared spectroscopy confirmed the retention of the reactive epoxide functionality of glycidyl methacrylate, which can enable further chemical derivatization as required for application in optoelectronics, sensing, separations, and biomedical devices.



Nanomedicine

Current Hurdles of Nanomedicines

The field of nanomedicine has significantly influenced research areas such as drug delivery, diagnostics, theranostics, and regenerative medicine; however, the further development of this field will face significant challenges at the regulatory level if related guidance remains unclear and unconsolidated.

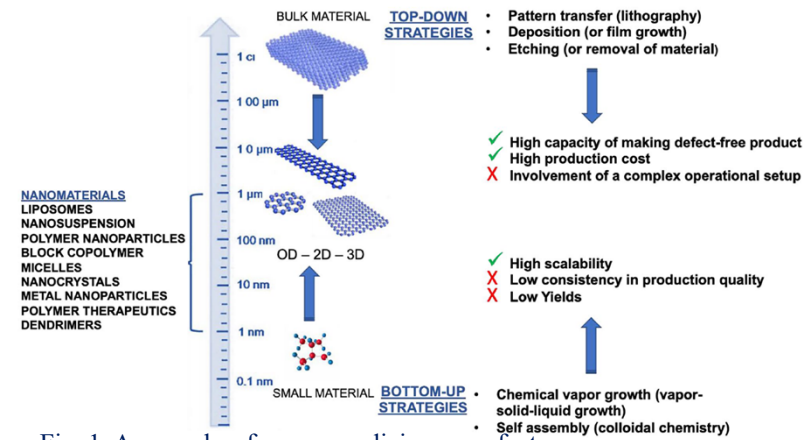


Fig. 1. Approaches for nanomedicine manufacture.

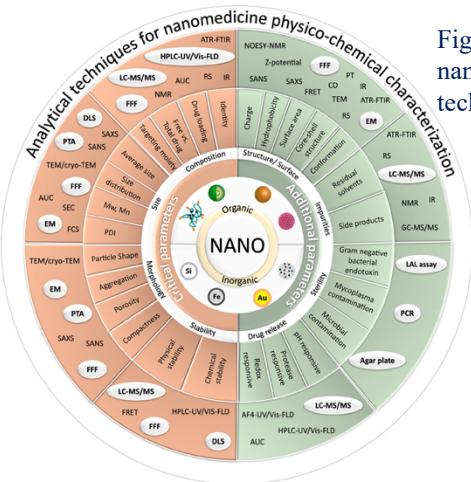


Fig. 3. Critical and additional parameters of nanomedicines and corresponding analytical techniques for their characterization.

The major challenges associated with nanomedicine regulation.

- Lack of a unified definition or classification of nanomedicines/nanomaterials.
- Lack of agreed regulations .
- Analytical methods differ for each nanomaterial.
- PK profiles diverge from standardized constituent materials.
- Stability issues after scale-up for manufacturing.

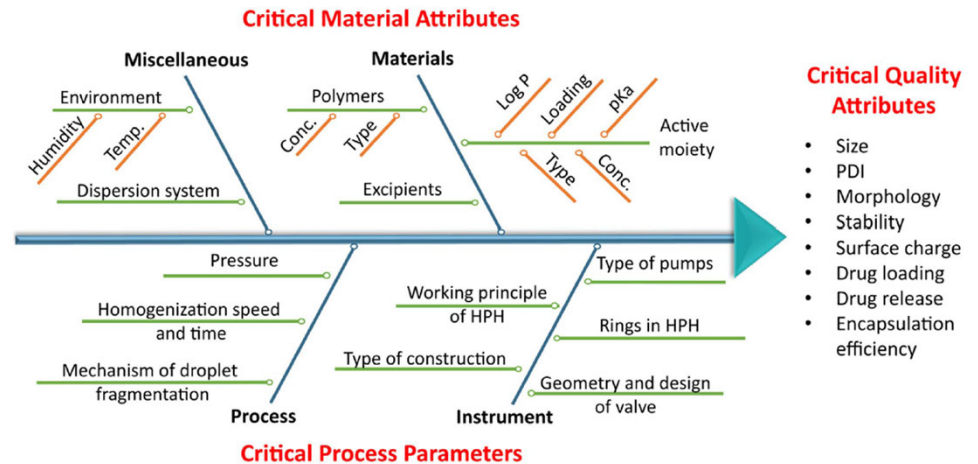


Fig. 2. Representation of those **critical material attributes (CMA)** and **critical process parameters (CPP)** that cause discrepancy and variability of **critical quality attributes (CQA)** during the rational design and production of nanomedicines.

Despite the promising advances made in preclinical animal models, the clinical translation of nanomedicines remains a slow, biased, and often failed affair. There exists a **general lack of specific protocols**, and the **characterization of materials and biological mechanisms** and the statistical analyses often employed remain inadequate. Moreover, the vast and significant **heterogeneity of models adopted**, a reluctance to share results, and the **inaccuracy of study design** have hampered the translation of nanomedicines into late clinical trial stages.

Nanotechnology for COVID-19

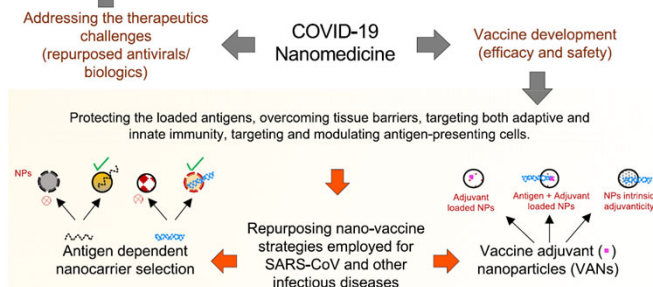
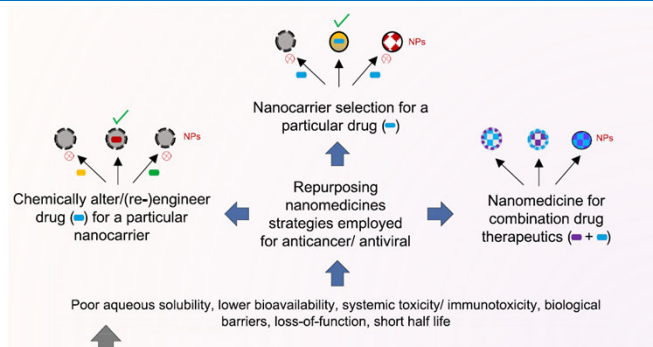


Figure 4. Nanomedicine strategies for COVID-19 therapeutics and vaccine development.

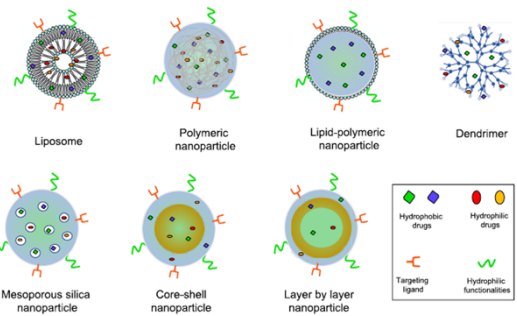
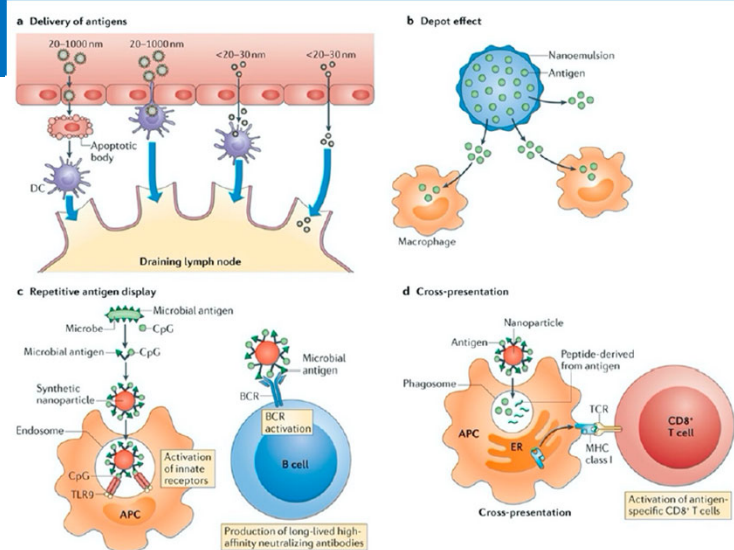


Figure 5. Nanocarrier platforms utilized for combination drug therapeutics.



Chauhan 2020, Nanotechnology for COVID-19- Therapeutics and Vaccine Research

Figure 6. Nanoparticle-based immune response modulation. (a) Antigen delivery by nanoparticles (size-dependent penetration and tissue or organ targeting). (b) Depot effect provides a prolonged and sustained release of stable antigen. (c) Repetitive antigen display as a result of the antigen presentation on the nanoparticle surface assists the receptor activation on APCs and B cells and (d) cross presentation of the antigen delivered by the nanoparticles (cytosolic delivery) to activate antigen specific CD8+ T cells. Antigen-presenting cell (APC); dendritic cell (DC); endoplasmic reticulum (ER); B cell receptor (BCR); T cell receptor (TCR).

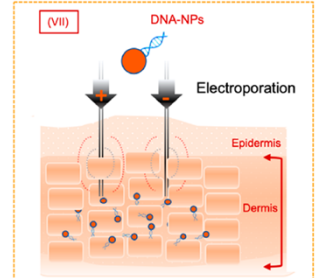
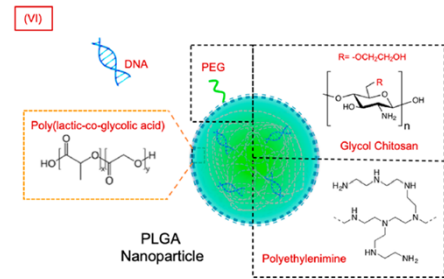
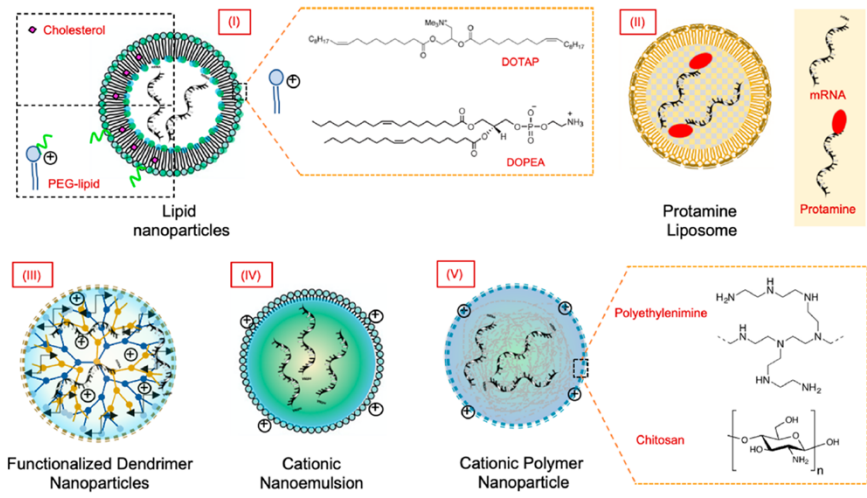
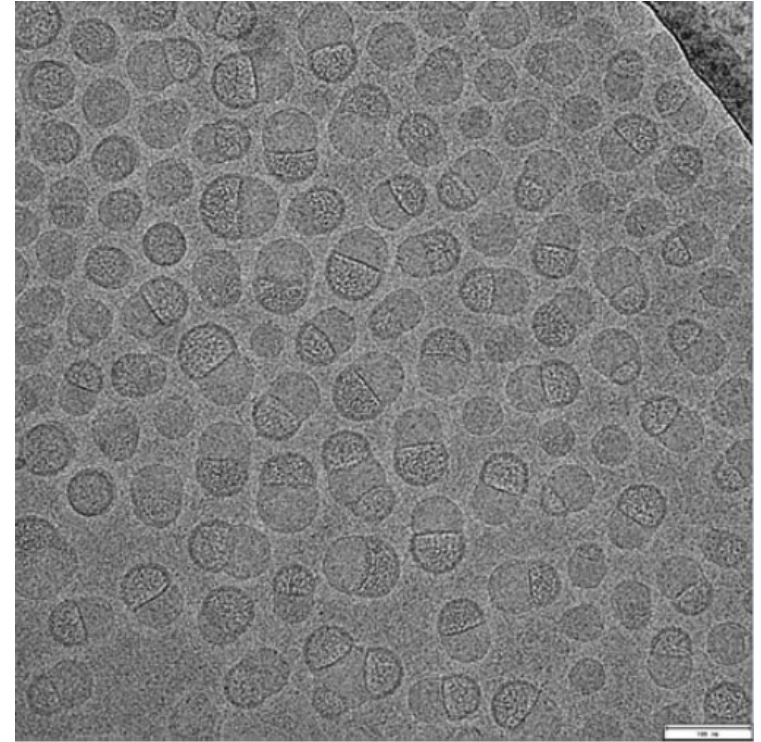
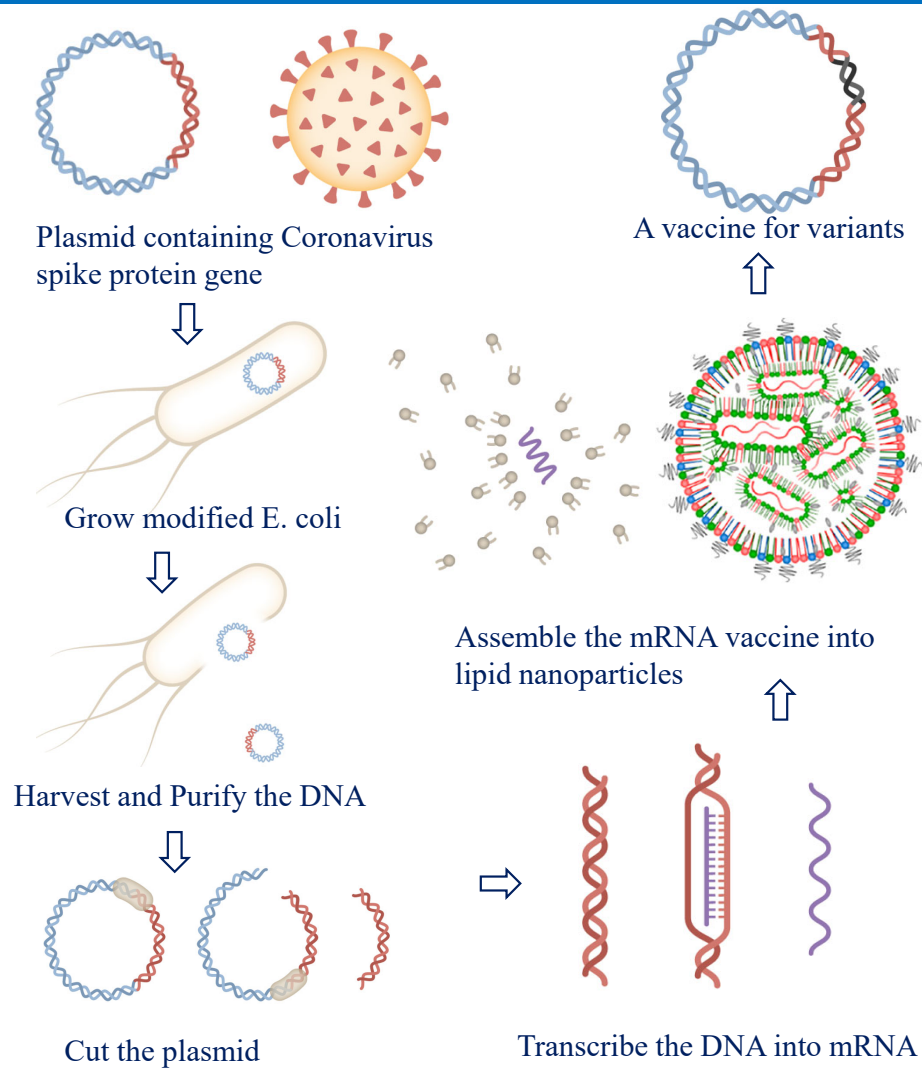


Figure 7. Major delivery methods for mRNA and DNA vaccines. (I-V) Nanocarrier for mRNA delivery, (VI) nanocarriers for DNA delivery, and (VII) electroporation technology for the intradermal delivery of DNA vaccines.

mRNA COVID-19 Vaccine



Brader 2021, Encapsulation state of messenger RNA inside lipid nanoparticles. *Biophys. J.* 120: 1-5.

Elia 2021, Design of SARS-CoV-2 hFc-conjugated receptor-binding domain mRNA vaccine delivered via lipid nanoparticles, *ACS Nano*

<https://www.nytimes.com/interactive/2021/health/pfizer-coronavirus-vaccine.html?referringSource=articleShare>

The Shape Structure Concept of Lipids.

ABSTRACT: RNA-based therapeutics have shown great promise in treating a broad spectrum of diseases through various mechanisms including knockdown of pathological genes, expression of therapeutic proteins, and programmed gene editing. Due to the inherent instability and negative-charges of RNA molecules, RNA-based therapeutics can make the most use of delivery systems to overcome biological barriers and to release the RNA payload into the cytosol. Among different types of delivery systems, lipid-based RNA delivery systems, particularly lipid nanoparticles (LNPs), have been extensively studied due to their unique properties, such as simple chemical synthesis of lipid components, scalable manufacturing processes of LNPs, and wide packaging capability. LNPs represent the most widely used delivery systems for RNA-based therapeutics, as evidenced by the clinical approvals of three LNP-RNA formulations, patisiran, BNT162b2, and mRNA-1273. This review covers recent advances of lipids, lipid derivatives, and lipid-derived macromolecules used in RNA delivery over the past several decades. We focus mainly on their chemical structures, synthetic routes, characterization, formulation methods, and structure–activity relationships. We also briefly describe the current status of representative preclinical studies and clinical trials and highlight future opportunities and challenges.

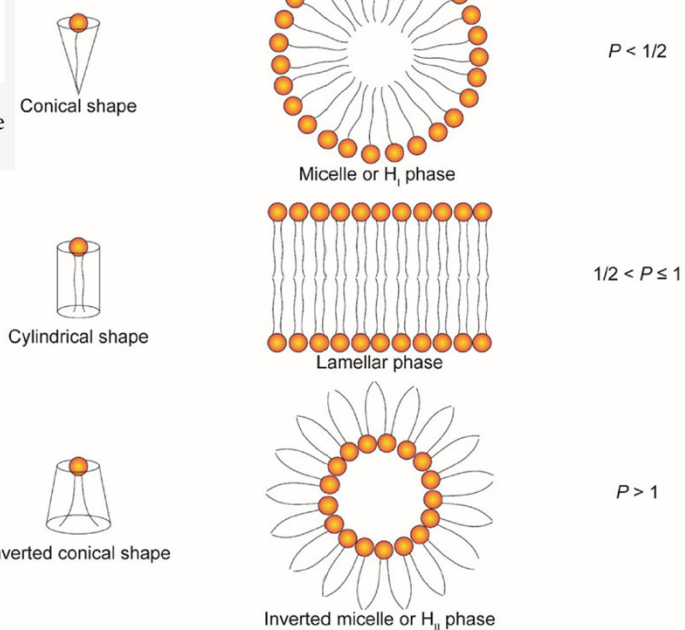
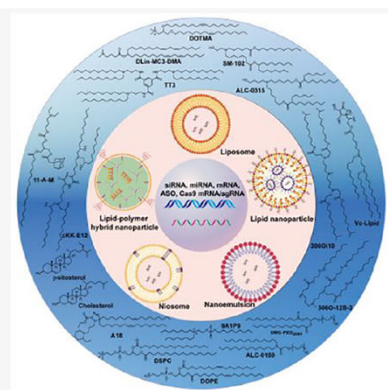


Figure 3. Schematic illustration of the shape structure concept of lipids.

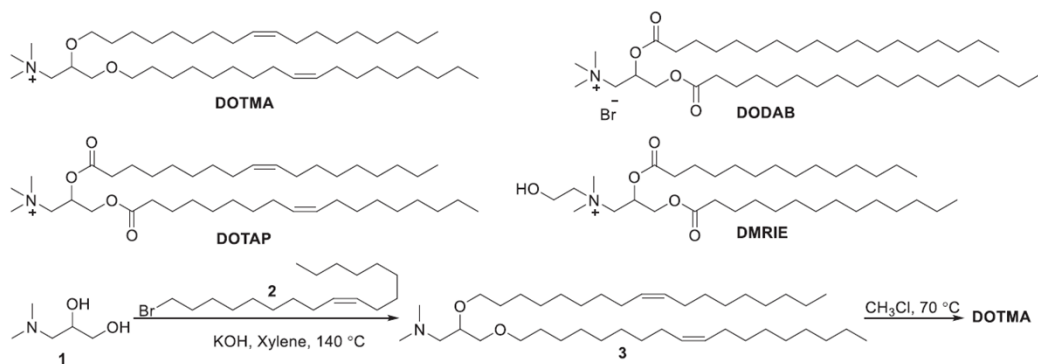


Figure 4. Chemical structures and synthesis of DOTMA and its analogs.

Stability of Gene Therapy Products

Improving Stability for Gene Therapy Products (By [Angelo DePalma, PhD](#), 2021)

After the genetic constructs are manufactured, doses must be stored, shipped, and stored again as they await dosing in far-flung test sites. The physical integrity of doses in these situations is paramount. The formulation, including buffers, cryoprotectants, and general storage conditions, were critical for maintaining stability. Standard storage practices involving **buffer, glycerol, and -80°C** storage could compromise gene delivery systems. In addition to requiring dry ice shipping such formulations also require **extensive dilution before administration to reduce glycerol toxicity**.

For cell therapies, storage and handling of both cells and viral vectors are quite diverse and present numerous issues for **long-term cryopreservation**, and to **maintain viability and activity post-thaw**. While we may approach a virus like AAV as nothing more than a complex protein biologic, we need to understand the impact of these factors on the virus. Viability can be measured several ways. **Cells from cryopreserved thaw can be measured directly in cell counters using a combination of nuclear and live/dead stains such as DAPI, acridine orange, or propidium iodide**. For activity assays, **viability** can be measured using the same combination of stains, as well as MTT or other functional killing assays.



Lipids

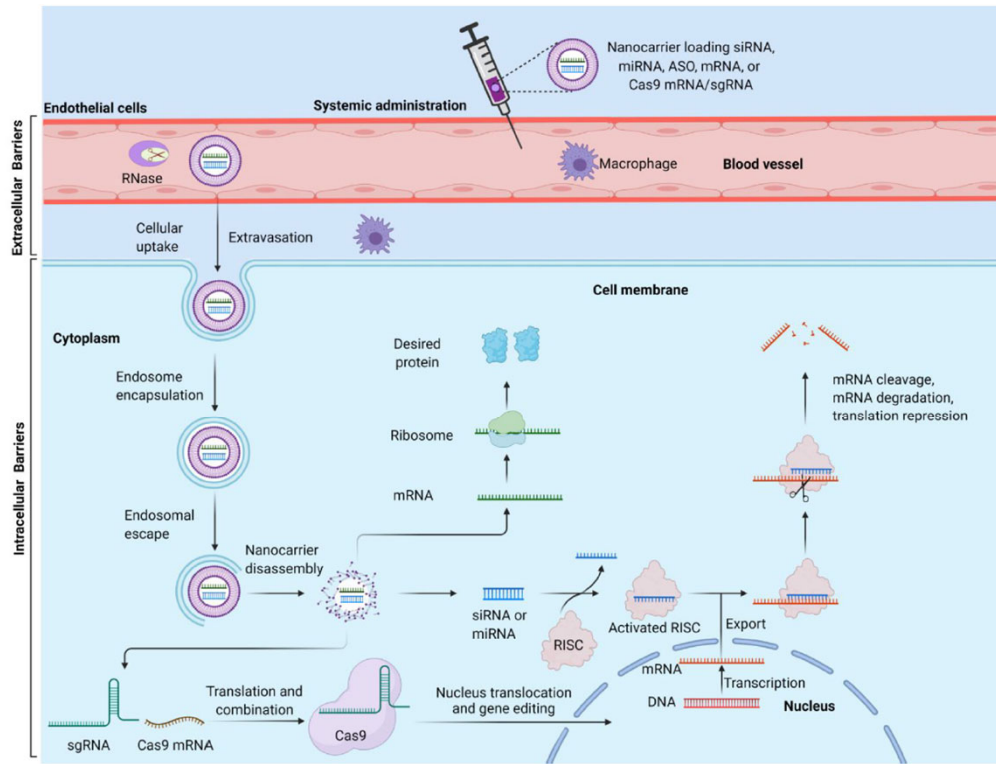
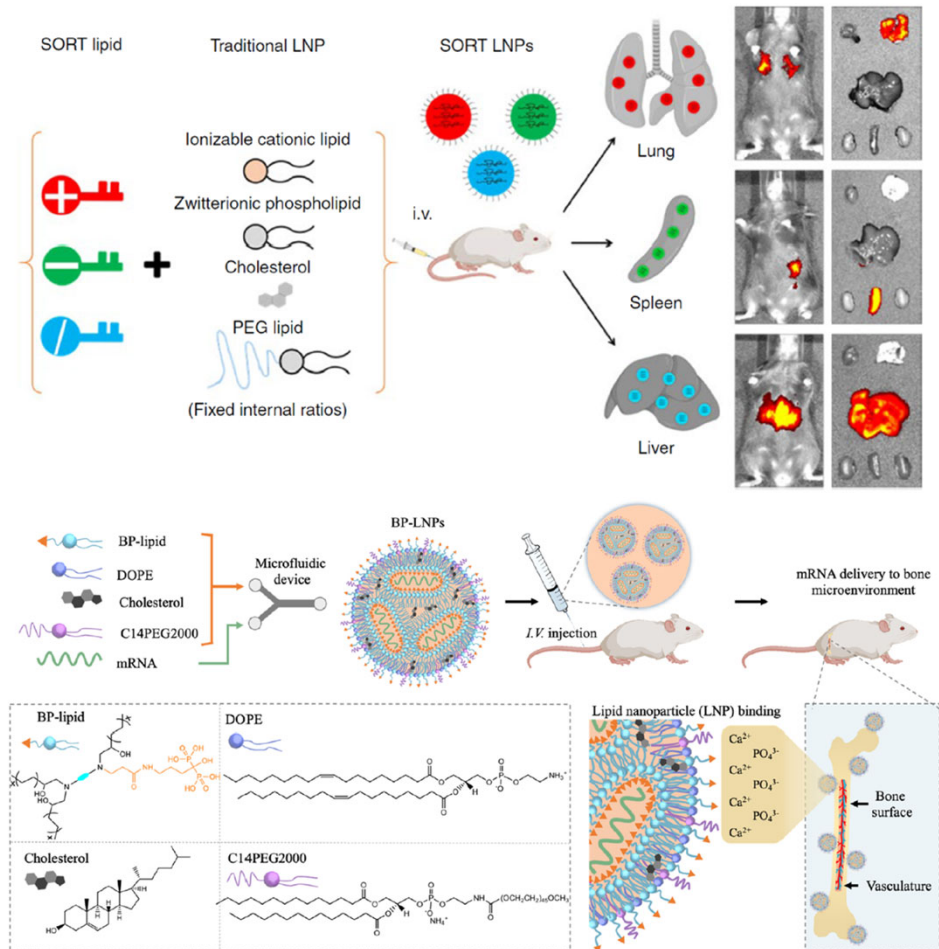


Figure 1. Schematic illustration of the extracellular and intracellular barriers to effective systemic delivery of RNAs and the mechanism of RNA-based therapeutics. Figure was created with BioRender.com.

Zhang 2021, Lipids and Lipid Derivatives for RNA Delivery



Xu 2023, Recent advances in site-specific lipid nanoparticles for mRNA delivery

Lipid Nanoparticles

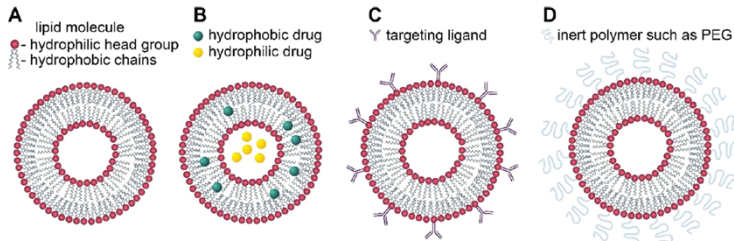


Figure 1. Schematic representation of (A) liposome, (B) liposome encapsulating hydrophobic and hydrophilic drugs, (C) immunoliposome functionalized with targeting ligands, and (D) sterically stabilized (“stealth”) liposome functionalized with inert polymers such as PEG.

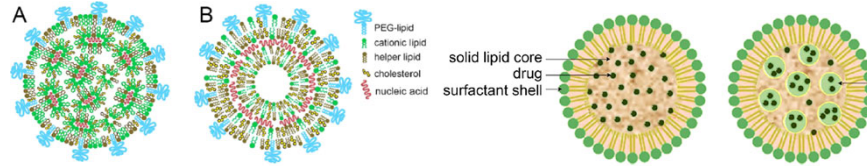


Figure 2. Suggested structures of lipid nanoparticle nucleic acid carriers: nucleic acids organized in inverse lipid micelles inside the nanoparticle (A); nucleic acids intercalated between the lipid bilayers (B).

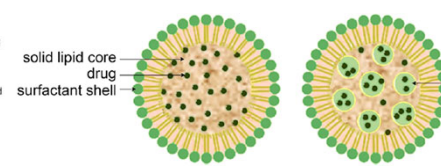


Figure 3. Schematic presentation of a solid lipid nanoparticle (left) and a nanostructured lipid carrier (right).

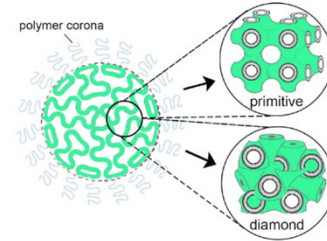


Figure 4. Cubosomes are nanoparticles comprising lipid in a bicontinuous bilayer cubic phase (either primitive or diamond type).

Lipid nanoparticles (LNPs) play a key role in effectively protecting and transporting mRNA to cells. LNPs exhibit more complex architectures and enhanced physical stabilities than liposomes (an early version of LNPs)

Note: Liposome ≠ LNP

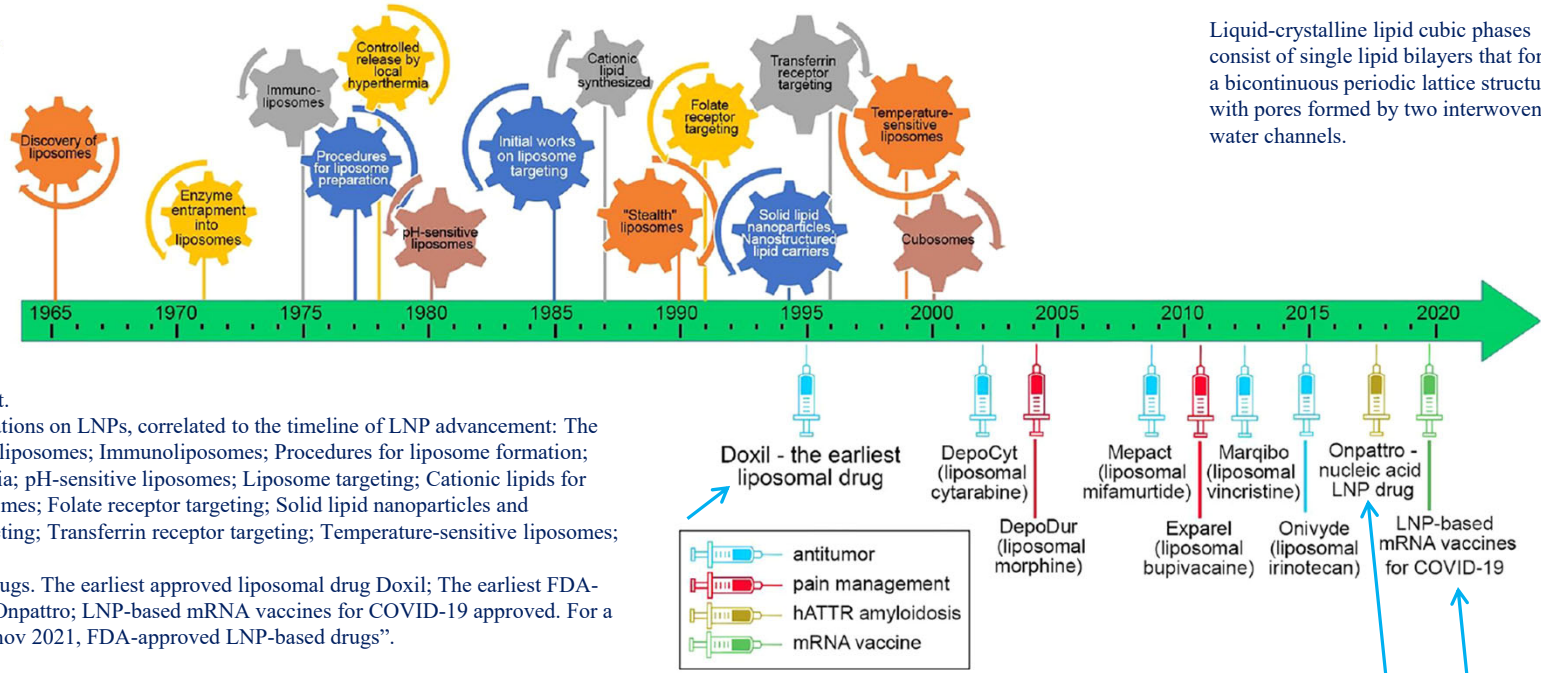


Figure 5. Timeline of liposome/LNP advancement.

(Upper part) Technological advancement. Publications on LNPs, correlated to the timeline of LNP advancement: The discovery of liposomes; Enzyme entrapment into liposomes; Immunoliposomes; Procedures for liposome formation; Thermoresponsive liposomes to local hyperthermia; pH-sensitive liposomes; Liposome targeting; Cationic lipids for gene delivery; Long-circulating (“Stealth”) liposomes; Folate receptor targeting; Solid lipid nanoparticles and nanostructures lipid carriers; HER2 receptor targeting; Transferrin receptor targeting; Temperature-sensitive liposomes; Stimuli-responsive liposomes; Cubosomes.

(Lower part) Examples of FDA-approved LNP drugs. The earliest approved liposomal drug Doxil; The earliest FDA-approved LNP-based nucleic acid (siRNA) drug Onpattro; LNP-based mRNA vaccines for COVID-19 approved. For a full list of approved LNP-based drugs, see “Tenchov 2021, FDA-approved LNP-based drugs”.

Tenchov 2021, Lipid Nanoparticles - From liposomes to mRNA vaccine delivery, a landscape of research diversity and advancement

Niosomes

ABSTRACT: Niosomes are a type of vesicular nanocarrier exploited for enhancing the therapeutic efficacy of various drugs in clinical practice. Niosomes comprise a bilayer hydrophobic membrane enclosing a central cavity filled with an aqueous phase, and therefore, they can encapsulate and deliver both hydrophobic and hydrophilic substances. Niosomal nanocarriers are preferred over other bilayer structures such as liposomes due to their chemical stability, biodegradability, biocompatibility, low production cost, low toxicity, and easy storage and handling. In addition, the niosomal membrane can be easily modified by the inclusion of ligands or stimulus-sensitive segments for achieving targeted delivery and triggered release of the encapsulated cargo. This mini-review outlines the current advances in designing functional niosomes and their use as platforms for developing advanced drug and gene delivery systems.

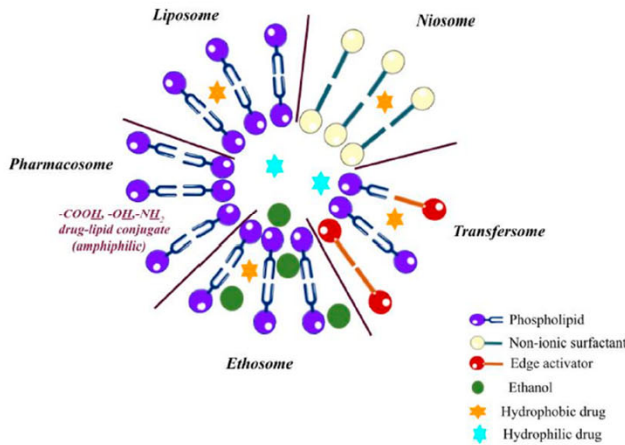
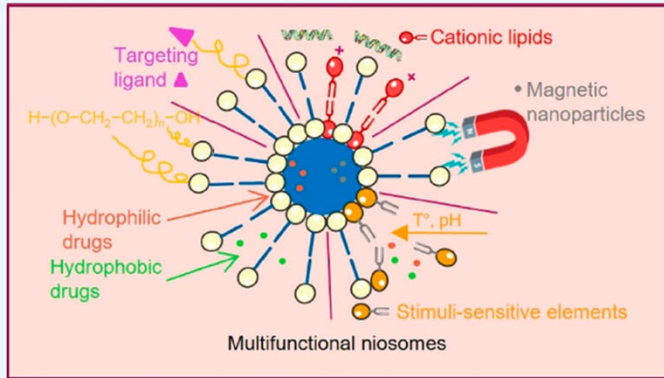


Figure 1. Sketch of different types of vesicular nanocarriers.

Niosomes are vesicular systems formed by nonionic surfactants via self-assembly in aqueous solution assisted by physical agitation or elevated temperature.² The use of nonionic surfactants as membrane forming constituents instead of phospholipids overcomes many of the disadvantages associated with liposomes, such as insufficient chemical stability, predisposition of phospholipids to oxidation, high production cost, necessity of special handling, and storage conditions.³ Their specific structure—an inner aqueous compartment surrounded by a hydrophobic membrane—allows incorporation (and codelivery, respectively) of hydrophobic and hydrophilic drug molecules.¹ Furthermore, niosomes are osmotically active, nontoxic, non-immunogenic, biocompatible, and biodegradable. Initially reported in the 1970s as a feasible approach in the cosmetic industry, niosomes were patented by L’Oreal in the 1980s as a cosmetic product.² Their favorable characteristics determine the increased research interest, as well the wide exploitation beyond the scope of cosmetic industry. Over the years, niosomes have been investigated as a promising drug delivery platform for various routes of administration—oral, parenteral, dermal/transdermal, ocular, and pulmonary (Figure 2).^{1,3}

Momekova 2023, Nanoarchitectonics of multifunctional niosomes for advanced drug delivery

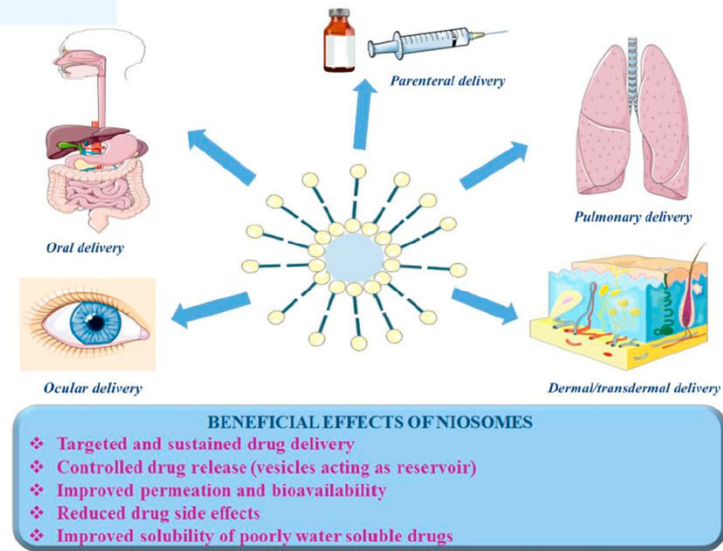


Figure 2. Beneficial effects of niosomes in accordance with the most commonly used delivery routes.

Biomimetic Nanoparticles for Targeted Drug Delivery

As numerous diseases are associated with **increased local inflammation**, directing drugs to the inflamed sites can be a powerful therapeutic strategy. One of the common characteristics of **inflamed endothelial cells** is the up-regulation of vascular cell adhesion molecule-1 (VCAM-1). Here, the specific affinity between very late antigen-4 (VLA-4) and VCAM-1 is exploited to produce a **biomimetic nanoparticle formulation** capable of targeting inflammation. **The plasma membrane from cells genetically modified to constitutively express VLA-4** is coated onto polymeric nanoparticle cores, and the resulting cell membrane-coated nanoparticles exhibit enhanced affinity to target cells that overexpress VCAM-1 in vitro. **A model anti-inflammatory drug, dexamethasone, is encapsulated into the nanoformulation**, enabling improved delivery of the payload to inflamed lungs and significant therapeutic efficacy in vivo. Overall, this work leverages the unique advantages of **biological membrane coatings to engineer additional targeting specificities** using naturally occurring target-ligand interactions.

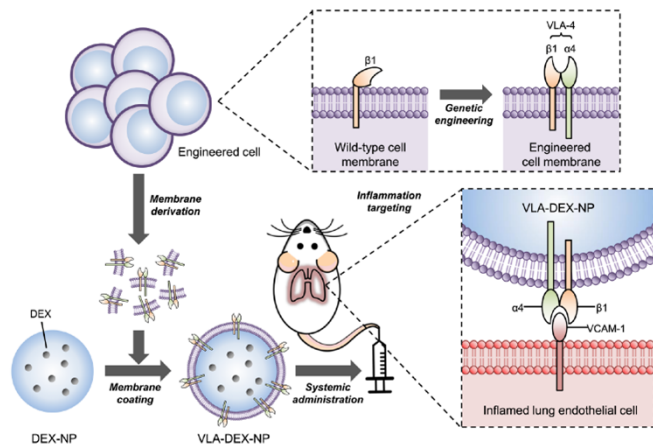


Fig. 1. Schematic illustration of genetically engineered cell membrane-coated nanoparticles for targeted drug delivery to inflamed lungs. Wild-type cells were genetically engineered to express VLA-4, which is composed of integrins $\alpha 4$ and $\beta 1$. Then, the plasma membrane from the genetically engineered cells was collected and coated onto dexamethasone-loaded nanoparticle cores (DEX-NP). The resulting VLA-4-expressing cell membrane-coated DEX-NP (VLA-DEX-NP) can target VCAM-1 on inflamed lung endothelial cells for enhanced drug delivery. (PLGA 50:50 (0.66 dl/g; LACTEL). For DEX-loaded PLGA cores, 500 μ L of PLGA (50 mg/ml) in dichloromethane (DCM; Sigma-Aldrich) was mixed with 500 μ L of DEX (10 mg/ml) in acetone.)

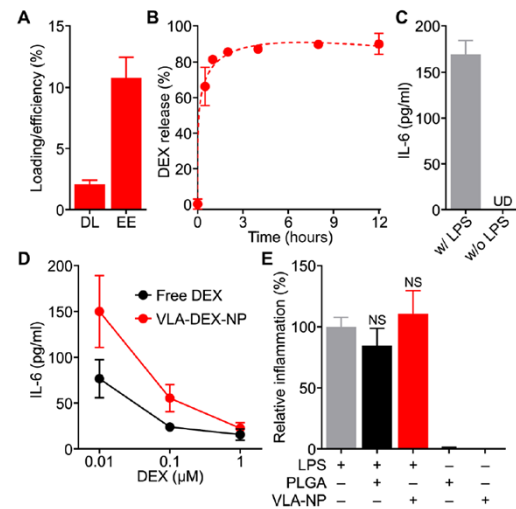


Fig. 4. Drug loading and in vitro activity. (A) Drug loading (DL) and encapsulation efficiency (EE) of dexamethasone (DEX) into VLA-NP (n = 3, mean \pm SD). (B) Drug release profile of VLA-DEX-NP (n = 3, mean \pm SD). The data were fitted using the Peppas-Sahlin equation (dashed line). (C) Secretion of IL-6 by LPS-treated DC2.4 cells (n = 3, mean \pm SD). UD, undetectable. (D) Secretion of IL-6 by LPS-treated DC2.4 cells preincubated with DEX in free form or loaded into VLA-NP (n = 3, mean \pm SD). (E) Relative inflammatory response, as measured by IL-6 secretion, of DC2.4 cells treated with LPS only, LPS and PLGA nanoparticles, LPS and VLA-NP, PLGA nanoparticles only, or VLA-NP only; all of the nanoparticles were empty without DEX loading (n = 3, mean \pm SD). NS, not significant (compared to the LPS-only group), one-way analysis of variance (ANOVA).

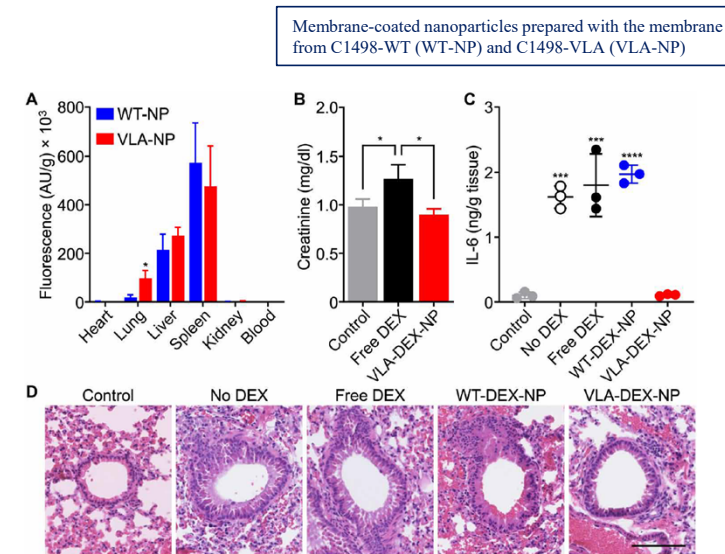


Fig. 5. In vivo targeting, safety, and therapeutic efficacy. (A) Biodistribution of WT-NP or VLA-NP in a lung inflammation model 6 hours after intravenous administration (n = 3, mean \pm SD). *P < 0.05, Student's t test. AU, arbitrary units. (B) Creatinine levels in the plasma of mice after repeated daily administrations for 9 days with free DEX or VLA-DEX-NP (n = 3, mean \pm SD). *P < 0.05, one-way ANOVA. (C) IL-6 levels in the lung tissue of mice intratracheally challenged with LPS and then treated intravenously with vehicle solution, free DEX, WT-DEX-NP, or VLA-DEX-NP (n = 3, mean \pm SD). ***P < 0.001, ****P < 0.0001 (compared to VLA-DEX-NP), one-way ANOVA. (D) Representative hematoxylin and eosin-stained lung histology sections of mice intratracheally challenged with LPS and then treated intravenously with vehicle solution, free DEX, WT-DEX-NP, or VLA-DEX-NP (scale bar, 100 μ m).

Biomimetic Nanobiomaterials

The design of next-generation nanobiomaterials requires **precise engineering of both physical properties of the core material and chemical properties of the material's surface to meet a biological function**. A bio-inspired modular and versatile technology was developed to allow biodegradable polymeric nanoparticles to **circulate through the blood for extended periods of time** while also acting as a detoxification device. To mimic red blood cells, **physical and chemical biomimicry** are combined to enhance the biological function of nanomaterials in vitro and in vivo. The anisotropic shape and membrane coating synergize to **resist cellular uptake and reduce clearance from the blood**. This approach enhances the detoxification properties of nanoparticles, markedly improving survival in a **mouse model of sepsis**. The anisotropic membrane-coated nanoparticles have **enhanced biodistribution and therapeutic efficacy**. These biomimetic biodegradable nanodevices and their derivatives **have promise** for applications ranging from detoxification agents, to drug delivery vehicles, and to biological sensors

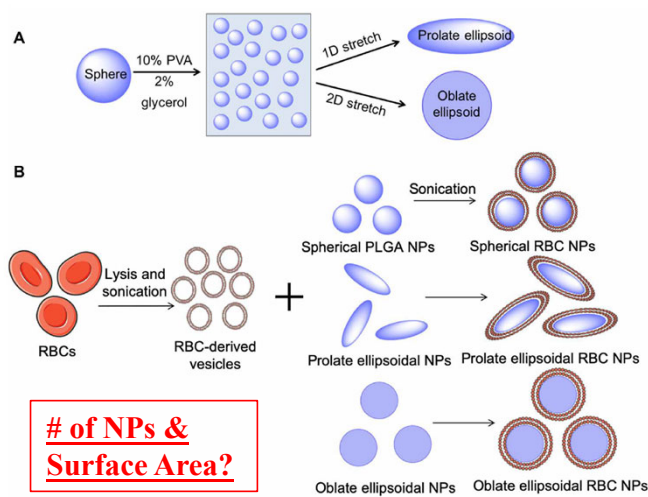


Fig. 1. Schematic of anisotropic nanoparticle fabrication and RBC membrane coating. (A) Spherical PLGA nanoparticles (NPs) were synthesized and cast into a thin plastic film of 10% polyvinyl alcohol (PVA) and 2% glycerol. Particles were then stretched under heat in one or two dimensions (2D) to generate prolate or oblate ellipsoidal particles, respectively. (B) RBCs underwent hypotonic lysis and were then sonicated to generate sub-200 nm vesicles. RBC-derived vesicles were then coated onto PLGA nanoparticles of all shapes under sonication.

Ben-Aklva 2020, Biomimetic anisotropic polymeric nanoparticles coated with red blood cell membranes for enhanced circulation and toxin removal

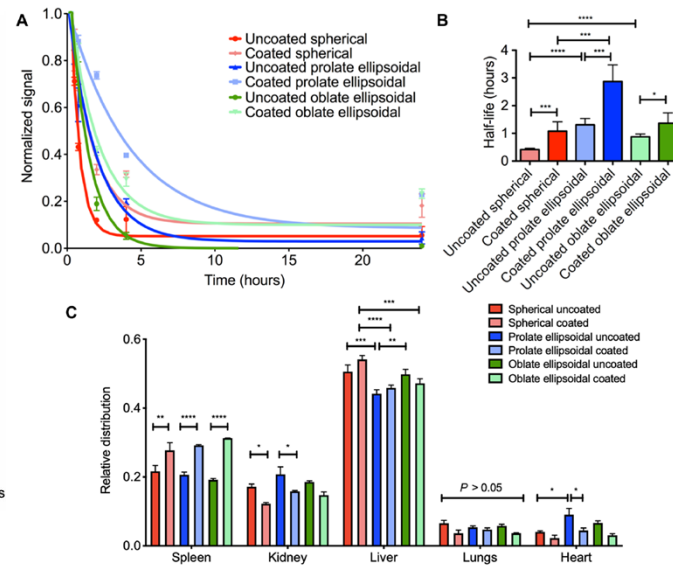


Fig. 4. In vivo clearance and biodistribution of nanoparticles. (A) Blood elimination of nanoparticles following intravenous administration as assessed by fluorescence readings of the blood sample (dots) and fit to a single exponential decay model (lines). (B) Particle bloodstream half-life was derived from the exponential fit of blood decay curves and was increased for RBC membrane-coated particles and prolate ellipsoidal particles. (C) Mice were euthanized after 24 hours, and organs were dissected out and imaged. Data are shown as means \pm SEM (n = 3 mice per group).

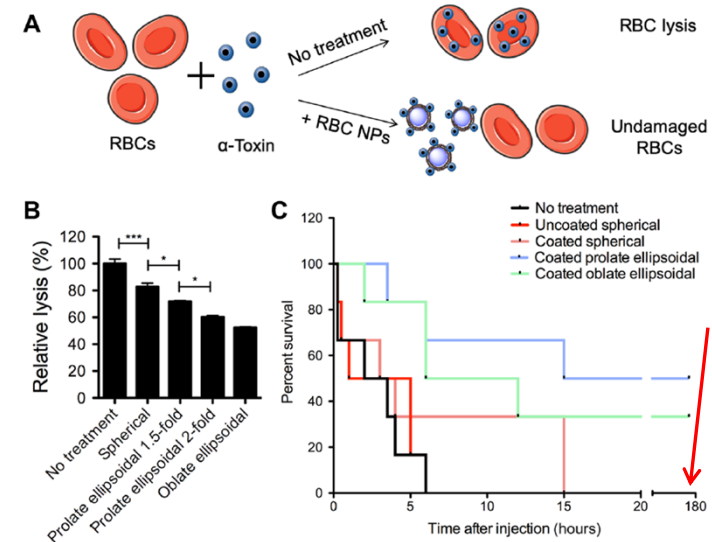
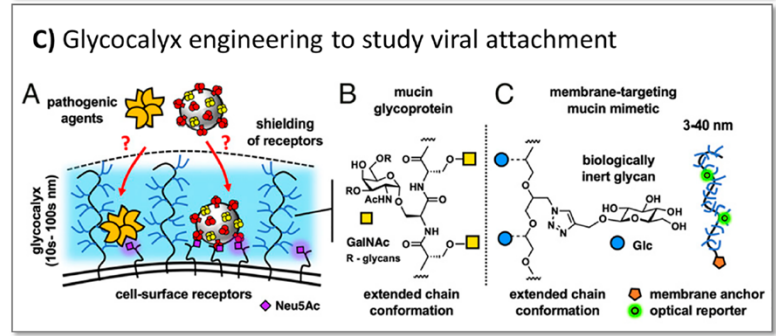
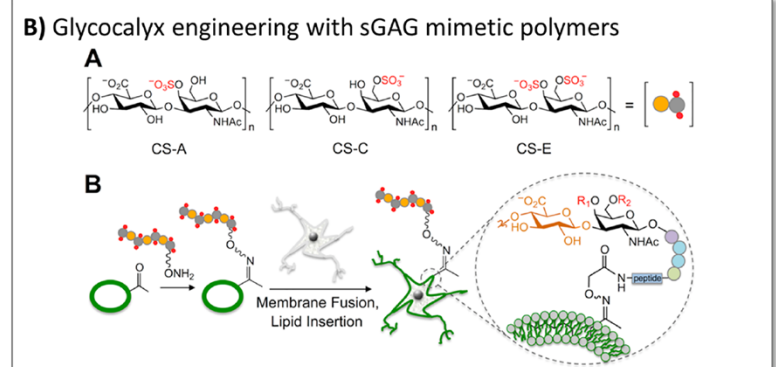
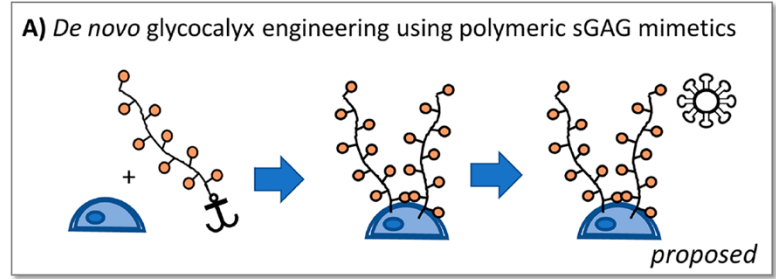
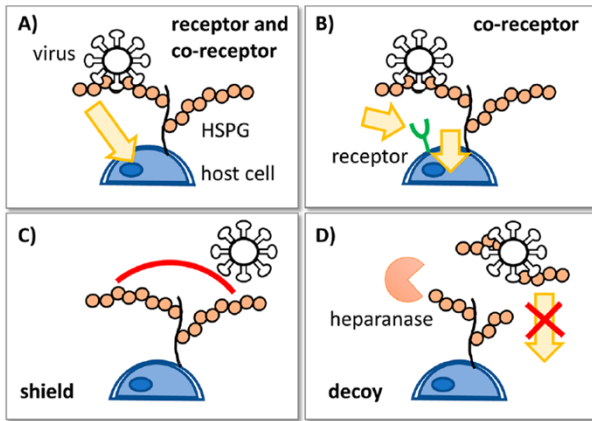
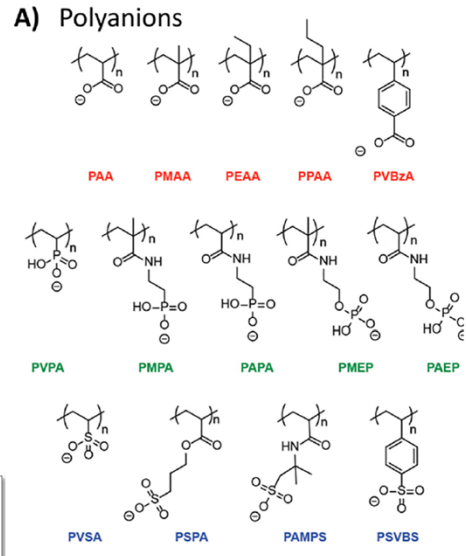
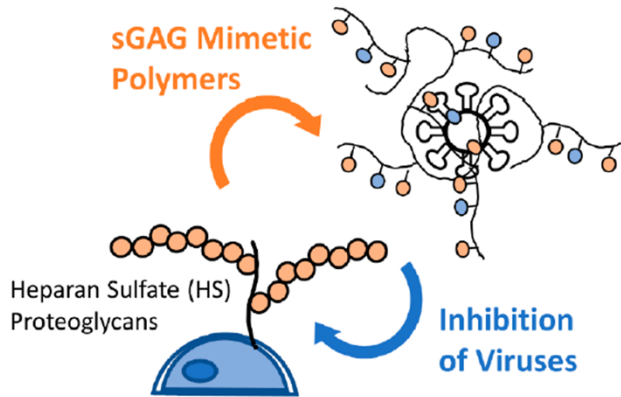


Fig. 5. Anisotropic RBC membrane-coated nanoparticles as detoxification treatment. (A) Schematic of mechanism of RBC coated nanoparticles (NPs) as detoxification treatment. RBC NPs neutralize alpha toxin by binding toxin that would otherwise bind the body's RBCs and cause lysis. (B) In vitro evaluation of hemolytic toxin absorption by RBC-coated nanoparticles. The anisotropic particles were able to absorb significantly more alpha toxin as evidenced by reduction in relative lysis. Data are shown as means \pm SEM (n = 4 replicates). (C) Survival following intravenous alpha toxin administration followed by nanoparticle administration (n = 6 mice per group). Mice receiving prolate ellipsoidal RBC-coated nanoparticles had a significant long-term survival benefit compared to spherical coated nanoparticle, and both anisotropic particle groups had a significant survival benefit over uncoated particles.

Polymers for Viral Targeting



Polymer Micelles

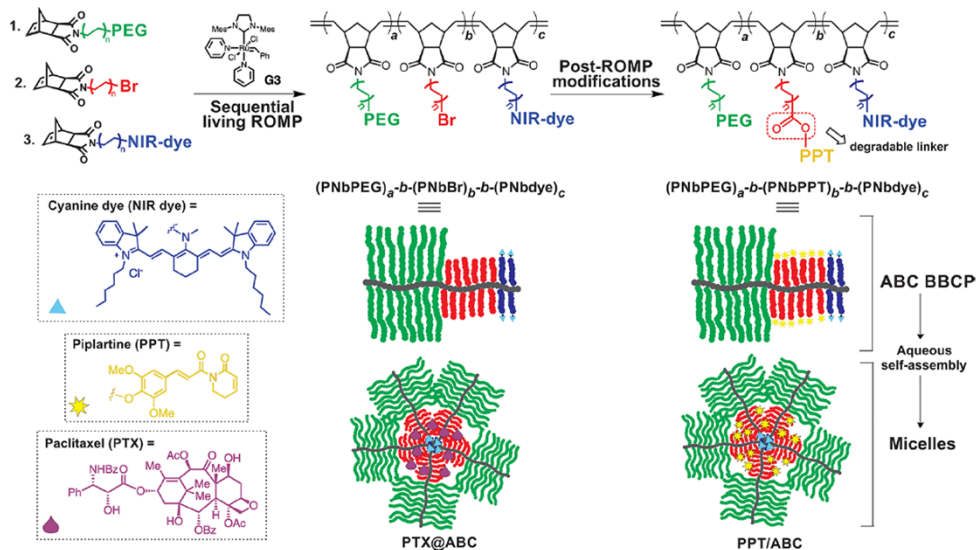


Figure 1. Schematic illustration of the synthesis of well-defined amphiphilic brush block copolymers (BBCPs) and the preparation of multifunctional fluorescent polymeric micelles from BBCPs

Braga 2021, Near-Infrared Fluorescent Micelles from Poly(norbornene) Brush Triblock Copolymers for Nanotheranostics

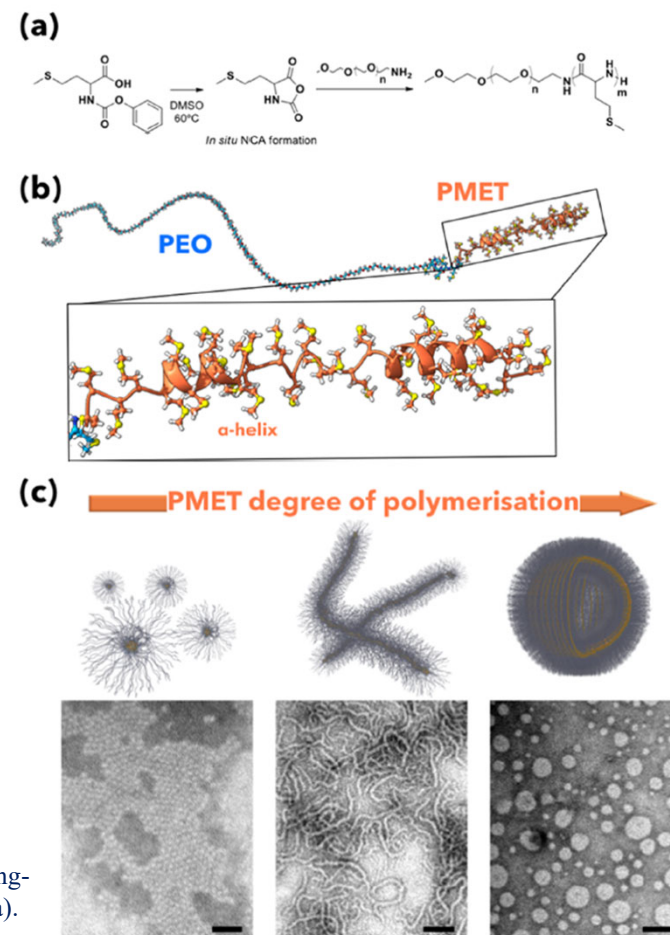
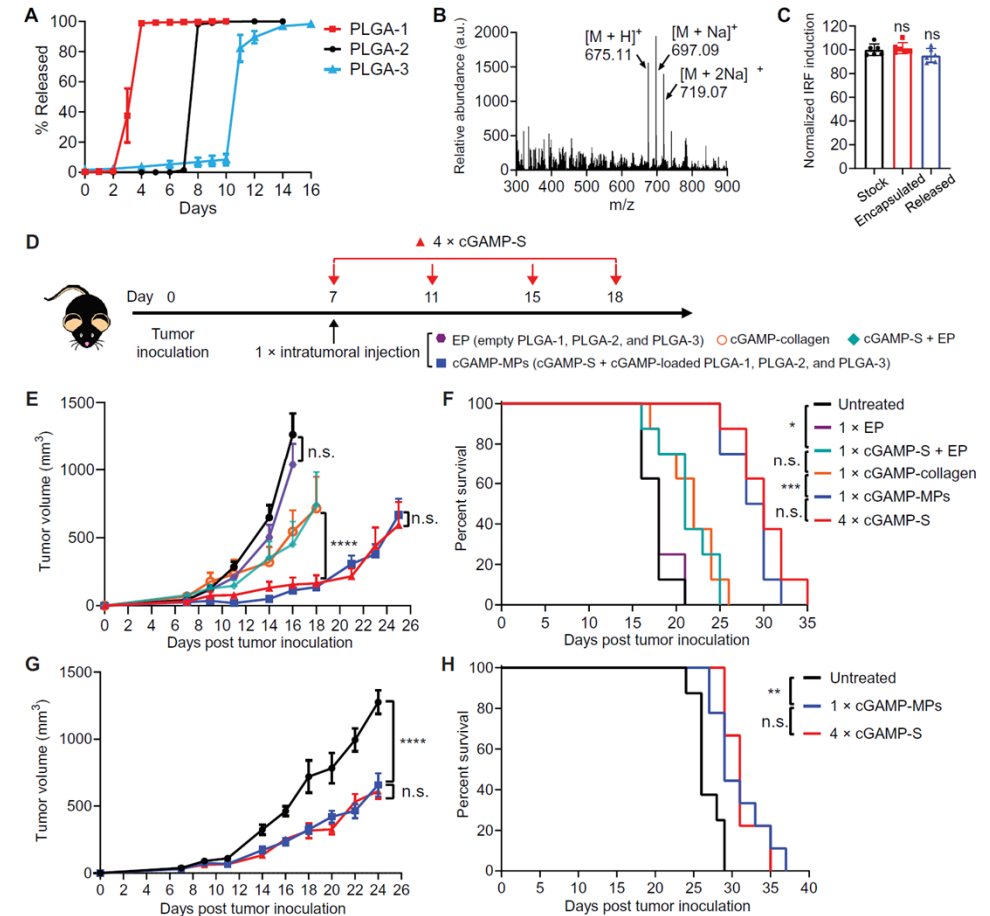
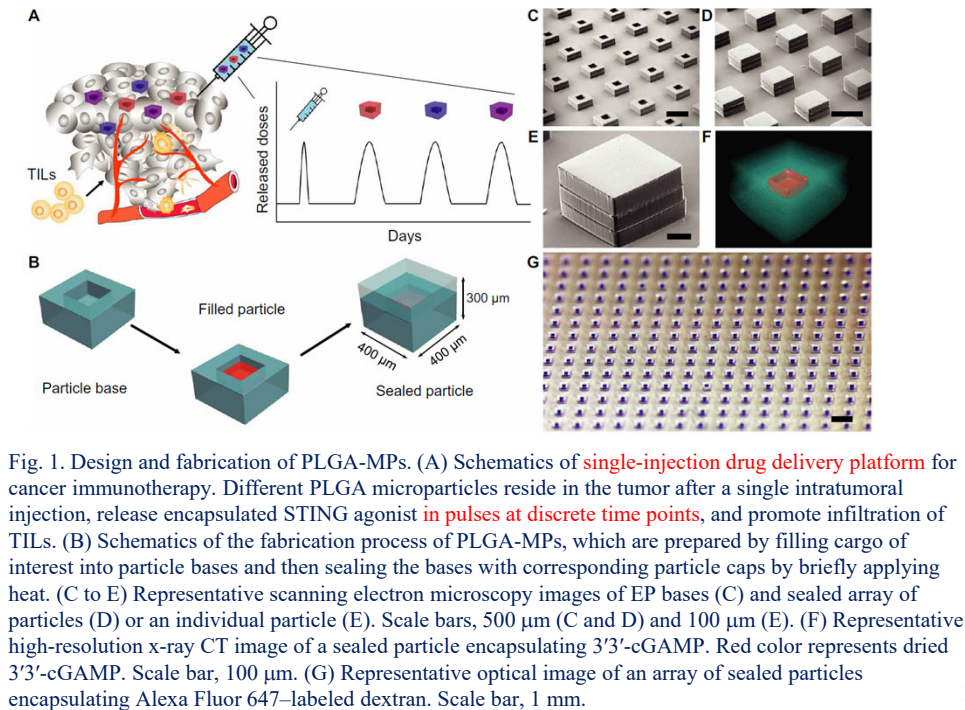


Figure 1. Schematic representation of the “one-pot” synthesis. Synthesis scheme for the ring-opening polymerization (ROP) of activated urethane of methionine in DMSO as solvent (a). Molecular model of the PEO-PMET diblock copolymer showing the partial folding of the polypeptide (b). Scheme showing the evolution from spherical micelles to cylindrical micelles to vesicles as a function of the PMET degree of polymerization with relative transmission electron micrographs (c). Scale bar = 100 nm.

Duro-Castano 2021, One-Pot Synthesis of Oxidation-Sensitive Supramolecular Gels and Vesicles

PLGA Microparticles for Long-term, Pulsatile Release

Activation of the stimulator of interferon gene (STING) pathway within the tumor microenvironment has been shown to generate a strong antitumor response. Although local administration of STING agonists has promise for cancer immunotherapy, the dosing regimen needed to achieve efficacy requires **frequent intratumoral injections over months**. Frequent dosing for cancer treatment is associated with poor patient adherence, with **as high as 48% of patients failing to comply**. Multiple intratumoral injections also disrupt the tumor microenvironment and vascular networks and therefore increase the risk of metastasis. Here, we developed **microfabricated poly(lactic-co-glycolic acid) (PLGA) particles that remain at the site of injection and release encapsulated STING agonist as a programmable sequence of pulses at predetermined time points that mimic multiple injections over days to weeks**. A single intratumoral injection of STING agonist-loaded microparticles triggered potent local and systemic antitumor immune responses, inhibited tumor growth, and prolonged survival as effectively as multiple soluble doses, but with reduced metastasis in several mouse tumor models.



Lu 2020, Engineered PLGA microparticles for long-term, pulsatile release of STING agonist for cancer immunotherapy

Universal Sensor for Betacoronaviruses

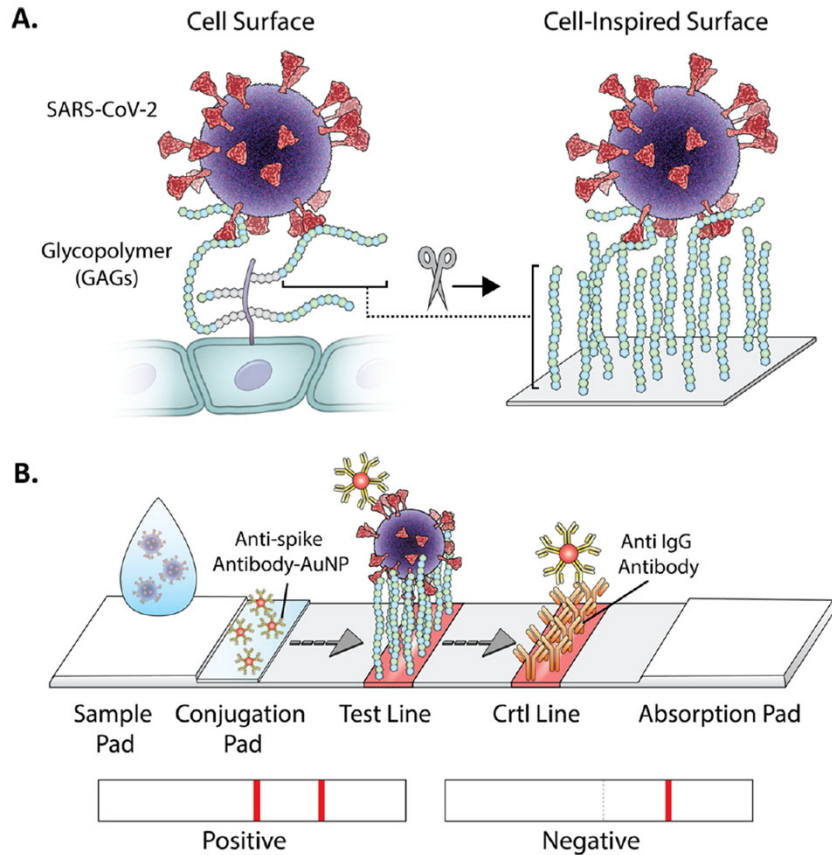


Figure 1. Graphical illustration of (A) virus interaction with GAGs on the cell surface and (B) on the GlycoGrip lateral flow (LF) biosensor for detecting SARS-CoV-2. The sample is deposited on the sample pad and migrates toward the conjugate. The conjugated antibodies bind the virus and migrate to the test line, where the bound target analyte is captured by the glycopolymers.

Kim 2022, GlycoGrip-Cell Surface-Inspired Universal Sensor for Betacoronaviruses

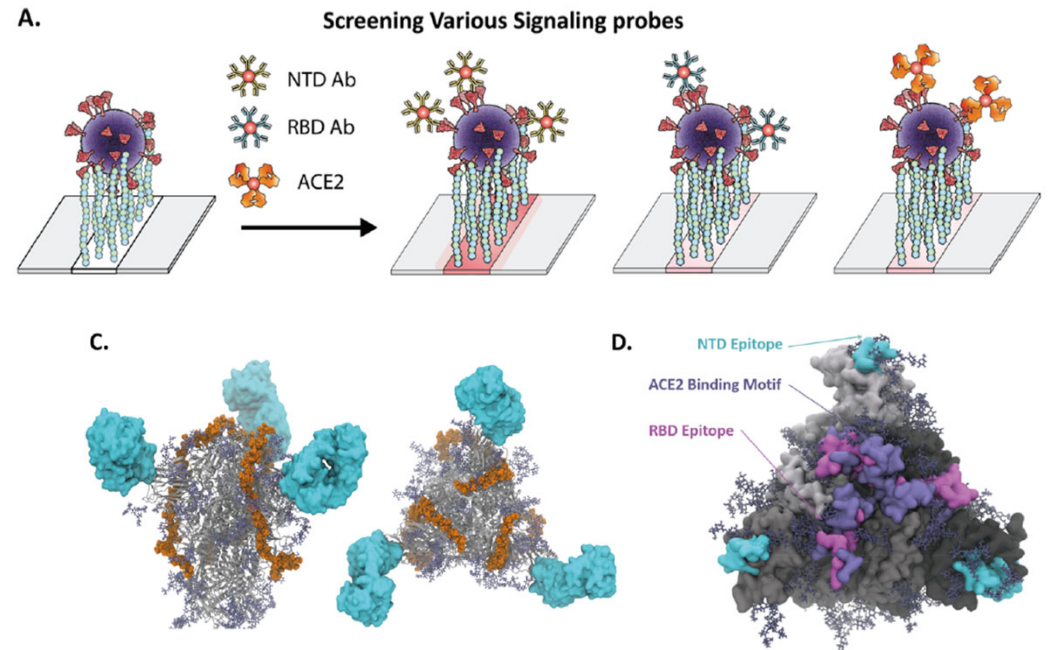


Figure 4. (A) Schematic illustration of our screening of various signaling probe candidates on heparin (HEP)-based lateral flow (LF) strip and (B) corresponding screening result with 30 and 5 min incubation. (C) Alignment of hep40mer and the N-terminal domain (NTD) Ab to the spike. (D) Computational model of NTD and the receptor binding domain (RBD, epitopes (4A8 and REGN10933, respectively) along with the angiotensin converting enzyme 2 (ACE2), binding motif. (E) Accessible surface area calculated from the RBD epitope (REGN10933), ACE2 binding motif, and NTD epitope (4A8). Dark blue bars indicate the size of the interface area as seen in Cryo-EM structures for the RBD, ACE2, and NTD binding footprints (6XDG, 6M17, and 7C2L, respectively). p values < 0.05 (*), 0.01 (**), and 0.001 (***) determined using a two-way ANOVA with Tukey's post hoc test.

Liquid Metal Drug Delivery Systems

Among various materials, transformable and easily handled **liquid metals (LMs)**, which have exceptional multifunctionality, might be suitable for creating **the convergence concept with cutting-edge technologies**, including optics, electronics, printing, robotics, and nanotechnologies. In particular, Ga- and Ga-based LM alloys are promising soft materials for various applications because of their **low toxicity, excellent electrical and thermal conductivities, and fluidity at near-room temperature**. More interestingly, Ga-based LM particles continue to exhibit both fluidic and metallic properties and are valuable for versatile functionalization in health monitoring devices and therapeutics.

EGaIn: Eutectic gallium–indium. Galinstan: Gallium–indium–tin.

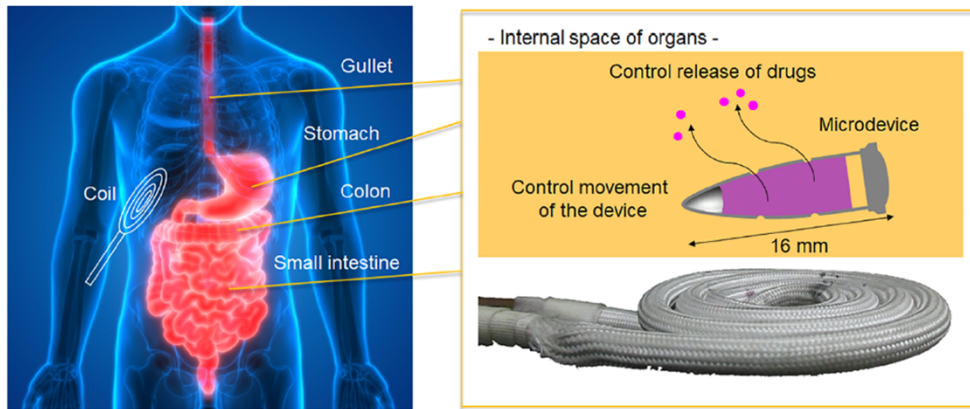


Figure 2. Application of a LM-based healthcare device. The schematic illustration represents the potential application of an alternating magnetic field-driven ingestible microdevice in digestive organs.

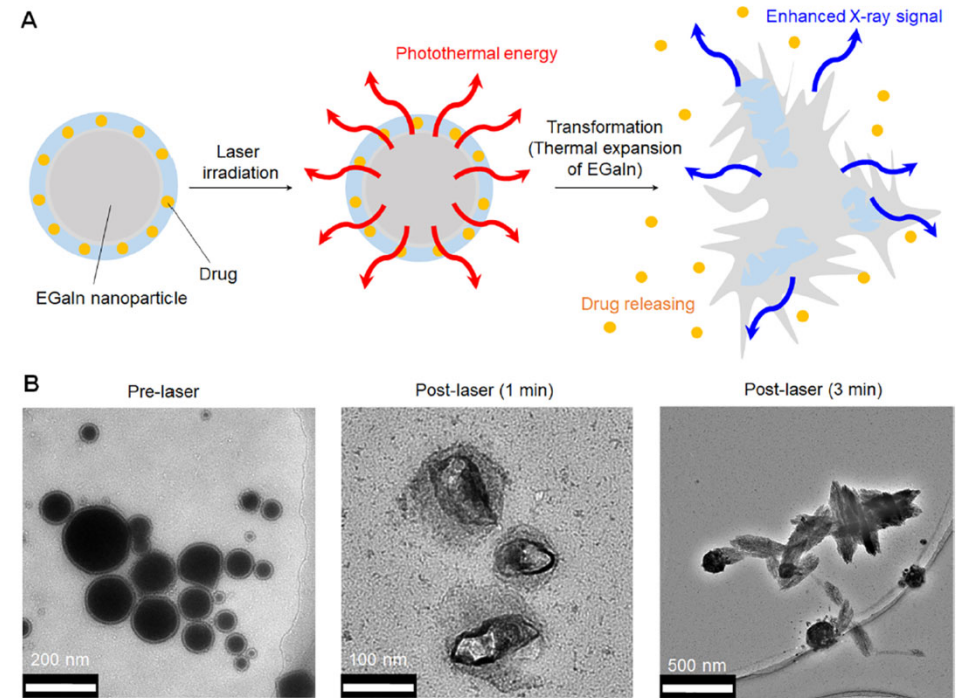


Figure 3. Medicinal application using the fluidity of LMs via light energy. (A) Schematic illustration of light-induced transformable EGaIn LM nanocapsules. (B) Transmission electron microscopic images of light-induced transformable EGaIn LM nanocapsules before and after laser irradiation for 1 and 3 min.

The New Antimicrobial Magic Bullet

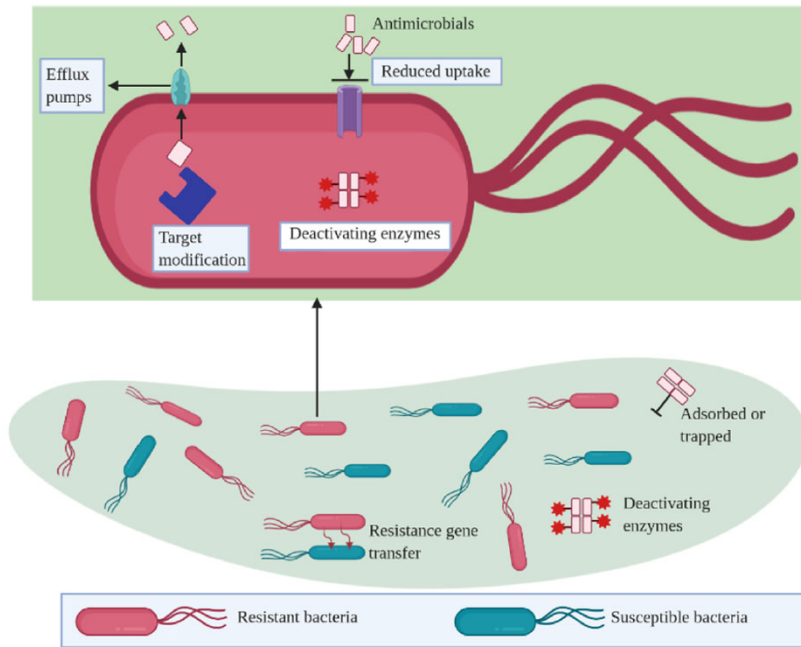


Figure 1. Antimicrobial resistance mechanisms toward conventional antibiotics. The resistance can happen in different ways: (1) bacteria mutate, communicate, and share resistance genes with one another, which results in spread of resistance genes across bacteria population; (2) resistant bacteria can harbor intracellular/extracellular enzymes that limit the binding of, degrade, or deactivate the antibiotics; (3) entry of antimicrobials into bacterial cells is limited; (4) efflux pumps, which in most cases are upregulated in resistant bacteria, actively transport antimicrobials outside the bacteria; and (5) the complex nature of the bacteria extracellular polymeric substances restricts the penetration of antimicrobials into bacterial cells.

Ndayishimiye 2022, Nanomaterials- The new antimicrobial magic bullet

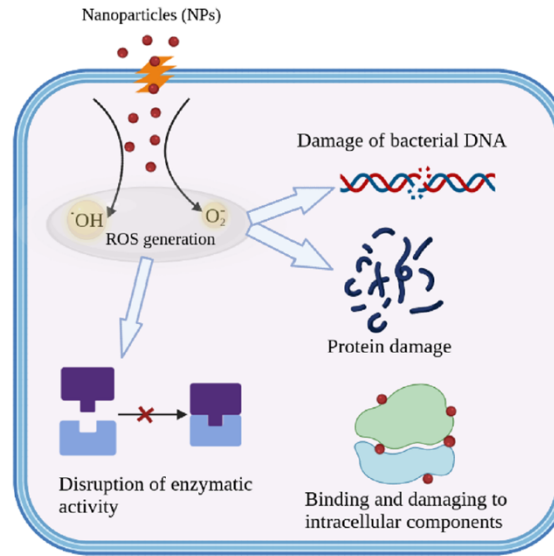
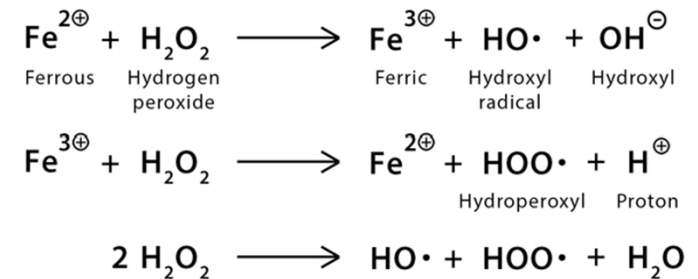


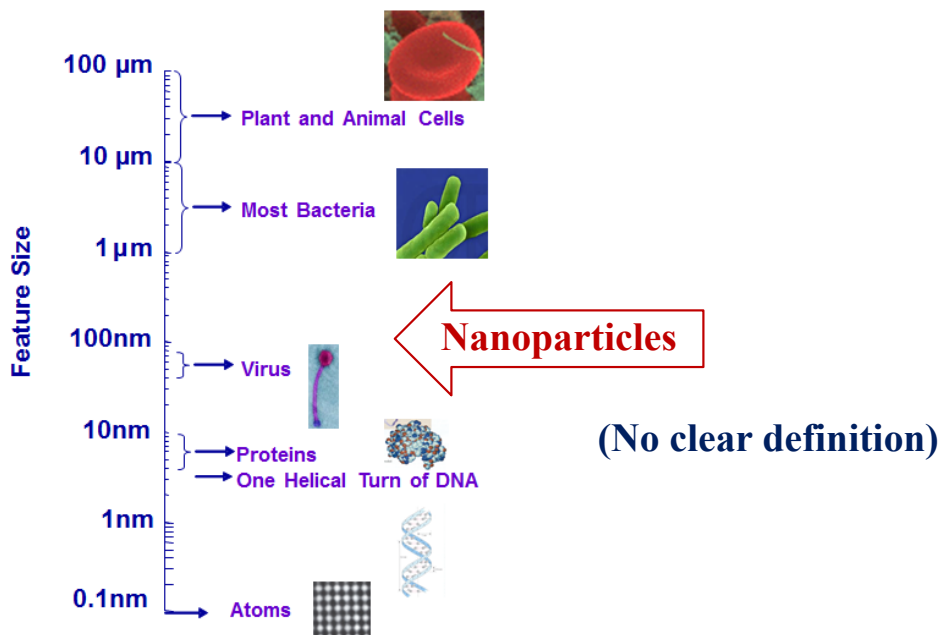
Figure 5. Some NPs (silver NPs, titanium oxide NPs, etc.) exert their antibacterial activity by producing (for example, through Fenton reactions) reactive oxygen species (ROS) inside the bacterial cell, which through different mechanisms cause bacteria death. Meanwhile NPs can directly bind to other bacterial intracellular components (like ribosomes, bacterial chromosomes, and plasmid) and cause the inhibition of bacterial intracellular activity.

Fenton Reaction

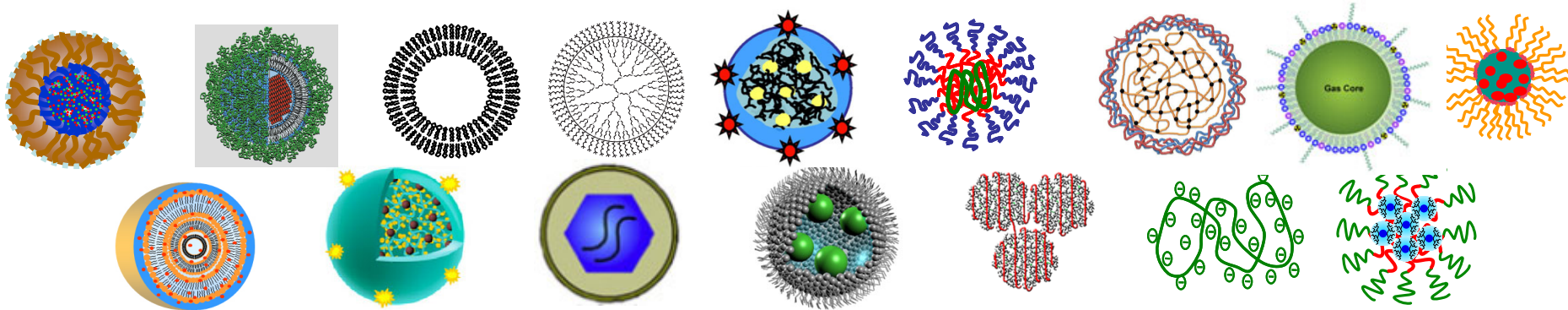


Iron and hydrogen peroxide are capable of oxidizing a wide range of substrates and causing biological damage. The reaction, referred to as the Fenton reaction, is complex and capable of generating both hydroxyl radicals and higher oxidation states of the iron. (C.C. Winterbourn 1995, Toxicity of iron and hydrogen peroxide: the Fenton reaction, Toxicol Lett. 1995 Dec;82-83:969-74. doi: 10.1016/0378-4274(95)03532-x).

Research on Nanotechnology Formulations



Almost all papers on such nanoparticles end up with the same conclusion: nanotechnology has great potential for drug delivery. It is true. The question, then, is to ask what can be done to turn this potential into tangible outcomes, *i.e.*, formulations that can benefit patients. It would be counterproductive only to talk about the potential for another decade. To achieve tangible outcomes, they first need to be defined. This, in turn, requires understanding the goals, which may depend on individuals.



Magic Bullet Against Enemy

Paul Ehrlich's Magic Bullet

Selective targeting to a bacterium
without affecting other organisms.



Selective killing

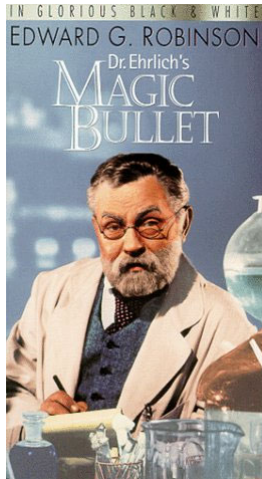
A drug that goes straight to their intended
cell-structural targets to treat disease.



interacts with



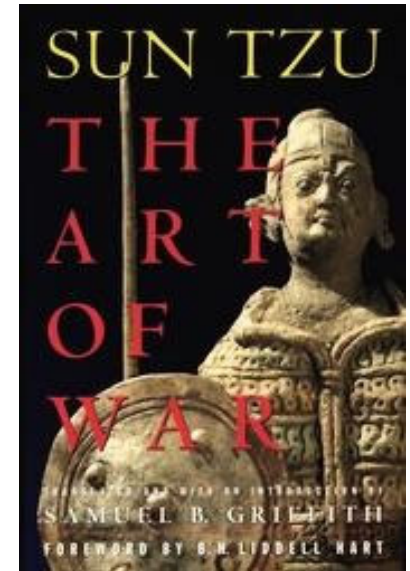
Nobel Prize 1908



The Art of War (孫子兵法)

(Sūn Zū Bīng Fǎ)

知己知彼 百戰百勝



The Art of War against Diseases

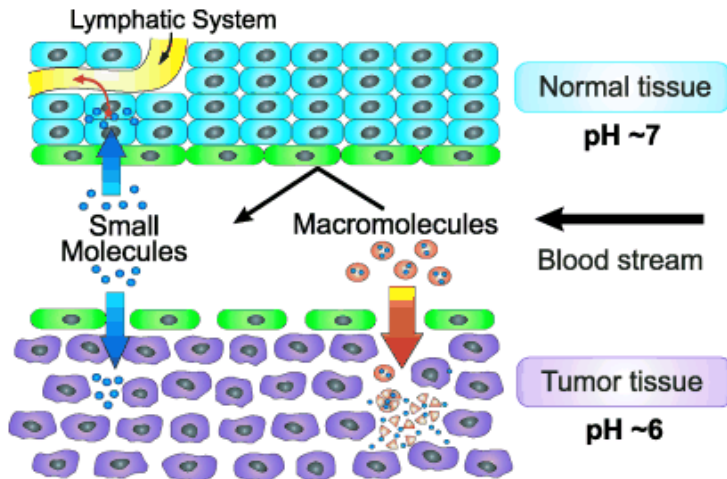
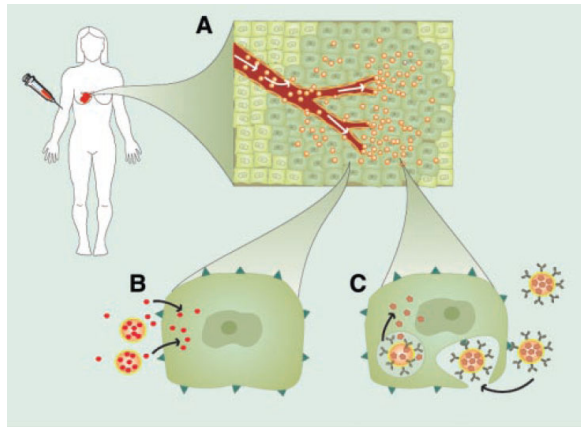
Know the properties of the drug delivery systems in vitro and in vivo.
Know the properties (heterogeneity and dynamic states) of the body.

Nanomedicine Hype

Current Understanding on Drug Targeting of I.V. Administered Systems

Passive Targeting:

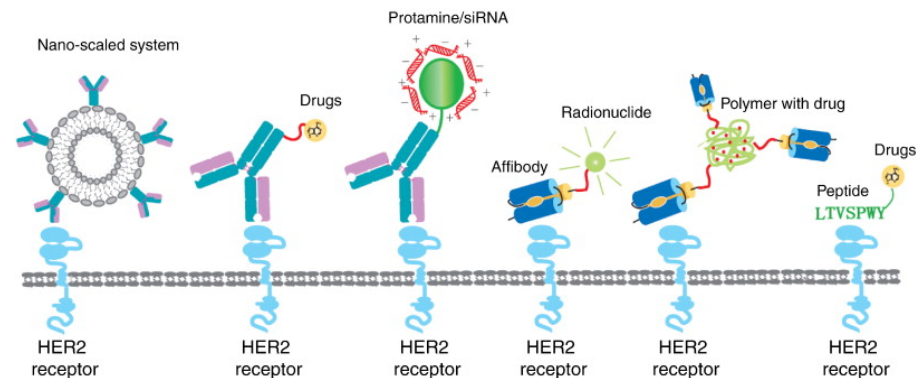
Delivery of plain nanoparticles by blood circulation



Active Targeting:

Delivery of ligand-coated nanoparticles by blood circulation

Ligand binds to target cell surface only if nanoparticle formulations reach the target!



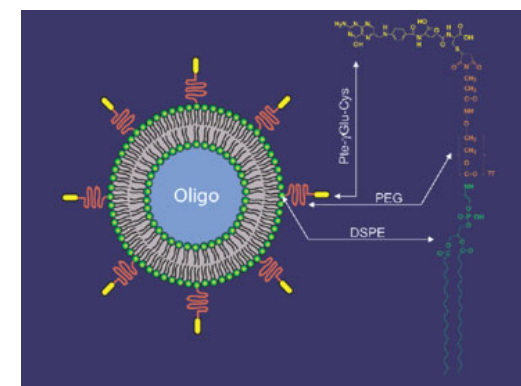
The role of HER2 in cancer therapy and targeted drug delivery.
W. Tai, R. Mahato, . Cheng: J. Control. Release 146 (3) 264-275, 2010

EPR Effect: Enhanced permeability and retention effect

Targeting In Vitro Cell Culture is not Targeting

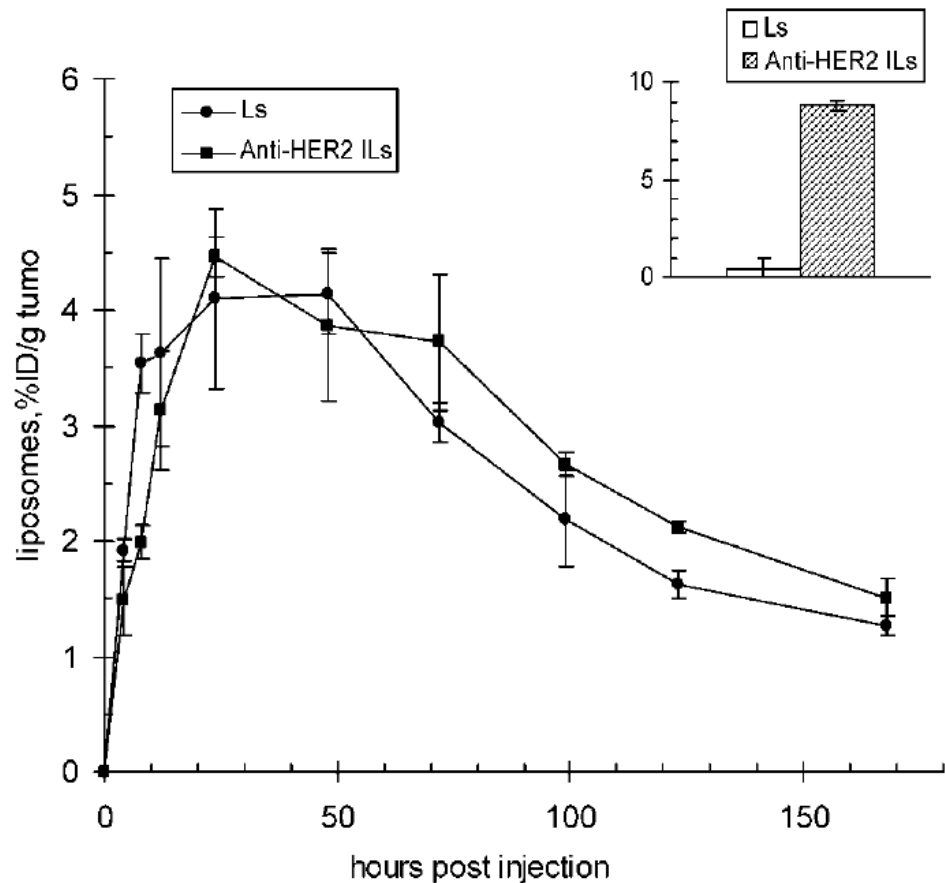
The objective of this study was to investigate the use of folate-targeted liposomes for the delivery of encapsulated oligonucleotides to folate receptor (FR)-positive tumor cells in vitro and in vivo. This project involved the synthesis and biological evaluation of many folate-PEG-lipid conjugates, where the chemical form of the folate moiety (pteroyl) and the length of the PEG linker chain were varied widely. Folate-targeted oligonucleotide-containing liposomes were prepared using conventional methods, and the extent of cell uptake was evaluated using, among others, the FR positive KB cell line. Oligonucleotide-loaded folate-targeted liposomes were found to rapidly associate with the KB cells, and saturation was typically reached within the first hour of incubation at 37 degrees C. Nearly 100,000 liposomes per cell were bound or internalized at saturation. Importantly, cell association was blocked by a large excess folic acid, thus reflecting the FR-specific nature of the cell interaction.

Full targeting potential was achieved with PEG linkers as low as 1000 in molecular weight, and pteroyl moieties bearing glycine or gamma-aminobutyryl residues juxtaposed to the pteroyl moiety were also effective for targeting, provided that a terminal cysteine moiety was present at the distal end of the PEG chain for added hydrophilicity. **When tested in vivo, folate-targeted liposomes were found to deliver approximately 1.8-fold more oligonucleotide to the livers of nude mice (relative to the nontargeted PEG-containing formulations); however, no improvement in KB tumor uptake was observed.** We conclude from these results that folate liposomes can effectively deliver oligonucleotides into folate receptor-bearing cells in vitro, but additional barriers exist in vivo that prevent or decrease effective tumor uptake and retention.



C. P. Leamon, S.R. Cooper, and G.E. Hardee:
Folate-liposome-mediated antisense oligodeoxynucleotide
targeting to cancer cells: Evaluation in vitro and in vivo.
Bioconjugate Chem. 14: 738-747, 2003

No Active Targeting by Antibody-Coated Nanoparticles



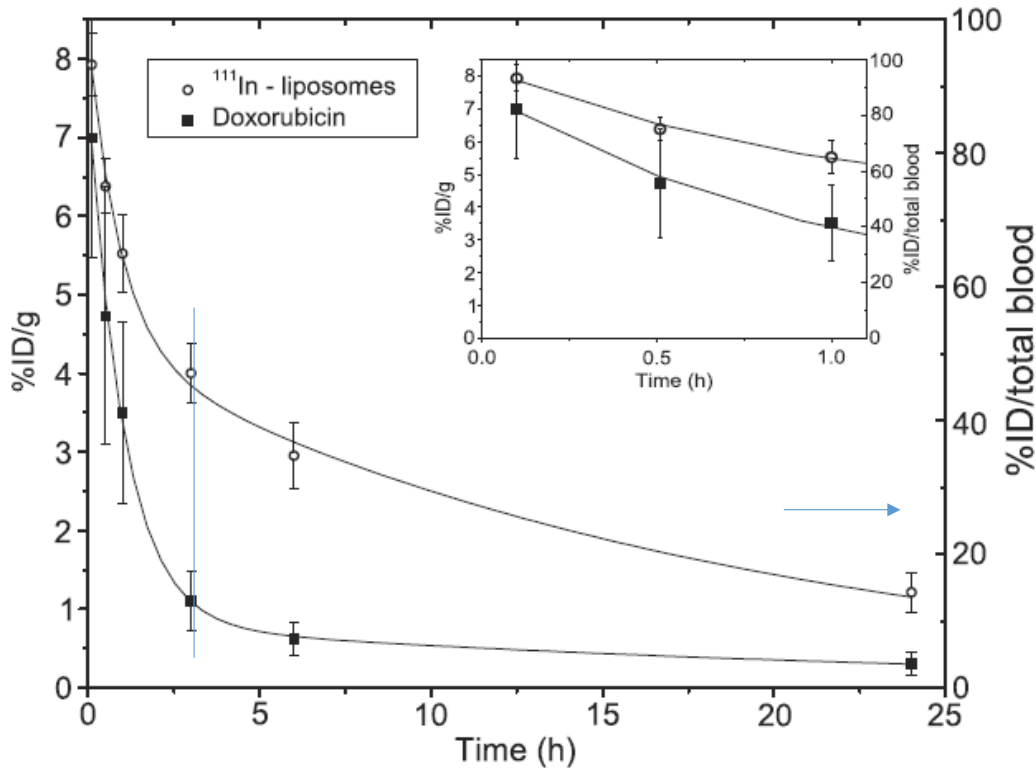
Abstract

We describe evidence for a novel mechanism of monoclonal antibody (MAB)-directed nanoparticle (immunoliposome) targeting to solid tumors in vivo. Long-circulating immunoliposomes targeted to HER2 (ErbB2, Neu) were prepared by the conjugation of anti-HER2 MAB fragments (Fab' or single chain Fv) to liposome-grafted polyethylene glycol chains. MAB fragment conjugation did not affect the biodistribution or long-circulating properties of i.v.-administered liposomes. However, antibody-directed targeting also did not increase the tumor localization of immunoliposomes, as both targeted and nontargeted liposomes achieved similarly high levels (7-8% injected dose/g tumor tissue) of tumor tissue accumulation in HER2-overexpressing breast cancer xenografts (BT-474). Studies using colloidal gold-labeled liposomes showed the accumulation of anti-HER2 immunoliposomes within cancer cells, whereas matched nontargeted liposomes were located predominantly in extracellular stroma or within macrophages. A similar pattern of stromal accumulation without cancer cell internalization was observed for anti-HER2 immunoliposomes in non-HER2-overexpressing breast cancer xenografts (MCF-7). Flow cytometry of disaggregated tumors posttreatment with either liposomes or immunoliposomes showed up to 6-fold greater intracellular uptake in cancer cells due to targeting. Thus, in contrast to nontargeted liposomes, anti-HER2 immunoliposomes achieved intracellular drug delivery via MAB-mediated endocytosis, and this, rather than increased uptake in tumor tissue, was correlated with superior antitumor activity. Immunoliposomes capable of selective internalization in cancer cells in vivo may provide new opportunities for drug delivery. (Cancer Res 2006; 66(13): 6732-40)

Dmitri B. Kirpotin, Daryl C. Drummond, Yi Shao, M. Refaat Shalaby, Keelung Hong, Ulrik B. Nielsen, James D. Marks, Christopher C. Benz and John W. Park

Antibody targeting of long-circulating lipidic nanoparticles does not increase tumor localization but does increase internalization in animal models. Cancer Res. 66: 6732-6740, 2006.

Drug vs. Drug Carrier



Blood kinetics of ^{111}In labeled TSLs containing doxorubicin. The percentage of the injected dose (%ID) is plotted per gram blood (left axis) and for the total blood (right axis). The blood clearance can be described with a biexponential time dependence.

Doxorubicin is released from liposome prematurely, and those liposomes reaching the target tumor may not even have the drug.

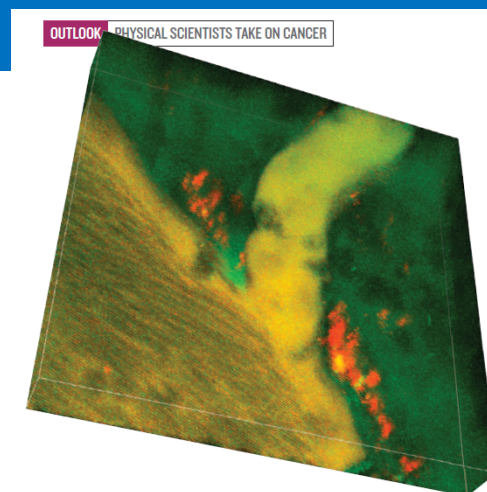
Mariska de Smet, Edwin Heijman, Sander Langereis, Nicole M. Hijnen, Holger Gröll
Magnetic resonance imaging of high intensity focused ultrasound mediated drug delivery from temperature-sensitive liposomes: An in vivo proof-of-concept study.
J. Control. Release 150: 102-110, 2011.

Failed Clinical Trials of Nanoscale Drug Carriers

NANOTECHNOLOGY

Carrying drugs

Traditional chemotherapies can be toxic but nano-sized carriers can keep them out of healthy tissue and take old drugs to new places.



A reconstructed 3D image showing the accumulation of 30-nm nanoparticles (green) in a pancreatic tumour.

Table 1: Nanoscale drug carriers in clinical trials in 2012.

NANOMEDICINE IN CLINICAL TRIALS

Several nanoscale drug carriers are currently in clinical trials.

Company	Drug	Formulation	Status	Description
Calando Pharmaceuticals	CALAA-01	A polymer nanocarrier containing gene-silencing RNA	Phase I	A polymer nanocarrier holds RNA that silences a gene in solid tumours needed for DNA synthesis and replication
BIND Biosciences	BIND-014	A polymer nanocarrier targeted to cancer cells carries docetaxel	Phase I	Targets solid or metastatic prostate cancer cells by binding to prostate-specific membrane antigen
Nippon Kayaku	NK105	A polymer nanocarrier containing paclitaxel	Phase III	Looking for progression-free survival in patients with metastatic or recurrent breast cancer
NanoCarrier	Nanoplatin (NC-6004)	A polymer nanocarrier containing cisplatin	Phase I/II	Evaluating Nanoplatin in combination with gemcitabine in patients with advanced or metastatic pancreatic cancer, with the aim of reducing kidney toxicity compared with cisplatin alone
Cerulean Pharma	CRLX101	A pH-sensitive polymer nanocarrier releases camptothecin in the acidic environment of cancer cells	Phase II	Separate studies testing CRLX101 in advanced non-small cell lung cancer and in ovarian cancer

Updated Status

Terminated in 2013

Terminated in 2016

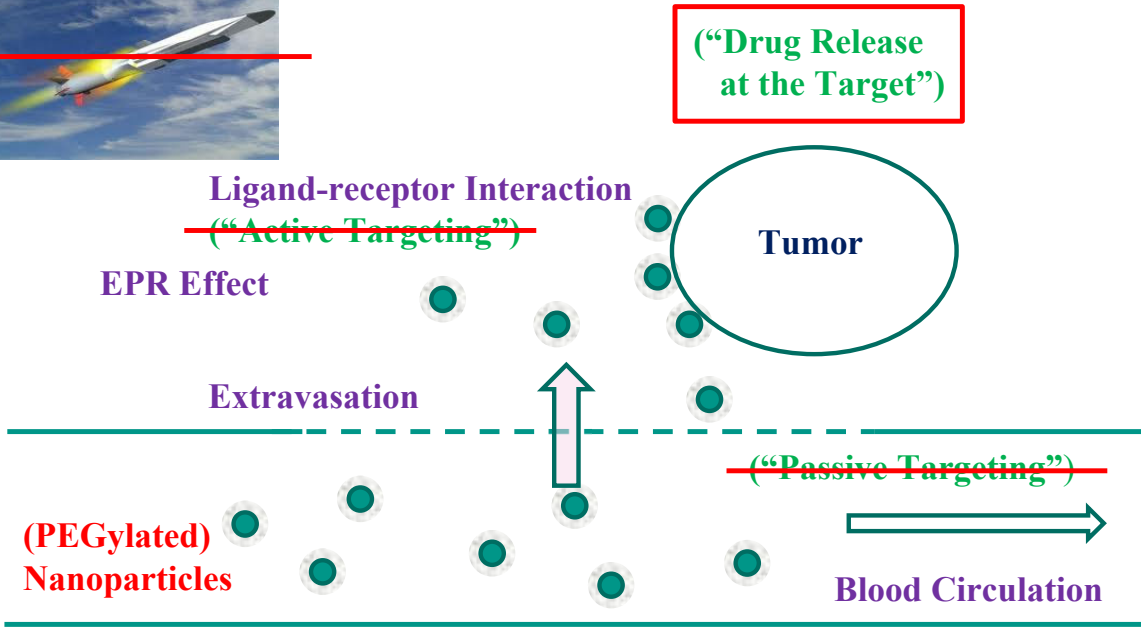
Terminated in 2016

Terminated in 2014

Terminated in 2016

K. Bourzac. Nanotechnology: Carrying drugs. Nature, 491 (2012) S58-S60.

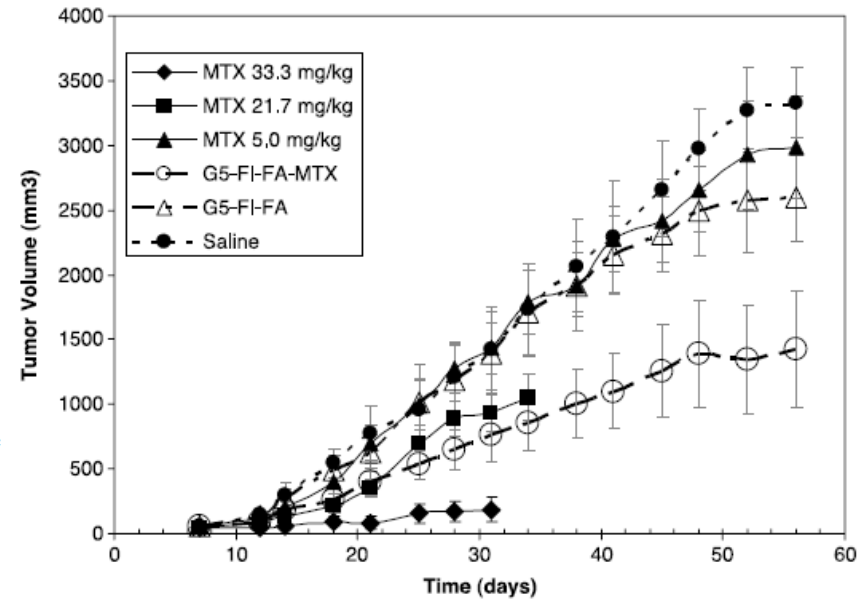
Nanomedicine: Myths and Facts



Nanoparticle Targeting of Anticancer Drug Improves Therapeutic Response in Animal Model of Human Epithelial Cancer

Jolanta F. Kukowska-Latallo,¹ Kimberly A. Candido,¹ Zhengyi Cao,¹ Shraddha S. Nigavekar,² Istvan J. Majoros,¹ Thommey P. Thomas,¹ Lajos P. Balogh,¹ Mohamed K. Khan,² and James R. Baker, Jr.¹

¹University of Michigan Center for Biologic Nanotechnology and ²Department of Radiation Oncology, University of Michigan Health System, Ann Arbor, Michigan

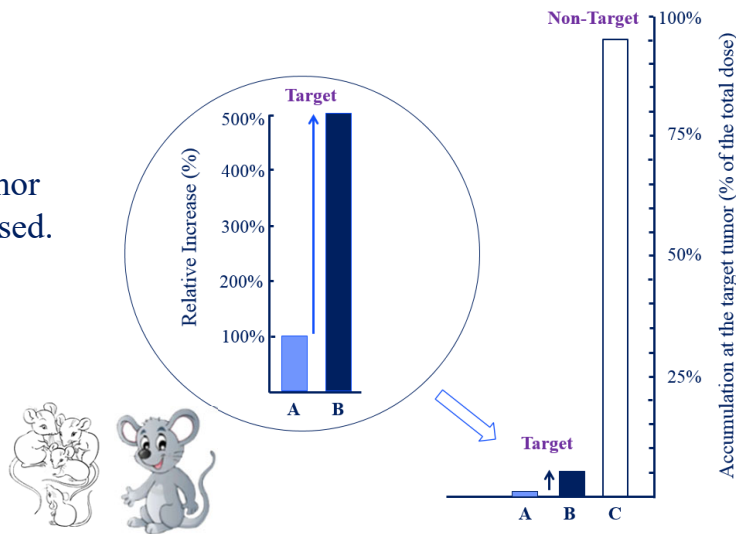


Nanomedicine: Assumptions and Facts in Targeted Drug Delivery

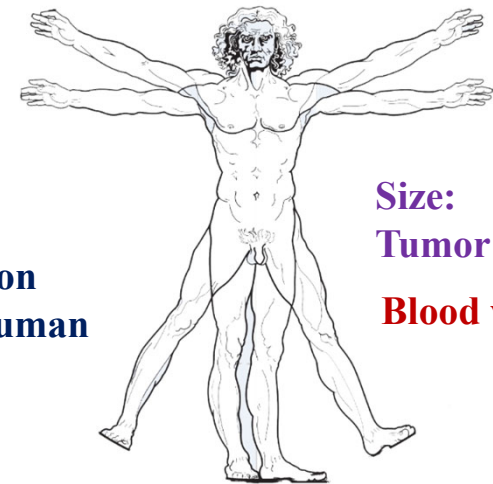
Assumptions used in targeted drug delivery by nanoparticles and the facts	
Assumptions	Facts
Nanoparticles deliver a drug to the target better than the solution control.	The improvement observed is small, usually from around 1% to 2% of the total administered dose.
PEGylation extends blood circulation time.	Only for a small fraction of the total nanoparticles.
Nanoparticles reach tumor by passive targeting.	Only 1~2% of the total dose.
Nanoparticles reach tumor by the EPR effect	But the EPR effect is not proven in humans.
Nanoparticles release a drug at the target tumor.	But only 1~2% of the total dose.



The target tumor cells are exposed.



Lack of Translation
from Mouse to Human



Size:
Tumor vs. Body
Blood volume

The Mechanisms of Nanoparticle Delivery to Solid Tumours

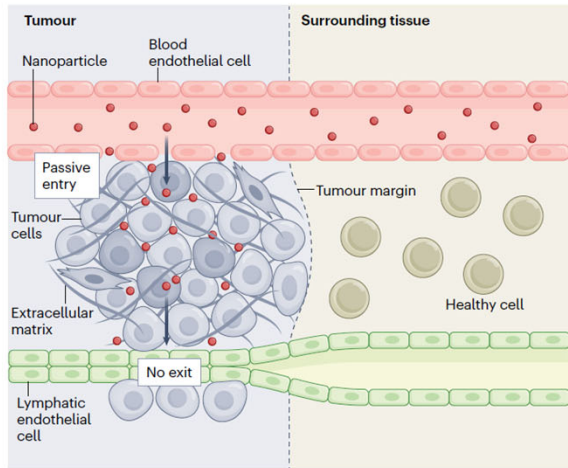


Fig. 2 | EPR mechanism of nanoparticle delivery. The enhanced permeability and retention (EPR) mechanism postulates that nanoparticles enter the tumour through gaps in the tumour blood vessel wall. Once nanoparticles are inside the tumour, the EPR effect suggests that nanoparticles are unable to exit owing to the collapse of the tumour lymphatics. The combination of nanoparticle entry and the absence of exit results in nanoparticle retention inside the tumour.

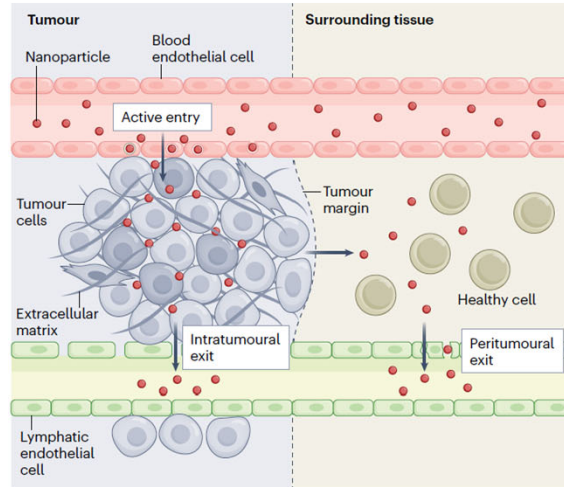


Fig. 3 | ATR mechanism of nanoparticle delivery. The active transport and retention (ATR) mechanism of nanoparticle delivery states that nanoparticles enter the tumour through both active and passive transport mechanisms. Active transport mechanisms include transcytosis mediated by nanoparticle transport endothelial cells, vesicle-vacuolar organelles and migrating cells. These active transport mechanisms are dominant over passive transport, which includes gaps and fenestrations. After entering the tumour, nanoparticles are retained owing to interactions with tumour cellular and acellular components. These tumour components sequester nanoparticles, thus slowing their transport from the entry site to the exit site. Nanoparticles exit the tumour via intratumoural or peritumoural lymphatics. Nanoparticles reach the peritumoural lymphatics by transporting out of the tumour at the tumour margin and accumulating in the tissues surrounding the tumour.

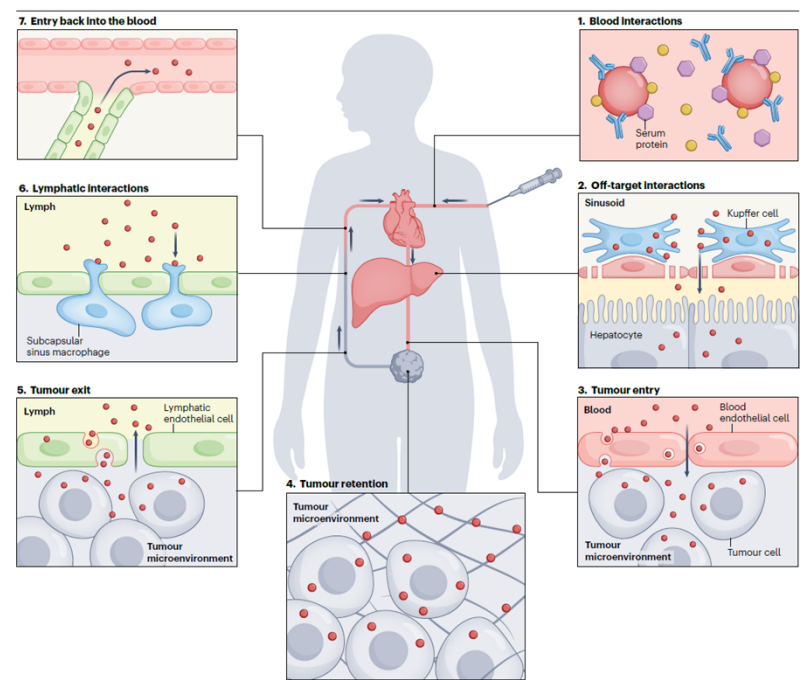


Fig. 4 | The delivery journey of cancer nanomedicine. The journey of nanoparticles once administered into the body. (1) Nanoparticles are administered into the blood, where they adsorb blood serum proteins. (2) Nanoparticles encounter non-tumour tissues, which sequester the nanoparticles and prevent tumour delivery. In addition to the liver, other organs, such as the spleen and kidneys, clear nanoparticles from the circulation. (3) Nanoparticles enter the tumour predominantly via active transport processes such as transcytosis (shown). Other mechanisms include vesiculo-vacuolar organelles and migrating cell effects. Passive transport mechanisms, such as interendothelial gaps, play a minor role. (4) Nanoparticles are retained inside the tumour owing to interactions with tumour cells and acellular components. (5) Nanoparticles exit the tumour predominantly via the lymphatics. Both lymphatic channels and vesicle-vacuolar organelle mechanisms of exit are shown. Tumour blood vessels contribute a minor role to nanoparticle exit. (6) Nanoparticles are transported through the lymphatic circulation, where they encounter immune cells in the lymphatic vessels and lymph nodes, which sequester nanoparticles. (7) Nanoparticles are transported back to the blood circulation via the right lymphatic trunks (shown) or thoracic duct. Nanoparticles then repeat this cycle (returning to the first step) until they are cleared from circulation. Nanoparticles, cells and organs are not drawn to scale.

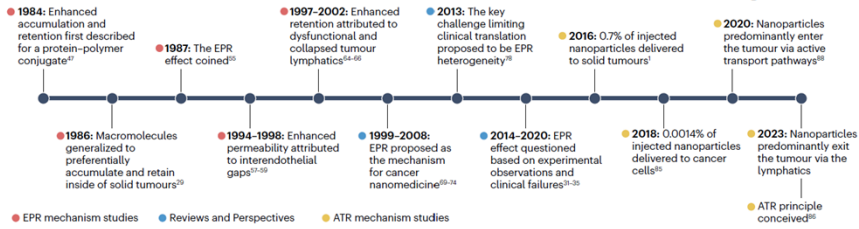
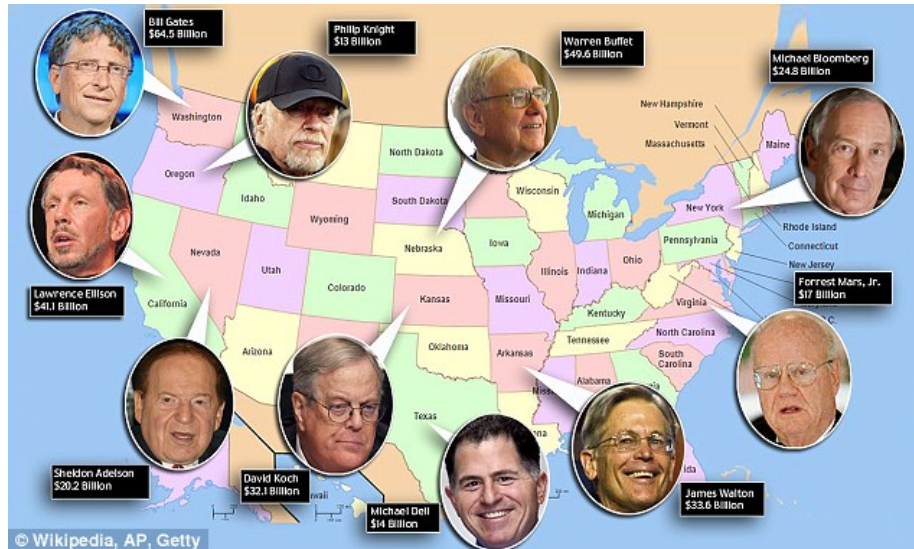


Fig. 1 | Timeline of the mechanisms of nanoparticle delivery to solid tumours. The timeline highlights key studies or a sequence of studies that led to the formulation of the enhanced permeability and retention (EPR) effect (red points) and the active transport and retention (ATR) principle (yellow points) and Perspectives are included (blue points).

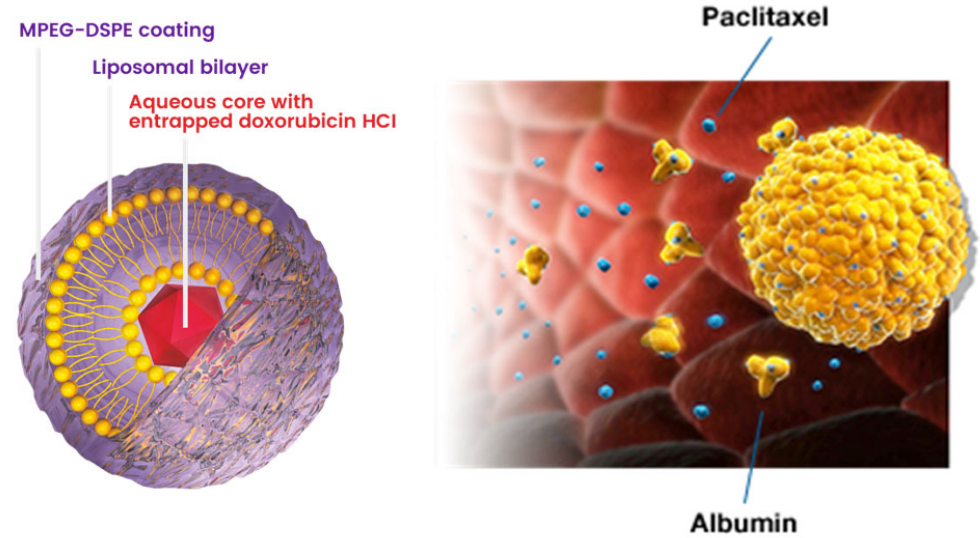
Problems of the Nanomedicine Field

Billionaires



The above billionaires are all Americans.
Therefore, all Americans are billionaires.

Clinically Effective Drugs against Cancer



The above drugs are all nanoparticles.
Therefore, all nanoparticles are clinically effective.

Different Interpretation of the Same Data

An elephant can be described by many different ways.
But which is the characteristic description of an elephant?

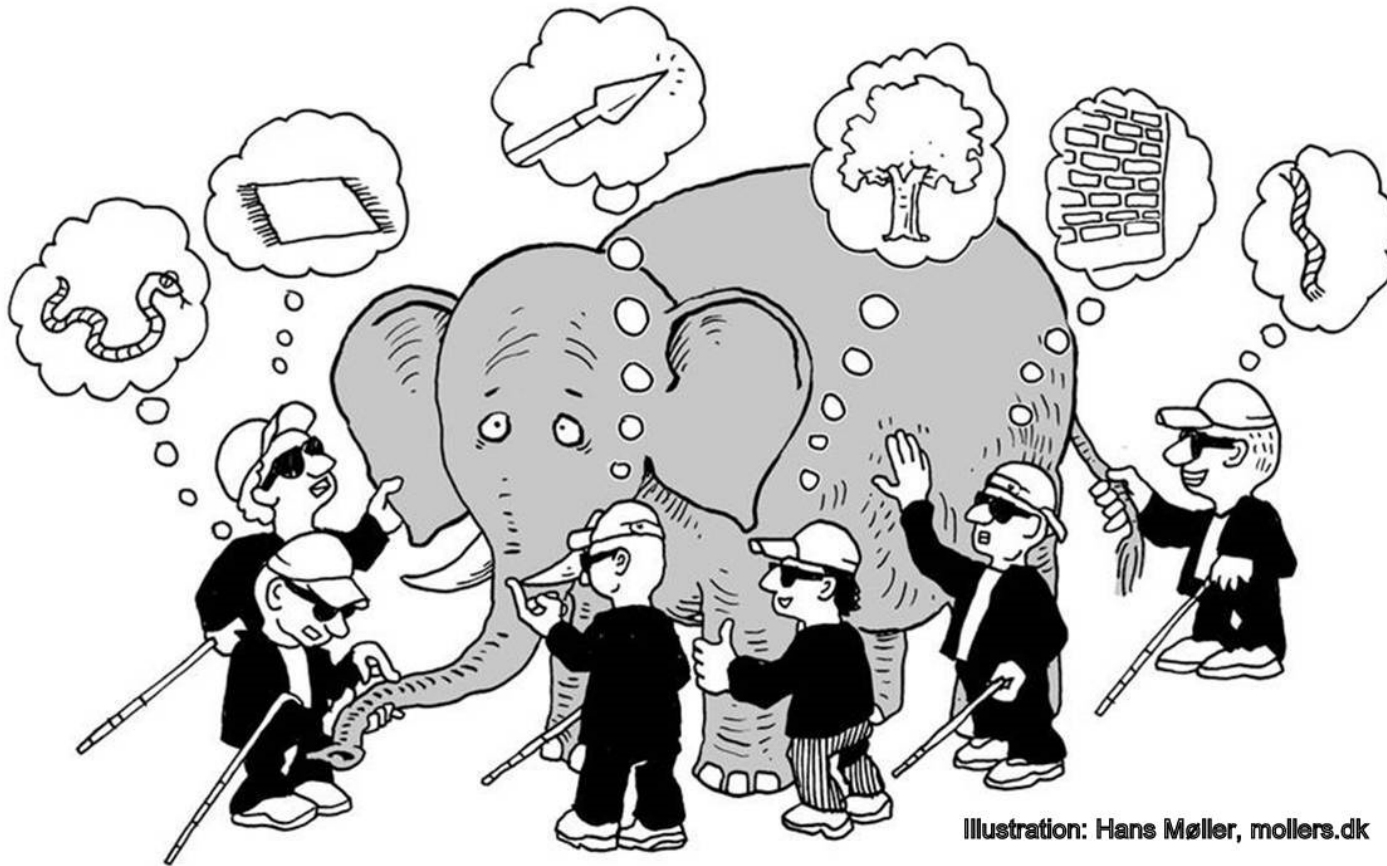


Illustration: Hans Møller, mollers.dk

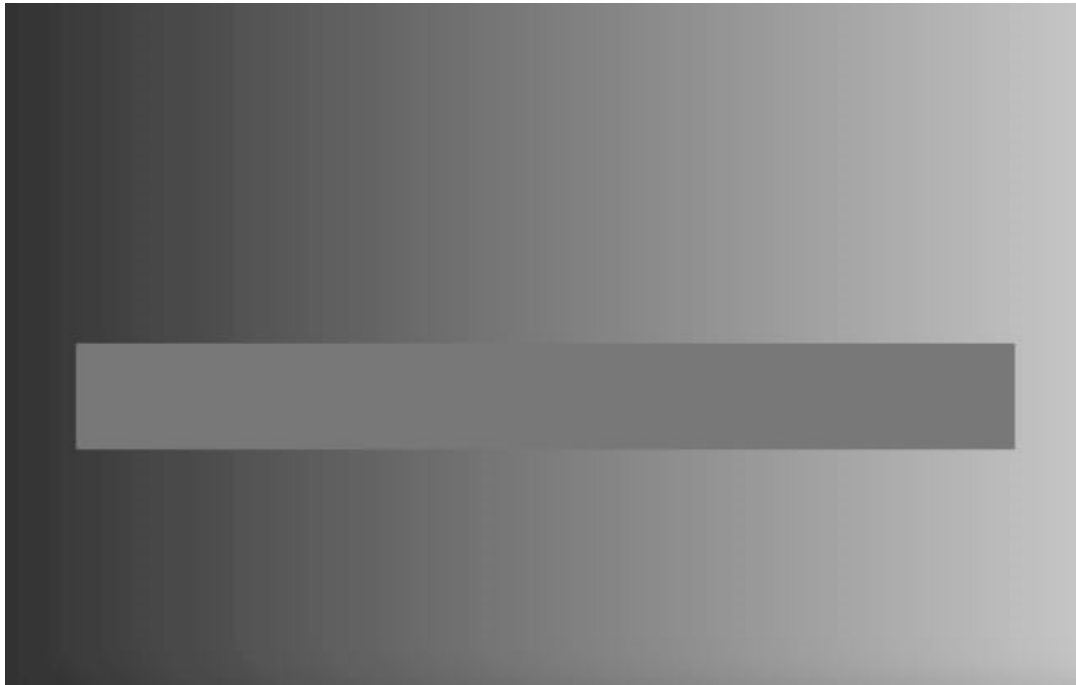
Ask Questions To Make Sure!

Professor Allan Hoffman



Idea: Peter Reid. University of Edinburgh

The Gray Bar in This Image Appears to be a Shaded Gradient.



https://www.buzzfeed.com/hikaruyoza/optical-illusions?utm_term=.evdyg5Z7b#.eg8GoryZ0

The Beginning of the End of the Nanomedicine Hype



journal of controlled release

OFFICIAL JOURNAL OF THE CONTROLLED RELEASE SOCIETY
AND THE JAPANESE SOCIETY OF DRUG DELIVERY SYSTEM

The Cancer Survivor's Journey

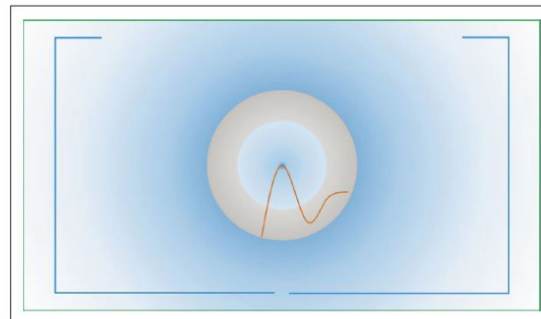
- 1 vitamin to 17 daily pills
- 1 MRI
- 2 PET Scans
- 12 Neulasta Injections - long bone pain
- 12 Atropine injections - disabled speech
- >19 hospitalisations for chemo s/e
- 28+ CT scans with radioactive dye
- 31 trips to the ER
- 72 experimental pancreatic vaccines
- 62 chemotherapy infusions
- \$100,000 spent in medical bills
- >84 trips to Hopkins - 75% in snowstorms
- >90 bags of fluid
- >133 days and 70 nights in a hospital
- >230 doctors' appointments
- 225 minutes of high dose radiation
- 360 lovenox injections
- 420 Lab draws

Obtaining the first ever image of an invisible black hole was made possible by a new algorithm developed by graduate student, Katie Bouman, [6] who was not bound to conventional wisdom. If a young scientist with a fresh mind can make an invisible black hole visible, a young drug delivery scientist with untethered ideas can also make invincible cancer vincible. The metrics of success or progress in our field should be based on whether a drug delivery system has saved cancer patients, not on the potential to cure or the number of publications [7]. We should never lower the goal or adjust the objective [8]. We should stop patting each other on the back, and should be more critical of each other with an expectation of real progress that will make clinical impact. Let's make Lora and all of the courageous cancer patients fighting daily to survive proud of what we do.



journal of controlled release

OFFICIAL JOURNAL OF THE CONTROLLED RELEASE SOCIETY
AND THE JAPANESE SOCIETY OF DRUG DELIVERY SYSTEM

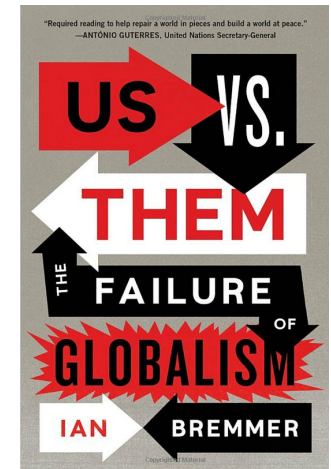
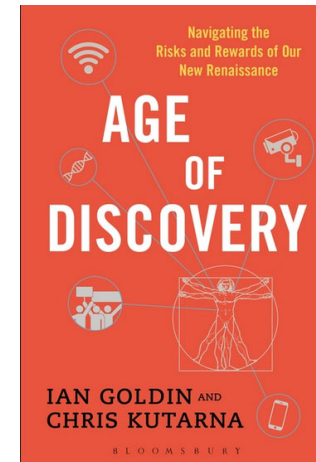
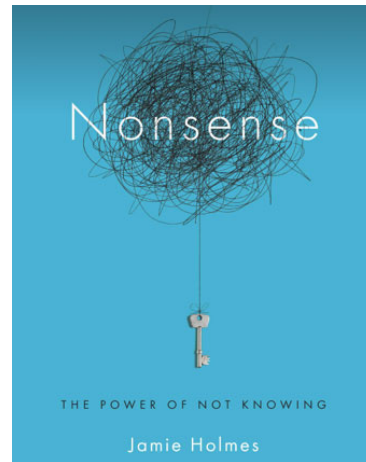
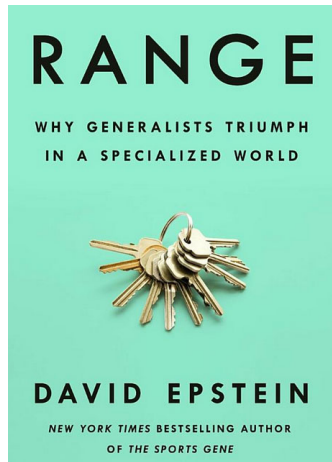


COVER STORY

The beginning of the end of the nanomedicine hype

Doing research is like a painter trying to capture a beautiful sunrise reflected on water on canvas. The difficulty is that it lasts only 5 min and it is too short to capture it by painting. Only repeated attempts to capture the moment will lead the painter to reproduce the image. Claude Monet said, "I have done what I could as a painter". Scientists do what they can do without exaggeration and hype. Science is hard and it does not become easier simply because someone comes up with trendy names with a lot of promotion. To avoid this problem, the current funding systems have to change to support conservative scientists who have diverse, meaningful research ideas. The recent NCI's announcement is encouraging, as it marks the beginning of shifting resources to nurture unpretentious scientists who do research, without any fanfare, on what matters in real life.

Science The Endless Frontier



Functional fixedness.

The man with a hammer =
The man with nanomedicine,
lacking the far transfer ability.

One tidy theoretical
formula with a single lens
**bends every event to fit its
ideas.** This does not work on
ill-defined problems.

The future is uncertain. We
must train the next generation
of scientists for the uncertain
future to **solve problems that
have no easy answer, to learn
failure is a part of progress,**
and to keep an open mind and
empathize with different
viewpoints.

Scientists should be able to
navigate the risks and
rewards, build the ability to
**shift resources and focuses
to a completely unexpected
direction,** continue relentless
improvements by challenging
paradigms, and mix ideas to
enrich humanity.

History shows that **people
give their best when their
best is required of them.**
That day is here now.

Human beings have
evolved to use their natural
ingenuity to create the
tools they need to survive

Concepts, ideas, and potentials in research articles are just the first step. It is the execution that makes the real difference.

The drug delivery field needs more implementations in clinical applications.

<https://www.hiv.gov/hiv-basics/overview/history/hiv-and-aids-timeline>

The Dangers of Nanoparticles

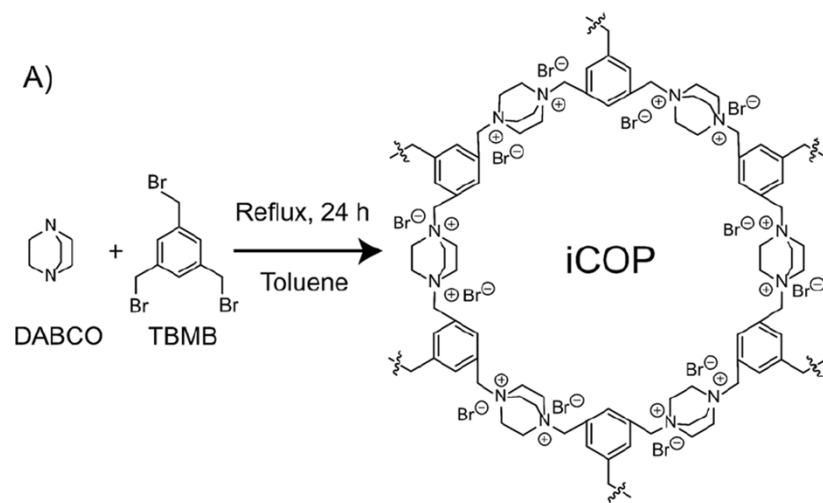
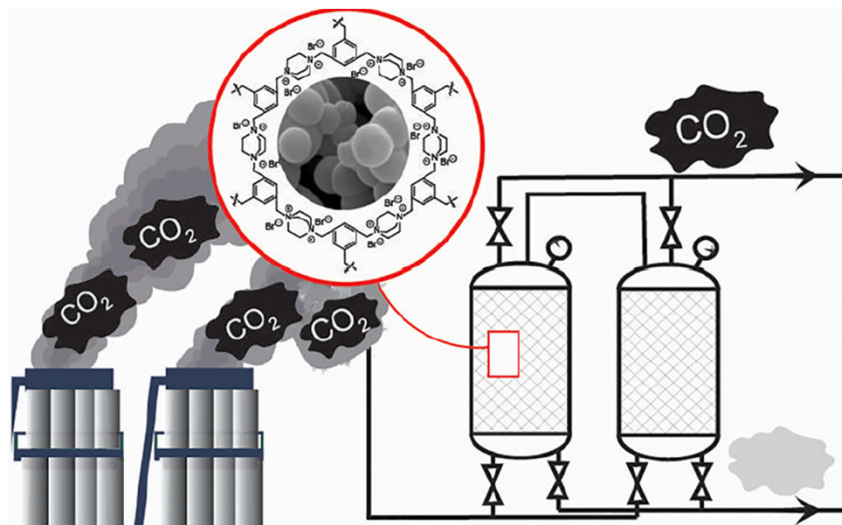
Nanoparticles made of plastics (nanoplastics) are polluting the Earth. They ferry in hazardous chemicals and help them accumulate up the food chain.

We breathe, inhale, and ingest them, and we are not aware of it.

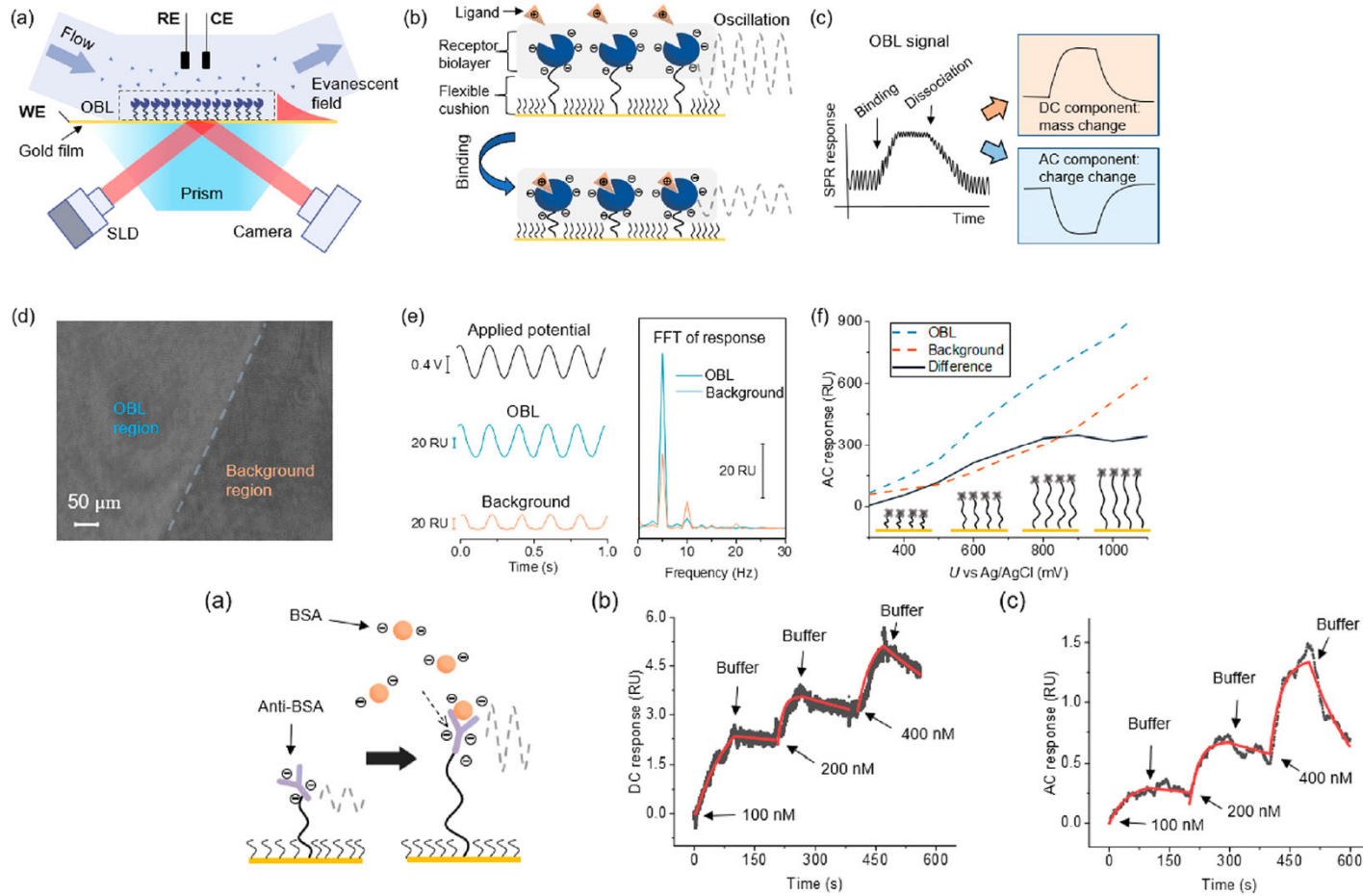
Nanomaterials & Their Applications

Ionic Covalent Organic Polymers for CO₂ Capture

ABSTRACT: We report on a scalable synthetic pathway to produce an ionic covalent organic polymer (iCOP) via the Menshutkin reaction. This one-step synthetic procedure avoids the need for postmodification of a COP and the use of ionic monomers. The as-synthesized materials precipitate as nanoparticles. The physical and chemical properties of the nanomaterials are characterized, and their sorption capacity for carbon dioxide (CO₂) capture is evaluated. The results indicate that the iCOP has a CO₂ uptake capacity of ~1.5 mmol/g at 1 bar and 293 K. The synthesized materials are considered green, and the proposed one-step approach is cost-effective when compared with other approaches used to synthesize porous materials for adsorption.



Electrical Modulation of a Flexible Nanobiolayer



Thermal Reflow of Polymers

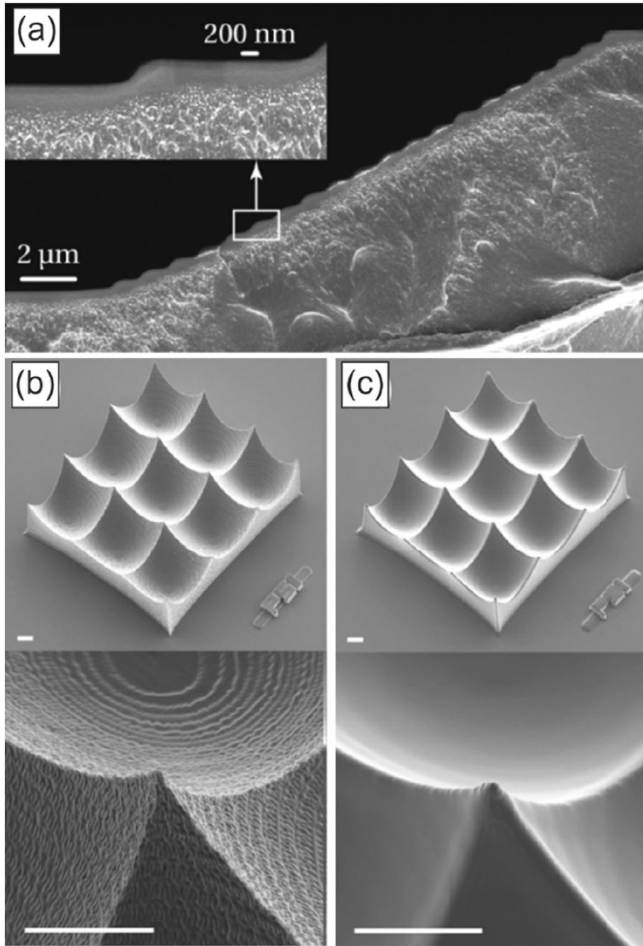


Fig. 14. SEM micrographs for PMMA microscopic structures (a-b) before and (c) after reflow: (a) cross-section of vacuum UV (VUV) created low M_w and low T_g section on top of unmodified bulk section for a microscopic step profile, (b) 3×3 lenslets after replication in PMMA, (c) VUV exposed and reflowed surface with ultra-smooth surface finish and minimal effects on the total (bulk) geometry

In micro- and nanofabrication, thermal reflow generally describes the concept of reshaping initial patterns into new profiles. While the initial structure can be obtained from efficient standard processes, the reshaped and new profile can most often only be obtained with reasonable efforts by reflow. In non-technical applications, reflow is like melting sugar grains into droplets or merging them into a smooth crust of caramelized sugar on a Crème brûlée. On the technical side, one prominent example is the fabrication of microlenses, i.e., lenses with curved surfaces and some tens of micrometer up to a few millimeters in diameter.

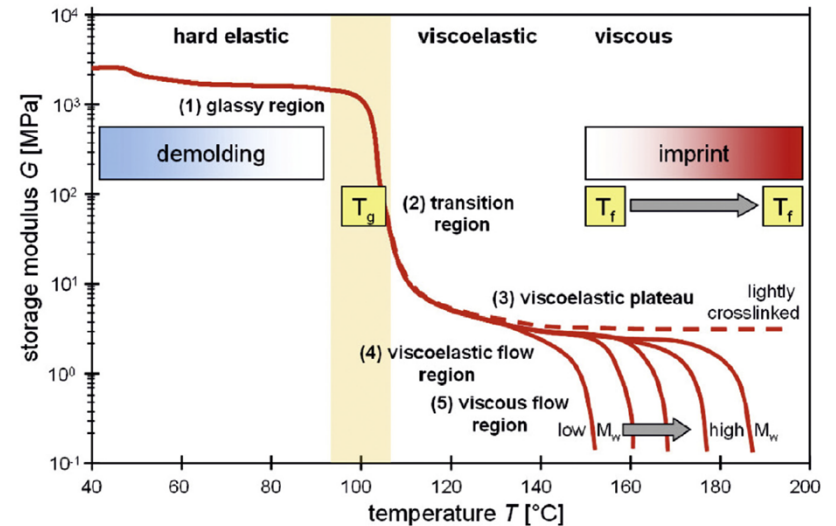


Fig. 2. (a) Mechanical properties of polymers dependent on temperature, molecular weight, and crosslinking (Ref [58]., modified from Ref [59]). Schematic for a polymer with a T_g around 100 °C for normal process conditions.

Nanowood

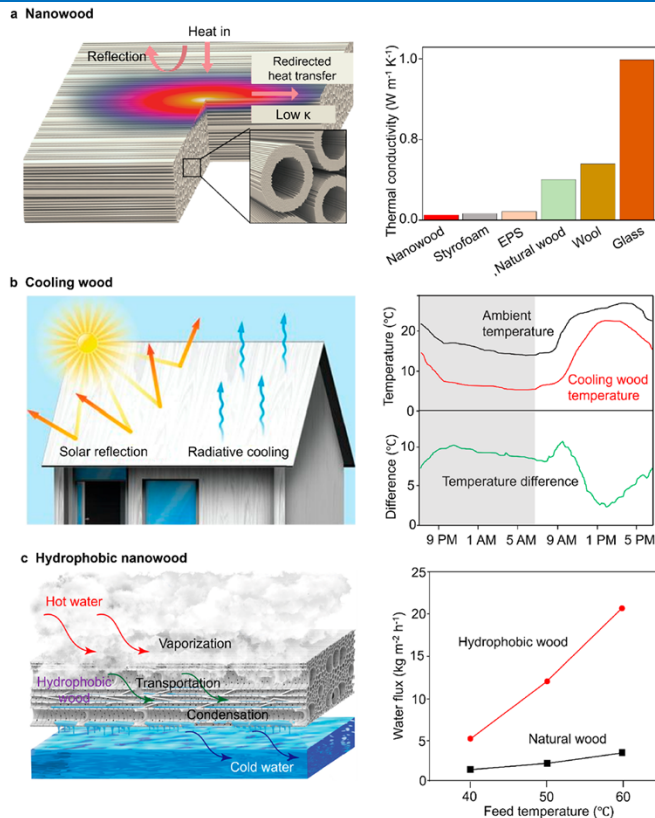


Figure 6. Delignification of wood toward thermal-management material. (a) Near-complete delignification reduces the thermal conductivity of wood by removing high thermal-conductivity lignin and creating more nanopores. Near-complete delignification endows the nanowood with a thermal conductivity of $\sim 0.03 \text{ W} \cdot \text{m}^{-1} \cdot \text{K}^{-1}$, which is lower than those of thermally insulating materials, such as Styrofoam, expanded polystyrene (EPS), wool, and grass. (b) Near-complete delignification and compression result in the cooling wood with a temperature lower than ambient temperature, in which the temperature reduces $>9^{\circ}\text{C}$ during the night and $>4^{\circ}\text{C}$ between 11 am and 2 pm due to the coverage of the cooling wood. (c) Nearcomplete delignification and hydrophobic modification via fluoroalkylsilane treatment prepare the hydrophobic wood enabling thermal-efficient distillation with a high flux of water.

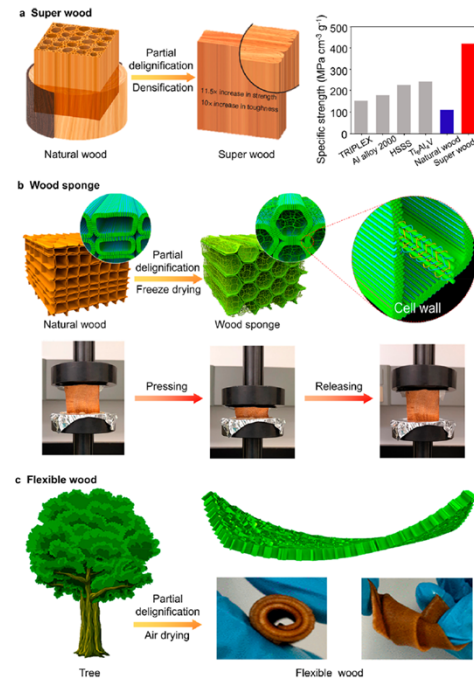


Figure 5. Partial delignification of wood toward lightweight structural

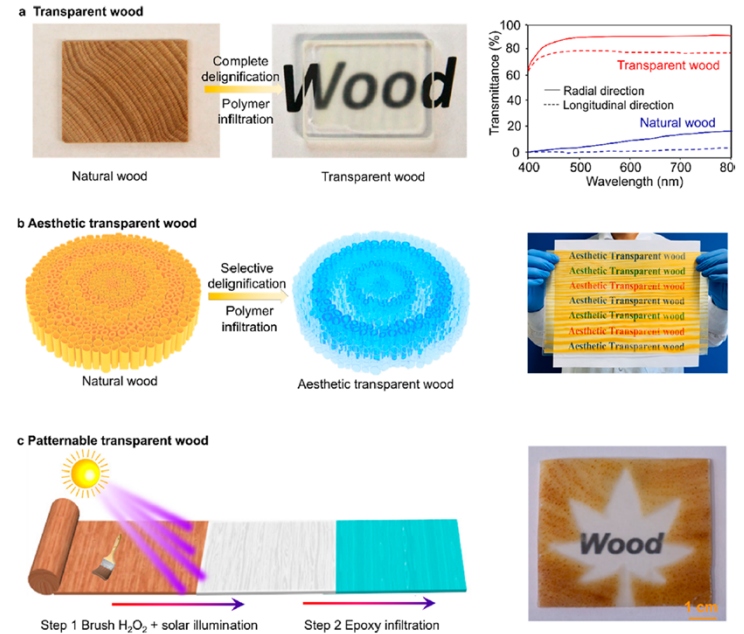


Figure 7. Delignified wood-polymer composites toward light-management materials. (a) Delignification and polymer infiltration modulate the optical performance of wood via making wood transparent. The transparent wood features a transparency of 90% in the radial direction and almost 80% in the longitudinal direction, both of which are much higher than the natural wood. (b) Spatial-selective delignification and polymer infiltration enables a high transparency and aesthetic patterns of wood, thus constructing an aesthetic transparent wood. (c) Solar-assisted chemical brushing strategy for manufacture the patternable transparent wood. The most lignin of wood is reservation and just light-absorbing chromophores of lignin are removed, which endows the patternable transparent wood with high strength and flexibility, as well as reducing the consumption of energy and chemicals.

Nanocellulose

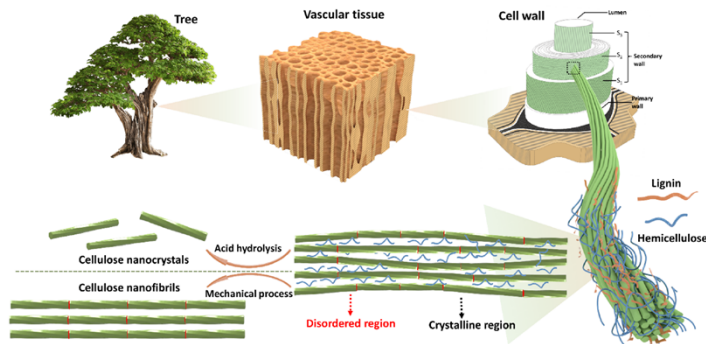


Figure 2. Schematic representation of the plant cell wall and cellulose fiber structure. CNFs and CNCs are extracted from cellulose fibers using mechanical process and chemical methods (oxidation or acid hydrolysis), respectively.

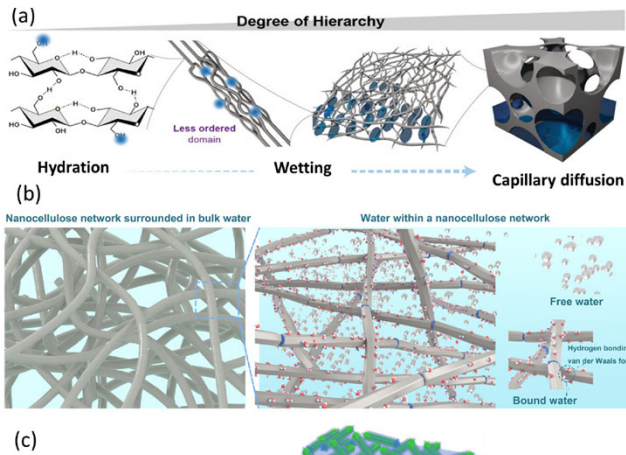


Figure 6. Schematic representation of wetting and hydration of nanocellulose. (a) Water and nanocellulose interactions from a supramolecular hierarchical point of view.²⁶ (a) Adapted from ref 26 under the terms of CC BY. Copyright 2020 John Wiley and Sons. (b) Wetting of cellulose nanofibers, highlighting the different states of water (bulk, free, and bound water) within nanocellulose networks. (c) Wetting of cellulose nanocrystals (in green) surrounded by adsorbed water (light blue)²⁷ (c) Adapted with permission from ref 27. Copyright 2015 American Chemical Society.

Solhi 2023, Understanding nanocellulose–water interactions. Turning a detriment into an asset

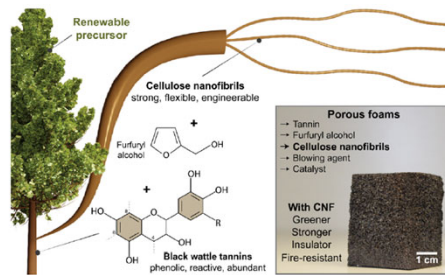


Figure 1. Left: Overall scheme of the preparation of tannin-furfuryl alcohol rigid foams reinforced with CNF. CNF is added as a wall reinforcer to replace chemical crosslinkers, here benchmarked by formaldehyde. The resulting CNF-containing tannin-furfuryl alcohol foams display thermal insulation capacity, fire self-extinguishing character, and are stronger and more sustainable than those containing chemical crosslinkers. Right: Porous foams are produced from plant-based building blocks. The chemical structure displayed represents a major group of compounds identified in black wattle tannins, including proanthocyanidin, which can polymerize from carbons 4, 6, and 8 to form a tridimensional macromolecule.^{24–26}

Missio 2022, Nanocellulose removes the need for chemical crosslinking in tannin-based rigid foams

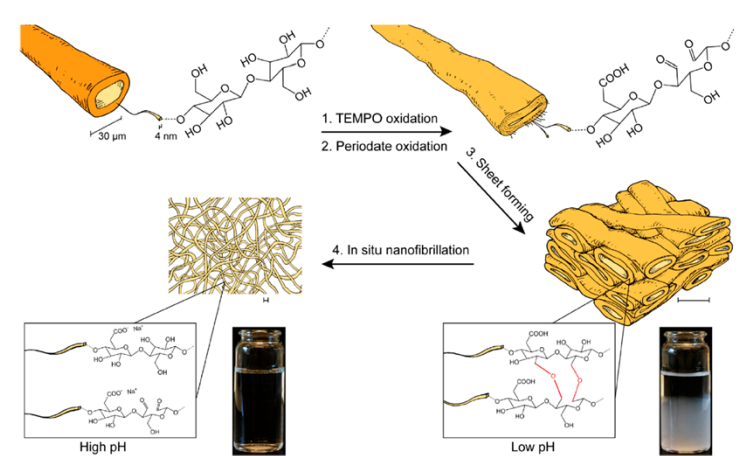


Figure 1. Scheme of sequential TEMPO and periodate oxidation followed by sheet forming and subsequent in situ nanofibrillation in the formed sheet. The inset photographs of vials represent SFF dispersions before and after stimuli-induced nanofibrillation.

Gorur 2020, Self-fibrillating cellulose fibers- rapid in situ nanofibrillation to prepare strong, transparent, and gas barrier nanopapers

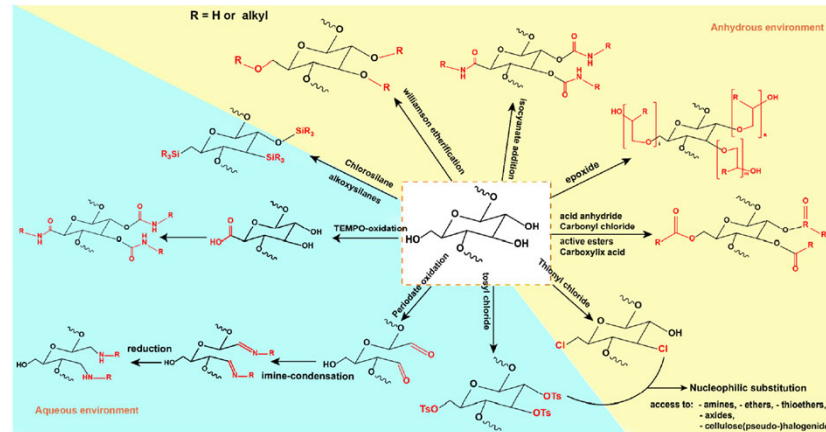


Figure 7. Most common initial reactions of cellulose, as the foundation for more elaborate modifications and their compatibility (blue)/sensitivity (yellow) to water.

Polydimethylsiloxane Vitrimer for Ultra-thin Durable Hydrophobic Films

dyn-PDMS: polydimethylsiloxane network strands and dynamic boronic ester crosslinks. Dyn-PDMS can also be utilized to fabricate superhydrophobic surfaces ($\theta_a > 150^\circ$) on textured substrates by a variety of techniques like spin-coating and dip-coating.

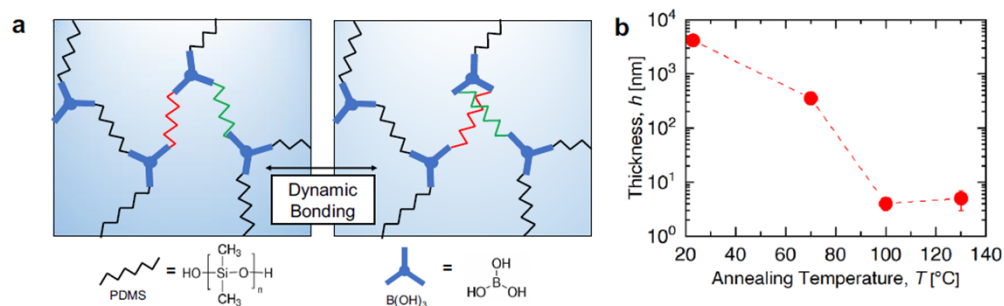


Fig. 1 Molecular design and characterizations of dyn-PDMS. **a** Schematic and chemical structure of a dynamic network made with PDMS strands and boric acid through transesterification. Green and red strands highlight the dynamic bond exchange.

b Correlation between the coating thickness and annealing temperature for $550 \text{ g} \cdot \text{mol}^{-1}$ PDMS.

Fabrication of superhydrophobic dyn-PDMS sample.

A solution of 1.7:1 PDMS to boric acid was prepared by dissolving the boric acid in 3 mL of IPA and mixing with the 1 mL PDMS in a 20 mL vial at 60 °C. The solution was then stirred at 110 °C on a hot plate and most IPA evaporated. When the solution in the vial decreased to 2 mL, the solution was in a 1:1 ratio of PDMS to IPA. The etched aluminum substrate was washed sequentially with ethanol/water/IPA and blown dry. 150 μL of 1.7:1 dyn-PDMS solution was pipetted onto the 2 cm² substrate and spun coat following the same procedure as all above samples. The substrate was cured in a vacuum oven at 110 °C for 17 h.

Ma 2021, Ultra-thin self-healing vitrimer coatings for durable hydrophobicity

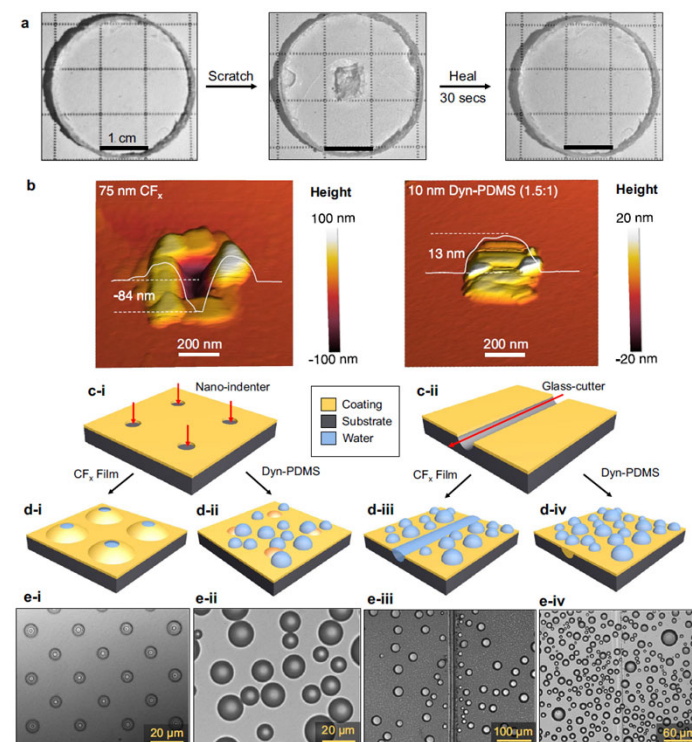


Fig. 2 Self-healing of dyn-PDMS films. **a** Optical top-view images of a bulk dyn-PDMS cylinder healing at room temperature after being scratched in the center using a razor and healed at room temperature after 1 psi of pressure was applied. **b** Response of the materials to AFM area scratches with a contact force of 2 μN . The area scratch was performed at the center $200 \text{ nm} \times 200 \text{ nm}$ area, and left permanent damage on CF_x (left image), while the self-healing dyn-PDMS film (right image) was left with a bump of materials covering the damaged hole. Inset color bar: surface height from low (black) to high (white). **c** Comparison of dyn-PDMS and CF_x thin-film hydrophobicity. Schematic showing the observed response of the coating to (c-i) artificial nano-indented pinholes and (c-ii) scratches. During steam condensation, optical microscopy images revealed that (d-i and e-i) water blisters formed beneath pinholes on the CF_x film, while (d-ii and e-ii) no blisters formed on the dyn-PDMS film. Top-view optical microscopy images showed (e-iii) droplets pinned near the linear water film on the CF_x coating after scratching, while (e-iv) the scratch on the dyn-PDMS sample recovered and healed as evidenced by droplets nucleating directly on the scratch without signs of pinning.

Organogel

Soft hydrogels and organogels combined with suitable solvents are commonly employed for the cleaning of dirty surfaces, especially when the substrate is susceptible to swelling and its functionality is compromised by the solvent itself. **The benefits of gels rely on their capability to entrap the solvent to minimize substrate damage and to adapt their shape to maximize the contact with the surface**, necessary to achieve good cleaning efficiency. Traditionally, natural resins, such as dammar and shellac, have been widely used for the preparation of varnishes. With the passing of time, natural resins change their chemical, optical, and mechanical properties because of the oxidative actions of light, air, and the interaction with pollutants. The most common procedure for the removal of the discolored and degraded varnishes consists in applying solvents with cotton swabs. However, this approach is extremely risky for the painting because **the solvent action is highly uncontrollable and leads to saponification, swelling, and leaching of the painting layer components**, with decrease of the surface mechanical strength. A valid alternative is **the use of gels able to exert a controlled solvent action**. Consequently, **chemical and physical gels** have become popular for the removal of aged varnishes or coatings from artwork surfaces through a “press and peel” approach.

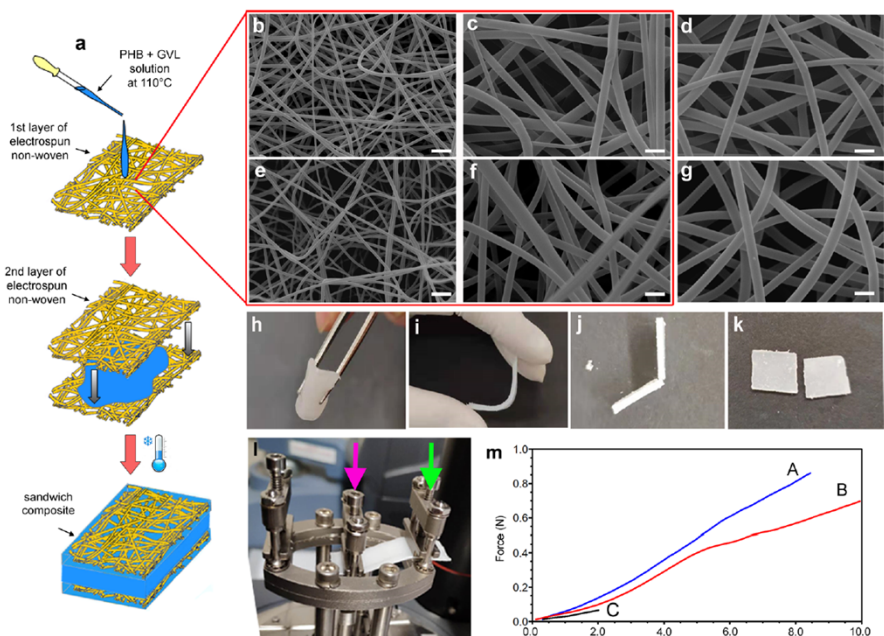


Figure 1. Sketch describing the preparation of PA6,6/PHB-GVL and PVA/PHB-GVL sandwich-like composites (a). SEM images of PA6,6 (b,c) and PVA (e,f) fibers at different magnifications; PA6,6 (d) and PVA (g) fibers after immersion in GVL for 1 min at 110 °C and dried at RT. Representative pictures of sandwich-like composite (h,i) and PHB-GVL gel (j,k) showing the different mechanical resistance of the two types of materials under bending. (l) Single cantilever configuration for sample mounting, where the green arrow indicates the fixed clamp and the pink arrow indicates the movable clamp (a representative composite sample is mounted in the picture). (m) Force-displacement curves of PA6,6/PHB-GVL composite (blue, A), PVA/PHB-GVL composite (red, B), and PHB-GVL gel (black, C): composites resist up to 10 mm bending, whereas the gel breaks at 2 mm. Scale bar: 6 μm (b,e); 2 μm (c,d,f,g).

Materials. γ -Valerolactone (GVL), PHB, poly(vinyl alcohol) (PVA) ($M_w = 85,000\text{--}124,000$ g/mol, 87–89% hydrolyzed), 1,1,1,3,3,3-hexafluoro-2-propanol (HFIP), absolute ethanol (EtOH), and γ -butyrolactone (BL) were purchased from Sigma-Aldrich. PA6,6 (Zytel E53 NC010) was kindly provided by DuPont.

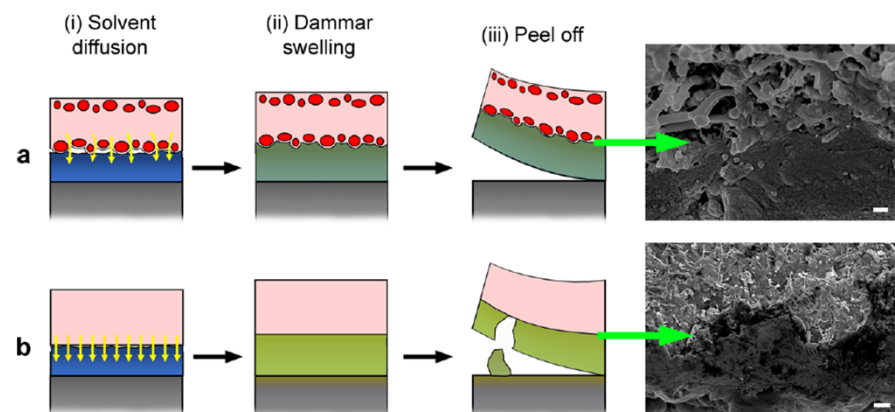


Figure 8. Schematic representation of the mode of action of (a) sandwich-like composites and (b) PHB-GVL organogel for the cleaning of dammar varnish. (i) Solvent diffusion from the gel phase to the varnish (solvent is depicted by yellow arrows): in the sandwich-like composites GVL diffusion is limited by the presence of the fibrous layer (fibre sections are depicted as red circles). (ii) dammar swelling: dammar swells after GVL absorption from the gel phase by following either the rough surface morphology of the composites (a) or the smooth surface of the organogel (b). Higher swelling is expected in the case of organogel compared to the composites, given the higher GVL diffusion from the former. (iii) Removal of the cleaning material by peeling off: dammar layer is effectively peeled off by using composites thanks to its good mechanical adhesion with the rough surface (see SEM image), whereas residual solvent and fragments of dammar can remain on the paint when organogel is used, due to its worse adhesion with the gel (see SEM image).

Jia 2020, Organogel coupled with microstructured electrospun polymeric nonwovens for the effective cleaning of sensitive surfaces

Micro/Nanomotors

Micro/nanomotors designed for environmental applications contain functional materials that enable their swimming at the microscale and removal of pollutants from the contaminated water. The choice of the functional material depends on the target pollutants.

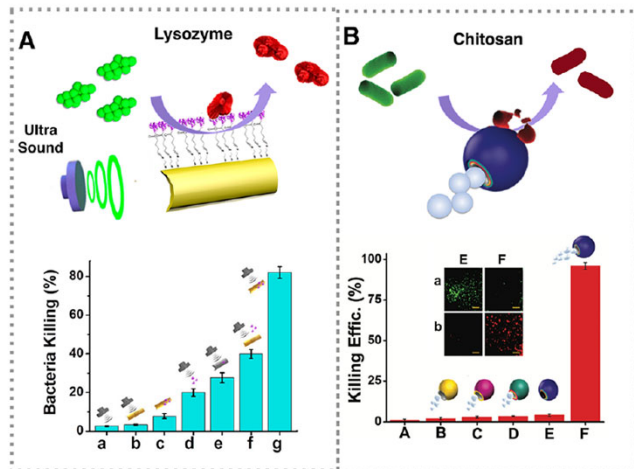


Figure 4. Removal of pathogenic microorganisms by (A) ultrasound propelled nanomotors containing lysozyme, (B and C) chitosan and silver nanoparticle-coated bubble propelled magnesium-based micromotors.

Pathogenic Microorganisms. The presence of pathogens in the water is a leading cause for the increase in diseases such as cholera and typhoid. **Common disinfection methods use chemicals (chlorine, chloramines, and ozone) or physical processes (UV light and heat) or a combination of both** due to the high resistance of some pathogens. However, the high doses of these disinfectants can be harmful or may leave toxic byproducts. **Micromotors focused on the removal of pathogenic bacteria from contaminated water, integrating on their structures several bactericidal materials or molecules such as enzymes, polymers, and metals have been developed.** Additionally, these micromotors can be designed for the selective isolation and destruction of bacteria by the modification of their structure with aptamers, antibodies, protein receptors, and target enzymes. Campuzano et al. described the first example of micromotors for capturing and isolating bacteria. First, Ni/Au layers were deposited by ebeam vapor deposition on the outer surface of electrosynthesized polyaniline (PANI)/Pt tubular micromotors. Afterward, the Au surface was modified using mercaptoundecanoic acid and NHS/EDC chemistry for the subsequent incorporation of the lectin receptor. Once the lectin-modified micromotors were placed in H₂O₂ solution, they selectively bind to the Escherichia coli (E. coli) surface by antibody–antigen interactions and capture E. coli while swimming. Later, the same research group demonstrated the first use of nanomotors for killing bacteria. The team used porous gold nanowires (p-AuNWs) propelled with an external ultrasound (US) source and **functionalized their surface with lysozyme, an antibacterial peptidoglycan-hydrolase (muramidase activity) enzyme** (Figure 4A) able to damage specifically the protective wall of bacteria. The p-AuNWs were fabricated using template electrosynthesis of different metal layers: (i) Ag sacrificial layer, (ii) Au layer, and (iii) Au–Ag layer being liberated after silver removal. The surface was chemically modified with cysteamine, which forms Au–S bonds and provides N-terminal groups to the AuNWs, for the subsequent use of glutaraldehyde molecule as a linker of proteins. Two kinds of bacteria, Micrococcus lysodeikticus and E. coli, were rapidly destroyed by these named “nanofighters” in comparison with static lysozyme–AuNWs and free lysozyme. This fact was attributed to the enhancement of lysozyme–bacteria interactions because of the fluid mixing generated by the nanomotors motion. After this pioneering approach, several studies have described different micromotors decorated with other antibacterial molecules, such as chitosan or silver-based materials. **Spherical water propelled micromotors made of chitosan/alginate poly(lactide-co-glycolide)/alginate/gold/ magnesium (Chi/Alg/PLGA/Au/Mg) have been reported for E. coli decontamination** (Figure 4B). Chitosan is a hydrophilic polycationic biopolymer industrially obtained by N-deacetylation of chitin and is able to interact with negatively charged cell membranes, such as bacteria walls, leading to the leakage of proteinaceous and other intracellular constituents. These chitosan-based micromotors showed a high bactericidal effect while they were swimming in comparison with the static analogous and the nonchitosan-based micromotors. As in the previous study, the autonomous propulsion of the Chi/Alg/PLGA/Au/Mg micromotors in drinking-water provided fluid mixing and, consequently, improved the chitosan-micromotor contact with bacteria interactions and its bactericidal efficiency.

Polymer Membranes for Water Treatment

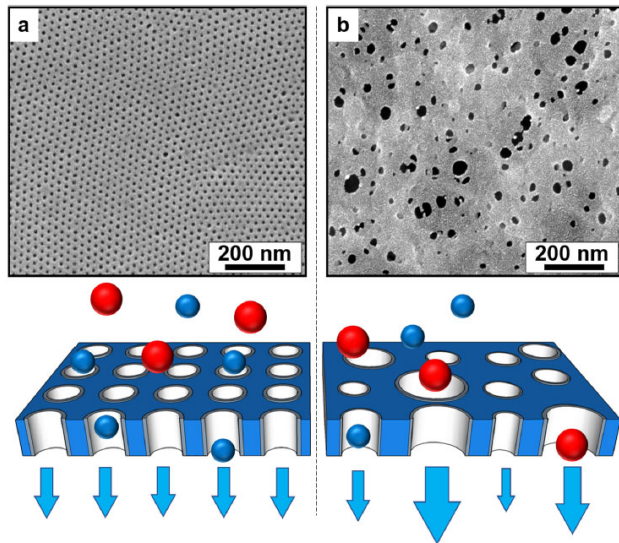


Fig. 2 Scanning electron micrographs of **a** a self-assembled block polymer membrane and **b** a commercial membrane made using a standard phase separation process. The highly-ordered nanostructure of the self-assembled membrane offers the potential for higher performance (i.e., higher throughput and more selective) separations relative to commercial membranes because the well-defined, narrow pore size distribution produces highly-selective filters, and generates a uniform flow distribution through each pore. The blue and red spheres represent solutes of varied size being filtered from solution. The width of the blue arrows is proportional to the volumetric flow through the associated pore. Solute selectivity and a uniform residence time for fluid flowing through the membrane pores are essential in the development of functional membranes for advanced applications.

Zhang 2018, Fit-for-purpose block polymer membranes for water treatment

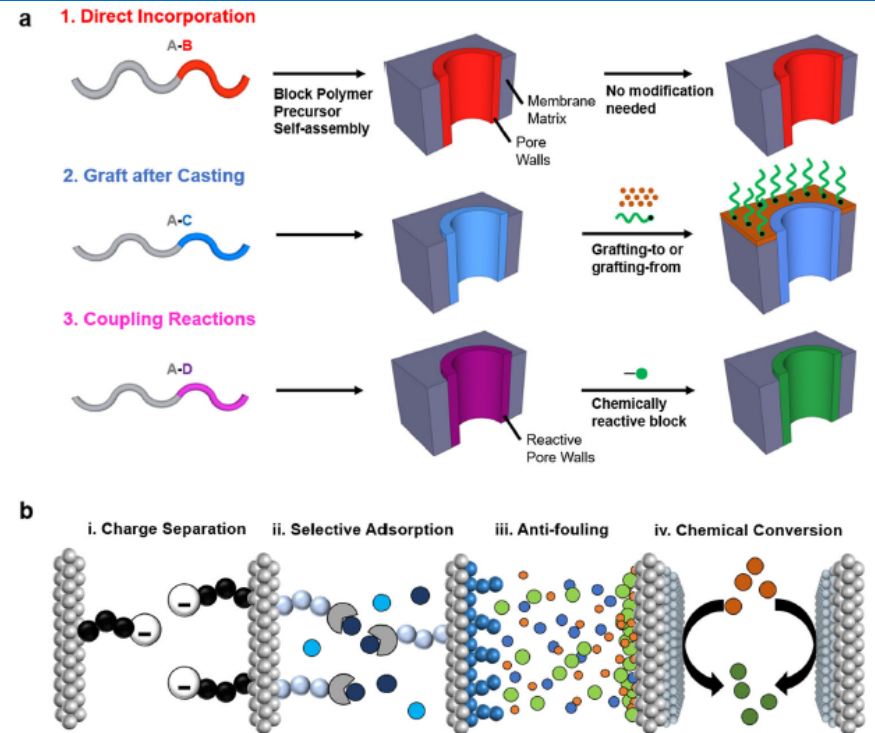


Fig. 6 a Functional moieties can be introduced into the pore wall chemistries of membranes made from block polymer precursors through three mechanisms. (1) The functional chemistry (red block) can be incorporated into the precursor block polymer prior to membrane fabrication. With the identification of suitable SNIPS parameters, a self-assembled membrane with functional pore walls that require no further functionalization reactions is generated. (2) The block polymer chemistry facilitates formation of a self-assembled structure. Subsequently, the surface of the membrane is modified using a coating (orange dots) to which functional chemistries are attached (green brushes). (3) The pore wall-lining block (magenta) is designed as a reactive chemistry that can be converted to a variety of functional chemistries through coupling reactions that are consistent with roll-to-roll processes. b An illustration of the broad range of potential applications where membranes with functional pore wall chemistries could be utilized.

Water Treatment Membrane

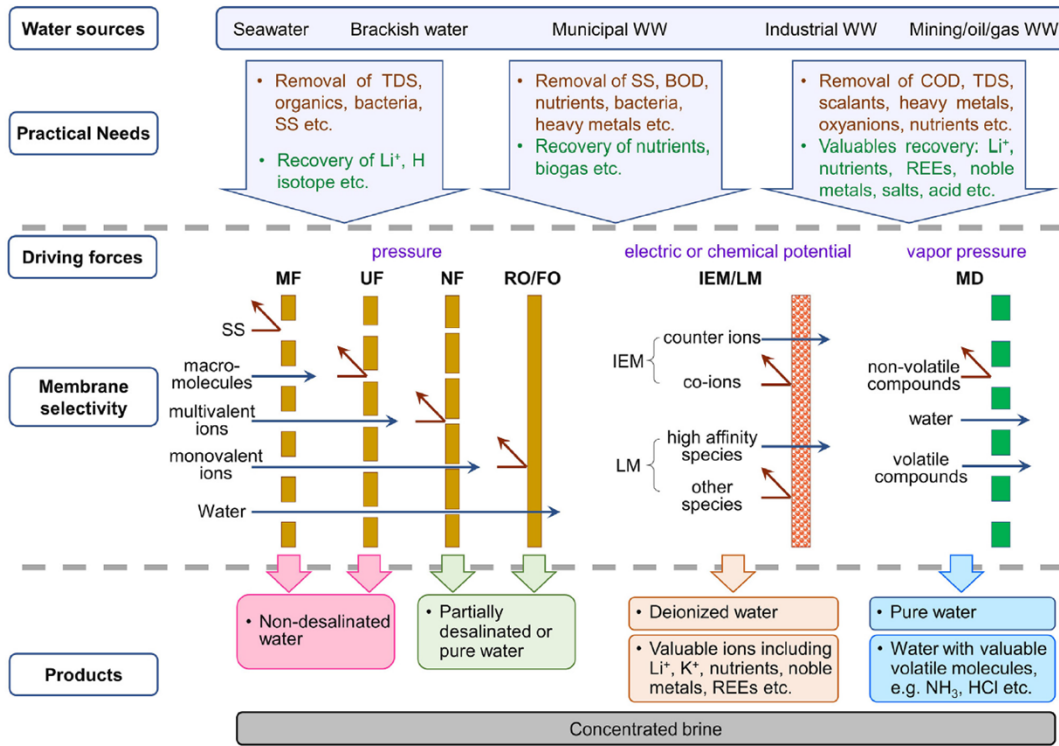


Figure 1. Water treatment membranes and their separation functions in water treatment. WW: wastewater; TDS: total dissolved solids; SS: suspended solids; BOD: biochemical oxygen demand; COD: chemical oxygen demand; REEs: rare earth elements. Microfiltration (MF), ultrafiltration (UF), nanofiltration (NF), reverse osmosis (RO), forward osmosis (FO), and membrane distillation (MD). Ion-exchange membranes (IEM), and liquid membranes (LM).

Zuo 2021, Selective membranes in water and wastewater treatment- Role of advanced materials

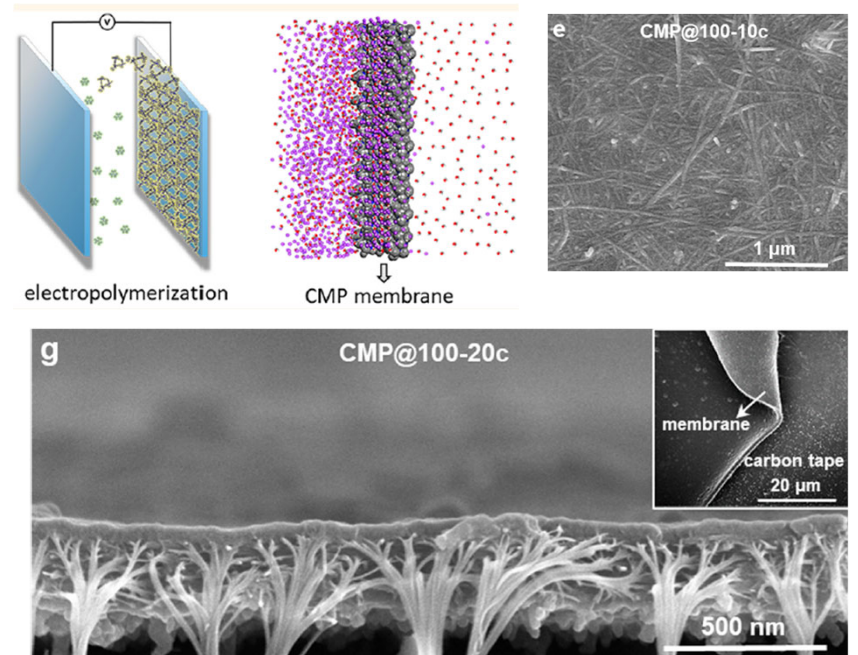


Figure 1. Membrane preparation and morphology. (a) Schematic illustration of the electropolymerization process. (e) Surface SEM image of CMP@100-10c. (g) Cross-sectional SEM image of CMP@100-20c. The inset SEM image shows the flexibility of the composite membrane.

Zhou 2021, Precise sub-angstrom ion separation using conjugated microporous polymer membranes

Centrifugal Microfluidic Discs

ABSTRACT: A fully integrated device for salivary detection with a sample-in-answer-out fashion is critical for noninvasive point-of-care testing (POCT), especially for the screening of contagious disease infection. Microfluidic paper-based analytical devices (μ PADs) have demonstrated their huge potential in POCT due to their low cost and easy adaptation with other components. This study developed a generic POCT platform by integrating a centrifugal microfluidic disc with μ PADs to realize sample-to-answer salivary diagnostics. Specifically, a custom centrifugal microfluidic disc integrated with μ PADs is fabricated, which demonstrated a high efficiency in saliva treatment. To demonstrate the capability of the integrated device for salivary analysis, the SARS-CoV-2 Nucleocapsid (N) protein, a reliable biomarker for SARS-CoV-2 acute infection, is used as the model analyte. By the chemical treatment of the μ PAD surface, and by optimizing the protein immobilization conditions, the on-disc μ PADs were able to detect the SARS-CoV-2 N protein down to 10 pg mL^{-1} with a dynamic range of $10\text{--}1000 \text{ pg mL}^{-1}$ and an assay time of 8 min. The integrated device was successfully used for the quantification of the N protein of pseudovirus in saliva with high specificity and demonstrated a comparable performance to the commercial paper lateral flow assay test strips.

KEYWORDS: microfluidic paper-based analytical devices, centrifugal microfluidic disc, salivary diagnostics, SARS-CoV-2, point-of-care testing

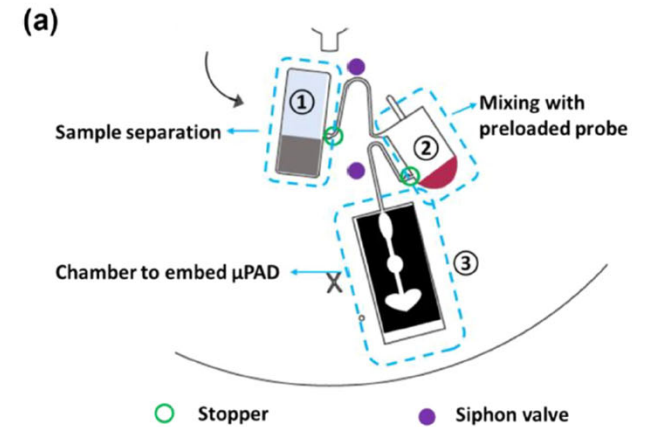
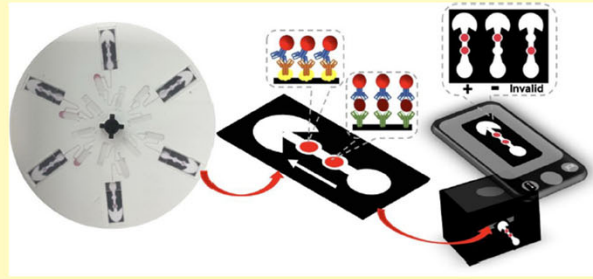
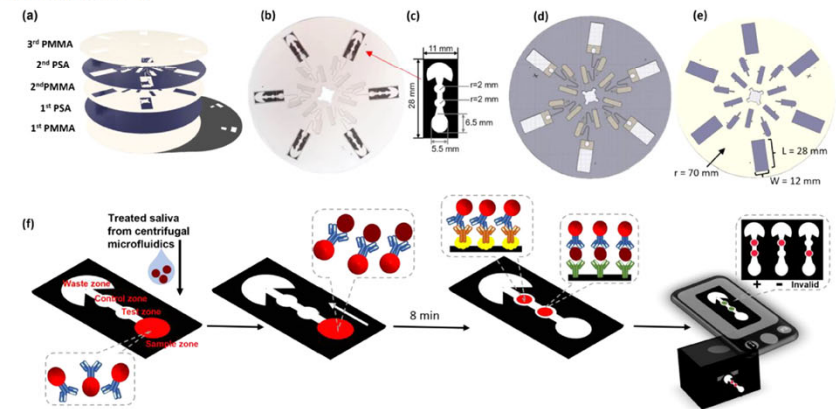


Figure 1. (a) Schematic diagram of on-disc saliva sample preparation procedures.

Scheme 1. (a) Components of the Centrifugal Microfluidic Disc Including Three Layers of PMMA and Two Layers of PSA; (b) Photo of the Centrifugal Microfluidic Disc Integrated with μ PADs; (c) Dimensions of the μ PADs Assembled in the Centrifugal Microfluidic Disc; (d) Top View of the Configuration of 1st PMMA, 1st PSA, and 2nd PMMA; (e) Bottom View of the Configuration of 2nd PSA and 3rd PMMA; (f) Assay Process on μ PADs for the Rapid Detection of Salivary SARS-CoV-2 Nucleocapsid Protein



Integrated Microfluidic Chip

ABSTRACT: Rapid and accurate antimicrobial prescriptions are critical for bloodstream infection (BSI) patients, as they can guide drug use and decrease mortality significantly. The traditional antimicrobial susceptibility testing (AST) for BSI is time-consuming and tedious, taking 2–3 days. Avoiding lengthy monoclonal cultures and shortening the drug sensitivity incubation time are keys to accelerating the AST. Here, we introduced a bacteria separation integrated AST (BSI-AST) chip, which could extract bacteria directly from positive blood cultures (PBCs) within 10 min and quickly give susceptibility information within 3 h. The integrated chip includes a bacteria separation chamber, multiple AST chambers, and connection channels. The separator gel was first preloaded into the bacteria separation chamber, enabling the swift separation of bacteria cells from PBCs through on-chip centrifugation. Then, the bacteria suspension was distributed in the AST chambers with preloaded antibiotics through a quick vacuum-assisted aliquoting strategy. Through centrifuge-assisted on-chip enrichment, detectable growth of the phenotype under different antibiotics could be easily observed in the taper tips of AST chambers within a few hours. As a proof of concept, direct AST from artificial PBCs with *Escherichia coli* against 18 antibiotics was performed on the BSI-AST chip, and the whole process from bacteria extraction to AST result output was less than 3.5 h. Moreover, the integrated chip was successfully applied to the diagnosis of clinical PBCs, showing 93.3% categorical agreement with clinical standard methods. The reliable and fast pathogen characterization of the integrated chip suggested its great potential application in clinical diagnosis.

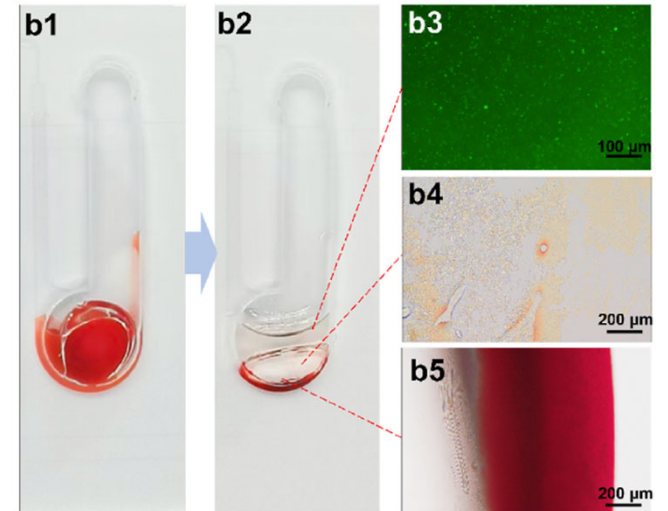
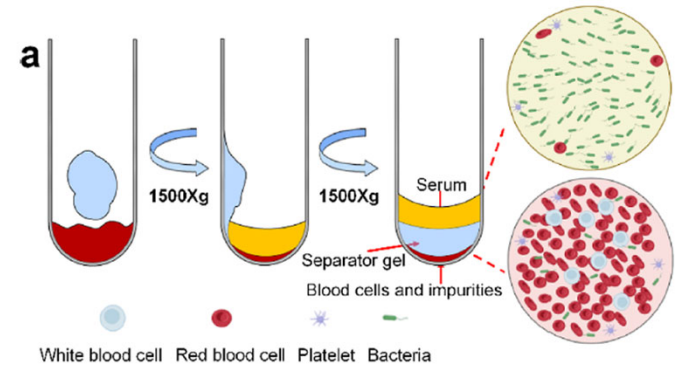
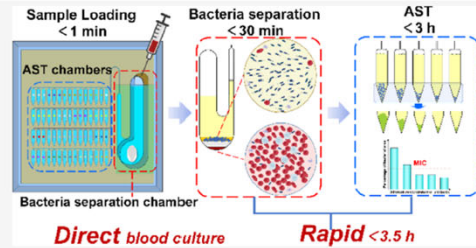


Figure 3. Principle of bacteria separation from PBCs with separator gel. (a) Thixotropic properties of separator gel and delamination of PBCs during centrifugation. (b1,b2) Photographs of the bacteria separation chamber. (b3) Bacteria layer. (b4) Separator gel layer. (b5) Blood cells and impurities layer.

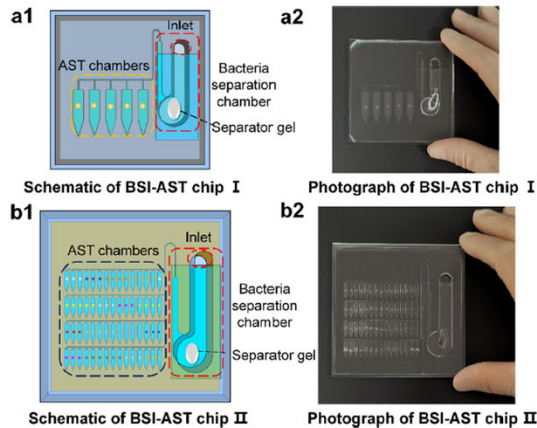


Figure 1. Schematic overview of the design and fabrication of the BSI-AST chip. (a1,a2) Schematic and photograph of BSI-AST chip I. (b1,b2) Schematic and photograph of BSI-AST chip II.